The gravitational path integral in early universe cosmology

Dissertation zur Erlangung des akademischen Grades

doctor rerum naturalium

(Dr. rer. nat.)

im Fach Physik: Spezialisierung:
Theoretische Physik

eingereicht an der
Mathematisch-Naturwissenschaftlichen Fakultät der Humboldt-Universität zu Berlin
von

Caroline Cécile C. Jonas

Präsidentin der Humboldt-Universität zu Berlin:

Prof. Dr. Julia von Blumenthal

Dekanin der Mathematisch-Naturwissenschaftlichen Fakultät:

Prof. Dr. Caren Tischendorf

Gutachter:

1. Prof Dr. Hermann Nicolai
2. Prof Dr. Olaf Hohm
3. Prof Dr. Claus Kiefer

Tag der mündlichen Prüfung: 27/06/2023

Abstract

The path integral quantization of semi-classical gravity is one of the most promising approaches to unify quantum mechanics and general relativity. In this thesis, we investigate the consequences of applying this path integral approach to the cosmology of the very early universe, for which this unification is crucial. In the first part, we focus on the no-boundary proposal, which constructs a non-singular beginning of the universe by relying on the gravitational path integral of general relativity. We prove that the no-boundary solution survives the addition of higher-order corrections to the gravity action. These correction terms usually arise in high-energy completions of general relativity such as string theory, so our analysis indicates that semi-classical results may still hold at the perturbative level of full quantum gravity. We then include a scalar field in the new no-boundary proposal, defined in the Lorentzian formalism as a sum over geometries with fixed initial momentum. Our results are key to confirming the viability of the proposal, as scalar fields are the simplest example of matter fields, which must be included in a realistic theory of the early universe. They also highlight the non-causality puzzle of the no-boundary proposal in the presence of matter fields, for which we offer new perspectives. The second part of the thesis deals with the path integral treatment of more general early universe models. First we test the validity of the semi-classical limit of these models with the finite amplitude criterion, which severely constrains for instance higher-order theories of gravity and favors the no-boundary proposal and emergent universes. At last, we apply Kontsevich and Segal's complex metric criterion to cosmological backgrounds. This criterion tests the path integral convergence of any quantum field theory on a given metric background. Applied in the context of quantum cosmology, it leads to a new understanding of the gravitational path integral in the no-boundary proposal, rules out generic quantum bounces, and stresses the limitation of the minisuperspace ansatz for classical transitions in de Sitter spacetime.

Zusammenfassung

Die Pfadintegral-Quantisierung der semi-klassischen Gravitation ist einer der vielversprechendsten Ansätze zur Vereinheitlichung von Quantenmechanik und allgemeiner Relativitätstheorie. In dieser Arbeit untersuchen wir die Konsequenzen der Anwendung dieses Pfadintegralansatzes auf die Kosmologie des sehr frühen Universums, für die diese Vereinheitlichung entscheidend ist. Im ersten Teil konzentrieren wir uns auf den no-boundary proposal, der einen nicht-singulären Anfang des Universums konstruiert, indem er sich auf das gravitative Pfadintegral der allgemeinen Relativitätstheorie stützt. Wir beweisen, dass die no-boundary Lösung das Hinzufügen von Korrekturen höherer Ordnung zur Gravitationswirkung überlebt. Diese Korrekturterme treten normalerweise in hochenergetischen Ergänzungen der allgemeinen Relativitätstheorie auf, wie z.B. in der Stringtheorie. Unsere Analyse deutet also darauf hin, dass semi-klassische Ergebnisse auch in der perturbative Störungstheorie der vollständigen Quantengravitation gültig sind. Anschließend beziehen wir ein Skalarfeld in den neuen no-boundary proposal ein, der im Lorentz-Formalismus als Summe über Geometrien mit festem Anfangsimpuls definiert ist. Unsere Ergebnisse sind der Schlüssel zur Bestätigung der Gültigkeit des neuen no-boundary proposals, denn Skalarfelder sind das einfachste Beispiel für Materiefelder, die in einer realistischen Theorie des frühen Universums enthalten sein müssen. Außerdem verdeutlichen sie das Nichtkausalitätsrätsel des no-boundary proposals in Gegenwart von Materiefeldern, für das wir neue Perspektiven aufzeigen. Der zweite Teil der Arbeit befasst sich mit der Pfadintegralansatz für allgemeineren Modellen des frühen Universums. Zunächst testen wir die Gültigkeit des semi-klassischen Limits dieser Modelle mit dem Kriterium der endlichen Amplitude, das z.B. Theorien höherer Ordnung der Gravitation stark einschränkt und den no-boundary proposal sowie emergente Universen begünstigt. Schließlich wenden wir das Kriterium der komplexen Metrik von Kontsevich und Segal auf kosmologische Hintergründe an. Dieses Kriterium prüft die Pfadintegralkonvergenz einer beliebigen Quantenfeldtheorie auf einem gegebenen metrischen Hintergrund. Im Kontext der Quantenkosmologie angewandt, führt es zu einem neuen Verständnis des gravitativen Pfadintegrals im no-boundary proposal, schließt generische quantum bounces aus und unterstreicht die Limitierung des Minisuperspace-Ansatzes für klassische Übergänge in der de-Sitter-Raumzeit.

Declaration of authorship

I declare that I have completed the thesis independently using only the aids and tools specified. I have not applied for a doctor's degree in the doctoral subject elsewhere and do not hold a corresponding doctor's degree. I have taken due note of the Faculty of Mathematics and Natural Sciences PhD Regulations, published in the Official Gazette of Humboldt-Universität zu Berlin no. 42/2018 on 11/07/2018.

Potsdam, February 21, 2023.
Caroline Jonas

Contents

List of publications

The present thesis is based on the following publications:

[1] *No-boundary solutions are robust to quantum gravity corrections*, Caroline Jonas and Jean-Luc Lehners, December 2020 in Phys. Rev. D 102 (2020) 123539.

[2] *Cosmological consequences of a principle of finite amplitudes*, Caroline Jonas and Jean-Luc Lehners and Jérôme Quintin, May 2021 in Phys. Rev. D 103 (2021) 103525.

[3] *Revisiting the no-boundary proposal with a scalar field*, Caroline Jonas and Jean-Luc Lehners and Vincent Meyer, February 2022 in Phys. Rev. D 105 (Feb, 2022) 043529.

[4] *Uses of complex metrics in cosmology*, Caroline Jonas and Jean-Luc Lehners and Jérôme Quintin, August 2022 in J. High Energ. Phys. 2022, 284 (2022).

Introduction

The twentieth century saw the occurrence of two total paradigm shifts concerning the understanding of the laws governing physics, on the one hand at the microscopic level with the development of quantum mechanics, and on the other hand at very large scales with general relativity. Quantum theory challenges our daily experience of the world, yet its predictions at the scale of the atoms and even up to molecular size, have been experimentally checked to such an extreme level of accuracy that it would be absurd to dispute it. Nevertheless, even though our classical world can be shown to emerge from the quantum description through the phenomenon of decoherence [5, 6], there is no experimental proof that the quantum theory will continue to be valid when we consider inaccessible regimes of extreme density of matter, such as those we expect to have existed in the very early universe.

Throughout this thesis, we will assume that quantum theory is indeed universal: it must be valid for any scales and regimes of matter. Given this initial assumption, the core purpose of this work is to understand **what is the quantum state of the very early universe**, and what are the tools we can use to probe the quantumness of this epoch.

So far, we have only been able to observe[1] the universe back to the cosmic microwave background state [7], about 380 000 years after the "big bang". In the future, it is possible that we gain experimental access to even earlier states, for example through neutrinos cosmic background, or even through the detection of primordial gravitational waves. Nevertheless, the cosmic microwave background is already telling us something about the quantum nature of the early universe, as we have good reason to think that its temperature variations are the direct offspring of quantum density fluctuations. In this work we push this question further and ask: how can we assess the quantum nature not only of fluctuations but also of the background geometry itself?

To investigate this, we mainly resort to the gravitational path integral and its semi-classical limit, when $\hbar \to 0$. This tool allows to define one instance of truly quantum background for the early universe, the no-boundary state. It further permits to construct theoretical criteria that can check the consistency of early universe models at the semi-classical level, based on the convergence of the path integral for matter fields and for gravity. Interestingly, we find a connection between these semi-classical consistency cri-

[1] Here observe means "measure with light signals". We will see later on that we have evidence for the validity of the universe model from much early times.

teria and the swampland program [8, 9]. This program aims to identify which low energy effective models cannot possibly emanate from the full UV-complete theory of quantum gravity. We find in this work intriguing resemblances between some of the swampland conditions and the conditions arising from our semi-classical criteria, possibly indicating that swampland constraints are not only features of the full quantum gravity, but already of its semi-classical limit. This may also hint toward possible first principles underlying those semi-classical criteria, such as unitarity, causality, etc.

This thesis is organized as follow: the first two chapters are introductory and present the general framework and state-of-the-art of quantum cosmology. In chapter 1 we expose the salient features of general relativity and the ensuing hot big bang evolution model and then present the simplest inflationary model, based on a massive scalar field. Then in chapter 2, we review the state-of-the-art of quantum cosmology, and in particular of the no-boundary proposal which will play a key role in our work. In the third and fourth chapters, we present new results on the no-boundary proposal developed in the course of this thesis. Specifically, chapter 3 studies the viability of no-boundary solutions for general relativity supplemented by higher-order terms (based on the results published in [1]), while chapter 4 investigates the inclusion of a scalar field in the no-boundary solution, using the new no-boundary prescription as a sum over regular metrics (results published in [3]). Finally, in the two last chapters, we take a step back with respect to the no-boundary proposal, and investigate criteria for the consistent definition of the gravitational wavefunction, from a semi-classical perspective. In chapter 5, we show how the requirement of obtaining convergent cosmological amplitudes from the gravitational path integral imposes strict conditions on possible early universe models. We find that the scenarios best suited to this criterion are the no-boundary proposal and loitering universes (results published in [2]). At last, chapter 6 considers the implications of the complex metric criterion, devised by Kontsevich and Segal as a convergence criterion on matter field's path integrals in quantum field theory, on theories of the early universe involving complex geometries (results published in [4]).

Unless otherwise stated, we use the following conventions in this thesis: partial derivatives are generally written as: $f_{,x} \equiv \frac{\partial f}{\partial x}$. An upper dot refers specifically to a partial derivative with respect to the coordinate time t. We work in four-dimensional spacetime and utilize the mostly positive signature of the metric.

Chapter 1

The standard model of cosmology

In this thesis we will study various models describing the evolution of our universe, with an emphasis on its beginning. For a very long time, the universe was believed to be in a stationary state. This view was challenged by the advent of general relativity in the early twentieth century. The initial purpose of general relativity was to reconcile the theory of gravitation with the principle of relativity, which restricts the propagation of interactions to a finite speed. Though this theory still admitted some static solutions (Einstein's static solution originally motivated him to introduce the cosmological constant Λ), it was gradually understood that general relativity, together with the assumptions of isotropy and homogeneity of the universe, led to what we call the standard hot big bang evolution. In this chapter, we first review this construction and then, we describe the flatness and horizon problem which arise from the initial conditions required by this model. We then describe the most popular solution to these problems, namely the inflationary scenario, while stressing its weaknesses and the puzzles it leaves unsolved.

1.1 General relativity and the hot big bang evolution

General relativity (GR) describes gravity as the curvature of spacetime sourced by matter. It departs from Newton's preceding theory of gravitation, that viewed gravity as an attractive force between any two masses. The latter assumed that time was an absolute quantity, but this premise got contradicted when Maxwell discovered that the electromagnetic waves propagate at a finite speed, the speed of light c, which led Einstein in 1905 to the theory of special relativity. In special relativity, space and time are coordinates on a four-dimensional manifold, and the structure of spacetime is determined by the Minkowski metric, which is a non dynamical quantity that determines the proper distance between any two events, $\mathrm{d}s^2 = -c^2\mathrm{d}t^2 + \mathrm{d}\vec{x}^2$. By allowing the metric of spacetime to become a dynamical object, Einstein then obtained in 1915 the theory of general relativity, where spacetime gets curved by the matter and energy it contains.

A key observation at the center of general relativity is **the equivalence principle**. First formulated by Galilei, it states that in pure vacuum, the speed of a free falling object

does not depend on its mass, meaning that gravity and acceleration are in fact equivalent. Locally, gravity can therefore always be removed by selecting the appropriate accelerated frame: it can be entirely described by a local change of frames (i.e., transformation of spacetime coordinates), $x'^{\alpha} \to x^{\mu} = x^{\mu}(x'^{\alpha})$. In other words, gravity is completely determined by the dynamical metric $g_{\mu\nu}(x)$ depending on arbitrary spacetime coordinates $\{x^{\mu}\}$:

$$\mathrm{d}s^2 \equiv \eta_{\alpha\beta}\mathrm{d}x'^{\alpha}\mathrm{d}x'^{\beta} = g_{\mu\nu}(x)\mathrm{d}x^{\mu}\mathrm{d}x^{\nu} \quad \Rightarrow \quad g_{\mu\nu}(x) = \eta_{\alpha\beta}\frac{\partial x'^{\alpha}}{\partial x^{\mu}}\frac{\partial x'^{\beta}}{\partial x^{\nu}}\,. \tag{1.1.1}$$

The equivalence principle is then formally equivalent to the requirement that dynamical equations are invariant under the change of frames: $x'^{\alpha} \to x^{\mu}$. This transformation is called a diffeomorphism in differential geometry, so the equations describing gravity must be **diffeomorphism invariant**. From the Newtonian limit, we know that the equations for gravity must contain second-order differential operators. The simplest non-trivial second-order operator that is diffeomorphism invariant is the **Riemann tensor**:

$$R^{\lambda}{}_{\mu\rho\nu} \equiv \partial_{\nu}\Gamma^{\lambda}_{\mu\rho} - \partial_{\rho}\Gamma^{\lambda}_{\mu\nu} + \Gamma^{\alpha}_{\mu\rho}\Gamma^{\lambda}_{\alpha\nu} - \Gamma^{\alpha}_{\mu\nu}\Gamma^{\lambda}_{\alpha\rho}\,, \tag{1.1.2}$$

where the Christoffel symbols $\Gamma^{\mu}_{\nu\rho}$ are defined by:

$$\Gamma^{\mu}_{\nu\rho} = \frac{1}{2}g^{\mu\alpha}\left(\partial_{\nu}g_{\alpha\rho} + \partial_{\rho}g_{\nu\alpha} - \partial_{\alpha}g_{\nu\rho}\right). \tag{1.1.3}$$

We can also obtain the so-called Ricci two-indices tensor and Ricci scalar, constructed from one Riemann tensor and the metric as:

$$R_{\mu\nu} \equiv R^{\lambda}{}_{\mu\lambda\nu} \quad \text{(Ricci tensor)}\,; \tag{1.1.4}$$

$$R \equiv g^{\mu\nu}R_{\mu\nu} \quad \text{(Ricci scalar)}\,. \tag{1.1.5}$$

The action for gravity must be a scalar quantity constructed only from the metric $g_{\mu\nu}$ and the Riemann tensor $R^{\lambda}{}_{\mu\nu\rho}$, as these fully encapsulate the geometry and curvature of spacetime. We hence write an ansatz of the form:

$$S = \int \mathrm{d}^4x\sqrt{-g}\left[a + bR + cR_{\mu\nu}R^{\mu\nu} + dR_{\mu\nu\rho\sigma}R^{\mu\nu\rho\sigma} + eR_{,\nu}R^{,\nu} + \cdots\right], \tag{1.1.6}$$

where $g \equiv \det(g_{\mu\nu})$ is the determinant of the metric, and the factor $\sqrt{-g}$ serves to render the four-volume element d^4x diffeomorphism invariant. By dimensional analysis, we find that b has the dimension of an energy squared, $[b] \sim [\text{energy}]^2$. At this point, we take a step back to ask ourselves, what is the range of energy for which we expect this theory to be valid? We are constructing a purely classical field theory. We know from quantum mechanics and the quantization of other classical field theories such as electromagnetism, that quantum effects appear when we consider very small length scales, or equivalently

very large energy scales. In this context, we usually express all quantities in GeV by using the natural system of units where $c = \hbar = k_{\rm B} = 1$. When considering gravity, we have one additional fundamental constant, the Newtonian constant G. This means that a theory treating gravity at a quantum level would be best described by a system of units where $c = \hbar = k_{\rm B} = 8\pi G = 1$. This system of units defines a mass scale, the (reduced) Planck mass $M_{\rm Pl} \equiv \sqrt{\frac{\hbar c}{8\pi G}} = 4.341 \cdot 10^{-9}$kg, corresponding to a length $\ell_{\rm Pl} \sim 10^{-33}$cm and an energy scale of about 10^{18} GeV. This defines the typical scale for which quantum effects are expected in gravitation. Back to equation (1.1.6), the coupling constant b must be of order: $[b] \sim [\text{energy}]^2 \;\Rightarrow\; b \sim G^{-1} \sim M_{\rm Pl}^2$, but then for any scale larger than the Planck scale $\ell \gg \ell_{\rm Pl}$ (i.e., for the classical regime we want to describe), the Ricci scalar scales as $R \sim 1/\ell^2$ so that

$$bR \sim M_{\rm Pl}^2 \cdot \frac{1}{\ell^2} \ll \text{constant} \cdot R^2 \sim \text{constant} \cdot \frac{1}{\ell^4}\,. \tag{1.1.7}$$

At the classical level, we can neglect all terms of order larger than 1 in the Riemann tensor, unless we assume unnaturally large dimensionless coupling constants $\sim 10^{100}$. Later in this thesis, we will consider theories which extend the action (1.1.6) and include higher orders of the Riemann tensor, precisely in order to describe the quantum corrections to general relativity.

The action for general relativity (1.1.6) eventually reduces to the Einstein-Hilbert action:

$$S_{\text{E-H}} = \frac{1}{16\pi G}\int \mathrm{d}^4x\sqrt{-g}\,(R - 2\Lambda)\,, \tag{1.1.8}$$

where Λ is the cosmological constant. The associated equations of motion are called the **Einstein field equations**, and they can be derived from the action (1.1.8) supplemented by a matter action $S_{\rm Matter}$, by using the variational principle:

$$R_{\mu\nu} - \frac{1}{2}g_{\mu\nu}R - \Lambda g_{\mu\nu} = 8\pi G\, T_{\mu\nu}\,. \tag{1.1.9}$$

$T^{\mu\nu}$ is the stress energy tensor which derives from the matter action,

$$T^{\mu\nu} \equiv \frac{2}{\sqrt{-g}}\frac{\delta S_{\rm Matter}}{\delta g^{\mu\nu}}\,. \tag{1.1.10}$$

The above sets the formalism of general relativity. On top of recovering the Newtonian theory in the appropriate limit (nearly flat spacetime $g_{\mu\nu} \simeq \eta_{\mu\nu}$, non-relativistic matter $v \ll 1$ and without cosmological constant $\Lambda = 0$), general relativity made new predictions departing from Newtonian gravity which have been tested to an exquisite level of accuracy. In particular, it predicted the deflection angle of light due to the gravitational field of a massive object (experimentally tested during the 1919 solar eclipse), and precession of the perihelion of Mercury. The linear approximation of the field equations led to the prediction in 1918 of gravitational waves, whose first evidence was given by the energy loss

of the Hulse-Taylor binary [10], and that are now extensively studied by the LIGO/Virgo collaboration [11]. Finally, general relativity also predicted the existence of black holes, whose first confirmed instance was the X-ray source Cygnus X-1 observed in 1971 [12].

Having recalled the key features of general relativity, we focus on its application to the evolution of our whole universe. Friedmann found in 1924[1] that the Einstein field equations possessed a solution for a spatially homogeneous and isotropic universe, yet expanding in time. The assumption of spatial homogeneity and isotropy is known as the cosmological principle, and it was since then found to be valid in our universe to a very good approximation on large scales, most spectacularly by the cosmic microwave background (CMB), whose latest measurement by the Planck satellite [7] is reproduced in figure 1.1. Friedmann's spatially homogeneous and isotropic solution is given by the

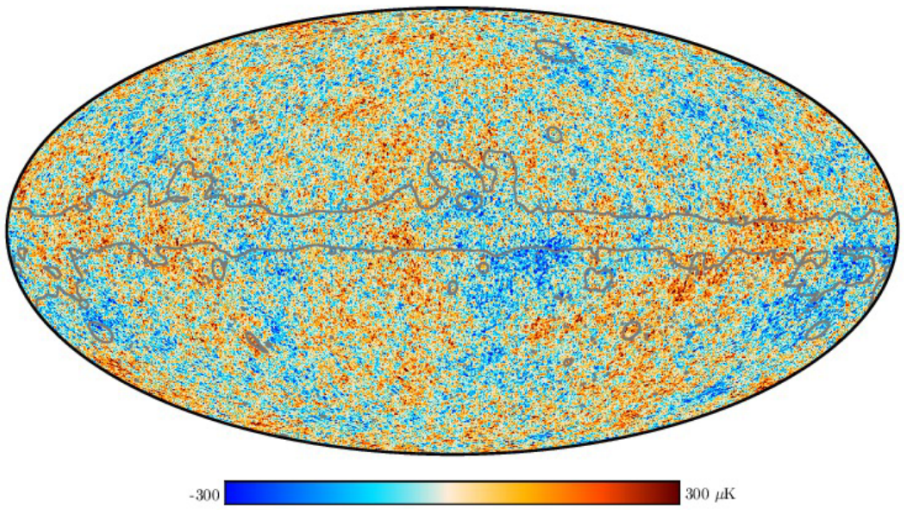

Figure 1.1: All-sky map of the fluctuations of temperature observed in the cosmic microwave background by the Planck's satellite. The average temperature is $T_{\text{CMB}} = 2.72548 \pm 0.00057K$, and the fluctuations range from $-300\mu K$ to $+300\mu K$, thus representing a ratio of variation of about $\delta T/T \sim 10^{-4}$. Picture taken from [7].

FLRW metric:

$$\mathrm{d}s^2 = -N(t)^2\mathrm{d}t^2 + a(t)^2\left(\frac{\mathrm{d}r^2}{1-kr^2} + r^2\mathrm{d}\Omega_2^2\right) . \tag{1.1.11}$$

Locally, this is the unique spatially homogeneous and isotropic metric in four dimensions, but globally there might be different spacetimes associated with different topologies. The FLRW metric only depends on two functions of time, the lapse $N(t)$ and the scale factor $a(t)$. This represents a drastic reduction of the number of degrees of freedom: instead of a metric whose evolution varies at every single point in spacetime, we find an evolution only in time: our system is described by two functions, instead of infinitely many. k is the spatial curvature, that can take values 0, 1 and -1, corresponding respectively to a spatially flat, closed and open universe. Plugging this metric into Einstein's field equations (1.1.9), and assuming a stress-energy tensor accounting for a perfect fluid matter with

[1] This solution was also found by Lemaître in 1927, and then by Robertson and Walker in 1935, hence the name Friedmann-Lemaître-Robertson-Walker (FLRW).

equation of state $p(t) = w\rho(t)$,

$$T^{\mu\nu} = p(t)g^{\mu\nu} + (\rho(t) + p(t))\, u^\mu u^\nu \,, \tag{1.1.12}$$

where $\rho(t)$ is the energy density, $p(t)$ the pressure and u^μ the four-velocity, we obtain the Friedmann constraint and equations of motion of the homogeneous and isotropic universe:

$$\begin{cases} \dfrac{3\dot{a}^2}{a^2N^2} + \dfrac{3k}{a^2} = \Lambda + 8\pi G\rho \quad \text{(Friedmann constraint)}\,, \\ \dfrac{2\ddot{a}}{aN^2} + \dfrac{\dot{a}^2}{a^2N^2} + \dfrac{k}{a^2} = \Lambda - 8\pi G p \quad \text{(acceleration equation)}\,, \\ a\dot{\rho} + 3\dot{a}(\rho + p) = 0 \quad \text{(continuity equation)}\,. \end{cases} \tag{1.1.13}$$

The Hubble rate is defined by $H(t) \equiv \dot{a}(t)/a(t)$ and represents an important quantity in observational cosmology. The measured quantity nowadays is of about $H(t_0) \equiv H_0 \simeq 70\,\mathrm{km\,s^{-1}Mpc^{-1}}$ [2].

Depending on the matter content of the universe and its equation of state, the FLRW equations (1.1.13) yield different regimes of evolution for the scale factor. We distinguish three types of matter content in the universe:

1. **Radiation** (photons): radiation is characterized by the equation of state: $p_\gamma = \rho_\gamma/3$. By using the continuity equation in (1.1.13), we find that

$$\rho_\gamma(t) = \rho_\gamma(t_0) \cdot \frac{a(t_0)^4}{a(t)^4}\,.$$

2. **Non-relativistic matter** (ordinary and cold dark matter): ordinary matter is characterized by $p_\mathrm{M} = 0$, $\rho_\mathrm{M} \neq 0$. Thus the continuity equation yields the time dependence:

$$\rho_\mathrm{M} = \rho_\mathrm{M}(t_0) \cdot \frac{a(t_0)^3}{a(t)^3}\,.$$

3. **Vacuum energy** (cosmological constant): In equations (1.1.13), the cosmological constant terms can be understood as an additional type of matter with energy density $\rho_\Lambda \equiv \Lambda/(8\pi G)$ and pressure $p_\Lambda \equiv -\Lambda/(8\pi G)$. This energy density is thus time-independent. Note that if we only have a cosmological constant in an otherwise empty universe, the solution to the Einstein fields' equations (1.1.9) is the de Sitter ($\Lambda > 0$) or Anti-de Sitter ($\Lambda < 0$) spacetime. In these cases the scalar curvature R is proportional to the cosmological constant. The de Sitter spacetime plays an important role because it gives an approximate solution when the universe is dominated by the vacuum energy, as in the late universe.

[2] The Planck's measurement gives $H_0 = 66.88 \pm 0.92\,\mathrm{km\,s^{-1}Mpc^{-1}}$ [7], while the local measurement based on the distance-redshift velocity relation for Cepheids and type Ia supernovae yields $H_0 = 73.00 \pm 1.75\,\mathrm{km\,s^{-1}Mpc^{-1}}$ [13]. The tension between these values is still unexplained and it provoked a reconsideration in recent years of the standard model of cosmology.

With the above matter content, the Friedmann equation in (1.1.13) becomes:

$$H^2 + \frac{k}{a^2} = \frac{8\pi G}{3}\left(\rho_\gamma + \rho_{\mathrm{M}} + \rho_\Lambda\right), \tag{1.1.14}$$

$$\Rightarrow \text{ at } t = t_0: \quad 1 + \frac{k}{a(t_0)^2 H_0^2} = \frac{8\pi G}{3H_0^2}\left(\rho_\gamma(t_0) + \rho_{\mathrm{M}}(t_0) + \rho_\Lambda\right). \tag{1.1.15}$$

The quantity $\rho_{\mathrm{c}} \equiv 3H_0^2/(8\pi G)$ is called the critical density[3]. The equation (1.1.15) provides the abundances ratio of each matter content at present time $t = t_0$. $\Omega_\gamma \equiv \rho_\gamma(t_0)/\rho_{\mathrm{c}}$ is the radiation abundance, $\Omega_{\mathrm{M}} \equiv \rho_{\mathrm{M}}(t_0)/\rho_{\mathrm{c}}$ is the matter abundance and $\Omega_\Lambda \equiv \rho_\Lambda/\rho_{\mathrm{c}}$ is the cosmological constant abundance. By similarly defining the spatial curvature abundance as $\Omega_k \equiv -k/(a(t_0)^2 H_0^2)$, we can rewrite equation (1.1.15) as $1 = \Omega_\gamma + \Omega_{\mathrm{M}} + \Omega_\Lambda + \Omega_k$. Using the time dependencies of the energy density for the different matter types, we can express the Friedmann equation in term of the energy density abundances:

$$H(t)^2 = H_0^2\left[\Omega_\Lambda + \Omega_{\mathrm{M}}\frac{a(t_0)^3}{a(t)^3} + \Omega_\gamma\frac{a(t_0)^4}{a(t)^4} + \Omega_k\frac{a(t_0)^2}{a(t)^2}\right]. \tag{1.1.16}$$

This equation yields three different regimes of evolution depending on which term dominates the energy content (1.1.16) in time. From experimental data (Planck 2018), we measure that $\Omega_\Lambda = 0.6847 \pm 0.0073$, $\Omega_{\mathrm{M}} = 0.315 \pm 0.007$, $\Omega_k = 0.0007 \pm 0.0019$ [4] [7] and $\Omega_\gamma = 5.38 \cdot 10^{-5}$ [14]. Therefore at present time, the term ρ_Λ dominates the equation (1.1.16) and leads to a **cosmological constant dominated epoch** with an approximate exponential evolution for the scale factor (approximate de Sitter spacetime):

$$a(t) \simeq a(t_0)\exp\left(\sqrt{\frac{\Lambda}{3}}(t - t_0)\right), \quad H(t) = \sqrt{\frac{\Lambda}{3}}. \tag{1.1.17}$$

When going backward in time, the scale factor $a(t)$ shrinks, and the matter and radiation terms $\Omega_{\mathrm{M}}/a(t)^3$ and $\Omega_\gamma/a(t)^4$ grow until they turn by turn dominate the equation (1.1.16). First we reach a time t_1 where $\rho_{\mathrm{M}}(t_1) = \rho_\Lambda(t_1)$ and we enter a **matter dominated epoch** where the scale factor approximately evolves as:

$$a(t) \simeq a(t_1)\left(\frac{t}{t_1}\right)^{2/3}, \quad H(t) = \frac{2}{3t} \text{ and } \rho_{\mathrm{M}}(t) = \frac{1}{6\pi G t^2}. \tag{1.1.18}$$

Going further back in time, we reach a second time t_2 where $\rho_\gamma(t_2) = \rho_{\mathrm{M}}(t_2)$ and we reach a **radiation dominated epoch** where

$$a(t) \simeq a(t_2)\left(\frac{t}{t_2}\right)^{1/2}, \quad H(t) = \frac{1}{2t} \text{ and } \rho_\gamma(t) = \frac{3}{32\pi G t^2}. \tag{1.1.19}$$

[3] It is called critical density because depending whether its ratio with the present total energy density $(\rho_\gamma^0 + \rho_{\mathrm{M}}^0 + \rho\Lambda)$ is smaller, equal or larger to 1, the spatial curvature of our present universe will be open, flat or closed.

[4] This explains why our late-universe model is named the ΛCDM model, since the two largest components of the energy content nowadays are due to the vacuum energy and to cold dark matter.

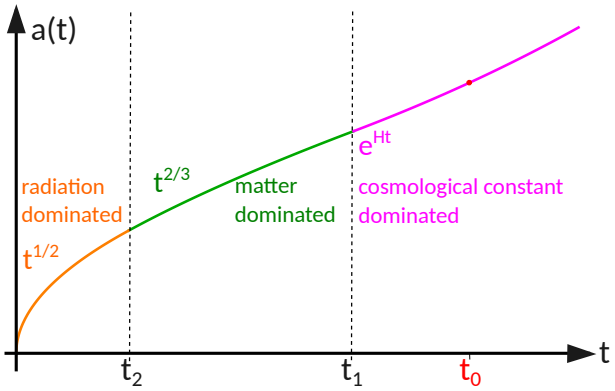

Figure 1.2: Approximated regimes of evolution of the scale factor in time following the hot big bang model. Present time t_0 is represented by a red dot, and is estimated to be 13.8 billion years. The transition from radiation to matter dominated epoch takes place about 50 000 years after the big bang. The transition from matter dominated to cosmological constant dominated phase takes place about 10 billion years after the big bang, very recently compared to the total age of the universe.

These three regimes of evolution are depicted in Figure 1.2. Note that these scaling solutions are obtained because we have approximated the spatial curvature term Ω_k to be 0, as is expected from the Planck data currently.

The radiation and matter dominated equations (1.1.18) and (1.1.19) both imply that at some point in time, $a \to 0$ and $\rho \to +\infty$. This corresponds to the so-called big bang or cosmological singularity. The above analysis does not include quantum effects, but these cannot be neglected anymore when $\rho \to +\infty$. The model breaks down when $\rho \sim M_{\mathrm{Pl}}^4$, which corresponds to a time scale of $t \sim 1/M_{\mathrm{Pl}} \sim 10^{-43}\,\mathrm{s}$. The evolution described above is theoretically valid up to that point, which enables to get to states with very large densities, larger even than the density inside atomic nuclei.

This model was first proposed by Gamow et al. in 1948 and postulated that the state of the early universe was in a thermal equilibrium at a certain temperature and density. Going back in time, we reach hotter and denser states, and this led to two predictions. First, the transition from a fully ionized plasma (opaque to radiation) into a gas of neutral atoms (transparent to radiation) when the temperature reaches the binding energy of electrons in hydrogen atoms (13.6 eV), leaves a black body radiation remnant, the CMB, which was observed for the very first time in 1965 by Penzias and Wilson. The CMB is in a sense the first picture of our universe, dated back to 380 000 years after the big bang. Similarly, from the transition at the nuclear binding energy ($\sim 1\,\mathrm{MeV}$), Gamow et al. predicted the primordial abundance of helium in the universe to be one quarter of the original neutrons and protons [15]. The abundance of other light elements such as deuterium and lithium can also be predicted this way, and these predictions agree well with the abundances found in very early stars, for which the abundances due to the star nucleosynthesis did not yet supplant the former. This transition happened about 1 second after the big bang, and is the earliest experimental evidence of the hot big bang evolution. We however continue to have a good understanding of earlier times and

matter states until the so called electroweak scale at energy $\sim 1\,\text{TeV}$, equivalent to about $t \sim 10^{-14} - 10^{-12}$s, because we can probe those energies and study the equivalent state of matter with experiments on Earth such as the Large Hadron Collider at CERN.

Overall, the hot big bang model is a very good approximation of our early universe, despite its apparent simplicity. However as we will discuss in the next section, in addition to the fact that this theory cannot be trusted above the Planck scale, it requires initial conditions that are problematic and lead to worrying puzzles, preventing us to obtain a consistent picture of the early universe.

1.2 Puzzles of the hot big bang model and the inflationary paradigm

The hot big bang evolution necessitates to start from an initial state with very special conditions: it must be extremely spatially homogeneous, isotropic and flat. Assuming that the universe started in such a fine-tuned state is very unnatural, and instead it appeals to search for an explanation of these initial conditions, which is in particular the aim of the no-boundary proposal we will present in chapter 2. But even if we take for granted that the initial state[5] of our universe was highly spatially homogeneous, isotropic and flat, by assuming only the hot big bang evolution we encounter nonsensical puzzles. Though these puzzles could be relegated to the quantum gravity phase before the Planck time, the mechanism of inflation [16, 17] enables to get rid of them through a mechanism taking place well after the Planck time. Inflation relies on a quantum field theory on curved background approach, which implies that it treats the background as a classical quantity, on top of which quantum fluctuations are considered. This way, the inflationary model can also generate the density perturbations that are observed in the CMB and that seed the large structures in our universe, from primordial quantum fluctuations.

1.2.1 The horizon problem

The horizon problem results from the very high spatial homogeneity and isotropy observed in the CMB spectrum. For a static universe described by a Minkowski spacetime as in special relativity, the finite bound on the speed of propagation c implies that any two events whose spatial separation ℓ is larger than $c \cdot \Delta t$, where Δt is their time separation, cannot be causally connected.

In an expanding universe, the size of the causal horizon $\ell(t)$ is deformed by the Hubble rate of expansion $H(t) = \dot{a}(t)/a(t)$:

$$\frac{\mathrm{d}\ell}{\mathrm{d}t} = c + \frac{\dot{a}(t)}{a(t)} \cdot \ell\,, \;\Leftrightarrow\; \ell(t) = c \cdot a(t) \int_{t_{\text{ini}}}^{t} \frac{\mathrm{d}t'}{a(t')} = c \cdot t^{\alpha} \int_{t_{\text{ini}}}^{t} \frac{\mathrm{d}t'}{t'^{\,\alpha}} \quad \text{for } a(t) \propto t^{\alpha}\,. \tag{1.2.1}$$

[5] As defined by Guth in [16], the initial state of the hot big bang model can be taken as a state of the universe colder than the Planck scale, e.g. for $T \sim 10^{17}$GeV, to avoid quantum effects.

When the initial time $t_{\rm ini} \to 0$, the above integral converges for $\alpha < 1$ and yields $\ell(t)|_{t_{\rm ini}=0} = \dfrac{t}{1-\alpha}$. Therefore, at the time of recombination of electrons, which approximately corresponds to the CMB time, the size of the causal horizon is $\ell_{\rm CMB} \sim 3\, t_{\rm CMB}$, because we are in the matter dominated epoch for which $\alpha = 2/3$. After the expansion of the universe, we observe this causal region at present time as a region of size:

$$\ell(t_0) \equiv \ell_{\rm CMB} \cdot \frac{a(t_0)}{a(t_{\rm CMB})} \sim 3\, t_{\rm CMB}^{1/3} t_0^{2/3}\,. \tag{1.2.2}$$

The angular region we observe in the sky now and that should have been causally connected at the time of the CMB has a size of $\theta \simeq \ell(t_0)/(3t_0) = (t_{\rm CMB}/t_0)^{1/3} = 2^\circ$, since $t_{\rm CMB} \sim 5 \cdot 10^5$ years and $t_0 \sim 15 \cdot 10^9$ years. Following this argument, we should not expect correlations in the CMB between regions separated by more than 2 degrees. Nevertheless, we observe that the temperature of the universe at the time of the CMB is the same with fluctuations of the order $\delta T/T \sim 10^{-4}$ in the whole sky. This absurd over-homogeneity of the CMB compared to expectations from the hot big bang evolution is the horizon problem, and would require that the setting of the initial conditions violates causality.

1.2.2 The flatness problem

The flatness problem follows from the very small spatial curvature that is measured today. The Friedmann equation (1.1.14) provides a measuring tool of the spatial curvature of the universe:

$$\frac{k}{a^2 H^2} = \Omega - 1\,, \text{ where } \Omega \equiv 8\pi G\, \frac{\rho_\gamma + \rho_{\rm M} + \rho_\Lambda}{3H^2}\,. \tag{1.2.3}$$

For the spatially flat case $k = 0$, we find that the quantity $\Omega = 1$ is time-independent. Otherwise, Ω is time dependent and in particular, for a scale factor $a \sim t^\alpha$ with $\alpha < 1$, we find that $H \sim 1/t$, so that $\Omega - 1 \sim k \cdot t^{2-2\alpha}$. At present time we measure $\Omega - 1 \sim 10^{-2}$, so evolving this quantity backward in time until for example the big bang nucleosynthesis time where $T \simeq 1\,\text{MeV}$, we find that the spatial curvature was $\Omega - 1 \sim 10^{-15}$. The other way around, it looks as if the initial value for the Hubble rate had been hugely fine-tuned so that the present universe was nearly spatially flat[6].

1.2.3 The inflationary mechanism

We have identified the two above puzzles by assuming that the hot big bang evolution was valid down to $t = 0$ with $a \sim t^\alpha$ and $\alpha < 1$. However, we have seen that we do not have experimental evidence for the hot big bang model before $t \sim 1\,\text{s}$. We could thus assume that there was a period of time, starting after the initial singularity ($t_i > 0$) and

[6]The flatness problem can also been seen without using any particular solution by simply considering the Friedmann equation (1.1.16). When the scale factor grows, the curvature term should naturally dominate at some point, but instead we observe it to be very small at present, meaning it must have started from an unnaturally small value in the past.

ending before this experimentally reachable time ($t_{\text{critical}} < t_{\text{exp}}$), during which the scale factor followed a different evolution.

What kind of evolution would enable to solve the horizon and flatness puzzles? In both cases, the problem boils down to the fact that for radiation and matter dominated phases, the quantity $1/(aH) \sim \dot{a}^{-1}$ (which is called the comoving Hubble radius) is growing monotonically and in a very large manner on the time period we are considering. Indeed for the flatness problem, the puzzle comes from the excessive growth of $\Omega - 1 \propto 1/(aH)^2$, and for the horizon problem, the puzzle ensues from the divergence of the horizon size: $\ell(t) = c\,a(t) \int \frac{\mathrm{d}t'}{a(t')} = c\,a(t) \int_{a_{\text{ini}}}^{a_{\max}} \frac{\mathrm{d}a}{a\dot{a}}$ diverges when we integrate on $a_{\max} \to \infty$ because $\dot{a}^{-1}$ grows largely with a. The divergence of the horizon size implies that we see regions in the CMB which should be causally disconnected, and despite this they all look extremely similar to one another.

Therefore, if instead the comoving Hubble radius $\dot{a}^{-1}$ was shrinking during a sufficiently long period before the start of the hot big bang evolution, we could solve these two problems simultaneously: the horizon size would converge and restrict to one causally connected region, while the $\Omega - 1$ quantity could start from a large value (say $\Omega - 1 \sim 1$) and shrink very much in order to reach a very small value at the beginning of the hot big bang evolution, which would be consistent with present observations despite its subsequent large growth.

In terms of equations, if the comoving Hubble radius has to shrink, then it means:

$$\frac{\mathrm{d}}{\mathrm{d}t}\left(\frac{1}{\dot{a}}\right) < 0 \;\Leftrightarrow\; \frac{\ddot{a}}{\dot{a}^2} > 0\,. \tag{1.2.4}$$

Therefore, we need a phase of accelerated expansion. This is the phase usual referred to as **the inflationary phase**. By combining the acceleration equation and the Friedmann equation (1.1.13) we get that for a perfect fluid $p = w\rho$,

$$\frac{2\ddot{a}}{a} = -8\pi G\,\rho\left(w + \frac{1}{3}\right)\,. \tag{1.2.5}$$

This means that we will have an inflationary phase only for $w < -1/3$. Note that, for a perfect fluid, the equations (1.1.13) yield the approximate scaling solution: $a \sim t^{2/(3+3w)}$, which is expanding ($H > 0$) only if $w > -1$. Therefore, the inflationary phase can be generated by a perfect fluid whose equation of state has $-1 < w < -1/3$. We can estimate the time period necessary for inflation to solve the problems. In practice, it turns out that the period of time needed to solve the puzzles is very short, in simple inflation models it would last only $10^{-36} - 10^{-34}\,\text{s}$ [18], so we see that this inflationary period can easily take place even before the electroweak time ($t_{\text{EW}} \sim 10^{-12}\,\text{s}$) and stay consistent with the hot big bang evolution.

We now turn to a practical implementation of this scenario based on quantum field theory on curved backgrounds, whose simplest instance is the **scalar field inflation** (see

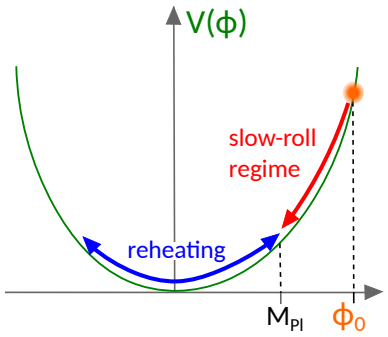

Figure 1.3: Sketch of the inflationary slow-roll mechanism. The inflaton field (in orange) starts from a value $\phi_0 > M_{\rm Pl}$ and rolls down the potential in the slow-roll regime, producing an accelerated expansion. When it exits this regime, it reaches an oscillatory phase, where reheating [19] takes place, leading to the creation of the standard model's particles and the advent of a thermodynamical state from which the hot big bang evolution follows.

for example [18]). We consider a theory of gravity minimally coupled to a scalar field (generically called the inflaton) with scalar potential $V(\phi)$, whose action reads:

$$S = \int \mathrm{d}^4x\sqrt{-g}\left(\frac{R}{16\pi G} - \frac{1}{2}g^{\mu\nu}\partial_\mu\phi\partial_\nu\phi - V(\phi)\right). \tag{1.2.6}$$

We consider an homogeneous scalar field, $\phi(t)$, and discuss this assumption later. We also choose a simple massive term for the potential[7]: $V(\phi) = m_\phi^2\phi^2/2$. The equations of motion associated with this action, again for an FLRW metric (1.1.11), are:

$$\begin{cases} H^2 + \dfrac{k}{a^2} = \dfrac{8\pi G}{3}\left(\dfrac{\dot\phi^2}{2} + \dfrac{m_\phi^2\phi^2}{2}\right); \\ \ddot\phi + 3H\dot\phi + m_\phi^2\phi = 0\,. \end{cases} \tag{1.2.7}$$

The "$3H\dot\phi$" in the scalar field equation is a friction term due to the expansion of the universe. If $H = 0$, the scalar field oscillates indefinitely in the potential, but when H becomes larger and larger, this oscillation gets more and more damped. We focus on a specific regime for which the oscillations are overdamped, characterized by: $\ddot\phi \ll 3H\dot\phi$ and $\dot\phi^2 \ll m_\phi^2\phi^2$. This is called the **slow-roll regime**, and in this regime the equations (1.2.7) become:

$$3H\dot\phi + m_\phi^2\phi \simeq 0\,, \quad H^2 \simeq \frac{8\pi G}{3}\frac{m_\phi^2\phi^2}{2}\,, \tag{1.2.8}$$

and their solution reads:

$$\phi(t) \simeq \phi_i - \frac{m_\phi}{\sqrt{12\pi G}}(t - t_i)\,. \tag{1.2.9}$$

From the slow-roll condition $\left|\dot\phi\right| \ll |m_\phi\phi|$, we deduce that this solution is valid only for $\phi(t) \gg \frac{1}{\sqrt{12\pi G}} \equiv \sqrt{\frac{2}{3}}M_{\rm Pl}$. Assuming that the initial scalar field value ϕ_i satisfies this

[7]This model for inflation has been ruled out by observations, but is one of the simplest model to present and understand the key features of the inflationary solution. Models that are more favored by current observations include for example the Higgs inflation [20] or the Starobinsky R^2 inflation [21].

condition, we find the solution for the scale factor as:

$$a(t) \simeq a_i \exp\left(\frac{m_\phi}{\sqrt{6}\, M_{\rm Pl}}\left(\phi_i(t-t_i) - \frac{M_{\rm Pl} m_\phi (t-t_i)^2}{\sqrt{6}}\right)\right). \tag{1.2.10}$$

We obtain the sought-after accelerated expansion, valid as long as $t - t_i \lesssim \sqrt{\frac{3}{2}}\,\phi_i/(M_{\rm Pl}\, m_\phi)$. When we reach $\phi_{\rm critical} = \sqrt{\frac{2}{3}} M_{\rm Pl}$, i.e., at $t_{\rm critical} - t_i = \sqrt{\frac{3}{2}}\,\phi_i/(M_{\rm Pl}\, m_\phi)$, the slow roll approximation breaks down and the accelerated expansion stops. The $\ddot{\phi}$ term in (1.2.7) cannot be neglected anymore, and we obtain an oscillatory behavior for the scalar field where reheating [19] takes place, giving rise in principle to all the standard model elementary particles. From then on the universe start following the hot big bang evolution described in the previous section (see figure 1.3 for an illustration). The total amount of expansion produced by the inflationary phase is of about $a_{\rm critical}/a_i \simeq \exp\left(\frac{\phi_i^2}{4M_{\rm Pl}^2}\right)$: the exponent $\phi_i^2/(4M_{\rm Pl}^2)$ is called the e-fold number and must be of order 60 for the flatness and horizon problem to be solved [16]. This means that for this model of inflation, we find that inflation must last for a period of time $\Delta t \equiv t_{\rm critical} - t_i = \sqrt{\frac{3}{2}}\frac{\phi_i}{M_{\rm Pl}\, m_\phi} \simeq 10^{-12}\,{\rm GeV}^{-1} \simeq 10^{-36}\,{\rm s}$ for $m_\phi \simeq 10^{13}\,{\rm GeV}$, which is the typical mass of the inflaton needed to explain density fluctuations in the CMB [18].

We now reflect on the assumptions entering this scenario. In addition to the assumption of spatial homogeneity and isotropy (FLRW metric), we have assumed that the scalar field was initially homogeneous and that it was varying slowly ($\dot{\phi}^2 \ll m_\phi^2 \phi^2$) implying an initial value $\phi_i \gg M_{\rm Pl}$. Inflation renders the setting of the initial conditions consistent with causality, but it still requires the initial state to be an homogeneous and isotropic space, and adds an homogeneous scalar field. The scalar potential must also comply with specific requirements for obtaining the slow roll regime. These assumptions are not explained by inflation. Besides our focus on the no-boundary proposal as a theory of initial conditions, in this thesis we will also show that some higher-order theories of gravity, such as quadratic gravity, may force (through the semi-classical criteria we develop) the universe to indeed start from such a very specific initial state. Inflation does not explain why the initial conditions for our universe have to be those specific ones, but it shows that at least these conditions are consistent and reasonable[8].

Another largely praised benefit of the inflationary scenario is that it can explain why on small scales, our present universe is so clumped, by taking into consideration quantum fluctuations of the scalar field. When distances inflate, these quantum perturbations get amplified and become classical, yielding a spectrum of density perturbations visible in the CMB. These small density perturbations then later lead to the formation of large structures such as galaxies, by the collapse of matter overdensities. However, this does

[8]The further assumption on the scalar field, $\phi_i \gg M_{\rm Pl}$, is also reasonable: the scalar field value is not an observable, but we can measure its energy density, $\dot{\phi}^2 + m_\phi^2 \phi^2$. In the classical regime, and as explained earlier, this energy density must be much smaller than the Planck density energy $\rho \sim M_{\rm Pl}^4$, while the mass of the scalar field must be much smaller than the Planck mass: $m_\phi^2 \cdot \phi^2 \ll M_{\rm Pl}^4$ and $m_\phi \ll M_{\rm Pl}$. Given the huge ratio between the Planck mass and the mass of standard particles, it is thus completely reasonable to assume that $\phi_i \gg M_{\rm Pl}$.

not represent a prediction, because different inflationary models, using different inflaton fields for instance (Higgs inflation [20], R^2 inflation [21], etc.) can lead to different values for the tensor-to-scalar ratio r of perturbations in the CMB (i.e., the ratio between the amplitudes of gravitational waves perturbations and of scalar temperature fluctuations).

Finally, we should mention that alternatives theories to inflation have been developed, in particular in the perspective of solving the Trans-Planckian problem of fluctuations [22], such as bouncing models and genesis scenarios, which can also solve the initial condition puzzles and provide the correct spectrum of scalar fluctuations observed in the CMB. They also generically lead to very different values for the tensor-to-scalar ratio r. We will come back to these alternatives in more detail in the fifth chapter of this thesis (see in particular section 5.3 for bounces and section 5.6 for genesis scenarios).

Chapter 2

Path integral and quantum cosmology

2.1 Why quantum cosmology?

In the previous chapter, we have reviewed the standard take on the early universe evolution, largely derived from applying general relativity to the whole, spatially homogeneous and isotropic universe. We have glanced at its many predictions and evidences, and introduced the mechanism of inflation for solving the initial condition's puzzles we encountered. However, we have already pointed out that this evolution breaks down when we reach the Planck scale, because there quantum effects cannot be ignored.

Since this evolution is based on GR, the straightforward method to describe the pre-Planck scale epoch would be to quantize gravity by quantizing GR, in a similar fashion to the quantization of electromagnetism in quantum electrodynamic, and to that of the weak and strong nuclear interactions in the Glashow-Weinberg-Salam theory and in quantum chromodynamic respectively. It is nonetheless now well known that GR is a non-renormalizable theory [23, 24, 25], i.e., it cannot be quantized by using the ordinary perturbative approach. Instead, other quantization approaches have been attempted. We will review some of them here below, though up to now, none of them proposed a completely satisfactory answer.

As the early universe cosmology can be very well approximated by the FLRW metric, the study of quantum cosmology presents a considerable advantage in that it requires drastically less degrees of freedom compared to the full quantum gravity theory. In practice, we say that we restrict to **minisuperspace**: instead of quantizing ten fields depending each on space and time coordinates, we restrict to only the scale factor and the lapse function, and most importantly they only depend on time. The number of degrees of freedom narrows down from an infinite number of evolution functions (several for each space coordinate) to only a few global functions. This implies a strict symmetry reduction whose validity must be checked a posteriori. In particular, we will encounter cases in this thesis where this symmetry reduction is too strong and removes some key elements of the

solutions. Nevertheless, the minisuperspace ansatz is generally very powerful, because it renders many otherwise too intricate calculations feasible, and thus represents a first step in our understanding of quantum gravity.

A first approach which appears very well suited to the study of the early universe, is the canonical quantization of gravity [26]. It relies on the Hamiltonian formulation of gravity, and on the Arnowitt-Deser-Misner (ADM) [27] foliation of spacetime in equal time hypersurfaces:

$$\mathrm{d}s^2 = -N^2(\mathrm{d}x^0)^2 + \gamma_{ij}(\mathrm{d}x^i + N^i\mathrm{d}x^0)(\mathrm{d}x^j + N^j\mathrm{d}x^0)\,, \tag{2.1.1}$$

where N is the lapse and N_i the shift vector, and they parametrize the evolution from one hypersurface to the next, while the 3-metric γ_{ij} describes the geometry on the hypersurfaces. This formulation is completely general and preserves the 10 degrees of freedom of GR (1 for the lapse, 3 for the shift vector and 9 for the three-dimensional metric). The FLRW metric (1.1.11) corresponds to the specific case where the shift vector is null and the lapse and three-dimensional metric are spatially homogeneous and isotropic. Using the ADM metric (2.1.1), it is easier to perform the appropriate Legendre transformation from the Lagrangian to the Hamiltonian action formulation (see e.g., [28, 29])

$$S = \int \mathrm{d}t\mathcal{L} = \int \mathrm{d}t\,\mathrm{d}^3x \left[\Pi^{ij}\gamma_{ij,t} - N\mathcal{H} - N^i\mathcal{H}_i\right], \tag{2.1.2}$$

where Π^{ij} is the conjugate momentum of the spatial metric γ_{ij}, ${}^{(3)}R$ is the intrinsic three-dimensional Ricci scalar based on that metric, and $\mathcal{H}$, $\mathcal{H}_i$ are the Hamiltonian and diffeomorphism constraints, that appear in the action with their associated Lagrange multipliers N and N^i. Those constraints explicitly read (γ is the determinant of the spatial metric and D_i is the covariant derivative based on it):

$$\begin{cases} \mathcal{H} = \dfrac{16\pi G}{\sqrt{\gamma}}\left(\Pi^{ij}\Pi_{ij} - \dfrac{(\Pi_l{}^l)^2}{2}\right) - \dfrac{\sqrt{\gamma}}{16\pi G}\,{}^{(3)}R\,; \\ \mathcal{H}_i = -16\pi G\, D_j\Pi_i{}^j\,; \end{cases} \tag{2.1.3}$$

and they give rise to the general constraint equations of canonical quantum gravity: $\mathcal{H} = 0$ and $\mathcal{H}_i = 0$. The three latter generate coordinate transformations in three-dimensional spacetime, similarly to the Gauß law in electrodynamic, while the first actually generates the dynamic of the system. By quantizing this theory (i.e., by transforming Poisson brackets into commutators), these constraints transform into conditions on the quantum state Ψ, representing the state of the whole universe, $\mathcal{H}\Psi = 0$ and $\mathcal{H}_i\Psi = 0$. The dynamical equation following from the first condition is called the Wheeler-de Witt equation. For instance in the case of an FLRW metric with a minimally coupled scalar field such as in

(1.2.6), the Wheeler-de Witt equation reads [29]:

$$\left[\frac{2\pi G}{3a}\frac{\partial}{\partial a}\left(a\frac{\partial}{\partial a}\right) - \frac{1}{2a^2}\frac{\partial^2}{\partial\phi^2} + a^4 V(\phi)\right]\Psi(a,\phi) = 0\,. \tag{2.1.4}$$

We make two remarks about this equation:

1. to obtain the expression (2.1.4), it is necessary to choose a certain factor ordering when transforming the momenta in functional differential operators, $\Pi^{ij} \to \frac{1}{i}\frac{\partial}{\partial\gamma_{ij}}$. It is common to choose the Laplace-Beltrami factor ordering as we did in (2.1.4) because it ensures the invariance of the kinetic term under configuration space's transformations [28]. This is however merely an arbitrary choice.

2. this dynamical equation contains second order derivatives, and therefore if we want to interpret it as an evolution equation similarly to the Schrödinger equations of quantum mechanics, we obtain negative probabilities: this theory doesn't respect unitarity[1].

The lack of unitarity causes a big hurdle in interpreting the Wheeler-de Witt equation and prevents the canonical quantization from generating a complete quantum cosmology theory. We thus move on to other quantization methods of gravity. In any case, the idea of a wavefunction of the universe obeying the Wheeler-de Witt equation is central to quantum cosmology and we will refer to it throughout this thesis.

Another approach to the quantization of gravity starts from string theory, which is a candidate for a full quantum gravity theory. In the chapters 3 and 5 of this thesis, we will review some aspects of string theory applied to the early universe cosmology.

We finally turn to the quantization procedure which we will mostly adopt in this work, the **path integral quantization**. It was originally proposed by Feynman as an alternative formulation of non-relativistic quantum theory [31], which constructs the wavefunction describing a quantum state as an integral summing over all the possible paths in configuration space linking an initial to a final coordinates position, and weighted by an exponential of the classical action multiplied by a factor i and divided by $\hbar$:

$$\Psi(x_i,t_i;x_f,t_f) = \int_{\{x_i,t_i\}}^{\{x_f,t_f\}} \mathcal{D}x\, e^{iS[x]/\hbar}\,, \tag{2.1.5}$$

where $\mathcal{D}x$ is a measure on the configuration space, while $S[x]$ is the action evaluated on the coordinates position x. This wavefunction was shown to satisfy the Schrödinger equation, proving the equivalence of this formulation with the more familiar Schrödinger's and Heisenberg's pictures of quantum mechanics. The path integral picture also allows for a straightforward semi-classical limit when $\hbar \to 0$: using the WKB approximation[2],

[1] It was recently shown in [30] that, for minisuperspace, unitarity can be recovered at the next-to-leading order in a Born-Oppenheimer approximation which makes a semi-classical time emerge.

[2] Developed in 1926 by Wentzel, Kramer and Brillouin, the WKB approximation is a method for approximating solutions to linear differential equations such as the Schrödinger's equation, valid when the amplitude of the wavefunction varies slowly compared to its phase.

the wavefunction (2.1.5) reduces to a sum over the classical, saddle point solutions:

$$\Psi(x_i, t_i; x_f, t_f) \simeq \mathcal{N} \sum_{\substack{\text{saddle} \\ \text{points}}} e^{iS_{\text{on-shell}}[\text{S.P.}]/\hbar} \,. \tag{2.1.6}$$

This formulation has been successfully adapted to field theory, where it provided one of the most efficient way of quantizing fields such as Yang-Mills. In this case we write the generating functional of Green's function as the path integral:

$$\mathcal{Z}[J] = \int \mathcal{D}\Phi \, e^{i(S[\Phi] + J_A \Phi^A)/\hbar} \,, \tag{2.1.7}$$

with $\mathcal{D}\Phi$ the measure on the fields Φ, and $S[\Phi]$ the action on those fields. $\mathcal{Z}[J]$ thus provides correlation functions and propagators for the field theory in the presence of the source J.

The path integral idea was first generalized to include gravity by Hawking in [32]. The amplitude of probability to go from a state with metric g_1 and matter field ϕ_1 at time t_1, to a second state with metric g_2 and matter fields ϕ_2 at time t_2 is then given by:

$$\langle g_1, \phi_1, t_1 | g_2, \phi_2, t_2 \rangle = \int \mathcal{D}g \, \mathcal{D}\phi \, e^{iS[g,\phi]/\hbar} \,, \tag{2.1.8}$$

where the path integral sums over all field configurations, including the metric, with the appropriate initial and final values.

This provides another way to construct the wavefunction of the universe which must be a solution to the Wheeler-de Witt equation above (2.1.4), and sets the context for the construction of the no-boundary proposal we now turn to.

2.2 The no-boundary proposal

In the first chapter, we have reviewed the initial condition's puzzles of the hot big bang evolution, and showed how inflation could relieve these tensions. However, the inflationary phase still requires some initial conditions. A possible way out of this never-ending search for initial conditions, is to postulate that the universe originally started in a compact and regular geometry, so no initial condition would have to be initially imposed [33]. Such a **no-boundary geometry** replaces the big bang singularity, and provides a definite prescription for the initial condition of the universe. In this sense, it gives a theory of initial conditions, which also yields different amplitudes for different final boundary conditions, given a certain model of the early universe[3].

In practice, the no-boundary proposal builds on the path integral approach for the quantization of gravity. It was formulated by Hartle and Hawking [33, 38] as an attempt

[3]Examples of early universe dynamical models which have been studied in this context are the slow-roll inflation and the ekpyrotic bouncing model. For both, no-boundary solutions were found as well as the emergence of late-time classicality, see [34, 35, 36, 37].

to define a **quantum theory of initial conditions** for the universe. The original proposal goes as follow: the quantum state of a spatially closed universe ($k = 1$) can be described by a wavefunction calculated using the Euclidean path integral of the Einstein-Hilbert action (1.1.8). The use of the Euclidean path integral, instead of the Lorentzian one as in the original Feynman's path integral [31], intends to make the oscillatory integral better defined and is equivalent to the latter by a Wick rotation to imaginary time. This path integral sums over all compact and regular four-geometries whose only boundary is a final three-geometry. The wavefunction is proven to be a solution of the Wheeler-de Witt equation [26]:

$$\Psi[h_{ij}] = \int_{\mathcal{M}} \mathcal{D}g\, e^{-\mathcal{I}_{\mathrm{E}}[g]}\,, \tag{2.2.1}$$

where the manifold $\mathcal{M}$, on which the path integral is summing, contains all compact and regular four-geometries having the Riemannian three-geometry h_{ij} as only boundary. This definition of the wavefunction can then be completed by including matter fields, in particular scalar fields, which can then lead to an inflationary phase [39, 40].

It is obvious that such compact and regular four-geometries cannot be Lorentzian, as it would otherwise contradict Penrose's singularity theorem [41], which states that Lorentzian manifolds generically possess an initial singularity in their past. The manifold $\mathcal{M}$ therefore consists of complex geometries. In particular, we expect these complex geometries to start in the Euclidean direction.

Having constructed a formal definition of the no-boundary wavefunction (2.2.1), the question is now whether we can actually use it to calculate anything. As already emphasized, the interest of quantum cosmology is that we can restrict to minisuperspace, and retain only one or two degrees of freedom for the gravitational sector such as the scale factor $a(t)$ and the lapse function $N(t)$. The practical implementation of the original no-boundary proposal hence restricts geometries to an FLRW type of metrics, in spatially closed space $k = 1$:

$$\mathrm{d}s^2 = N^2\mathrm{d}\tau^2 + a(\tau)^2\mathrm{d}\Omega_3^2\,, \tag{2.2.2}$$

where τ is the Euclidean time running from 0 to 1 by convention. The Euclidean action for gravity with a cosmological constant is given by

$$\mathcal{I}_{\mathrm{E}}[g_{\mu\nu}] = -\frac{1}{2}\int \mathrm{d}^4x\sqrt{g}\,(R - 2\Lambda) \propto \int_0^1 \mathrm{d}\tau\, aN\left[-\frac{a'^2}{N^2} + \frac{a^2\Lambda}{3} - 1\right], \tag{2.2.3}$$

where the prime denotes a derivative with respect to the Euclidean time τ. The equations of motion then read:

$$\begin{cases} -a'^2 + N^2 = \dfrac{\Lambda}{3}a^2N^2\,, \\ 2aa'' + a'^2 + N^2(a^2\Lambda - 1) = 0\,. \end{cases} \tag{2.2.4}$$

The solutions to these classical equations of motion are the **saddle point solutions** of the Euclidean path integral, that are also sometimes called *instantons*. One typical instance of such an instanton is depicted in figure 2.1. It consists of a four-dimensional

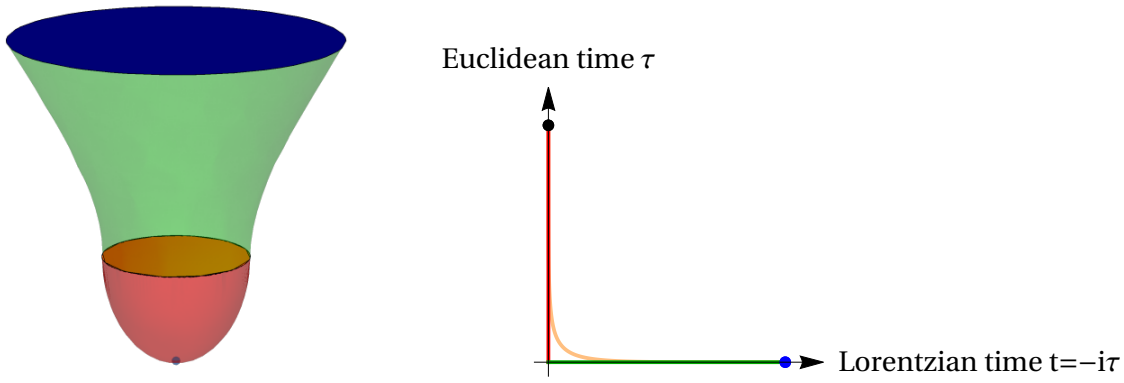

Figure 2.1: *Left:* Pictorial representation of an instanton: no-boundary geometry consisting in the gluing of a lower-half four-sphere (Euclidean solution, in red (2.2.5a)) onto the waist of the hyperboloid of a four-dimensional de Sitter (dS) space (Lorentzian solution, in green (2.2.5b)). This does not represent an evolution in time but instead one instanton geometry. Only the final upper hypersurface (in blue) is classical and has real field values. The real time evolution is given by a succession of such geometries, with larger and larger final hypersurfaces. *Right:* Contour in the complex time plane associated with the instanton geometry depicted to the left. We start from a purely Euclidean space at the South Pole of the instanton, and end in the purely Lorentzian direction on the final real hypersurface. Fuzzy instantons corresponding to more realistic geometries avoid the origin of the plot and describe a fully complex geometry as the light orange line suggests.

de Sitter hyperboloid (dS_4) glued at its waist onto the equator of a lower-half four-sphere (S^4). The metrics are given by the line elements

$$\mathrm{d}s^2_{S^4} = \mathrm{d}\tau^2 + \frac{\sin^2(H\tau)}{H^2}\mathrm{d}\Omega^2_{(3)}\,, \tag{2.2.5a}$$

$$\mathrm{d}s^2_{\mathrm{dS}_4} = -\mathrm{d}t^2 + \frac{\cosh^2(Ht)}{H^2}\mathrm{d}\Omega^2_{(3)}\,, \tag{2.2.5b}$$

where $\mathrm{d}\Omega^2_{(3)}$ is the metric on a three-sphere of constant radius $1/H$, and the two metrics are related to each other through the following Wick rotation:

$$t = -i\left(\tau - \frac{\pi}{2H}\right)\,. \tag{2.2.6}$$

Of course, realistic instantons have a completely regular geometry and do not present such a sharp change of signature from Euclidean to Lorentzian, which would otherwise induce a discontinuity. These are then fully complex and sometimes called *fuzzy instantons* [35], as shown by the light orange line on the right of figure 2.1.

In the semi-classical limit, the path integral is evaluated by summing over all saddle point solutions, leading to a definite expression for the wavefunction of a closed universe at the semi-classical level:

$$\Psi[a_\mathrm{f}, \tau_\mathrm{f}] \sim \mathcal{N} \sum_{\substack{\text{relevant}\\ \text{saddle points}}} e^{-\mathcal{I}[\text{saddle point}]}. \tag{2.2.7}$$

From this wavefunction, one can then extract the probabilities of different histories for

the universe.

This first original implementation of the no-boundary proposal faced several issues. The first and most notorious is the **conformal mode problem**. It appears whenever one considers the Euclidean action for gravity (2.2.3), because it is not positive definite. By performing a conformal transformation $\tilde{g}_{\mu\nu} = \Omega^2(x) g_{\mu\nu}$, the Ricci scalar transforms as $\tilde{R} = \Omega^{-2} R - 6\Omega^{-3}\Box\Omega$ [42], so that the Euclidean action,

$$\mathcal{I}[\tilde{g}] = -\frac{1}{16\pi G}\int \mathrm{d}^4x \sqrt{\det g}\left(\Omega^2 R + 6\Omega_{,\mu}\Omega^{,\mu}\right), \tag{2.2.8}$$

can be rendered as negative as desired by choosing a rapidly varying conformal factor $\Omega(x)$. The Euclidean action is then unbounded by below, and this means that the Euclidean path integral is not uniquely defined by the boundary conditions [42]: we need a precise prescription on how to integrate on Euclidean metrics.

The second obstacle encountered by the original implementation of the no-boundary proposal, is that requiring the quantum state to be defined by the sum over **compact** geometries (i.e., the scale factor is initially zero) that are also **regular** (i.e., the scale factor function and its derivatives must be continuous), appears to be in contradiction with the Heisenberg uncertainty principle of quantum mechanics. Indeed if one assumes that the geometries must have $a(\tau \to 0) = 0$ and must also satisfy the constraint equation (2.2.4), then we see that this implies $a'^2(\tau \to 0) = -N^2$. Therefore the quantum state is defined by a sum over geometries which have both their position and momentum fixed in $\tau \to 0$, challenging the uncertainty principle. The way out of this issue, is to instead sum only on geometries that are either compact, or regular initially. Of course the saddle point solutions, which are classical solutions to the equations of motion, will always be both compact and regular. But this will not be the case for other off-shell geometries over which the path integral is summing. In practice, we end up with two different choices[4] on how to define the no-boundary wavefunction:

- by **summing over compact geometries**, in the spirit of the original no-boundary proposal, this is the field space definition; or
- by **summing over regular geometries**, as in a more recent formulation we will describe later in this section, this is the momentum space definition.

Finally, the last difficulty with the original implementation of the no-boundary proposal, is that there is no prescription on how the sum over saddle points must be taken. By considering tensor perturbations on top of the background, the no-boundary wavefunction with final scale factor a_f and tensor perturbations amplitude φ in the pure gravity case with cosmological constant $\Lambda \equiv 3H^2$, is given in term of a sum over saddle points by

[4] Actually, in-between choices are also possible, such as Robin boundary conditions, see [43].

[44, 45]:

$$\Psi[a_{\rm f},\varphi] \approx \sum_{\substack{\text{relevant}\\ \text{saddle}\\ \text{points}}} \exp\left[\frac{i}{\hbar}S[N_\sigma(a_{\rm f},\varphi)]\right] = \sum_{\text{S.P.}} \exp\left[\pm\left(\frac{4\pi^2}{\hbar H^2} - \frac{\ell(\ell+1)(\ell+2)}{6\hbar H^2}\varphi^2\right)\right. \tag{2.2.9}$$
$$\left. \pm i\left(\frac{4\pi^2 H}{\hbar}\sqrt{a_{\rm f}^2 - H^{-2}}^3 + \frac{\sqrt{3}\ell(\ell+2)\bar{a}}{2\hbar H}\varphi^2\right)\right].$$

ℓ is the principal quantum number on the 3-sphere, and for tensor perturbations it must be larger than 2. There are four different saddle points N_σ, related by time reversal and complex conjugation. Saddle point values of the lapse are found as the solutions to the equation $\partial S_{\text{on-shell}}/\partial N = 0$, where $S_{\text{on-shell}}$ is the Einstein-Hilbert action evaluated on the classical solutions to the equations of motion. At background level for the pure gravity case, they read:

$$N_\sigma = \mp H^{-2}\left(i \pm \sqrt{H^2 a_{\rm f}^2 - 1}\right). \tag{2.2.10}$$

Neglecting the perturbations φ, the wavefunction (2.2.9) is weighted by $\exp[\pm 4\pi^2/(\hbar H^2)]$. If we had also included a scalar field, then we would get the replacement $H^2 = \Lambda/3 \to V(\phi_{\rm f})/3$: we get different weightings depending on the final scalar field value, $\phi_{\rm f}$. We also find that the phase grows with $a_{\rm f}^3$ for large values of the final scale factor ($a_{\rm f} \gg H^{-1}$): this means that this wavefunction predicts the emergence of a classical spacetime. Considering the perturbations, we find that they reproduce the expected Bunch-Davies vacuum [46] (quantum state which possess no quanta in the asymptotic past on a de Sitter background), only with the "+" sign in front of the amplitude part in (2.2.9). This "+" sign corresponds to the so-called Hartle-Hawking saddle points, which have a negative imaginary part ("-" sign in front in (2.2.10)), and so the tensor perturbations around these saddle points follow a Gaußian distribution: those saddle point geometries are stable. On the contrary, the Vilenkin saddle points [47], with a positive imaginary part of the lapse, have an inverse Gaußian distribution for their perturbations: the perturbations around the Vilenkin saddle points blow up, these are unstable geometries. From this calculation, it appears that in order to construct a stable wavefunction, the relevant saddle points on which we must sum are the Hartle-Hawking saddle points. This formed the basis of the Hartle-Hawking proposal constructed from the Euclidean Path Integral (2.2.1). But as we have seen above, this formulation carries along the problem of the conformal mode problem.

To evade the various limitations of the original no-boundary implementation, different approaches have been suggested in the last fifteen years. One [48] for instance uses **holography**, by constructing a dual formulation of the no-boundary dS wavefunction using the Euclidean anti-de Sitter/Conformal Field Theory (AdS/CFT) correspondence [49, 50]. AdS/CFT is a duality construction between a quantum gravity theory (e.g., string theories) defined on the bulk of an AdS spacetime and a quantum field theory

with conformal symmetry defined on the boundary of that spacetime. In this case one constructs an AdS geometric representation of the dS saddle points. The no-boundary amplitude is then computed from the partition function of the dual field theory, forming a dS/CFT correspondence.

Another approach [51], which we will rely upon in this work, suggests to consider rather the Lorentzian path integral formulation, and proposes a new tool to enable the evaluation of oscillating path integrals, namely the **Picard-Leschetz theory**. Working in the minisuperspace setting and rescaling the lapse function N conveniently, one can define a scale factor q whose kinetic term in the Einstein-Hilbert action is canonically normalized, such that the metric reads (for t the Lorentzian time):

$$\mathrm{d}s^2 = -\frac{N^2(t)}{q(t)}\mathrm{d}t^2 + q(t)\mathrm{d}\Omega_3^2\,. \tag{2.2.11}$$

In these new variables, the Einstein-Hilbert action (1.1.8) of a closed space ($k = 1$) and its equations of motion transform into:

$$S_{\text{E-H}} = 2\pi^2 \int_0^1 \mathrm{d}t \left[\frac{-3\dot{q}^2}{4N} + N(3 - \Lambda q)\right] \quad \Rightarrow \quad \begin{cases} \ddot{q} = \dfrac{2\Lambda}{3}N^2\,; \\ \dfrac{\dot{q}^2}{4N^2} + 1 = \dfrac{\Lambda}{3}q\,. \end{cases} \tag{2.2.12}$$

The classical solution with fixed Dirichlet boundary conditions in $t = 0$ and in $t = 1$ then reads:

$$\bar{q}(t) = \frac{\Lambda N^2}{3}t(t-1) + (q_1 - q_0)t + q_0\,. \tag{2.2.13}$$

Therefore, the full solution $q(t)$ is given by this classical solution $\bar{q}(t)$, plus some arbitrary fluctuation $\mathcal{Q}(t)$ satisfying the boundary conditions: $\mathcal{Q}(0) = \mathcal{Q}(1) = 0$ for the sum over compact metrics (Dirichlet-Dirichlet boundary conditions). This turns the path integral over the scale factor into a Gaußian integral that can be evaluated exactly:

$$\Psi[q_0, q_1] = \int_0^\infty \mathrm{d}N \exp\left[\frac{i}{\hbar}S_{\text{E-H}}[\bar{q}(t)]\right] \int_{\mathcal{Q}(0)=0}^{\mathcal{Q}(1)=1} \mathcal{D}\mathcal{Q} \exp\left[-\frac{2\pi^2 i}{\hbar}\int_0^1 \mathrm{d}t \frac{3\dot{\mathcal{Q}}^2}{4N}\right] \tag{2.2.14}$$

$$= \int_0^\infty \mathrm{d}N \sqrt{\frac{3\pi i}{2N\hbar}} \exp\left[\frac{i}{\hbar}S_{\text{E-H}}[\bar{q}(t)]\right]. \tag{2.2.15}$$

We are then left with a simple integral on the lapse N, a highly oscillating integral which does not converge when evaluated on the real axis. To evaluate it and give it meaning, we must deform the contour of integration into the complex plane. Using complex analysis, one can show that in the absence of singularities in the way, the contour of integration can be deformed, by following the steepest ascent path which intersect the original contour, into the steepest descent path, which interesect the steepest ascent path at the saddle point. The steepest ascent and descent paths are defined as the paths along which the amplitude of the integrand, $\exp(-\operatorname{Im}(S_{\text{E-H}}[\bar{q}(t)]))$ grows (respectively decreases) with the faster rate when starting from the saddle point. The integral is then

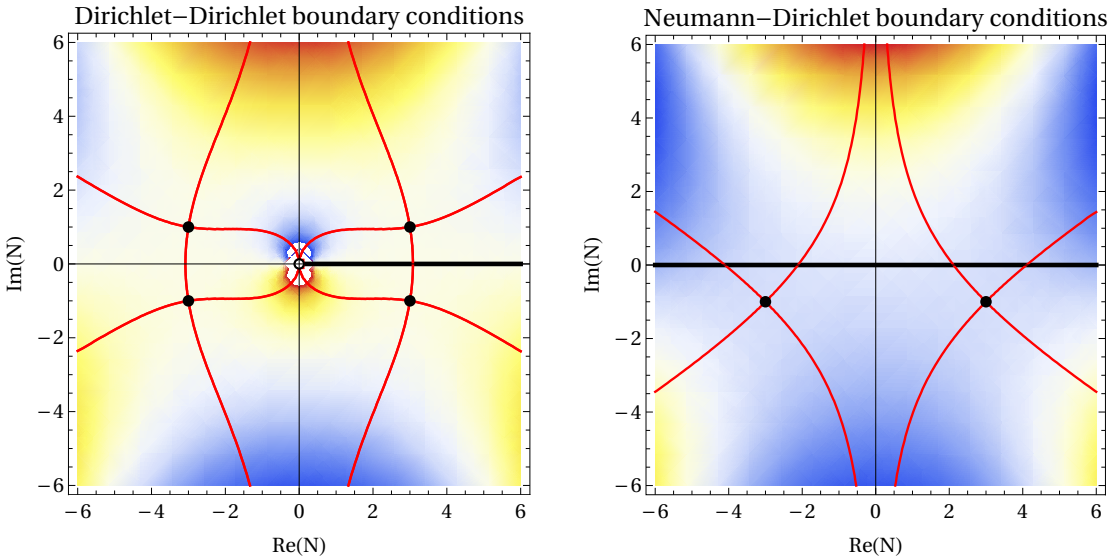

Figure 2.2: Regions of convergence/divergence of the path integral (the integrand tends to converge (diverge) the bluer (the redder)), steepest ascent and descent paths in red solid lines, and saddle points as black dots for the no-boundary solutions with Dirichlet boundary conditions (**sum over compact metrics**, with $q(0) = 0$ and $q(1) = 10H^{-2}$) on the left, and for Neumann boundary conditions (**sum over regular metrics**, with $q(1) = 10\,H^{-2}$) on the right. On the left, the real axis can be deformed following the steepest ascent into the steepest descent lines intersecting it at the saddle points in the upper half plane. These upper saddle points are unstable and correspond to the Vilenkin wavefunction. On the right, the sum over regular metrics automatically restricts to the stable lower saddle points that are then selected by the Picard-Lefschetz theory and yields to correct Hartle-Hawking result.

made convergent because by definition, the amplitude of the integrand rapidly goes to zero along the steepest descent path. A visual explanation is also provided in the caption of Figure 2.2. The result of this integral is given in the semi-classical approximation by the saddle point "selected" by this method. Applying this method, it was found in [51, 44] that the no-boundary proposal defined as a sum over compact geometries selects the Vilenkin, unstable saddle points (i.e., those on the upper half-plane on the left of figure 2.2). In fact, even by choosing a different initial contour of integrations, the unstable Vilenkin's saddle points are linked to the stable Hartle-Hawking ones through steepest descent contours, so that a contour of integration passing through the stable, lower-half plane saddle points will necessarily also sum over the unstable upper-half saddle points. This is the inconsistency of the no-boundary proposal defined as a over compact metrics. To remedy that, Ref. [52] suggested to sum rather on regular metrics, i.e., metrics starting with an initial zero momentum flow. This means that the boundary conditions are Neumann-Dirichlet boundary conditions: $\dot{q}(0) = 2Ni\,,\ q(1) = q_1\,,$ so the classical solution transforms into

$$\bar{q}_{\rm N}(t) = \frac{\Lambda N^2}{3}(t^2-1) + 2Ni(t-1) + q_1\,. \tag{2.2.16}$$

The scale factor integral over fluctuations also changes (see the Appendix of [53] for an

explicit calculation) and we find:

$$\Psi_{\rm N}[q_1] = \int_0^\infty {\rm d}N \exp\left[\frac{i}{\hbar} S_{\text{E-H}}[\bar{q}_{\rm N}(t)]\right] \int_{\dot{\mathcal{Q}}(0)=0}^{\mathcal{Q}(1)=0} \mathcal{D}\mathcal{Q} \exp\left[-\frac{2\pi^2 i}{\hbar}\int_0^1 {\rm d}t \frac{3\dot{\mathcal{Q}}^2}{4N}\right] \tag{2.2.17}$$

$$= \int_0^\infty {\rm d}N \sqrt{\frac{3\pi i}{\hbar}} \exp\left[\frac{i}{\hbar} S_{\text{E-H}}[\bar{q}_{\rm N}(t)]\right]. \tag{2.2.18}$$

With Neumann-Dirichlet boundary conditions, there are only two saddle points, which are the Hartle-Hawking saddle points (because we have already fixed the sign in the initial momentum, $\dot{q}(0) = +2Ni$). The Picard-Lefschetz theory applied in this case therefore automatically selects the stable saddle points (see right panel of figure 2.2), and we recover the Hartle-Hawking wavefunction, which at the background level gives $\Psi \sim e^{4\pi^2/(H^2\hbar)} \cdot \mathit{phase}$, and which with tensor perturbations φ and final scale factor $a_{\rm f}$ yields the wavefunction:

$$\Psi_{\rm N}(a_{\rm f}, \varphi) \approx \exp\left[\frac{4\pi^2}{\hbar H^2} - \frac{\ell(\ell+1)(\ell+2)}{6\hbar H^2}\varphi^2\right]$$
$$\times \left\{\exp\left[i\left(\frac{4\pi^2}{\hbar} H \sqrt{a_{\rm f}^2 - H^{-2}}^3 + \frac{\sqrt{3}\,\ell(\ell+2)\bar{a}}{2\hbar H}\,\varphi^2\right)\right] + \text{c.c.}\right\}. \tag{2.2.19}$$

This Picard-Lefschetz method was also applied for AdS black hole solutions, and it was found in [53] that Neumann initial boundary conditions are required to recover the thermodynamical results of black holes that can independently be calculated using the AdS/CFT correspondence.

This concludes our review of the state-of-the-art on the no-boundary proposal prior to this thesis. The next two chapters will present new results which develop further this set-up, and in particular the sum over regular metric formulation to which we include a scalar field minimally coupled to general relativity.

Part I

Progress in the no-boundary proposal

Chapter 3

Higher-order corrections to the no-boundary proposal

As emphasized in the introductory section on the no-boundary proposal, we consider the wavefunction of the universe defined as the Lorentzian path integral summing over all possible matter fields ϕ and geometries $g_{\mu\nu}$ with a specific initial condition, either a zero-size compact geometry, or a zero-momentum flow regular geometry. The wavefunction calculated on the final hypersurface h_{ij} with a final field content $\tilde{\phi}$ is therefore given by:

$$\Psi[h_{ij}, \tilde{\phi}] \equiv \int^{h_{ij}, \tilde{\phi}} \mathcal{D}\phi \, \mathcal{D}g_{\mu\nu} \, e^{\frac{i}{\hbar} S} \,, \tag{3.0.1}$$

where the action S is given by the usual Einstein-Hilbert action of general relativity, supplemented by a cosmological constant Λ and a Gibbons-Hawking-York (GHY) boundary term[1]:

$$S = \frac{1}{8\pi G} \int \mathrm{d}^4x \sqrt{-g} \left[\frac{R}{2} - \Lambda + \cdots \right] + \frac{1}{8\pi G} \int_{h_{ij}} \mathrm{d}^3y \sqrt{h} K \,. \tag{3.0.2}$$

The ellipsis stands for additional matter fields and higher-order corrections, stemming from UV-complete theories of gravity, such as string theories. The no-boundary proposal does not usually consider these corrections, and this is justified by the semi-classical treatment it is adopting.

The aim of this chapter is specifically to study the effect of these corrections on the existence of the no-boundary proposal. The fact that no-boundary solutions are robust to the addition of higher-order corrections is central in proving the validity of the no-boundary proposal as an early universe model. It implies that the no-boundary wavefunction, obtained in the semi-classical limit of gravity, will also hold for UV-complete theories of quantum gravity, without radical modifications.

The robustness of no-boundary solutions is actually highly non-trivial, because higher-

[1]The GHY boundary term must be added to the action in order to obtain a well-defined variational principle when we consider Dirichlet boundary conditions on a certain hypersurface [54, 55]. See chapter 5 of this thesis, equation (5.1.9) for a detailed definition.

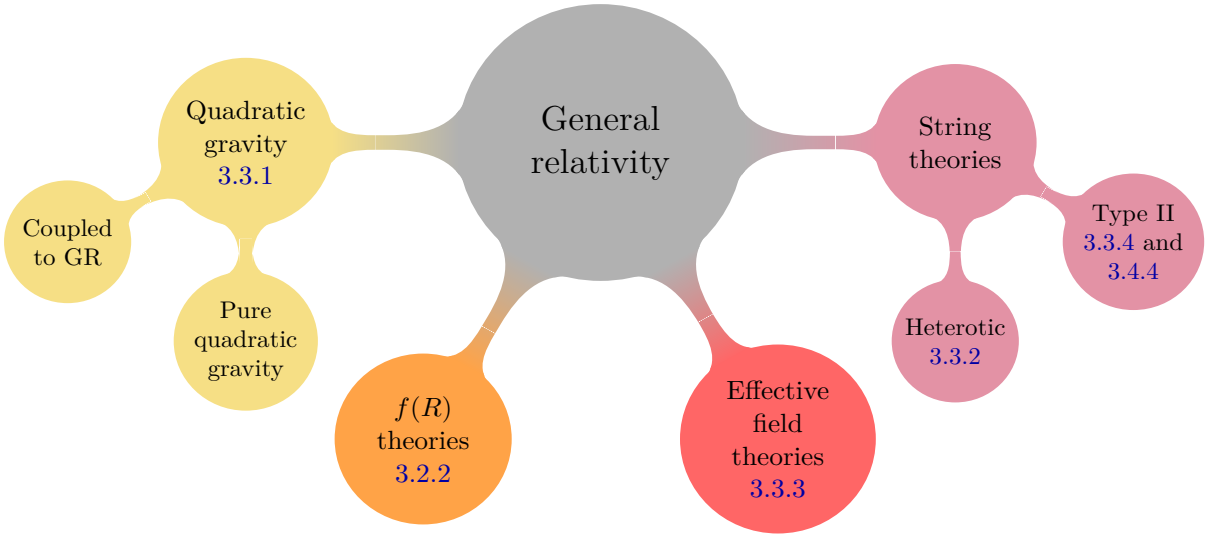

Figure 3.1: Theories containing higher-order corrections studied in this chapter.

order corrections typically consists of higher power of the Riemann tensor or even covariant derivatives thereof [2]. In a universe with scale factor $a(t)$, the Riemann tensor contains terms of the form:

$$\text{Riemann tensor} \sim \frac{1}{a^2}, \frac{\dot{a}^2}{a^2}, \frac{\ddot{a}}{a}. \tag{3.0.3}$$

Therefore, it is not guaranteed that regular solutions will continue to exist when $a \to 0$ in the presence of higher-order corrections. In this chapter we will show that thanks to the specific symmetry of the FLRW geometry, it is nevertheless the case. A regular no-boundary solution, modified by the higher-order corrections, continues to exist for a large class of higher-order theories, including all the known corrections stemming from string theory.

The plan of this chapter is as follow: in section 3.1 we set up the framework that will enable us to study the existence of regular no-boundary solutions in theories including higher-order corrections, by relying on specificities of the FLRW background. We also prove that restricting to homogeneous and isotropic backgrounds is sufficient for studying those solutions. In section 3.2, we derive conditions that must be fulfilled by an action composed of Riemann tensors in order to admit a regular no-boundary solution. We then study several theories containing higher-order corrections in section 3.3 and find they all fulfill this condition. Finally, we study the conditions stemming from covariant derivatives of the Riemann tensors in section 3.4, as these appear in the low energy effective action of type II string theory. The following four sections follow and present the results first published in [1].

[2] Higher-derivative theories have been little studied so far in the no-boundary context. We can cite for example Hawking and Luttrell [56] and Vilenkin [34] for quadratic gravity, and van Elst et al. for GR plus a cubic Ricci scalar term [57].

3.1 No-boundary ansatz

We consider the FLRW closed ($k = 1$) metric in the presence of a perfect fluid matter. Conversely to other parts of this thesis that deal with the no-boundary proposal, we use the usual FLRW metric with scale factor $a(t)$ and lapse function $N(t)$ only depending on time, such that:

$$\mathrm{d}s^2 = -N(t)^2\mathrm{d}t^2 + a(t)^2\left[\mathrm{d}\psi^2 + \sin^2\psi\left(\mathrm{d}\theta^2 + \sin^2\theta\mathrm{d}\phi^2\right)\right]. \tag{3.1.1}$$

ψ and θ range from 0 to π and ϕ ranges from 0 to 2π. For the fluid, we assume a stress-energy tensor of the perfect fluid form (1.1.12) and thus obtain again the FLRW equations of motion (1.1.13):

$$\begin{cases} \dfrac{\dot{a}^2}{N^2} + 1 = \dfrac{a^2}{3}\left(\Lambda + 8\pi G\rho\right), \\ \dfrac{2\ddot{a}}{aN^2} + \dfrac{\dot{a}^2}{a^2N^2} + \dfrac{1}{a^2} - \Lambda = -8\pi G p\,, \\ a\dot{\rho} + 3\dot{a}(\rho + p) = 0\,. \end{cases} \tag{3.1.2}$$

We are looking for a **regular solution** as $a(t) \to 0$ (we will choose the origin of the time coordinate such that this coincides with $t \to 0$). The equations (3.1.2) above imply that this can only be achieved if

$$\dot{a}^2(t \to 0) = -N^2 \quad ; \quad \ddot{a}(t \to 0) = 0 \quad ; \quad (\rho + p)(t \to 0) = 0\,. \tag{3.1.3}$$

These conditions (3.1.3) precisely define the no-boundary solution. The condition on $\dot{a}$ immediately implies that the metric is Euclidean near $t = 0$. The condition on the energy density and pressure implies that near $t = 0$, the only allowed form of matter must have the equation of state of a cosmological constant there, e.g., a scalar field that approaches a constant value at $t = 0$, i.e., for which $\dot{\phi}(t = 0) = 0$. No other form of matter is allowed near the "big bang" (also sometimes called the South Pole of the instanton), as this would destroy the regularity of the solution. This means that for our purposes we can ignore matter contributions and focus only on gravitational terms.

Additionally, we show that we can safely ignore anisotropies and inhomogeneities near the South Pole, so that the study of a FLRW background is sufficient to proof the existence of regular no-boundary solutions.

Consider a Bianchi IX metric,

$$\begin{aligned}\mathrm{d}s^2_{\mathrm{IX}} = -N^2\mathrm{d}t^2 + \frac{a^2}{4}\Big[&e^{\beta_+ + \sqrt{3}\beta_-}(\sin\psi\mathrm{d}\theta - \cos\psi\sin\theta\mathrm{d}\phi)^2 + e^{\beta_+ - \sqrt{3}\beta_-}(\cos\psi\mathrm{d}\theta + \sin\psi\sin\theta\mathrm{d}\phi)^2 \\ &+ e^{-2\beta_+}(\mathrm{d}\psi + \cos\theta\mathrm{d}\phi)^2\Big]\,;\end{aligned} \tag{3.1.4}$$

in (t, ψ, θ, ϕ) coordinates, with $\theta \in [0, \pi]$, $\phi \in [0, 2\pi]$ and $\psi \in [0, 4\pi]$. The anisotropies are specified by the functions $\beta_\pm(t)$. If we neglect matter fields, the constraint and equations

of motion for the Einstein-Hilbert action are

$$\begin{cases} \dfrac{3\dot{a}^2}{a^2} - \dfrac{3}{4}(\dot{\beta}_+^2 + \dot{\beta}_-^2) - \dfrac{N^2}{a^2}U(\beta_+, \beta_-) - N^2\Lambda = 0\,; \\ \dfrac{\dot{a}^2}{a^2N^2} + \dfrac{2\ddot{a}}{aN^2} + \dfrac{3}{4N^2}(\dot{\beta}_+^2 + \dot{\beta}_-^2) - \dfrac{1}{3a^2}U(\beta_+, \beta_-) - \Lambda = 0\,; \end{cases} \tag{3.1.5}$$

where the functional U is defined by:

$$U(\beta_+, \beta_-) = e^{-4\beta_+} + e^{2\beta_+ - 2\sqrt{3}\beta_-} + e^{2\beta_+ + 2\sqrt{3}\beta_-} - 2e^{2\beta_+} - 2e^{-\beta_+ - \sqrt{3}\beta_-} - 2e^{-\beta_+ + \sqrt{3}\beta_-}\,. \tag{3.1.6}$$

Close to $t = 0$, the no-boundary ansatz (3.1.3) leads to a regular solution if the conditions: $(\dot{\beta}_+^2 + \dot{\beta}_-^2)(t \to 0) = 0$ and $U(\beta_+, \beta_-)(t \to 0) = -3$ are satisfied. In this case, the anisotropies β_+ and β_- are necessarily going to zero when $t \to 0$. Similar arguments apply to inhomogeneities.

Therefore, as long as a homogeneous and isotropic solution exists, other solutions may exist that develop inhomogeneities and anisotropies away from the South Pole, while approaching the most symmetric solution at the South Pole. This remains true when considering more involved theories of gravity.

Close to the no-boundary point, it is sufficient to focus on the isotropic and homogeneous part of the metric, i.e., on the scale factor. To determine the existence of no-boundary solutions we use a Taylor series ansatz of the form:

$$\begin{cases} a(t) = a_1 t + \dfrac{a_3}{6}t^3 + \dfrac{a_4}{24}t^4 + \dfrac{a_5}{120}t^5 + \mathcal{O}(t^6)\,; \\ a_1^2 = -N^2\,. \end{cases} \tag{3.1.7}$$

We will examine whether **such a series solution continues to exist in the presence of quantum gravity corrections.**

We conclude this section by pointing out three important remarks on the no-boundary solution:

1. The regularity condition $\dot{a}^2(0) = -N^2$ leads to two complex conjugated solutions, $\dot{a}(0) = a_1 = \pm iN$. These correspond to the Vilenkin [47] and Hartle-Hawking [38] choices. In this chapter we do not distinguish between the two.

2. On its own, the coefficient $a_1 = \pm iN$ describes simple flat space. So the function $a(t) = a_1 \cdot t$ will always be a solution of any action constructed purely from Riemann tensors. What is unclear and that we will explore in the next sections, is whether for arbitrary actions composed of Riemann tensors, there exists non-vanishing a_i coefficients for some $i > 1$, which define a no-boundary solution regular in time.

3. The coefficient a_3 is related to the expansion rate of the universe. For general relativity in the presence of a cosmological constant $\Lambda \equiv 3H^2$, the no-boundary

solution in Euclidean time ($\tau = -iNt$) is given by:

$$a(\tau) = \frac{1}{H}\sin(H\tau) = \tau - \frac{1}{6}H^2\tau^3 + \cdots\,, \tag{3.1.8}$$

so that $a_1^2 = -N^2$, independently of H, and $a_3 \propto H^2$: the expansion rate is fixed. For generic theories that allow solutions with different expansion rates, we expect a_3 to remain a free parameter, labeling the different solutions. Solutions with different expansion rates will yield different actions, i.e., different probabilities.

3.2 Robustness to the addition of Riemann terms

We start by investigating the impact of adding terms of higher order in the Riemann tensor, without including covariant derivatives. As explained in the previous section, we can reduce our investigation to that of the scale factor in a closed FLRW universe, with metric (3.1.1). In this spacetime, the only non-vanishing components of the Riemann tensor $R^{\mu\nu}{}_{\rho\sigma}$ are of the form $R^{ab}{}_{ab}$ and $R^{ab}{}_{ba}$ with $a, b = 0, \ldots, 3$, $a \neq b$ and no summation on a and b implied. In the FLRW background, all scalar contractions composed of n Riemann tensors $R_{\mu\nu\rho\sigma}$ and $2n$ inverse metrics $g^{\mu\nu}$ can therefore be written as contractions of n $R^{ab}{}_{ab}$ or $R^{ab}{}_{ba}$ (where n can be any integer). Moreover, these 24 non-zero components have simple expressions in terms of the lapse and scale-factor functions: $\forall\ i, j = 1, 2, 3$ with $i \neq j$ and no summation on the indices implied,

$$R^{ij}{}_{ij} = \frac{\dot{a}^2 + N^2}{a^2N^2} \equiv A_1 \quad \text{and} \quad R^{0i}{}_{0i} = \frac{\ddot{a}N - \dot{a}\dot{N}}{aN^3} \equiv A_2\,. \tag{3.2.1}$$

We define a **Riemann term** to be any scalar combination of Riemann tensors and metric factors. Because of (3.2.1), any Riemann term can be written as a polynomial in A_1 and A_2 on a closed FLRW background. Basic examples are:

- the Ricci scalar: $R = 6(A_1 + A_2)$,
- the Ricci tensor squared: $R^{\mu\nu}R_{\mu\nu} = 12(A_1^2 + A_1A_2 + A_2^2)$,
- the Riemann tensor squared: $R^{\mu\nu\rho\sigma}R_{\mu\nu\rho\sigma} = 12(A_1^2 + A_2^2)$.

3.2.1 General action and constraint

Since all Riemann terms are polynomials in A_1 and A_2, the most general action containing only such terms is

$$S = \int \mathrm{d}^4x\sqrt{-g}\cdot f\left(R_{\mu\nu\rho\sigma}, g^{\alpha\beta}\right) = 2\pi^2\int \mathrm{d}t\ a^3N \sum_{p_1,p_2\in\mathbb{N}^2} c_{p_1,p_2}A_1^{p_1}A_2^{p_2}\,, \tag{3.2.2}$$

where c_{p_1,p_2} is a constant depending on the precise form of the function f for each couple $\{p_1, p_2\}$.

We can slightly manipulate this action to ease the calculation of the equations of motions later on. The lapse N is a non-dynamical variable whose equation of motion is a constraint on the system. Therefore, since we work in a gauge where N is constant, any term containing more than one power of $\dot{N}$ will drop from the equations of motion. Decomposing $A_2^{p_2}$ with the Newton formula,

$$A_2^{p_2} = \left(\frac{\ddot{a}}{aN^2} - \frac{\dot{a}\dot{N}}{aN^3}\right)^{p_2} = \sum_{l=0}^{p_2} \binom{p_2}{l} \left(-\frac{\dot{a}\dot{N}}{aN^3}\right)^{l} \left(\frac{\ddot{a}}{aN^2}\right)^{p_2-l}, \tag{3.2.3}$$

we see that only the terms $l = 0$ and $l = 1$ will survive, so we can replace:

$$\left(\frac{\ddot{a}N - \dot{a}\dot{N}}{aN^3}\right)^{p_2} \to \left(\frac{\ddot{a}}{aN^2}\right)^{p_2-1} \left(\frac{\ddot{a}}{aN^2} - p_2\frac{\dot{a}\dot{N}}{aN^3}\right). \tag{3.2.4}$$

We also rewrite

$$A_1^{p_1} = \left(\frac{\dot{a}^2 + N^2}{a^2N^2}\right)^{p_1} = \frac{1}{a^{2p_1}} \sum_{j=0}^{p_1} \binom{p_1}{j} \frac{\dot{a}^{2j}}{N^{2j}}. \tag{3.2.5}$$

The action (3.2.2) then reduces to

$$S = 2\pi^2 \sum_{p_1,p_2\in\mathbb{N}^2} c_{p_1,p_2} \sum_{j=0}^{p_1} \binom{p_1}{j} \int \mathrm{d}t \left[\frac{1}{N^{2p_2-1+2j}} \frac{\dot{a}^{2j}\ddot{a}^{p_2}}{a^{2p_1+p_2-3}} - p_2 \frac{\dot{N}}{N^{2p_2+2j}} \frac{\dot{a}^{2j+1}\ddot{a}^{p_2-1}}{a^{2p_1+p_2-3}}\right]. \tag{3.2.6}$$

We then calculate the constraint equation by varying this action (3.2.6) with respect to N. Using

$$\frac{\dot{N}}{N^{2p_2+2j}} = \frac{\mathrm{d}}{\mathrm{d}t}\left(-\frac{1}{2p_2+2j-1} \cdot \frac{1}{N^{2p_2+2j-1}}\right), \tag{3.2.7}$$

we rewrite (3.2.6) as

$$\begin{aligned} S = 2\pi^2 \sum_{p_1,p_2} c_{p_1,p_2} \sum_{j=0}^{p_1} \binom{p_1}{j} \int \frac{\mathrm{d}t}{N^{2p_2+2j-1}} \Bigg[& \frac{\dot{a}^{2j}\ddot{a}^{p_2}}{a^{2p_1+p_2-3}} - \frac{p_2}{2p_2+2j-1} \Bigg\{ (2j+1)\frac{\dot{a}^{2j}\ddot{a}^{p_2}}{a^{2p_1+p_2-3}} \\ & + (p_2-1)\frac{\dot{a}^{2j+1}\ddot{a}^{p_2-2}\dddot{a}}{a^{2p_1+p_2-3}} - (2p_1+p_2-3)\frac{\dot{a}^{2j+2}\ddot{a}^{p_2-1}}{a^{2p_1+p_2-2}} \Bigg\} \Bigg] \end{aligned} \tag{3.2.8}$$

$$\equiv 2\pi^2 \sum_{p_1,p_2} c_{p_1,p_2} \sum_{j=0}^{p_1} \binom{p_1}{j} \int \frac{\mathrm{d}t}{N^{2p_2+2j-1}} \cdot \mathcal{L}_{p_1,p_2,j}(a, \dot{a}, \ddot{a}, \dddot{a}). \tag{3.2.9}$$

Varying with respect to the lapse then yields

$$\delta_N S = 2\pi^2 \sum_{p_1,p_2} c_{p_1,p_2} \sum_{j=0}^{p_1} \binom{p_1}{j} \int \mathrm{d}t \left(\frac{-(2p_2+2j-1)\delta N}{N^{2p_2+2k}}\right) \cdot \mathcal{L}_{p_1,p_2,j}\ ; \tag{3.2.10}$$

from which we read the constraint equation:

$$0 = \frac{\delta S}{\delta N} = -2\pi^2 \sum_{p_1,p_2} c_{p_1,p_2} \sum_{j=0}^{p_1} \binom{p_1}{j} \frac{2p_2+2j-1}{N^{2p_2+2j}} \cdot \mathcal{L}_{p_1,p_2,j}\ ; \tag{3.2.11}$$

$$\Leftrightarrow\ 0=\frac{\delta S}{\delta N}=-2\pi^2\sum_{p_1,p_2}\frac{c_{p_1,p_2}}{N^{2p_2}}\frac{\ddot{a}^{p_2-1}}{a^{2p_1+p_2-2}}\sum_{j=0}^{p_1}\binom{p_1}{j}\frac{\dot{a}^{2j}}{N^{2j}}\Big[(2j-1)(1-p_2)a\ddot{a} \tag{3.2.12}$$
$$-p_2(p_2-1)\frac{a\dot{a}a^{(3)}}{\ddot{a}}+p_2(2p_1+p_2-3)\dot{a}^2\Big]\,.$$

Using Newton's binomial formula, we can resum:

$$\begin{cases}\displaystyle\sum_{j=0}^{p_1}\binom{p_1}{j}\frac{\dot{a}^{2j}}{N^{2j}}=\left(\frac{\dot{a}^2}{N^2}+1\right)^{p_1}=a^{2p_1}A_1^{p_1}\,;\\ \displaystyle\sum_{j=0}^{p_1}\binom{p_1}{j}j\frac{\dot{a}^{2j}}{N^{2j}}=p_1\frac{\dot{a}^2}{N^2}\left(\frac{\dot{a}^2}{N^2}+1\right)^{p_1-1}=p_1\frac{\dot{a}^2}{a^2N^2}a^{2p_1}A_1^{p_1}\,;\end{cases} \tag{3.2.13}$$

so the constraint equation (3.2.12) finally reduces to:

$$0=\frac{\delta S}{\delta N}=2\pi^2\sum_{p_1,p_2}c_{p_1,p_2}\Big[2p_1(p_2-1)\frac{a\dot{a}^2}{N^2}A_2^{p_2}A_1^{p_1-1}+(1-p_2)a^3A_2^{p_2}A_1^{p_1}$$
$$+p_2(p_2-1)\frac{a\dot{a}a^{(3)}}{N^4}A_2^{p_2-2}A_1^{p_1}-p_2(2p_1+p_2-3)\frac{a\dot{a}^2}{N^2}A_2^{p_2-1}A_1^{p_1}\Big]\,. \tag{3.2.14}$$

Since the equation of motion for the scale factor, obtained by varying the action with respect to a, is implied by the constraint equation (i.e., it can be obtained by deriving the constraint with respect to time), it is sufficient to restrict our analysis to the constraint equation (3.2.14).

3.2.2 Order by order equations with the no-boundary ansatz

We now insert the no-boundary ansatz into the Friedmann constraint equation (3.2.14) for the general action (3.2.6). We will then analyze the resulting equations order by order in t. This will provide conditions the action must obey in order to admit a regular no-boundary solution.

First, note that the constraint equation (3.2.14) (hence also the equation of motion), and the no-boundary conditions (3.1.3), are all invariant under the time reversal transformation

$$\begin{cases}t\to-t,\\ a\to-a,\end{cases}\quad\Rightarrow\quad a(-t)=-a(t)\,; \tag{3.2.15}$$

so the function a must be odd in t. Thus all coefficients of even powers of t in the Taylor expansion are zero, and the no-boundary ansatz (3.1.7) can be simplified into

$$\begin{cases}a(t)=a_1t+\dfrac{a_3}{6}t^3+\dfrac{a_5}{120}t^5+\mathcal{O}(t^7)\,;\\ a_1^2=-N^2\,.\end{cases} \tag{3.2.16}$$

The fact that a is an odd function of t implies that for any solution $a(t)$, there will always

exist a time-reversed solution, but both will have the same signature as the metric only depends on $a(t)^2$. For this second solution, the proper time runs in the opposite coordinate time direction t. Since there is also always a complex conjugate solution for each solution (see 1), this makes for four solutions in total.

We start by plugging (3.2.16) into the expressions for A_1 and A_2, obtaining the expansions

$$\begin{cases} A_1 = \dfrac{\dot{a}^2(t) + N^2}{a^2(t)N^2} = -\dfrac{a_3}{a_1^3} + \dfrac{\left(a_3^2 - a_1 a_5\right)}{12 a_1^4}\, t^2 + \dfrac{\left(a_3 a_5 - a_1 a_7\right)}{360 a_1^4}\, t^4 + \mathcal{O}(t^6)\,; \\ A_2 = \dfrac{\ddot{a}(t)}{a(t)N^2} = -\dfrac{a_3}{a_1^3} + \dfrac{\left(a_3^2 - a_1 a_5\right)}{6 a_1^4}\, t^2 - \dfrac{\left(10 a_3^3 - 13 a_1 a_3 a_5 + 3 a_1^2 a_7\right)}{360 a_1^5}\, t^4 + \mathcal{O}(t^6)\,. \end{cases} \tag{3.2.17}$$

The fact that these expansions start at order t^0 is non-trivial since A_1 and A_2 both contain powers of $a(t)$ in their denominators, so they could in principle have been singular as $t \to 0$. This is precisely what the no-boundary solution prevents. Moreover, the combination $A_2 - A_1$ only starts at order t^2.

Then we plug the no-boundary ansatz (3.2.16) into the Friedmann constraint equation (3.2.14) (see appendix A.1). Interestingly, even though we allow terms of arbitrary order in the Riemann tensor, **all coefficients of negative powers of t vanish automatically and the first non-trivial condition arises at order t**. From the two lowest non-trivial orders (t and t^3) we obtain two conditions on the coefficients c_{p_1,p_2}:

$$\text{Order } t: \quad \sum_{p_1,p_2} \frac{c_{p_1,p_2}}{N^{2P}} a_1^{4-P} a_3^{P-1} \left(p_2 - p_1\right) = 0\,; \tag{3.2.18}$$

$$\text{Order } t^3: \quad \sum_{p_1,p_2} \frac{c_{p_1,p_2}}{N^{2P}}\, a_1^{3-P} a_3^{P-2} \left(a_3^2 \cdot G_3[p_1,p_2] + a_1 a_5 \cdot G_5[p_1,p_2]\right) = 0\,; \tag{3.2.19}$$

where $P \equiv p_1 + p_2$ and

$$G_3[p_1,p_2] = \frac{1}{6}\left(p_1^2 - 15 p_1 + 6 - 4 p_2^2 + 12 p_2\right) \;;\; G_5[p_1,p_2] = \frac{p_1(1-p_1)}{6} - \frac{2p_2(1-p_2)}{3}\,. \tag{3.2.20}$$

A sufficient condition for satisfying (3.2.18) is to require:

$$\forall \{p_1,p_2\} \in \mathbb{N}^2\,, \quad c_{p_1,p_2} = c_{p_2,p_1}\,. \tag{3.2.21}$$

It turns out that this special case covers most known examples:

- any term of the form R^n, $\forall\, n \in \mathbb{N}$, satisfies (3.2.21) since $R = 6(A_1 + A_2)$. In particular this implies that $f(R)$ **theory**, and hence gravity plus a scalar field, will admit a regular no-boundary solution.

- quadratic terms and all their powers satisfy (3.2.21) since $R_{\mu\nu\rho\sigma}R^{\mu\nu\rho\sigma} = 6\,(A_1^2 + A_2^2)$ and $R_{\mu\nu}R^{\mu\nu} = 12\,(A_1^2 + A_1 A_2 + A_2^2)$. In particular, **quadratic gravity** possesses a

no-boundary solution.

Next we consider the condition (3.2.19). Provided the expression factoring a_5 is not zero, this condition determines the value of a_5 in terms of a_1 and a_3:

$$a_5 \cdot \sum_{p_1,p_2} \frac{c_{p_1,p_2}}{N^{2P}}\, a_1^{3-P} a_3^{P-2} G_5[p_1,p_2] = -\frac{a_3^2}{a_1} \cdot \sum_{p_1,p_2} \frac{c_{p_1,p_2}}{N^{2P}}\, a_1^{3-P} a_3^{P-2} G_3[p_1,p_2]\,. \tag{3.2.22}$$

When we are in the special case where (3.2.21) is satisfied, we can simplify (3.2.22) by symmetrizing the expressions G_3 and G_5 in the exchange of p_1 and p_2, and we find

$$a_5 = -\frac{a_3^2}{a_1} \cdot \frac{\sum_{p_1,p_2} \frac{c_{p_1,p_2}}{N^{2P}} a_1^{3-P} a_3^{P-2} \Big[4 - p_1(p_1+1) - p_2(p_2+1)\Big]}{\sum_{p_1,p_2} \frac{c_{p_1,p_2}}{N^{2P}} a_1^{3-P} a_3^{P-2} \Big[p_1(p_1-1) + p_2(p_2-1)\Big]}\,. \tag{3.2.23}$$

At higher orders in t the additionally appearing coefficients a_7, $a_9, \ldots$ are fixed in terms of the lower ones. Thus all theories of this form admit no-boundary solutions as $a \to 0$, with a_3 remaining a free parameter effectively corresponding to solutions with different expansion rates.

The single exception to this statement is the case where the left-hand side of (3.2.22) vanishes, in which case a_3 is fixed in terms of a_1. This corresponds to **ordinary general relativity** in the presence of a cosmological constant. Expanding the Friedmann constraint (first line of (3.1.2)) in this case, we find

$$a_3 = -\frac{a_1^3 \Lambda}{3}\ ;\ a_5 = -\frac{5a_3^2}{a_1} - 2a_1^2 a_3 \Lambda = \frac{a_1^5 \Lambda^2}{9}\ ;\quad \text{etc.} \tag{3.2.24}$$

For this theory the no-boundary solution corresponds to complexified de Sitter space with a fixed expansion rate determined by the cosmological constant.

In this section, we derived general conditions that the action must satisfy in order to possess a no-boundary solution. In the next section we will study specific examples of theories with higher-order corrections, and see that they fulfill those conditions.

Before that, we illustrate the non-triviality of the no-boundary regularity condition, by studying what goes wrong if the condition (3.2.18) is not satisfied. Even though these do not have a covariant expression, we consider the actions:

$$\int \mathrm{d}t\, a^3 N A_1\ ;\quad \text{or}\quad \int \mathrm{d}t\, a^3 N A_1 A_2^2\ ;\quad \text{etc,} \tag{3.2.25}$$

which violate the order t condition (3.2.18). The constraint equation for the action $\int \mathrm{d}t a^3 N A_1$ gives

$$(a_1^2 - N^2)t + a_1 a_3 t^3 + \mathcal{O}(t^5) = 0\,; \tag{3.2.26}$$

so even in the presence of matter (only appearing at order t^3), this would imply $a_1 = \pm N$, corresponding to Minkowski spacetime rather than Euclidean space near $a = 0$. This

is inconsistent with the no-boundary ansatz, and stresses that it is not enough for an approximately flat solution to exist near $a = 0$, it must also be Euclidean. Even that is not enough, as the next example shows: considering the action $\int \mathrm{d}t\, a^3 N A_1 A_2^2$ for instance, its constraint equation reads

$$\frac{2a_1 a_3^2}{N^6} t + \left(\frac{4a_1 a_3 a_5}{3N^6} - 2a_1^3 \Lambda \right) t^3 + \mathcal{O}(t^5) = 0 \; ; \tag{3.2.27}$$

where we have included a cosmological constant Λ and assumed the no-boundary relation $a_1^2 = -N^2$. The order t sets $a_3 = 0$, but then at the next order the constraint equation cannot be satisfied. Hence this action does not admit a no-boundary solution.

We now will apply these conditions to explicit examples of actions containing higher-order corrections, from quadratic gravity to string-theory corrections.

3.3 Application of the constraint to higher-order correction examples

3.3.1 Quadratic gravity

The most straightforward extension of Einstein gravity is **quadratic gravity**, analyzed in the no-boundary context in [56, 34]. Quadratic gravity is a renormalizable theory of gravity [58], but it suffers from the presence of a ghost, whose interpretation has been very much studied, but isn't yet fully understood [59, 60]. Besides, quadratic theory forms the building block of the inflationary model preferred by experimental data [61].

We first consider **pure quadratic gravity**, where the action only contains R^2 terms. This theory is scale invariant and its action reads

$$S_{\text{pure quad}} = \int \mathrm{d}^4x \sqrt{-g} \left(\alpha R^2 + \beta R_{\mu\nu} R^{\mu\nu} + \gamma R_{\mu\nu\rho\sigma} R^{\mu\nu\rho\sigma} \right) . \tag{3.3.1}$$

On closed FLRW background, we recall that

$$R^2 = 36 \left(A_1 + A_2 \right)^2 \; ; \; R_{\mu\nu} R^{\mu\nu} = 12 \left(A_1^2 + A_1 A_2 + A_2^2 \right) \text{ and } R_{\mu\nu\rho\sigma} R^{\mu\nu\rho\sigma} = 12 \left(A_1^2 + A_2^2 \right) .$$

In four dimensions, the Gauß-Bonnet term $\int \mathrm{d}^4x \sqrt{-g}\, \mathcal{G}$ is a topological invariant and does not contribute to the dynamics. On this background it reads

$$\mathcal{G} \equiv R^{\alpha\beta\gamma\delta} R_{\alpha\beta\gamma\delta} - 4 R^{\alpha\beta} R_{\alpha\beta} + R^2 = 24 A_1 A_2 \, ; \tag{3.3.2}$$

and the associated constraint equation obtained by inserting $\{p_1 = 1,\, p_2 = 1\}$ in (3.2.14) is automatically null. To study the dynamics the action can therefore effectively be reduced to

$$S^{\text{reduced}}_{\text{pure quad}} = 2\pi^2 \int \mathrm{d}t\, a^3 N\, \epsilon (A_1^2 + A_2^2) \quad ; \quad \text{with } \epsilon = 36\alpha + 12\beta + 12\gamma \, . \tag{3.3.3}$$

At first order in t, the constraint equation is automatically satisfied because the action (3.3.3) is symmetric in A_1 and A_2, and therefore satisfies the condition (3.2.21). At the next order, the constraint equation yields

$$\frac{(a_1 a_3^2 - a_1^2 a_5)}{N^4} \cdot t^3 + \mathcal{O}\left(t^5\right) = 0 \qquad \Rightarrow \;\; a_5 = a_3^2/a_1. \tag{3.3.4}$$

The coefficient a_3 is left undetermined, as expected from the scale invariance of the theory.

Next we consider **quadratic gravity coupled to ordinary GR**,

$$S_{\text{quad}} = \int \mathrm{d}^4x\sqrt{-g}\left(\frac{R}{16\pi G} - \frac{\Lambda}{8\pi G} + \frac{\omega}{3\sigma}R^2 - \frac{1}{2\sigma}C^2 + \epsilon\mathcal{G}\right), \tag{3.3.5}$$

where we wrote the action in terms of the Weyl tensor C, which vanishes for a FLRW metric:

$$C_{\mu\nu\rho\sigma}C^{\mu\nu\rho\sigma} = R_{\mu\nu\rho\sigma}R^{\mu\nu\rho\sigma} - 2R_{\mu\nu}R^{\mu\nu} + \frac{1}{3}R^2 = 0\,;$$

and the topological Gauß-Bonnet combination $\mathcal{G}$. Then the relevant part of the quadratic action for computing the dynamics on a FLRW background is

$$S_{\text{quad}}^{\text{reduced}} = 2\pi^2 \int \mathrm{d}t a^3 N\left[\frac{1}{8\pi G}\left(3A_1 + 3A_2 - \Lambda\right) + \frac{12\omega}{\sigma}(A_1^2 + A_2^2)\right]. \tag{3.3.6}$$

The constraint equation for this action is

$$\left(\alpha a_1^3\Lambda + \frac{a_3^2\beta}{a_1^3} - \frac{a_5\beta}{a_1^2} + 3\alpha a_3\right)\cdot t^3 + \mathcal{O}\left(t^5\right) = 0\,; \tag{3.3.7}$$

where $\alpha = \dfrac{1}{8\pi G}$ and $\beta = \dfrac{12\omega}{\sigma}$. The no-boundary solution is

$$a_5 = \frac{a_3^2}{a_1} + \frac{\alpha}{\beta}\Big(a_1^5\Lambda + 3a_1^2 a_3\Big)\,; \tag{3.3.8}$$

valid when $\alpha \sim \beta$ or $\alpha \ll \beta$. a_3 is again left undetermined.

When $\alpha \gg \beta$, the solution is instead

$$a_3 \;=\; \frac{-3a_1^3 \pm \sqrt{9a_1^6 - 4\frac{\beta}{\alpha}a_1^6\Lambda + 4\frac{\beta^2}{\alpha^2}a_1 a_5}}{2\beta/\alpha} \;\xrightarrow{\alpha\gg\beta}\; \begin{cases} -\dfrac{a_1^3\Lambda}{3} + \mathcal{O}\Big(\beta/\alpha\Big)\,; \\ -3a_1^3\dfrac{\alpha}{\beta} + \dfrac{a_1^3\Lambda}{3} + \mathcal{O}\Big(\beta/\alpha\Big)\,. \end{cases} \tag{3.3.9}$$

The first branch corresponds to the Einstein-Hilbert solution, while the second branch is not physical as it gives a solution with curvature a_3 bigger than the Planck scale (α), and a non smooth limit $\beta \to 0$. The second branch arises due to the presence of higher derivatives in the action, and is associated with the new scalar degree of freedom.

3.3.2 Heterotic string theory

The low-energy effective theory of **heterotic string theory** is the *Einstein – Maxwell – axion – dilaton* gravity, that contains a dilaton field ϕ, gauge fields F (Maxwell) and a 3-form H (the axion), see e.g., [62, 63]. At first order in the squared string length $\alpha' \sim \ell_s^2$, an S-matrix calculation in heterotic string theory leads to the effective Einstein frame action [63]:

$$S_{\text{heterotic}} = \frac{1}{2\kappa_D^2}\int \mathrm{d}^D x\sqrt{-g}\left(R - \frac{1}{2}(\partial\phi)^2 + \frac{\alpha'}{8}e^{-\phi/2}\left(\mathcal{G} + \frac{3}{16}(\partial\phi)^4\right) - V(\phi) + \cdots\right); \quad (3.3.10)$$

where the compactification leads to a potential $V(\phi)$ for the dilaton (in general we should expect additional terms). As discussed in section 3.1, the axion H and the gauge fields F are consistently set to zero. Additional scalar fields arising from the compactification will behave analogously to the dilaton, so we use the dilaton as a stand-in for all scalar fields. In the gravitational sector, the first correction in α' is given by the Gauß-Bonnet combination. It is not a topological term this time because it is multiplied by the dilaton $e^{-\phi/2}$, so we must include its effects. The constraint reads

$$\begin{aligned}\frac{\delta}{\delta N}\left(\mathcal{L}_{\text{heterotic}}\right) = \frac{\delta}{\delta N}\left(6a^3N(A_1+A_2)\right) - a^3\left[\frac{\dot\phi^2}{2} - \frac{\alpha'}{128}e^{-\phi/2}\dot\phi^4 + V(\phi)\right] \\ + 3\alpha' e^{-\phi/2}\frac{\delta}{\delta N}\left(a^3NA_1A_2\right) - \frac{3\alpha'}{2}\dot\phi\, e^{-\phi/2}\frac{\dot a a^2}{N^2}A_1 = 0\,, \end{aligned} \quad (3.3.11)$$

where the second line follows from

$$\frac{\delta}{\delta N}\left(a^3N\,A(N,\dot N,t)\,B(t)\right) = B\,\frac{\delta\left(a^3NA\right)}{\delta N} - \dot B\,\frac{\partial\left(a^3NA\right)}{\partial\dot N} \text{ for } A\equiv\mathcal{G} \text{ and } B\equiv e^{-\phi/2}\,. \quad (3.3.12)$$

Equation (3.3.11) is odd under the transformation $t\to -t$, $a\to -a$ and $\phi\to\phi$. The equation of motion for the scalar ϕ on the closed FLRW background and for a homogeneous field $\phi(t)$ is:

$$\begin{aligned}&\nabla^2\phi - \frac{\alpha'}{16}e^{-\phi/2}\left(\mathcal{G} + 3(\nabla_\mu\phi)(\nabla_\nu\phi)(\nabla^\mu\nabla^\nu\phi) + \frac{3}{2}\nabla^2\phi(\partial\phi)^2 - \frac{9}{16}\left(\partial\phi\right)^4\right) - V_{,\phi} = 0\,,\\ \Leftrightarrow\ &\ddot\phi - \frac{3\alpha'}{16}e^{-\phi/2}\left(8A_1A_2 + \frac{3}{2}\dot\phi^2\ddot\phi - \frac{3}{16}\dot\phi^4\right) - V_{,\phi} = 0\,. \end{aligned} \quad (3.3.13)$$

This equation is even under the time reversal $t\to -t$, $a\to -a$ and $\phi\to\phi$.

Do these equations ((3.3.11) and (3.3.13)) possess a no-boundary solution around $t=0$? From the transformation rules of these equations under time reversal, a solution must have $a(t)$ odd and $\phi(t)$ even with respect to time:

$$\begin{cases} a = a_1 t + \dfrac{a_3}{6}t^3 + \dfrac{a_5}{120}t^5 + \dots \\ \phi(t) = \phi_0 + \dfrac{\phi_2}{2}t^2 + \dfrac{\phi_4}{24}t^4 + \dots \end{cases} \quad (3.3.14)$$

This implies that ϕ must be constant at first order in time close to the South Pole in $t \to 0$. When plugging (3.3.14) in the constraint equation (3.3.11) and expanding in orders of t, the leading order reads

$$-\frac{3a_1 e^{-\phi_0/2}\alpha'}{2N^4}(a_1^2+N^2)\phi_2 t + \mathcal{O}(t^3) = 0\,; \tag{3.3.15}$$

solved by the usual no-boundary solution $a_1^2 = -N^2$. The ϕ equation (3.3.13) at leading order yields

$$\phi_2 - \frac{3a_3^2}{2a_1^6}\alpha' e^{-\phi_0/2} - V_{,\phi}(\phi_0) + \mathcal{O}(t^2) = 0\,. \tag{3.3.16}$$

This equation fixes ϕ_2 as a function of ϕ_0, a_1 and a_3. Implementing this solution for ϕ_2, the next order of the constraint equation gives us a cubic equation for a_3 in terms of a_1 and ϕ_0:

$$\left[-\frac{9a_3^3}{4a_1^8}\alpha'^2 e^{-\phi_0} + 6a_3\left(1 - e^{-\phi_0/2}\frac{\alpha' V_{,\phi}(\phi_0)}{4a_1^2}\right) - a_1^3 V(\phi_0)\right]t^3 + \mathcal{O}(t^5) = 0\,. \tag{3.3.17}$$

We conclude that the heterotic string action (3.3.10) possesses a family of no-boundary solutions, labeled by ϕ_0, the dilaton value at the South Pole.

3.3.3 General relativity as an Effective Field Theory

We just saw that the leading correction stemming from the heterotic string is a combination of quadratic terms in the Riemann tensor. More generally, when considering an **effective field theory treatment of general relativity**, we expect new couplings between matter fields and gravitational terms, in addition to the pure gravitational sector [64]. In our case we are particularly interested in couplings between scalar fields and gravity. We cannot treat them exhaustively, but we consider the first non-trivial couplings, and find no obstruction to the existence of no-boundary solutions. Specifically, we consider the effective theory of gravity and a scalar field up to fourth order in derivatives,

$$\begin{aligned} S_{\text{eff}} = \int \mathrm{d}^4x\sqrt{-g}\Big[&\frac{1}{16\pi G}(R-2\Lambda) + \frac{1}{2}g^{\mu\nu}\partial_\mu\phi\partial_\nu\phi - V(\phi) + c_1R^2 + c_2R_{\mu\nu}R^{\mu\nu} \\ &+ (d_1R^{\mu\nu} + d_2Rg^{\mu\nu})\partial_\mu\phi\partial_\nu\phi + d_3R\,V(\phi) + \cdots\Big]\,, \end{aligned} \tag{3.3.18}$$

for arbitrary coefficients c_1, c_2, d_1, d_2, d_3. Again on closed FLRW background with a homogeneous scalar field and up to total derivatives, this action reduces to

$$\begin{aligned} S_{\text{eff}} = 2\pi^2\int \mathrm{d}t\, a^3 N\Big[&\frac{1}{8\pi G}\big(3A_1 + 3A_2 - \Lambda\big) - \frac{\dot\phi^2}{2N^2} - V(\phi) + 12(3c_1+c_2)(A_1^2+A_2^2) \\ &- \big(3d_1A_2 + 6d_2(A_1+A_2)\big)\frac{\dot\phi^2}{2N^2} + 6d_3(A_1+A_2)\,V(\phi)\Big]. \end{aligned} \tag{3.3.19}$$

The full equations of motion for ϕ and N are:

$$\frac{a^3}{N}\Big[\ddot{\phi}+3H\dot{\phi}-N^2V_{,\phi}+6d_1\Big(A_2(\ddot{\phi}+2H\dot{\phi})+\frac{a^{(3)}}{aN^2}\dot{\phi}\Big)+6d_3(A_1+A_2)N^2V_{,\phi}$$
$$+12d_2\Big(\ddot{\phi}(A_1+A_2)+H\dot{\phi}(A_1+4A_2)+\frac{a^{(3)}}{aN^2}\dot{\phi}\Big)\Big]=0\quad\text{(equation for }\phi)\,; \tag{3.3.20}$$

$$a^3\Big[\frac{3A_1-\Lambda}{8\pi G}+\frac{\dot{\phi}^2}{2N^2}-V(\phi)-12(3c_1+c_2)\Big(\frac{2\dot{a}^2}{a^2N^2}A_1-\frac{2\dot{a}a^{(3)}}{a^2N^4}+\Big(\frac{\ddot{a}}{aN^2}-\frac{\dot{a}^2}{a^2N^2}\Big)^2\Big)$$
$$+6d_1\Big(\frac{\dot{\phi}^2}{N^2}\Big(\frac{\ddot{a}}{aN^2}-\frac{\dot{a}^2}{a^2N^2}\Big)-\frac{\dot{a}}{aN}\frac{\dot{\phi}\ddot{\phi}}{N^3}\Big)+6d_2\Big(\frac{\dot{\phi}^2}{N^2}A_1+\frac{2\ddot{a}}{aN^2}\frac{\dot{a}^2}{N^2}-\frac{2\dot{a}}{aN}\frac{\dot{\phi}\ddot{\phi}}{N^3}\Big)$$
$$+6d_3\Big(A_1V(\phi)+\frac{\dot{a}}{aN}\frac{\dot{\phi}}{N}V_{,\phi}\Big)\Big]=0\quad\text{(equation for }N)\,. \tag{3.3.21}$$

These equations are also odd under the time reversal $t\to-t$, $a\to-a$ and $\phi\to\phi$, so the ansatz (3.3.14) is appropriate. The equations of motion (3.3.20) and (3.3.21) then reduce to:

$$\frac{6a_1}{N^3}\left(a_1^2+N^2\right)\left(4d_2\phi_2+d_3N^2V_{,\phi}(\phi_0)\right)\cdot t+\mathcal{O}\left(t^3\right)=0\,, \tag{3.3.22}$$

$$-\frac{12}{a_1N^4}\cdot(3c_1+c_2)\left(3a_1^4+2a_1^2N^2-N^4\right)\cdot\frac{1}{t}+\frac{(a_1^2+N^2)}{a_1^2N^4}\Big(\frac{3a_1^3N^2}{8\pi G}-18a_1^2a_3(3c_1+c_2)$$
$$-2a_3(3c_1+c_2)N^2+6a_1^3d_3N^2V(\phi_0)\Big)\cdot t+\mathcal{O}\left(t^3\right)=0\,, \tag{3.3.23}$$

consistent with $a_1^2=-N^2$. Higher orders in t fix higher coefficients a_3, a_5, $\phi_2,\ldots$ in terms of ϕ_0 and a_1. For instance the next order of the ϕ equation gives

$$\frac{t^3}{N}\cdot\Big(4\phi_2(a_1^3-6a_3(d_1+4d_2))+a_1^2(a_1^3+12a_3d_3)V_{,\phi}(\phi_0)\Big)+\mathcal{O}(t^5)=0\,, \tag{3.3.24}$$

fixing the value of ϕ_2. This proves that even with higher derivative couplings, the scalar field does not diverge near the South Pole, but approaches a constant, just as for minimal coupling. Even if we cannot explicitly check all possible higher derivative couplings, we can assume that they will not yield any divergences, and focus on the gravitational sector only.

As a side remark, an effective treatment of general relativity leads to the appearance of non-local terms such as: $\int\sqrt{-g}R\frac{1}{\Box}R$ [64]. Those can have interesting implications in cosmology, see for example [65, 66, 67]. Expanding such terms around a specific background, we obtain an infinite series of terms containing more and more derivatives. In the section 3.4 below, we consider specific correction terms containing derivatives, but we are technically limited to a small, finite number of derivatives, so the study of non-local terms goes beyond the reach of our analysis.

3.3.4 Type II string theory in D=10 spacetime dimensions

The low-energy effective action, obtained by looking at quantum corrected amplitudes for four-graviton scattering in **type II string theory in** $D = 10$ **dimensions** order by order in α', reads [68, 69]:

$$S = \int \mathrm{d}^D x \sqrt{-G} \left(R + (\alpha')^3 \mathcal{E}^{(D)}_{(0,0)} \mathcal{R}^4 + (\alpha')^5 \mathcal{E}^{(D)}_{(1,0)} \nabla^4 \mathcal{R}^4 + (\alpha')^6 \mathcal{E}^{(D)}_{(0,1)} \nabla^6 \mathcal{R}^4 + \dots \right); \tag{3.3.25}$$

where G is the determinant of the D-dimensional metric, and $\mathcal{E}^{(D)}_{(p,q)}$ are coefficient functions stemming from the compactification. In this subsection we focus on the α'^3 type II correction to Einstein gravity within (3.3.25). It is given by the $\mathcal{R}^4$ term which is a special combination of four Riemann tensors defined as:

$$\mathcal{R}^4 = t_8^{ijklmnpq} t_8^{abcdefgh} R_{ijab} R_{klcd} R_{mnef} R_{pqgh} \,. \tag{3.3.26}$$

The eight-rank special tensor t_8 is given by (see chapter 9, appendix A of [70]):

$$\begin{aligned} t^{ijklmnpq} = & -\frac{1}{2}\epsilon^{ijklmnpq} \\ & -\frac{1}{2}\Big[\left(\delta^{ik}\delta^{jl} - \delta^{il}\delta^{jk}\right)\left(\delta^{mp}\delta^{nq} - \delta^{mq}\delta^{np}\right) + \left(\delta^{km}\delta^{ln} - \delta^{kn}\delta^{lm}\right)\left(\delta^{pi}\delta^{qj} - \delta^{pj}\delta^{qi}\right) \\ & \quad + \left(\delta^{im}\delta^{jn} - \delta^{in}\delta^{jm}\right)\left(\delta^{kp}\delta^{lq} - \delta^{kq}\delta^{lp}\right) \Big] \\ & +\frac{1}{2}\Big[\delta^{jk}\delta^{lm}\delta^{np}\delta^{qi} + \delta^{jm}\delta^{nk}\delta^{lp}\delta^{qi} + \delta^{jm}\delta^{np}\delta^{qk}\delta^{li} + \ 45 \text{ more terms obtained} \\ & \quad \text{by anti-symmetrizing on the pairs } ij,\ kl,\ mn \text{ and } pq \Big]. \end{aligned} \tag{3.3.27}$$

The quantity $\mathcal{R}^4$ is therefore a Riemann term, so we can determine if it will admit a no-boundary solution by simply looking at its structure in terms of A_1 and A_2 and see if it meets the condition (3.2.18). We compute[3] the explicit structure of $\mathcal{R}^4$ in terms of Riemann tensors:

$$\begin{aligned} \mathcal{R}^4 = & \ 12(R_{abcd}R^{abcd})^2 + 6R^{abcd}R_{ab}{}^{ij}(4R_{ij}{}^{kl}R_{cdkl} - R_{ic}{}^{kl}R_{jdkl}) - 12R_{abij}R_{cdkl}R^{abci}R^{djkl} \\ & + \frac{3}{2}R_{abij}R^{acid}R^{jl}{}_{ck}R^{bk}{}_{dl} + \frac{3}{4}R_{abij}R^{acid}R_{ckdl}R^{bkjl} \\ & +\epsilon^{ijklmnpq}R_{ij}{}^{ab}\Big[2R_{klef}R_{mn}{}^{ef}R_{pqab} - \frac{1}{2}R_{kl}{}^{ef}R_{mnae}R_{pqbf} - \frac{1}{2}R_{klae}R_{mn}{}^{fe}R_{pqbf} \\ & + 2R_{kl}{}^{ef}R_{mnab}R_{pqef} - \frac{1}{2}R_{klae}R_{mnbf}R_{pq}{}^{ef} + 2R_{klab}R_{mn}{}^{ef}R_{pqef}\Big] \\ & +\frac{1}{4}\epsilon^{ijklmnpq}\epsilon^{efghabcd}R_{ijab}R_{klcd}R_{efmn}R_{ghpq}. \end{aligned} \tag{3.3.28}$$

All the above expressions are originally valid only in 10 dimensions (an analogous structure is also expected in 11-dimensional supergravity, since the low-energy type II theories are related to 11-dimensional supergravity via circle compactifications [72]). The com-

[3] For this calculation we acknowledge the use of the xAct package of Mathematica [71].

pactification to four dimensions produces new fields (and different associated terms), when indices point in the internal dimensions. These new gauge and scalar fields depend on the details of the compactification, but as discussed in section 3.1, we expect gauge fields to be zero and scalar fields to be constant at the no-boundary point. Therefore, we can restrict to the part of (3.3.28) for which all indices point in the (four) external spacetime dimensions. In that case, all the terms containing an eight-rank tensor ϵ are set to zero, and we are left with:

$$\begin{aligned}\mathcal{R}^4\Big|_{\text{4d truncated}} &= 12(R_{\mu\nu}{}^{\rho\sigma}R^{\mu\nu}{}_{\rho\sigma})^2 + 6R^{\mu\nu}{}_{\rho\sigma}R_{\mu\nu}{}^{\xi\eta}(4R_{\xi\eta}{}^{\kappa\lambda}R^{\rho\sigma}{}_{\kappa\lambda} - R_{\xi}{}^{\rho\kappa}{}_{\lambda}R_{\eta}{}^{\sigma}{}_{\kappa}{}^{\lambda}) \\ &\quad - 12R_{\mu\nu}{}^{\xi\eta}R^{\rho\sigma}{}_{\kappa\lambda}R^{\mu\nu}{}_{\rho\xi}R_{\sigma\eta}{}^{\kappa\lambda} + \frac{3}{2}R^{\mu\nu}{}_{\xi\eta}R_{\mu\rho}{}^{\xi\sigma}R^{\eta}{}_{\lambda}{}^{\rho}{}_{\kappa}R_{\nu}{}^{\kappa}{}_{\sigma}{}^{\lambda} \\ &\quad + \frac{3}{4}R_{\mu\nu}{}^{\xi\eta}R^{\mu\rho}{}_{\xi\sigma}R_{\rho\kappa}{}^{\sigma\lambda}R^{\nu\kappa}{}_{\eta\lambda}\,; \end{aligned} \tag{3.3.29}$$

where $\mu, \nu, \rho, \sigma, \xi, \eta, \kappa, \lambda$ are spacetime indices running from 0 to 3. All the terms in expression (3.3.29) can be rewritten in terms of A_1 and A_2 through two quantities that we denote $\mathcal{R}_1$ and $\mathcal{R}_2$:

$$12(R_{\mu\nu}{}^{\rho\sigma}R^{\mu\nu}{}_{\rho\sigma})^2 = 12^3\left(A_1^4 + 2A_1^2A_2^2 + A_2^4\right) \equiv 12\mathcal{R}_1\,; \tag{3.3.30}$$

$$24R^{\mu\nu}{}_{\rho\sigma}R_{\mu\nu}{}^{\xi\eta}R_{\xi\eta}{}^{\kappa\lambda}R^{\rho\sigma}{}_{\kappa\lambda} = 8\cdot 12^2\left(A_1^4 + A_2^4\right) \equiv 24\mathcal{R}_2\,; \tag{3.3.31}$$

$$-6R^{\mu\nu}{}_{\rho\sigma}R_{\mu\nu}{}^{\xi\eta}R_{\xi}{}^{\rho\kappa}{}_{\lambda}R_{\eta}{}^{\sigma}{}_{\kappa}{}^{\lambda} = -12^2(A_1^4 + A_2^4) = -3\mathcal{R}_2\,; \tag{3.3.32}$$

$$-12R_{\mu\nu}{}^{\xi\eta}R^{\rho\sigma}{}_{\kappa\lambda}R^{\mu\nu}{}_{\rho\xi}R_{\sigma\eta}{}^{\kappa\lambda} = -12^2\cdot 4\left(A_1^4 + A_1^2A_1^2 + A_2^4\right) = -2\mathcal{R}_1 - 6\mathcal{R}_2\,; \tag{3.3.33}$$

$$\frac{3}{2}R^{\mu\nu}{}_{\xi\eta}R_{\mu\rho}{}^{\xi\sigma}R^{\eta}{}_{\lambda}{}^{\rho}{}_{\kappa}R_{\nu}{}^{\kappa}{}_{\sigma}{}^{\lambda} = 9\left(3A_1^4 + 2A_1^2A_2^2 + 3A_2^4\right) = \frac{1}{16}\mathcal{R}_1 + \frac{3}{8}\mathcal{R}_2\,; \tag{3.3.34}$$

$$\frac{3}{4}R_{\mu\nu}{}^{\xi\eta}R^{\mu\rho}{}_{\xi\sigma}R_{\rho\kappa}{}^{\sigma\lambda}R^{\nu\kappa}{}_{\eta\lambda} = 18\left(A_1^4 + 2A_1^2A_2^2 + A_2^4\right) = \frac{1}{8}\mathcal{R}_1\,. \tag{3.3.35}$$

The truncated $\mathcal{R}^4$ term in four-dimensions (3.3.29) then reads

$$\mathcal{R}^4\Big|_{\text{4d truncated}} = \frac{163}{16}\mathcal{R}_1 + \frac{123}{8}\mathcal{R}_2 = 1467(A_1^2 + A_2^2)^2 + 738(A_1^4 + A_2^4)\,. \tag{3.3.36}$$

Because the quantities $\mathcal{R}_1$ and $\mathcal{R}_2$ are both symmetric under the exchange of A_1 and A_2, they satisfy the condition (3.2.21), so the $\mathcal{R}^4$ term satisfies the leading order condition (3.2.18) and admits a no-boundary solution.

It can be surprising that this complicated scalar combination of four Riemann tensors possess such a simple expression in terms of A_1 and A_2, that is moreover symmetric in the exchange of A_1 and A_2. To prove that this is however not a general property of any scalar combination of Riemann tensors, we consider the terms:

$$R_{\mu\nu}{}^{\rho\sigma}R^{\mu\xi}{}_{\rho\sigma}R_{\xi\kappa}{}^{\nu\lambda}R^{\alpha\kappa}{}_{\alpha\lambda} = 48A_1^4 + 36A_2^4 + 48A_1A_2^3 + 24A_1^3A_2 + 60A_1^2A_2^2\,; \tag{3.3.37}$$

and

$$R^{\mu\nu}{}_{\xi\eta}R_{\mu\rho}{}^{\xi\sigma}R^{\rho\kappa}{}_{\nu\lambda}R_{\sigma\kappa}{}^{\eta\lambda} = 12(A_1^4 + A_1^2A_2^2 + A_2^4) + 12A_1(A_1^3 + A_1A_2^2 + 2A_2^3)\,. \tag{3.3.38}$$

These are both not symmetric under the exchange of A_1 and A_2. Still, they satisfy the leading order condition (3.2.18), and therefore admit a no-boundary solution.

In conclusion, known Riemann terms stemming from string theory have a structure allowing for the existence of no-boundary solutions. All covariant Riemann terms that we have studied actually allow for no-boundary solutions, and it would be very interesting if one could prove a general result in this line.

The next orders in α' of the type II string theory (3.3.25) are not Riemann terms anymore: they involve covariant derivatives acting on Riemann tensors. We cannot treat covariant derivative terms as systematically as we treated Riemann terms, because they depend on higher and higher time derivatives of the scale factor a. Instead, we study them on a case by case basis, starting with the easiest expressions and ending with the first string theory covariant derivative term, written schematically as $\nabla^4\mathcal{R}^4$ in (3.3.25).

3.4 Addition of covariant derivatives

When we start considering covariant derivatives as well, it is even less trivial that their contributions to the constraint equation still admit consistent and regular solutions. Riemann terms are linear combinations of A_1 and A_2, and these quantities only start at order t^0. Acting on them with time derivatives cannot lead to negative powers of t, that could bring singularities. But the covariant derivative is also composed of the Christoffel's symbol part: $\nabla\cdot \sim \partial\cdot + \Gamma\cdot$. For the FLRW closed metric, the time dependence of non zero Christoffel's symbols is:

$$g^{ki}\Gamma^0_{ij} \sim \frac{\dot{a}}{aN^2} \quad ; \quad \Gamma^i_{j0} \sim \frac{\dot{a}}{a} \quad \text{and} \quad \Gamma^i_{jk} \sim 1\,. \tag{3.4.1}$$

The quantity $\dot{a}/a \sim t^{-1}$ is singular, so covariant derivatives could introduce singularities into the constraint equation. Therefore we need to check term by term the existence of regular solutions in the presence of the specific covariant derivative terms we are interested in.

Consider again the time reversal transformation: $t \to -t,\ a \to -a$. On the closed FLRW background, for a generic action:

$$S = \int \mathrm{d}t\, a^3 N\ \mathcal{L}\,, \tag{3.4.2}$$

the constraint equation reads

$$\frac{\delta}{\delta N}\Big(a^3 N\mathcal{L}\Big) \equiv \frac{\partial\big(a^3 N\mathcal{L}\big)}{\partial N} - \frac{\mathrm{d}}{\mathrm{d}t}\left[\frac{\partial\big(a^3 N\mathcal{L}\big)}{\partial \dot{N}}\right] + \ldots\ = 0\ . \tag{3.4.3}$$

This constraint equation is odd under time reversal only if $\mathcal{L}$ is even under it. Because the terms A_1 and A_2 are even under time reversal, so are all Riemann terms. Since

the FLRW metric doesn't contain any mixed term g_{0i}, time derivatives always come in pairs. The Christoffel's symbols (3.4.1) with one zero index are odd under time reversal and they also always come in pairs or together with one time derivative. Therefore all covariant derivatives of Riemann terms are even under the time reversal, and their constraint equation is odd. We can thus once more use the reduced no-boundary ansatz (3.2.16) instead of the full ansatz (3.1.7).

In this section we study terms with up to four covariant derivatives acting on Riemann terms. We will therefore encounter expressions with up to four derivatives acting on the scale factor a. To ease upcoming expressions, we define

$$A_3 \equiv \frac{a^{(3)}}{aN^3} - \frac{\dot{a}\ddot{N}}{aN^4} - \left(\frac{3\dot{N}}{N^2} + \frac{\dot{a}}{aN}\right)A_2 \; ; \tag{3.4.4}$$

$$A_4 \equiv \frac{a^{(4)}}{aN^4} - \frac{\dot{a}N^{(3)}}{aN^5} - \frac{6\dot{N}}{N^2}A_3 - \left(\frac{6\dot{a}\dot{N}}{aN^3} + \frac{3\dot{N}^2}{N^4} + \frac{4\ddot{N}}{N^3}\right)A_2 - A_2^2 \; . \tag{3.4.5}$$

The calculations involving covariant derivatives are rather cluttered and won't be displayed here at full length. Instead, we explicitly investigate here the simplest example, arising when two covariant derivatives act on one Riemann tensor ($\nabla^2 R$), and delay the results of lengthier calculations to the appendices A.2 and A.3. Our final goal is to calculate the constraint equation and solution for terms of the form $\nabla^4 R^4$, which appear at the next-to-next-to-leading order (NNLO) in the type II low energy string theory effective action (3.3.25).

3.4.1 An explicit example: two covariant derivatives acting on one Riemann tensor

In this first subsection, we explicitly calculate the constraint equation of an action composed of a covariant derivative term. We focus on the simplest covariant derivative term possible,

$$\mathcal{A} \equiv \nabla^2 R = -6\left(A_4 + \frac{3\dot{a}}{aN}A_3 + 2A_2(A_2 - A_1)\right). \tag{3.4.6}$$

$\mathcal{A}$ is a scalar term composed of two covariant derivatives acting on one Riemann tensor. It is a total derivative so its constraint equation is necessarily null. We derive this explicitly here for the sake of illustration.

To compute the constraint equation of $\mathcal{A}$ we need to compute those of the terms A_4 and $\frac{\dot{a}}{aN}A_3$, or more precisely, of the actions:

$$S_{A_4} = \int \mathrm{d}t\, a^3 N A_4 \quad \text{and} \quad S_{\dot{a}A_3} = \int \mathrm{d}t\, a^3 N \frac{\dot{a}}{aN}A_3 \, . \tag{3.4.7}$$

The constraint equation for the action S_{A_4} is

$$0 = \frac{\partial(a^3 N A_4)}{\partial N} - \frac{\mathrm{d}}{\mathrm{d}t}\left[\frac{\partial(a^3 N A_4)}{\partial \dot{N}}\right] + \frac{\mathrm{d}^2}{\mathrm{d}t^2}\left[\frac{\partial(a^3 N A_4)}{\partial \ddot{N}}\right] - \frac{\mathrm{d}^3}{\mathrm{d}t^3}\left[\frac{\partial(a^3 N A_4)}{\partial N^{(3)}}\right]$$

$$\equiv \frac{\delta}{\delta N}\Big[a^3 N A_4\Big]. \tag{3.4.8}$$

Calculating the time derivatives one by one, we find:[4]

$$a^3 N\, A_4 = \frac{a^2 a^{(4)}}{N^3} - \frac{a\ddot{a}^2}{N^3} - \frac{6a^2 a^{(3)}\dot{N}}{N^4} + \frac{2a\dot{a}\ddot{a}\dot{N}}{N^4} - \frac{4a^2\ddot{a}\ddot{N}}{N^4} - \frac{a^2\dot{a}N^{(3)}}{N^4}; \tag{3.4.9}$$

$$\Rightarrow \quad \begin{cases} \dfrac{\partial(a^3 N\, A_4)}{\partial N} = -\dfrac{3}{N^4}\Big(a^2 a^{(4)} - a\ddot{a}^2\Big)\,; \\ \dfrac{\mathrm{d}}{\mathrm{d}t}\left[\dfrac{\partial(a^3 N\, A_4)}{\partial \dot{N}}\right] = \dfrac{1}{N^4}\Big(-6a^2 a^{(4)} + 2\dot{a}^2\ddot{a} + 2a\ddot{a}^2 - 10a\dot{a}a^{(3)}\Big)\,; \\ \dfrac{\mathrm{d}^2}{\mathrm{d}t^2}\left[\dfrac{\partial(a^3 N\, A_4)}{\partial \ddot{N}}\right] = \dfrac{1}{N^4}\Big(-4a^2 a^{(4)} - 8\dot{a}^2\ddot{a} - 8a\ddot{a}^2 - 16a\dot{a}a^{(3)}\Big)\,; \\ \dfrac{\mathrm{d}^3}{\mathrm{d}t^3}\left[\dfrac{\partial(a^3 N\, A_4)}{\partial N^{(3)}}\right] = \dfrac{1}{N^4}\Big(-a^2 a^{(4)} - 12\dot{a}^2\ddot{a} - 6a\ddot{a}^2 - 8a\dot{a}a^{(3)}\Big). \end{cases} \tag{3.4.10}$$

We can then plug these derivatives into (3.4.8), and find the constraint equation for the action S_{A_4}:

$$\frac{\delta}{\delta N}\Big[a^3 N A_4\Big] = \frac{1}{N^4}\Big(2\dot{a}^2\ddot{a} - a\ddot{a}^2 + 2a\dot{a}a^{(3)}\Big). \tag{3.4.11}$$

This is the procedure that is implicitly used for all further action terms. For $S_{\dot{a}A_3}$, the constraint equation is found to be

$$\frac{\delta}{\delta N}\left[a^3 N \frac{\dot{a}}{aN} A_3\right] = \frac{1}{N^4}\Big(-2a\dot{a}a^{(3)} + a\ddot{a}^2 - 2\dot{a}^2\ddot{a}\Big)\,. \tag{3.4.12}$$

In order to find the constraint equation for the full $\nabla^2 R$ (3.4.6), we only miss the term $A_2(A_2 - A_1)$. That is a simple $A_1^{p_1} A_2^{p_2}$ term whose contribution reads from (3.2.14):

$$\frac{\delta}{\delta N}\Big[a^3 N A_2\Big(A_2 - A_1\Big)\Big] = \frac{1}{N^4}\Big(2a\dot{a}a^{(3)} - a\ddot{a}^2 + 2\dot{a}^2\ddot{a}\Big)\,. \tag{3.4.13}$$

The constraint equation for $\mathcal{A}$ is therefore 0 as expected:

$$\begin{aligned} \delta\mathcal{A} \equiv \frac{\delta}{\delta N}\Big[a^3 N\mathcal{A}\Big] &= -6\left[\frac{\delta}{\delta N}\Big[a^3 N A_4\Big] + 3\frac{\delta}{\delta N}\left[a^3 N\frac{\dot{a}}{aN}A_3\right] + 2\frac{\delta}{\delta N}\Big[a^3 N A_2\Big(A_2 - A_1\Big)\Big]\right] \\ &= 0\,. \end{aligned} \tag{3.4.14}$$

3.4.2 General procedure

The method presented in the previous subsection enable us in theory to compute the constraint equation for any covariant derivatives term. The calculation is made even easier by using the following decomposition.

[4] All following expressions in this chapter are evaluated at constant lapse N, so we drop all terms containing more than one power of a derivative of N.

Suppose we know the constraint equations for the two actions:

$$S_A = \int \mathrm{d}t\, a^3 N\, A \quad \text{and} \quad S_B = \int \mathrm{d}t\, a^3 N\, B\ , \tag{3.4.15}$$

where A and B are functions of a, N and their time derivatives. Then the constraint equation for the action

$$S_{A\cdot B} = \int \mathrm{d}t\, a^3 N\, A\cdot B\,, \tag{3.4.16}$$

will be given by

$$\begin{aligned}
\frac{\delta}{\delta N}\Big[a^3 N\, A\cdot B\Big] = {} & A\cdot\frac{\delta}{\delta N}\Big[a^3 N\, B\Big] + B\cdot\frac{\delta}{\delta N}\Big[a^3 N\, A\Big] - a^3 A\cdot B \\
& - \dot{A}\cdot\left[\frac{\partial(a^3 N\, B)}{\partial\dot{N}} - 2\frac{\mathrm{d}}{\mathrm{d}t}\Big(\frac{\partial(a^3 N\, B)}{\partial\ddot{N}}\Big) + 3\frac{\mathrm{d}^2}{\mathrm{d}t^2}\Big(\frac{\partial(a^3 NB)}{\partial N^{(3)}}\Big)\right] \\
& + \ddot{A}\left[\frac{\partial(a^3 N\, B)}{\partial\ddot{N}} - 3\frac{\mathrm{d}}{\mathrm{d}t}\Big(\frac{\partial(a^3 NB)}{\partial N^{(3)}}\Big)\right] - A^{(3)}\frac{\partial(a^3 NB)}{\partial N^{(3)}} \\
& - \dot{B}\cdot\left[\frac{\partial(a^3 N\, A)}{\partial\dot{N}} - 2\frac{\mathrm{d}}{\mathrm{d}t}\Big(\frac{\partial(a^3 N\, A)}{\partial\ddot{N}}\Big) + 3\frac{\mathrm{d}^2}{\mathrm{d}t^2}\Big(\frac{\partial(a^3 NA)}{\partial N^{(3)}}\Big)\right] \\
& + \ddot{B}\left[\frac{\partial(a^3 N\, A)}{\partial\ddot{N}} - 3\frac{\mathrm{d}}{\mathrm{d}t}\Big(\frac{\partial(a^3 NA)}{\partial N^{(3)}}\Big)\right] - B^{(3)}\frac{\partial(a^3 NA)}{\partial N^{(3)}}\,.
\end{aligned} \tag{3.4.17}$$

This assumes that A and B depend on the third derivative of N at most, as will be the case in this chapter. It would be trivial to extend (3.4.17) to include higher orders. Using this decomposition, we can construct the constraint equations of more and more involved expressions of A_1, A_2, A_3 and A_4. For instance, we may consider the four following covariant expressions:

$$\begin{aligned}
&\mathcal{B}_1 \equiv (\nabla_\mu R_{\alpha\beta\gamma\delta})(\nabla^\mu R^{\alpha\beta\gamma\delta})\,; \quad \mathcal{B}_2 \equiv (\nabla_\mu R_{\alpha\beta})(\nabla^\mu R^{\alpha\beta})\,; \\
&\mathcal{B}_3 \equiv (\nabla_\mu R)(\nabla^\mu R) \qquad \text{and} \qquad \mathcal{B}_4 \equiv (\nabla_\mu R^{\mu}{}_{\alpha\beta\gamma})(\nabla_\nu R^{\nu\alpha\beta\gamma})\,.
\end{aligned} \tag{3.4.18}$$

They are expressed in terms of the quantities A_1, A_2 and A_3 as

$$-\frac{\mathcal{B}_1}{12} = A_3^2 + \frac{8\dot{a}^2}{a^2N^2}(A_2-A_1)^2\,; \quad -\frac{\mathcal{B}_2}{12} = A_3^2 + \frac{2\dot{a}}{aN}(A_2-A_1)A_3 + \frac{6\dot{a}^2}{a^2N^2}(A_2-A_1)^2\,; \tag{3.4.19}$$

$$-\frac{\mathcal{B}_3}{36} = A_3^2 + \frac{4\dot{a}}{aN}(A_2-A_1)A_3 + \frac{4\dot{a}^2}{a^2N^2}(A_2-A_1)^2\,; \quad -\frac{\mathcal{B}_4}{6} = \left[2(A_2-A_1)\frac{\dot{a}}{aN} + A_3\right]^2. \tag{3.4.20}$$

The constraint equation of these four expressions (3.4.18) thus only requires to calculate that of the actions:

$$S_{A_3} = \int \mathrm{d}t\, a^3 N A_3 \quad \text{and} \quad S_{\dot{a}(A_2-A_1)} = \int \mathrm{d}t\, a^3 N \frac{\dot{a}}{aN}\Big(A_2 - A_1\Big)\,; \tag{3.4.21}$$

and combine these using (3.4.17).[5]

To summarize, the constraint equation of any covariant derivative terms can be calculated by following the four subsequent steps:

1. Decompose the expression in terms of A_1, A_2, A_3 and A_4.[6]
2. Find the basic blocks needed to build each terms in this expression (in the previous example those were (3.4.21)), and compute their constraint equation.
3. Use the formula (3.4.17) (iteratively if needed) to combine the basic blocks and get the complete constraint equation for the initial covariant expression.
4. Plug in the no-boundary ansatz (3.2.16). This step is commutative with the previous one.

In the appendix A.2, we present the results of this method applied for the $\mathcal{B}$ terms (3.4.18) and for the following terms where four covariant derivatives act on two Riemann tensors:

$$\begin{aligned} &\mathcal{C}_1 \equiv \nabla^2 R_{\alpha\beta\gamma\delta}\, \nabla^2 R^{\alpha\beta\gamma\delta}\ ; && \mathcal{C}_2 \equiv \nabla^2 R_{\alpha\beta}\, \nabla^2 R^{\alpha\beta}\ ; && \mathcal{C}_3 \equiv \nabla^2 R\, \nabla^2 R\ ; \\ &\mathcal{C}_4 \equiv \nabla_\mu\nabla_\nu R_{\alpha\beta\gamma\delta}\nabla^\mu\nabla^\nu R^{\alpha\beta\gamma\delta}\ ; && \mathcal{C}_5 \equiv \nabla_\mu\nabla_\nu R_{\alpha\beta}\nabla^\mu\nabla^\nu R^{\alpha\beta}\ ; && \mathcal{C}_6 \equiv \nabla_\mu\nabla_\nu R\, \nabla^\mu\nabla^\nu R\ . \end{aligned} \tag{3.4.22}$$

It is essential for the existence of the no-boundary solution that the constraint equations of all these expressions always start at order t^3 and are regular in $t \to 0$, although in principle they could have started at order t^{-1} and be singular. This particularity will continue to hold for the cases of four derivatives acting on four Riemann tensor, to which we now turn.

3.4.3 Four covariant derivatives acting on four Riemann tensors

We can now evaluate the contributions to the constraint equation stemming from the $\nabla^4\mathcal{R}^4$ terms (these terms are discussed in more detail in [73], see also [74]). We focus on the truncated part of $\mathcal{R}^4$ (3.3.29):

$$\mathcal{R}^4\Big|_{\text{4d truncated}} = \frac{163}{16}\mathcal{R}_1 + \frac{123}{8}\mathcal{R}_2\,; \tag{3.4.23}$$

where we recall that $\mathcal{R}_1 = (R_{\alpha\beta\gamma\delta}R^{\alpha\beta\gamma\delta})^2$ and $\mathcal{R}_2 = R^{\alpha\beta}{}_{\gamma\delta}R_{\alpha\beta}{}^{\epsilon\zeta}R_{\epsilon\zeta}{}^{\eta\theta}R^{\gamma\delta}{}_{\eta\theta}$. When four covariant derivatives act on four Riemann tensors, we find three types of terms inequivalent up to integrations by part[7]

$$(\nabla R)^4 \quad ; \quad (\nabla^2 R)^2 R^2 \quad \text{and} \quad (\nabla^2 R)(\nabla R)^2 R\,. \tag{3.4.24}$$

[5] Note also that other terms like $R^{\mu\nu}(\nabla^2 R_{\mu\nu})$ or $R(\nabla^2 R)$ can be obtained from these $\mathcal{B}$ terms (3.4.18) by integrating by parts, since two terms differing by a total derivative lead to the same constraint equation.

[6] This is only valid for terms where at most four covariant derivatives are acting on Riemann tensors.

[7] The R here does not refer to the Ricci scalar but is a schematic way of writing the Riemann tensor without bothering about the indices.

For these three types, we now construct all possible independent terms where the four Riemann tensors are either $\mathcal{R}_1$ or $\mathcal{R}_2$.

Type 1: $(\nabla R)^4$ terms.

These terms can all be written as linear combinations of the four following terms:

$$\mathcal{D}_1 \equiv \left(\nabla_\mu R_{\alpha\beta\gamma\delta}\, \nabla^\mu R^{\alpha\beta\gamma\delta}\right)^2 ; \qquad \mathcal{D}_2 \equiv \left(\nabla_\mu R_{\alpha\beta\gamma\delta} \nabla_\nu R^{\alpha\beta\gamma\delta} \nabla^\mu R_{\epsilon\zeta\eta\theta} \nabla^\nu R^{\epsilon\zeta\eta\theta}\right) ;$$
$$\mathcal{D}_3 \equiv \left(\nabla_\mu R^{\alpha\beta}{}_{\gamma\delta} \nabla^\mu R_{\alpha\beta}{}^{\epsilon\zeta} \nabla_\nu R_{\epsilon\zeta}{}^{\eta\theta} \nabla^\nu R_{\eta\theta}{}^{\gamma\delta}\right); \qquad \mathcal{D}_4 \equiv \left(\nabla_\mu R^{\alpha\beta}{}_{\gamma\delta} \nabla_\nu R_{\alpha\beta}{}^{\epsilon\zeta} \nabla^\mu R_{\epsilon\zeta}{}^{\eta\theta} \nabla^\nu R_{\eta\theta}{}^{\gamma\delta}\right). \tag{3.4.25}$$

They are expressed in terms of A_1, A_2 and A_3 in the appendix A.3. Computing their contributions to the constraint equation requires the computation of the following constraint equations:

$$\Delta_1 \equiv \frac{\delta}{\delta N}\left[a^3 N\, A_3^4\right] = \frac{32(a_3^2 - a_1 a_5)^3}{9 a_1^{15}} t^3 + \mathcal{O}\left(t^5\right) ; \tag{3.4.26}$$

$$\Delta_2 \equiv \frac{\delta}{\delta N}\left[a^3 N \frac{\dot{a}^4}{a^4 N^4}(A_2 - A_1)^4\right] = \frac{(a_1 a_5 - a_3^2)^3}{72 a_1^{15}} \cdot t^3 + \mathcal{O}\left(t^5\right) ; \tag{3.4.27}$$

$$\Delta_3 \equiv \frac{\delta}{\delta N}\left[a^3 N \frac{\dot{a}^2}{a^2 N^2} A_3^2 (A_2 - A_1)^2\right] = \mathcal{O}\left(t^5\right) ; \tag{3.4.28}$$

$$\Delta_4 \equiv \frac{\delta}{\delta N}\left[a^3 N \frac{\dot{a}^3}{a^3 N^3} A_3 \big(A_2 - A_1\big)^3\right] = \frac{(a_1 a_5 - a_3^2)^3}{36 a_1^{15}} \cdot t^3 + \mathcal{O}\left(t^5\right) . \tag{3.4.29}$$

Combining these, we find the contributions to the constraint coming from the four $\mathcal{D}$ terms displayed in Appendix A.3. We stress here that up to order t^3, these four terms have the same structure involving the combination $a_3^2 - a_1 a_5$ (α_i are specific numerical factors):

$$\delta\mathcal{D}_i = \alpha_i \frac{(a_3^2 - a_1 a_5)^3}{a_1^{15}} t^3 + \mathcal{O}(t^5) . \tag{3.4.30}$$

Type 2: $(\nabla^2 R)^2 R^2$ terms

In this case we can construct eight different independent expressions (also expressed in terms of A_1, A_2, A_3, A_4 in appendix A.3):

$$\mathcal{E}_1 \equiv \nabla^2 R_{\alpha\beta\gamma\delta}\left(\nabla^2 R^{\alpha\beta\gamma\delta}\right) R_{\epsilon\zeta\eta\theta} R^{\epsilon\zeta\eta\theta} ; \qquad \mathcal{E}_2 \equiv \nabla_\mu \nabla_\nu (R_{\alpha\beta\gamma\delta}) \nabla^\mu \nabla^\nu (R^{\alpha\beta\gamma\delta}) R_{\epsilon\zeta\eta\theta} R^{\epsilon\zeta\eta\theta} ;$$
$$\mathcal{E}_3 \equiv \left((\nabla^2 R_{\alpha\beta\gamma\delta}) R^{\alpha\beta\gamma\delta}\right)^2 ; \qquad \mathcal{E}_4 \equiv \nabla_\mu \nabla_\nu (R_{\alpha\beta\gamma\delta}) \nabla^\mu \nabla^\nu (R_{\epsilon\zeta\eta\theta}) R^{\alpha\beta\gamma\delta} R^{\epsilon\zeta\eta\theta} ;$$
$$\mathcal{E}_5 \equiv \nabla^2 R^{\alpha\beta}{}_{\gamma\delta}\left(\nabla^2 R_{\alpha\beta}{}^{\epsilon\zeta}\right) R_{\epsilon\zeta}{}^{\eta\theta} R^{\gamma\delta}{}_{\eta\theta} ; \qquad \mathcal{E}_6 \equiv \nabla_\mu \nabla_\nu (R^{\alpha\beta}{}_{\gamma\delta}) \nabla^\mu \nabla^\nu (R_{\alpha\beta}{}^{\epsilon\zeta}) R_{\epsilon\zeta}{}^{\eta\theta} R^{\gamma\delta}{}_{\eta\theta} ;$$
$$\mathcal{E}_7 \equiv \nabla^2 R^{\alpha\beta}{}_{\gamma\delta}\left(\nabla^2 R_{\epsilon\zeta}{}^{\eta\theta}\right) R_{\alpha\beta}{}^{\epsilon\zeta} R^{\gamma\delta}{}_{\eta\theta} ; \qquad \mathcal{E}_8 \equiv \nabla_\mu \nabla_\nu (R^{\alpha\beta}{}_{\gamma\delta}) \nabla^\mu \nabla^\nu (R_{\epsilon\zeta}{}^{\eta\theta}) R_{\alpha\beta}{}^{\epsilon\zeta} R^{\gamma\delta}{}_{\eta\theta} .$$

Type 3: $(\nabla^2 R)(\nabla R)^2 R$ **terms**

The possible terms constructed from $\mathcal{R}_1$ and $\mathcal{R}_2$ are (see again appendix A.3)

$$\begin{aligned}
\mathcal{F}_1 \equiv&(\nabla^2 R_{\alpha\beta\gamma\delta})R^{\alpha\beta\gamma\delta}\nabla_\mu R_{\epsilon\zeta\eta\theta}\nabla^\mu R^{\epsilon\zeta\eta\theta}\ ; \quad \mathcal{F}_2 \equiv (\nabla_\mu\nabla_\nu R_{\alpha\beta\gamma\delta})R^{\alpha\beta\gamma\delta}\nabla^\mu R_{\epsilon\zeta\eta\theta}\nabla^\nu R^{\epsilon\zeta\eta\theta}\ ;\\
\mathcal{F}_3 \equiv&(\nabla^2 R_{\alpha\beta\gamma\delta})R_{\epsilon\zeta\eta\theta}\nabla_\mu R^{\alpha\beta\gamma\delta}\nabla^\mu R^{\epsilon\zeta\eta\theta}\ ; \quad \mathcal{F}_4 \equiv (\nabla_\mu\nabla_\nu R_{\alpha\beta\gamma\delta})R_{\epsilon\zeta\eta\theta}\nabla^\mu R^{\alpha\beta\gamma\delta}\nabla^\nu R^{\epsilon\zeta\eta\theta}\ ;\\
\mathcal{F}_5 \equiv&\Big(\nabla^2 R^{\alpha\beta}{}_{\gamma\delta}\Big)R_{\alpha\beta}{}^{\epsilon\zeta}\nabla_\mu R_{\epsilon\zeta}{}^{\eta\theta}\nabla^\mu R^{\gamma\delta}{}_{\eta\theta}\ ; \quad \mathcal{F}_6 \equiv \nabla_\mu\nabla_\nu(R^{\alpha\beta}{}_{\gamma\delta})R_{\alpha\beta}{}^{\epsilon\zeta}\nabla^\mu R_{\epsilon\zeta}{}^{\eta\theta}\nabla^\nu R^{\gamma\delta}{}_{\eta\theta}\ ;\\
\mathcal{F}_7 \equiv&\Big(\nabla^2 R^{\alpha\beta}{}_{\gamma\delta}\Big)R_{\epsilon\zeta}{}^{\eta\theta}\nabla_\mu R_{\alpha\beta}{}^{\epsilon\zeta}\nabla^\mu R^{\gamma\delta}{}_{\eta\theta}\ ; \quad \mathcal{F}_8 \equiv \nabla_\mu\nabla_\nu(R^{\alpha\beta}{}_{\gamma\delta})R_{\epsilon\zeta}{}^{\eta\theta}\nabla^\mu R_{\alpha\beta}{}^{\epsilon\zeta}\nabla^\nu R^{\gamma\delta}{}_{\eta\theta}\ .
\end{aligned}$$

To compute the contribution to the constraint equation stemming from the $\mathcal{E}$ and $\mathcal{F}$ terms, we must compute those of the 31 following building blocks:

$$\begin{aligned}
&\gamma_1 = A_1^2A_2^2(A_2-A_1)^2\,; \quad \gamma_2 = A_2^4(A_2-A_1)^2\,; \quad \gamma_3 = A_1A_2^3(A_2-A_1)^2\,;\\
&\gamma_4 = A_1^2A_4^2\,; \quad \gamma_5 = A_2^2A_4^2\,; \quad \gamma_6 = A_1A_2^2(A_2-A_1)A_4\,;\\
&\gamma_7 = A_2A_3^2A_4\ ; \quad \gamma_8 = A_1A_2(A_2-A_1)A_3^2\ ; \quad \gamma_9 = \frac{\dot a}{aN}A_1^2A_2(A_2-A_1)A_3\,;\\
&\gamma_{10} = \frac{\dot a}{aN}A_2^3(A_2-A_1)A_3\ ; \quad \gamma_{11} = \frac{\dot a}{aN}A_1A_2^2(A_2-A_1)A_3\,; \quad \gamma_{12} = \frac{\dot a}{aN}A_1^2A_3A_4\,;\\
&\gamma_{13} = \frac{\dot a}{aN}A_1A_2A_3A_4\,; \quad \gamma_{14} = \frac{\dot a}{aN}A_2^2A_3A_4\,; \quad \gamma_{15} = \frac{\dot a}{aN}A_1A_3^3\,;\\
&\gamma_{16} = \frac{\dot a}{aN}A_2A_3^3\,; \quad \gamma_{17} = \frac{\dot a^2}{a^2N^2}A_1^2A_2(A_2-A_1)^2\,; \quad \gamma_{18} = \frac{\dot a^2}{a^2N^2}A_1A_2^2(A_2-A_1)^2\,;\\
&\gamma_{19} = \frac{\dot a^2}{a^2N^2}A_2^3(A_2-A_1)^2\,; \quad \gamma_{20} = \frac{\dot a^2}{a^2N^2}A_1^2A_3^2\ ; \quad \gamma_{21} = \frac{\dot a^2}{a^2N^2}A_1A_2A_3^2\,;\\
&\gamma_{22} = \frac{\dot a^2}{a^2N^2}A_2^2A_3^2\ ; \quad \gamma_{23} = \frac{\dot a^2}{a^2N^2}A_1^2(A_2-A_1)A_4\,; \quad \gamma_{24} = \frac{\dot a^2}{a^2N^2}A_1A_2(A_2-A_1)A_4\,;\\
&\gamma_{25} = \frac{\dot a^2}{a^2N^2}A_2^2(A_2-A_1)A_4\,; \quad \gamma_{26} = \frac{\dot a^3}{a^3N^3}A_1^2(A_2-A_1)A_3\,; \quad \gamma_{27} = \frac{\dot a^3}{a^3N^3}A_1A_2(A_2-A_1)A_3\,;\\
&\gamma_{28} = \frac{\dot a^3}{a^3N^3}A_2^2(A_2-A_1)A_3\ ; \quad \gamma_{29} = \frac{\dot a^4}{a^4N^4}A_1^2(A_2-A_1)^2\,; \quad \gamma_{30} = \frac{\dot a^4}{a^4N^4}A_1A_2(A_2-A_1)^2\,;\\
&\gamma_{31} = \frac{\dot a^4}{a^4N^4}A_2^2(A_2-A_1)^2\,.
\end{aligned}$$

We denote $\Gamma_i \equiv \dfrac{\delta}{\delta N}\Big[a^3N\,\gamma_i\Big]$, the constraint contributions from these basic expressions. All $\mathcal{E}$ and $\mathcal{F}$ terms are linear combinations of the γ terms, so their constraint equations will be equal to the same linear combination of the corresponding Γ.

First we compute the contributions from all the γ terms, and plug them in the no-boundary ansatz (3.2.16). Then we expand all Γ's to order t^3. Only nine out of these 31 terms actually start at order t^{-1} (as generically expected of terms where four covariant derivatives act on Riemann terms). They are, to leading order,[8]

$$\Gamma_{23} = \Gamma_{24} = \Gamma_{25} = -\frac{2a_3^2\Big(a_3^2 - a_1a_5\Big)}{a_1^{13}t} \quad ; \quad \Gamma_{26} = \Gamma_{27} = \Gamma_{28} = -\frac{2a_3^2\Big(a_3^2 - a_1a_5\Big)}{3a_1^{13}t}\ ; \tag{3.4.31}$$

[8] These equalities are only valid at order t^{-1}.

$$\text{and} \quad \Gamma_{29} = \Gamma_{30} = \Gamma_{31} = -\frac{a_3^2\left(a_3^2 - a_1 a_5\right)}{3a_1^{13}t} \ . \tag{3.4.32}$$

In the $\mathcal{E}$ and $\mathcal{F}$ terms, these nine terms appear in the eleven following combinations that start at least at order t:

$$\begin{aligned}
&\frac{\delta}{\delta N}\left[\frac{\dot{a}^2}{a^2N^2}(A_2 - A_1)^3 A_4\right] \equiv \Gamma_{23} - 2\Gamma_{24} + \Gamma_{25} = \mathcal{O}(t^3) \ ; \\
&\frac{\delta}{\delta N}\left[\frac{\dot{a}^2}{a^2N^2}A_1(A_2 - A_1)^2 A_4\right] \equiv \Gamma_{24} - \Gamma_{23} = \mathcal{O}(t) \ ; \\
&\frac{\delta}{\delta N}\left[\frac{\dot{a}^2}{a^2N^2}A_2(A_2 - A_1)^2 A_4\right] \equiv \Gamma_{25} - \Gamma_{24} = \mathcal{O}(t) \ ; \\
&\frac{\delta}{\delta N}\left[\frac{\dot{a}^3}{a^3N^3}A_3(A_2 - A_1)^3\right] = \Delta_4 \equiv \Gamma_{26} - 2\Gamma_{27} + \Gamma_{28} = \mathcal{O}(t^3) \ ; \\
&\frac{\delta}{\delta N}\left[\frac{\dot{a}^3}{a^3N^3}A_3A_1(A_2 - A_1)^2\right] \equiv \Gamma_{27} - \Gamma_{26} = \mathcal{O}(t) \ ; \\
&\frac{\delta}{\delta N}\left[\frac{\dot{a}^3}{a^3N^3}A_3A_2(A_2 - A_1)^2\right] \equiv \Gamma_{28} - \Gamma_{27} = \mathcal{O}(t) \ ; \\
&\frac{\delta}{\delta N}\left[\frac{\dot{a}^4}{a^4N^4}(A_2 - A_1)^4\right] = \Delta_2 \equiv \Gamma_{29} - 2\Gamma_{30} + \Gamma_{31} = \mathcal{O}(t^3) \ ; \\
&\frac{\delta}{\delta N}\left[\frac{\dot{a}^4}{a^4N^4}A_1(A_2 - A_1)^3\right] \equiv \Gamma_{30} - \Gamma_{29} = \mathcal{O}(t) \ ; \\
&\frac{\delta}{\delta N}\left[\frac{\dot{a}^4}{a^4N^4}A_2(A_2 - A_1)^3\right] \equiv \Gamma_{31} - \Gamma_{30} = \mathcal{O}(t) \ ; \\
&\frac{\delta}{\delta N}\left[\frac{\dot{a}^3}{a^3N^3}A_1^2(A_2 - A_1)\left(A_3 - \frac{\dot{a}}{aN}(A_2 - A_1)\right)\right] \equiv \Gamma_{26} - 2\Gamma_{29} = \mathcal{O}(t) \ ; \\
&\frac{\delta}{\delta N}\left[\frac{\dot{a}^2}{a^2N^2}A_1^2(A_2 - A_1)\left(A_4 - \frac{\dot{a}}{aN}A_3 - \frac{4\dot{a}^2}{a^2N^2}(A_2 - A_1)\right)\right] \equiv \Gamma_{23} - \Gamma_{26} - 4\Gamma_{29} = \mathcal{O}(t).
\end{aligned}$$

Interestingly, the cancellations go even further and the contributions at order t also vanish identically. The full expressions, which start at order t^3, are listed in the appendix A.3. Schematically, the order t^3 contribution of all $\delta\mathcal{F}$ terms can be written as

$$\delta\mathcal{F} = \frac{\left(a_3^2 - a_1a_5\right)t^3}{a_1^{15}}\left[\lambda_1\left(a_3^2 - a_1a_5\right)^2 + \lambda_2 a_1a_5\left(a_3^2 - a_1a_5\right) + \lambda_3 a_1a_3\left(a_3a_5 - a_1a_7\right)\right] + \mathcal{O}(t^5)\,; \tag{3.4.33}$$

where λ_1, λ_2 and λ_3 take different numerical values for each combination of derivatives. As for the $\mathcal{E}$ terms, their contribution to the constraint is of the form

$$\begin{aligned}
\delta\mathcal{E} = \frac{t^3}{a_1^{15}}\Big[&\mu_1\left(a_3^2 - a_1a_5\right)^3 + \mu_2\, a_1a_5\left(a_3^2 - a_1a_5\right)^2 + a_1a_3\left(\mu_3\, a_5a_3 + \mu_4\, a_1a_7\right)\left(a_3^2 - a_1a_5\right) \\
&+ \mu_5\, a_1^2a_3a_5\left(a_3a_5 - a_1a_7\right) + \mu_6\, a_1^2a_3^2\left(a_1a_9 - a_3a_7\right)\Big] + \mathcal{O}(t^5)\,;
\end{aligned} \tag{3.4.34}$$

where μ_i are numerical factors varying for each case.

All pieces are eventually in place to compute the constraint equation of the type II

string theory effective action up to fifth order in α' (3.3.25), and assess the existence of a no-boundary solution for this action.

3.4.4 Constraint equation for type II string theory

The type II effective string action (3.3.25), compactified to four dimension, reads:

$$S^{4D}_{\text{type II}} = \frac{1}{2\kappa^2}\int \mathrm{d}^4x\sqrt{-g}\Big[R-(\partial\phi)^2-2V(\phi)+(\alpha')^3\mathcal{E}_{(0,0)}\mathcal{R}^4+(\alpha')^5\mathcal{E}_{(1,0)}\nabla^4\mathcal{R}^4+\mathcal{O}(\alpha'^6) \\ +\cdots\Big].$$

We have included a single scalar field with a potential $V(\phi)$, but the ellipsis stands for many additional scalars and gauge fields. The precise form of the action depends on the details of the compactification, but once again we can restrict to a constant scalar field and null gauge field since we focus on the no-boundary point 3.1. Similarly, the contributions in higher powers of α' must be thought of as containing compactification-dependent coefficient functions θ, δ_i, ϵ_i and η_i, in front of the specific combinations $\mathcal{D},\mathcal{E},\mathcal{F}$ that we introduced in section 3.4.3:

$$\mathcal{E}_{(0,0)}\mathcal{R}^4=\theta\left(\mathcal{R}_1+\frac{246}{163}\mathcal{R}_2\right)\quad\text{and}\quad\mathcal{E}_{(1,0)}\nabla^4\mathcal{R}^4=\sum_{i=1}^{4}\delta_i\mathcal{D}_i+\sum_{i=1}^{8}\epsilon_i\mathcal{E}_i+\sum_{i=1}^{8}\eta_i\mathcal{F}_i\,. \tag{3.4.35}$$

Does this theory admit no-boundary solutions? As demonstrated in the previous section, the constraint equation, that provides the litmus test for the existence of regular solutions, does not receive α' corrections at order t^{-1} nor at order t when the no-boundary ansatz (3.2.16) is plugged in, due to the specific form of the $\mathcal{D},\mathcal{E},\mathcal{F}$ terms. This rather astonishing result may have an underlying explanation in the fact that no-boundary solutions approach Euclidean flat space smoothly near the South Pole, so that covariant derivatives acting on the corresponding Riemann tensors are suppressed. In fact, the first non-trivial contributions to the constraint equation arise at order t^3, where the constraint takes the form:

$$\begin{aligned}&-6a_3t^3-2V(\phi_0)a_1^3t^3+(\alpha')^3\mathcal{E}_{(0,0)}\left[2205\cdot\frac{2a_3^2}{a_1^9}\left(3a_1a_5-4a_3^2\right)t^3-2934\cdot\frac{a_3^2}{a_1^9}\left(2a_3^2-a_1a_5\right)t^3\right]\\&+(\alpha')^5\mathcal{E}_{(0,1)}\left[\#_1\cdot\frac{\left(a_3^2-a_1a_5\right)^3}{a_1^{15}}t^3+\#_2\cdot\frac{a_5\left(a_3^2-a_1a_5\right)^2}{a_1^{14}}\right.\\&\qquad+\left[\#_3\cdot a_3^2a_5+\#_4\cdot a_1a_3a_7\right]\frac{a_3^2-a_1a_5}{a_1^{14}}+\#_5\cdot\frac{a_3a_5\left(a_3a_5-a_1a_7\right)}{a_1^{13}}\\&\qquad\left.+\#_6\cdot\frac{a_3^2\left(a_1a_9-a_3a_7\right)}{a_1^{13}}\right]=0\,.\end{aligned} \tag{3.4.36}$$

Here we denoted the South Pole dilaton value as $\phi(0)=\phi_0$ and the numerical coefficients at order α'^5 by $\#_i$. In the absence of higher order corrections we would have learned that

$a_3 = -\frac{V(\phi_0)}{3}a_1^3$, i.e., that the initial expansion rate depends on the location of the scalar field on the potential. Once the higher order terms are added, new families of solutions arise, and depending on the coefficient functions, a_5, a_7 and even a_9 can enter the order t^3 of the constraint equation. At higher orders in t, higher order terms in the series expansion for a also appear, and in this manner higher coefficients continue to be given in terms of the lower order ones. Also, for terms with more derivatives, such as terms of the form $\nabla^6\mathcal{R}^4$, we expect higher Taylor series coefficients of the scale factor a to arise, similarly to the results for $\mathcal{C}$ terms (see appendix A.2). For perturbative solutions, a self-consistency check will be that the solutions should have a smooth limit as $\alpha' \to 0$ (similarly to the limit $\beta \to 0$ for quadratic gravity 3.3.1). Overall, given the current knowledge about α' corrections, perturbative no-boundary solutions do exist in type II string theory.

3.5 Discussion

In this chapter, we have assessed the ability of the no-boundary proposal to survive the addition to GR of perturbative quantum corrections, that are generically expected to arise in cosmology when we approach the big bang singularity (see chapter 1), which is precisely the context in which the no-boundary proposal is useful. From known theories, we expect these corrections to contain Riemann tensors and covariant derivatives thereof. We have derived generic conditions that correction terms consisting only of Riemann tensors must satisfy for no-boundary solutions to exist. We have then showed that these conditions are in particular satisfied by $f(R)$ gravity, quadratic gravity, Gauß-Bonnet gravity, heterotic string theory and type II string theory at the order $(\alpha')^3$. Moreover, we have proved that (at least certain) terms containing covariant derivatives of the Riemann tensor can also allow for a no-boundary solution. In particular we showed it was the case for the type II string theory up to order α'^5. This opens the question of whether string theory in general has a structure that allows for the existence of no-boundary solutions, but also of whether one could generically prove that all covariant (derivative) Riemann terms lead to actions admitting a no-boundary solution.

The results presented in this chapter furnish a crucial consistency check of the no-boundary proposal, and they also suggest that results found at the semi-classical level from the gravitational path integral can continue to hold in perturbative quantum gravity.

Chapter 4

Inclusion of matter fields in the no-boundary description

As explained in the introductory chapter 2.2, the recent development of the no-boundary proposal suggests that a definition of the wavefunction of the universe based on the field space, i.e., summing over initially compact metrics in the path integral, cannot be made consistent [44]. Instead, a momentum space definition, where the path integral sums over initially regular metrics, has been advocated in [52]. Further support to this new no-boundary proposal came from the study of the gravitational path integral in the presence of a negative cosmological constant [53]. There, boundary conditions equivalent to those of the momentum space definition of the no-boundary are needed in order to recover the result expected for the wavefunction from the AdS/CFT correspondence [75]. The standard no-boundary proposal is then obtained by analytically continuing the cosmological constant from negative to positive values [76]. In the third chapter of this thesis, we have shown that no-boundary on-shell solutions, which are both compact and regular at the South Pole, continue to exist when we extend the Einstein-Hilbert action for gravity, and include higher-order corrections stemming for example from string theory. This important result attests of the no-boundary solution consistency at the level of (perturbative) quantum gravity. In that chapter, we also showed that within the no-boundary proposal, the only matter field allowed must have an equation of state that approaches that of a cosmological constant at the South Pole. This is in particular the case of a scalar field ϕ which tends to a constant value close to $t = 0$, i.e., such that $\dot{\phi}(t = 0) = 0$. Therefore, a necessary step in proving the consistency of the no-boundary proposal is to show that it is also robust to the inclusion of such a scalar matter field. This was already studied at great length in the past [39, 40], for the field space no-boundary definition.

In the present chapter we study the inclusion of a scalar matter field into the momentum space definition of the no-boundary proposal. The results of our study, presented in [3], are that:

- similarly to the pure gravity case, the regularity condition implies that the wavefunction of the universe has **no momentum flow** at the the South Pole;

- the regularity condition is not unique in this case, but leads to a family of initial conditions parameterized by γ (that can in some specific cases be interpreted as the initial scalar field value);
- saddle point geometries are always regular, but are compact only for certain values of γ. These compact geometries are generically paired up with a non-compact geometry;
- non-compact saddle point geometries appearing alongside compact ones are always subdominant to them in the path integral defining the no-boundary wavefunction;
- dominant saddle point geometries lead to a WKB wavefunction (and hence predict a classical spacetime) only for inflationary regions of the scalar field potential.

In our analysis, we focus on four different scalar field potentials, all presenting different physical features, but that can be parameterized in a common manner. In particular, we study one **inflationary potential containing a slow-roll region** (see section 4.2), one **negative AdS-like potential** extending the AdS gravitational path integral case [53] (see section 4.3), one **exponential potential** which also allows for inflationary scaling solutions at the classical level (see section 4.4), and finally an unrealistic hyperbolic sine potential (see 4.5). Those different potentials are presented in more details in next section 4.1 and displayed in figure 4.1.

The results found in this chapter and summarized here above lead to some puzzling conclusions concerning the no-boundary wavefunction definition. In contrast with the field space no-boundary definition, here the regularity condition does not uniquely fix the initial conditions for the scale factor and the scalar field. Additional conditions must be met in order to define the wavefunction consistently, for example here we request the existence of compact saddle points. These additional requirements may imply a non-causal behavior of the solution, in the sense that the initial scalar field value depends on the final values of the scale factor and scalar field. We discuss this unphysical consequence at a larger extent in the discussion section 4.6 of this chapter. We also come back to it in chapter 6, where we discuss a new criterion filtering complex metrics in quantum gravity, that brings new lights on the question of scalar fields.

4.1 Set-up and models

In this chapter we consider once more the no-boundary wavefunction of the universe, $\Psi[h_{ij}, \Phi_{\rm f}]$, as a functional of a three-dimensional hypersurface h_{ij} and of a scalar field final configuration $\Phi_{\rm f}$ living on the hypersurface. The arguments $[h_{ij}, \Phi_{\rm f}]$ represent a late, classical state of the universe (for example a post-inflationary state), and the wavefunction yields probabilities for different consistent histories of the universe [35]. As recalled in 2.2, the no-boundary wavefunction is defined by a **Lorentzian** path integral summing over a

subset $\mathcal{M}$ of four-manifolds with metric $g_{\mu\nu}$, and over matter field configurations Φ:

$$\Psi[h_{ij}, \Phi_{\rm f}] \equiv \int_{\mathcal{M}} \mathcal{D}g_{\mu\nu}\, \mathcal{D}\Phi\, e^{iS[g_{\mu\nu},\Phi]/\hbar}\,. \tag{4.1.1}$$

Evaluating this path integral exactly is a longstanding goal of quantum cosmology but presently out of reach. Instead one usually resorts to a minisuperspace ansatz of the FLRW form for the metric. Here in addition, we restrict the matter configuration to a homogeneous scalar field.

4.1.1 Classical action and equations of motion

The action consists of the Einstein-Hilbert action for GR, minimally coupled to a scalar field:

$$S_\Phi = \int \mathrm{d}^4x\sqrt{-g}\left(\frac{R}{16\pi G} - \frac{1}{2}g^{\mu\nu}\partial_\mu\Phi\partial_\nu\Phi - \tilde{V}(\Phi)\right) - \frac{1}{8\pi G}\int \mathrm{d}^3x\sqrt{h}\,K. \tag{4.1.2}$$

The second term we recall is the GHY term evaluated on the final hypersurface, necessary when imposing Dirichlet boundary conditions to make the variational principle consistent. $\tilde{V}(\Phi)$ is the scalar field potential. For normalization reasons and later convenience, we write the minisuperspace metric as:

$$\mathrm{d}s^2 = \frac{2G}{3\pi}\left(-\frac{N^2}{a^2(t)}\mathrm{d}t^2 + a^2(t)\mathrm{d}\Omega_3^2\right). \tag{4.1.3}$$

As stated earlier, we restrict to a homogeneous scalar field: $\Phi(x^\mu) \equiv \Phi(t)$. Then, we can rescale the scalar potential and field and get rid of all numerical factors in the action:

$$\begin{cases} \phi(t) \equiv \sqrt{\dfrac{4\pi G}{3}}\Phi(\tau)\,, \\ V(\phi) \equiv \dfrac{16G^2}{9}\tilde{V}(\Phi)\,, \end{cases} \Rightarrow\; S_\Phi = \frac{1}{2}\int N\mathrm{d}\tau\left(1 - \frac{a^2\dot{a}^2}{N^2} + \frac{a^4\dot{\phi}^2}{N^2} - a^2V(\phi)\right) - \left[\frac{a^3\dot{a}}{2N}\right]^0. \tag{4.1.4}$$

The last term in the action is a surface term on the initial boundary $t = 0$.

The class of scalar potential we explore here both offer a rich variety of physically interesting features, and render the path integral analytically feasible. These models were first studied by Garay et al. when including scalar fields in the original (field space defined) no-boundary proposal in [39]:

$$V(\phi) = \alpha\cosh(2\phi) + \beta\sinh(2\phi)\,, \quad \text{with} \;\; \alpha, \beta \in \mathbb{R}\,. \tag{4.1.5}$$

The equations of motion obtained from the action (4.1.4) are analytically solvable for any parameters α and β, but this becomes apparent after performing the change of variables $(a, \phi) \to (x, y)$:

$$x \equiv a^2\cosh(2\phi)\,; \quad y \equiv a^2\sinh(2\phi)\,. \tag{4.1.6}$$

The action (4.1.4) in these new variables reads:

$$S_\Phi[x,y] = \frac{1}{2}\int N\mathrm{d}t\left(\frac{\dot{y}^2-\dot{x}^2}{4N^2}+1-\alpha x-\beta y\right)-\left[\frac{x\dot{x}-y\dot{y}}{4N}\right]^0 , \tag{4.1.7}$$

and the associated equations of motions are:

$$\frac{\dot{x}^2-\dot{y}^2}{4N^2}+1=\alpha x+\beta y\,, \tag{4.1.8}$$

$$\ddot{x}=2N^2\alpha\,,\ \ddot{y}=-2N^2\beta\,. \tag{4.1.9}$$

The solution to these equations is straightforward, but to express it we first need to fix boundary conditions on x and y.

4.1.2 Boundary conditions for x and y

From the action (4.1.7), it is natural to define the conjugated momenta to the variable x and y as

$$\Pi_x(t)\equiv\frac{\dot{x}}{2N}\,;\quad \Pi_y(t)=\frac{\dot{y}}{2N}\,. \tag{4.1.10}$$

The boundary conditions are fixed by requiring the variational problem to be well-defined[1], in particular, its surface terms must vanish:

$$\delta S_\Phi \supset \frac{1}{2}\Big[y\,\delta\Pi_y-x\,\delta\Pi_x\Big]^0+\frac{1}{2}\Big[\Pi_y\,\delta y-\Pi_x\,\delta x\Big]^1=0\,. \tag{4.1.13}$$

We thus have to impose a condition on the momenta at the initial boundary: $\Pi_x(t=0)\equiv\Pi_x^0$ and $\Pi_y(t=0)\equiv\Pi_y^0$. The constraint equation (4.1.8) when $x,y\to 0$ imposes the following regularity condition:

$$(\Pi_x^0)^2-(\Pi_y^0)^2=-1\,. \tag{4.1.14}$$

Therefore we can parameterize the initial momenta as $\Pi_x^0\equiv i\cosh(2\gamma)$ and $\Pi_y^0\equiv i\sinh(2\gamma)$, making explicit the fact that **there remains one free parameter** γ, which specifies the initial conditions. At the final boundary we impose the usual Dirichlet conditions: $x(t=1)\equiv x_\mathrm{f}$ and $y(t=1)\equiv y_\mathrm{f}$.

[1] Alternatively, the boundary conditions can be determined by examining the Wheeler-de Witt equation, i.e., the operator version of the constraint (4.1.8) obtained in momentum space by replacing $x,y\to i\frac{\mathrm{d}}{\mathrm{d}\Pi_{x,y}}$:

$$\left(\Pi_x^2-\Pi_y^2+1-i\alpha\frac{\mathrm{d}}{\mathrm{d}\Pi_x}-i\beta\frac{\mathrm{d}}{\mathrm{d}\Pi_y}\right)\Psi=0\,. \tag{4.1.11}$$

Requiring the wavefunction to have no momentum flow initially (regularity condition [76]) implies

$$\left.\frac{\mathrm{d}\Psi}{\mathrm{d}\Pi_{x,y}}\right|_0=0\quad\Rightarrow\quad(\Pi_x^0)^2-(\Pi_y^0)^2=-1\,, \tag{4.1.12}$$

that is the same boundary condition we obtain from the first method (4.1.14). The other way around, this proves that the regularity condition yields the no momentum flow requirement for the wavefunction.

One main difficulty we will discuss in the next sections concerns the determination and interpretation of the value of γ. Studies of the stability against perturbations in pure gravity [43, 52, 53] impose a further condition on the conjugate momenta, namely that the sign of the imaginary part of Π_x^0 must be chosen positive: $\mathrm{Im}\,(\Pi_x^0) > 0$. This condition is equivalent to choosing the Hartle-Hawking wavefunction [38] over the tunneling Vilenkin wavefunction [47].

4.1.3 Performing the path integrals

Boundary conditions being fixed, we can now write the classical solutions to the equations of motion (4.1.9):

$$\begin{cases} \bar{x}(t) = \alpha N^2(t^2-1) + 2N\Pi_x^0(t-1) + x_\mathrm{f}\,, \\ \bar{y}(t) = -\beta N^2(t^2-1) + 2N\Pi_y^0(t-1) + y_\mathrm{f}\,. \end{cases} \tag{4.1.15}$$

Similarly to the case without scalar field 2.2, the path integrals on x and y are carried out by expanding around these classical background: $x(t) = \bar{x}(t) + \mathcal{X}(t)\,,\ y(t) = \bar{y}(t) + \mathcal{Y}(t)$ where $\mathcal{X}(t)$ and $\mathcal{Y}(t)$ are arbitrary fluctuations satisfying the boundary conditions: $\dot{\mathcal{X}}(0) = \dot{\mathcal{Y}}(0) = 0$ and $\mathcal{X}(1) = \mathcal{Y}(1) = 0$. Expanding the action (4.1.7) in these fluctuations, we find:

$$S_\Phi[x,y] = S_\Phi[\bar{x}(t),\bar{y}(t)] + \frac{1}{2}\int N\mathrm{d}t\left(\frac{\dot{\mathcal{Y}}^2 - \dot{\mathcal{X}}^2}{4N^2}\right) + \left[\frac{\dot{\bar{y}}\mathcal{Y} - \dot{\bar{x}}\mathcal{X}}{4N}\right]^1 - \left[\frac{x\dot{\mathcal{X}} - y\dot{\mathcal{Y}}}{4N}\right]^0 . \tag{4.1.16}$$

The first term is the on-shell action, independent of the fluctuations. From the integrand, the term linear in the fluctuations $\mathcal{X}$ and $\mathcal{Y}$ has vanished thanks to the equations of motion (4.1.9), and we are left only with the quadratic terms. The two surface terms in $t = 0$ and $t = 1$ displayed here also vanish thanks to the boundary conditions on the fluctuations. The no-boundary wavefunction is then:

$$\Psi[x_\mathrm{f}, y_\mathrm{f}, \gamma] = \int \mathrm{d}N\, e^{iS_\Phi[\bar{x}(t),\bar{y}(t)]/\hbar} \cdot \int_{\dot{\mathcal{X}}(0)=0}^{\mathcal{X}(1)=0} \mathcal{D}\mathcal{X} \int_{\dot{\mathcal{Y}}(0)=0}^{\mathcal{Y}(1)=0} \mathcal{D}\mathcal{Y}\, e^{\frac{i}{2\hbar}\int \mathrm{d}\tau \frac{\dot{\mathcal{Y}}^2 - \dot{\mathcal{X}}^2}{4N}} . \tag{4.1.17}$$

The fluctuations integrals are Gaußian but with mixed Neumann-Dirichlet boundary conditions. Such path integrals were calculated explicitly in the appendix of [53] and simply yield a numerical factor:

$$\Psi[x_\mathrm{f}, y_\mathrm{f}, \gamma] = \frac{8\hbar}{\pi}\int \mathrm{d}N e^{iS_\Phi[\bar{x}(t),\bar{y}(t)]/\hbar}\,. \tag{4.1.18}$$

The result of these fluctuation integrals can be verified indirectly by using the Wheeler-de Witt equation, see appendix B.1. The numerical factor obtained from this calculation is an overall constant that changes the measure but doesn't affect relative probabilities. We drop it in subsequent calculations.

4.1.4 Defining the lapse integral

The no-boundary wavefunction at this stage is simply given by an ordinary integral over the lapse N, (4.1.18). The integrand consists in the exponential of the on-shell action:

$$S_{\text{on-shell}}[x_{\text{f}}, y_{\text{f}}, \gamma] \equiv S_{\Phi}[\bar{x}(t), \bar{y}(t)] = \frac{1}{2}\Big[\frac{N^3}{3}(\alpha^2 - \beta^2) + N^2(\alpha\Pi_x^0 + \beta\Pi_y^0) - N(\alpha x_{\text{f}} + \beta y_{\text{f}}) + y_{\text{f}}\Pi_y^0 - x_{\text{f}}\Pi_x^0\Big]. \tag{4.1.19}$$

We can use the WKB semi-classical approximation to evaluate the lapse integral, and then apply **Picard-Lefshetz theory** (see section 2.2). For this we need to calculate the saddle point geometries, which are specified by the lapse value solving the saddle equation:

$$\frac{\delta}{\delta N} S_{\text{on-shell}}[x_{\text{f}}, y_{\text{f}}, \gamma]\Big|_{N_{\text{saddle}}} = 0\,, \quad \text{(saddle equation)}. \tag{4.1.20}$$

$$\Rightarrow \begin{cases} N^{\pm}_{\text{saddle}} = \dfrac{-(\alpha\Pi_x^0 + \beta\Pi_y^0) \pm \sqrt{(\alpha\Pi_x^0 + \beta\Pi_y^0)^2 + (\alpha^2 - \beta^2)(\alpha x_{\text{f}} + \beta y_{\text{f}})}}{\alpha^2 - \beta^2}\,, & (\alpha \neq \beta)\,; \\ N^0_{\text{saddle}} = \dfrac{1}{2}\dfrac{x_{\text{f}} + y_{\text{f}}}{\Pi_x^0 + \Pi_y^0}\,, & (\alpha = \beta)\,. \end{cases} \tag{4.1.21}$$

For any set of boundary conditions $\{x_{\text{f}}, y_{\text{f}}, \gamma\}$, the scalar potentials (4.1.5) with $\alpha \neq \beta$ possess two saddle point geometries specified by $N^{\pm}_{\text{saddle}}$, while the exponential potential ($\alpha = \beta$) has one saddle point geometry determined by N^0_{saddle}. The parameter γ fixes the initial momenta values Π_x^0 and Π_y^0, ensuring the regularity of the saddle point geometries in $t = 0$. However, the initial field values are not fixed in this setting, so saddle point geometries are not necessarily compact there. In fact, compactness only occurs for specific values of γ.

By prescription, we define the no-boundary wavefunction for a final set of boundary conditions, $\{x_{\text{f}}, y_{\text{f}}\}$, as a sum over the γ values which lead to at least one compact saddle point (SP) geometry, i.e.,

$$\Psi[x_{\text{f}}, y_{\text{f}}] \equiv \sum_{\substack{\gamma \text{ s.t.} \\ \text{one SP is} \\ \text{compact}}} \Psi[x_{\text{f}}, y_{\text{f}}, \gamma]\,. \tag{4.1.22}$$

This prescription gives a generalization of the path integral that includes a sum on specific boundary conditions. In the spirit of the path integral, each history is weighted by the exponential of the on-shell action only, which is why in equation (4.1.22), we give an equal weight to the wavefunctions with different γ values. In fact, this prescription is very similar to that used implicitly in earlier implementations of the no-boundary proposal such as [35]. With the difference that these used Dirichlet initial boundary conditions for the scale factor and scalar field, compact saddle point geometry were selected by adjusting the initial scalar field boundary condition depending on the final fields values. This sort

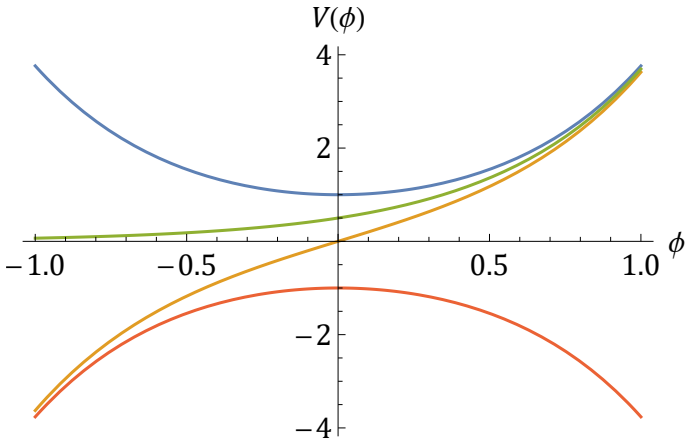

Figure 4.1: Prototypical scalar field potentials, $V(\phi) = \alpha \cosh(2\phi) + \beta \sinh(2\phi)$, studied in this chapter. Blue curve: hyperbolic cosine $\alpha = 1$, $\beta = 0$ (slow-roll potential 4.2). Red curve: negative hyperbolic cosine $\alpha = -1$, $\beta = 0$ (AdS-like potential 4.3). Green curve: exponential potential $\alpha = \beta = 1/2$ (see 4.4). And finally orange curve: hyperbolic sine $\alpha = 0$, $\beta = 1$.

of non-causal definition of the wavefunction appears ubiquitous when considering the no-boundary wavefunction including scalar fields, and forms the main puzzle mentioned in the introduction to this chapter. We will discuss this issue again in section 4.6. Note that another prescription could be equally valid, and remove the non-causality puzzle: by integrating over any value of γ, and then arguing that only compact saddle points dominate the path integral, for example by using the complex metric criterion of chapter 6. Indeed, we will see in the upcoming sections that non-compact geometries are characterized by $V(\phi_0) = 0$: this implies that their initial scalar field value is very complex, which would be ruled out by the complex metric criterion [77].

The plan for the next sections is to study in detail the definition (4.1.22) for some prototypical scalar potentials, depicted in figure 4.1.

4.2 Slow-roll potential

The hyperbolic cosine potential (in blue in figure 4.1) is the most relevant example to study: it is **inflationary** and exhibits a **slow-roll region** for small absolute values of the scalar field. Moreover, this model reduces to gravity with a cosmological constant (though with the addition of scalar fluctuations) when the scalar field vanishes. We therefore expect to recover the known no-boundary wave function in this limit. In fact, it turns out that this potential is the only one (of those we will study here) where a classical spacetime is predicted for large values of the scale factor[2].

[2]This result was already discussed in [39].

4.2.1 Compactness condition for the saddle point geometries

There are two saddle point geometries specified by the lapse values (4.1.21):

$$N^{\pm}_{\text{saddle}} = -i\cosh(2\gamma) \pm \sqrt{a_{\text{f}}^2\cosh(2\phi_{\text{f}}) - \cosh^2(2\gamma)}\,. \tag{4.2.1}$$

The constraint equation (4.1.8), $(\dot{x}^2 - \dot{y}^2)/(4N^2) + 1 = x$, must be satisfied and together with the regularity condition (4.1.14), it implies that $x(t=0) = 0$. Since the scale factor is given by $a(t)^2 = \sqrt{x(t)^2 - y(t)^2}$, the saddle point geometries (4.2.1) will be initially compact if and only if:

$$y(t=0) = 0 \quad \text{(compactness condition)}. \tag{4.2.2}$$

By using the equations of motion together with the classical solution, we find that this condition is satisfied only when the lapse value specifying the geometry is equal to:

$$N_{\text{compact}} = \frac{y_{\text{f}}}{2\Pi^0_y} = \frac{a_{\text{f}}^2\sinh(2\phi_{\text{f}})}{2i\sinh(2\gamma)}\,. \tag{4.2.3}$$

Therefore, saddle point geometries are compact if and only if: $N_{\text{saddle}} = N_{\text{compact}}$, which in this case leads to the equation:

$$a_{\text{f}}^2\sinh^2(2\phi_{\text{f}}) + 4\sinh(2\gamma)\sinh(2\gamma - 2\phi_{\text{f}}) = 0\,. \tag{4.2.4}$$

Solving this equation (4.2.4) for $\gamma \in \mathbb{C}$ yields three solutions, each valid in a different region of the phase space of final field values, $(a_{\text{f}}, \phi_{\text{f}})$:

$$\begin{cases} \gamma^{\text{I}}_{\mp} = \dfrac{\phi_{\text{f}}}{2} \mp \dfrac{i}{2}\,\text{arcsin}\left(|\sinh(\phi_{\text{f}})|\sqrt{a_{\text{f}}^2\cosh^2(\phi_{\text{f}}) - 1}\right); \\ \gamma^{\text{II}}_{\mp} = \dfrac{1}{2}\cosh^{-1}\left(\sqrt{1 + \dfrac{\sinh^2(2\phi_{\text{f}})}{4}\left(2 - a_{\text{f}}^2\cosh(2\phi_{\text{f}}) \mp \sqrt{\left(2 - a_{\text{f}}^2\cosh(2\phi_{\text{f}})\right)^2 - a_{\text{f}}^4}\right)}\right); \\ \gamma^{\text{III}}_{\mp} = \mp\dfrac{1}{2}\cosh^{-1}\left(\dfrac{1}{2}\sinh(2\phi_{\text{f}})\sqrt{a_{\text{f}}^2\cosh(2\phi_{\text{f}}) - 2 \mp \sqrt{\left(a_{\text{f}}^2\cosh(2\phi_{\text{f}}) - 2\right)^2 - a_{\text{f}}^4}}\right) \\ \qquad\quad + i\left(\dfrac{\pi}{4} + n\dfrac{\pi}{2}\right) \quad \text{with } n \in \{-1, 0\}. \end{cases} \tag{4.2.5}$$

To avoid clutterness, we postpone the derivation of the above formulae to the appendix B.2. The three regions of validity in the phase space $(a_{\text{f}}, \phi_{\text{f}})$, represented in figure 4.2, are:

$$\begin{cases} \text{region I:} & a_{\text{f}}^2\cosh^2(\phi_{\text{f}}) > 1 \;\&\; a_{\text{f}}^2\sinh^2(\phi_{\text{f}}) < 1\,; \\ \text{region II:} & a_{\text{f}}^2\cosh^2(\phi_{\text{f}}) < 1\,; \\ \text{region III:} & a_{\text{f}}^2\sinh^2(\phi_{\text{f}}) > 1\,. \end{cases} \tag{4.2.6}$$

Now that we have expressed the values of γ entering the no-boundary wavefunction definition (4.1.22), we can apply the Picard-Lefschetz method for evaluating the lapse

integral in (4.1.18). This yields the steepest descent contours emanating from the saddle point lapse values, on which the lapse integral can be defined by a sum of convergent integrals. In the semi-classical approximation (to leading order in $\hbar$), the integral is given by the corresponding sum on the saddle point lapse values.

4.2.2 Region I: complex saddle points.

For each of the two values $\gamma^{\mathrm{I}}_{\mp}$, equation (4.2.1) gives two complex saddle point lapse values. Out of these four saddle point geometries, only two are compact. This is because, for a given γ value, only one choice of sign in (4.2.1) can match with the required value (4.2.3) for a compact geometry, so the other choice of sign leads to a non-compact saddle point geometry. The regularity condition (4.1.14) is nevertheless satisfied on these non-compact saddles, because the scalar potential $V(\phi)$ vanishes at $t = 0$. The reason is that, by extending the fields to the complex plane, the potential becomes a holomorphic (in fact entire) function. From Picard's little theorem (see appendix B.3), entire functions generically vanish at certain field value(s). The appearance of non-compact but regular saddle point geometries is therefore a generic property when considering complex field values.

Numerical example

We illustrate this case by one numerical example for $a_{\mathrm{f}} = 1$ and $\phi_{\mathrm{f}} = 0.5$. In figure 4.3, we show the evolution of the complex field values a and ϕ for the lapse values corresponding to the four saddle point geometries. The lapse values come in pair with opposite real parts. They correspond to complex conjugate scale factor and scalar field. From the figure, it is evident that two saddle point geometries are initially compact ($\mathrm{Re}[a(0)] = \mathrm{Im}[a(0)] = 0$),

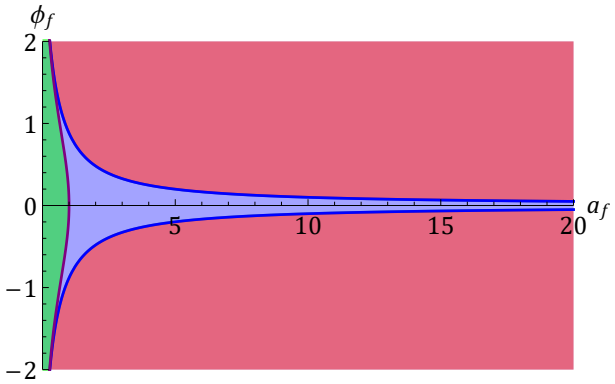

Figure 4.2: Phase space regions (4.2.6). Region I is in blue, region II is in green and region III is in red. The purple curve is the condition $a_{\mathrm{f}}^2 \cosh^2(\phi_{\mathrm{f}}) = 1$, and the blue curve is the condition $a_{\mathrm{f}}^2 \sinh^2(\phi_{\mathrm{f}}) = 1$.

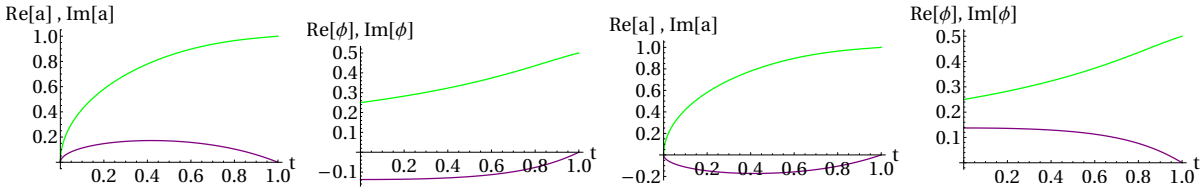

(a) Complex fields at $N_+[\gamma_-]$.

(b) Complex fields at $N_-[\gamma_+]$.

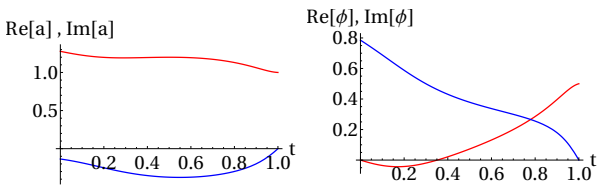

(c) Complex fields at $N_-[\gamma_-]$.

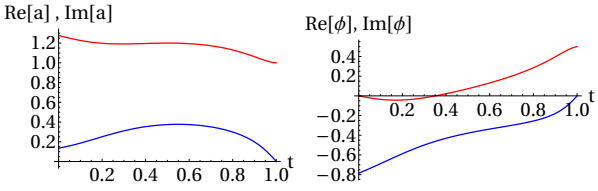

(d) Complex fields at $N_+[\gamma_+]$.

Figure 4.3: Numerical evolution for fields in region I. Parameters: $\alpha = 1$, $\beta = 0$ and $a_{\rm f} = 1$, $\phi_{\rm f} = 0.5$ (complex N). $\gamma_\mp = 0.25 \mp 0.137i$ and the saddle point lapse values are $N_+[\gamma_-] = 0.521 - 0.853i$, $N_-[\gamma_+] = -0.521 - 0.853i$, $N_-[\gamma_-] = -0.804 - 1.317i$, $N_+[\gamma_+] = 0.804 - 1.317i$. $N_+[\gamma_-]$ and $N_-[\gamma_+]$ are the compact saddle points. The graphs show the time evolution of the scale factor a and the scalar field ϕ for the four saddle point lapse values. Real parts in green for compact and in red for non-compact saddle points. Imaginary parts in purple for compact and in blue for non-compact saddles.

while the two other aren't. In all cases, the initial scalar field value is fully complex:

$$\begin{cases} \phi(t=0) = \pm i\dfrac{\pi}{4}\,, & \text{(non-compact SP);} \\ \phi(t=0) = \lim\limits_{t\to 0}\dfrac{1}{2}\text{arctanh}\left(\dfrac{\bar{y}(t)}{\bar{x}(t)}\right) = \dfrac{1}{2}\text{arctanh}\left(\dfrac{\Pi_y^0}{\Pi_x^0}\right) \equiv \gamma\,, & \text{(compact SP).} \end{cases} \tag{4.2.7}$$

This implies that **for compact saddle point geometries, the value of γ can be interpreted as the initial scalar field value:** $\phi(t=0) = \gamma$. Finally, all field values of a and ϕ become real on the final hypersurface $t = 1$. In figure 4.4, we draw the steepest

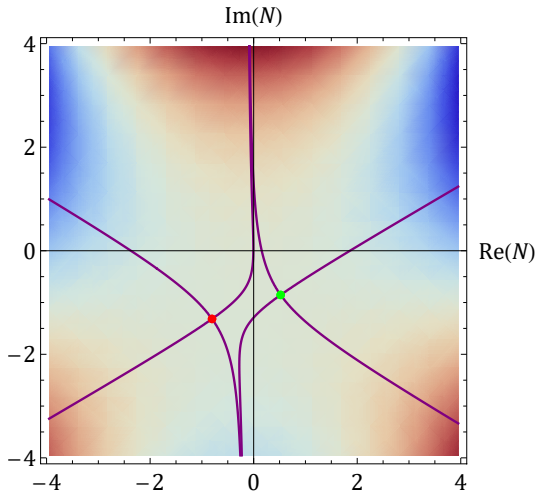

(a) $N_+[\gamma_-]$ (green dot) and $N_-[\gamma_-]$ (red dot).

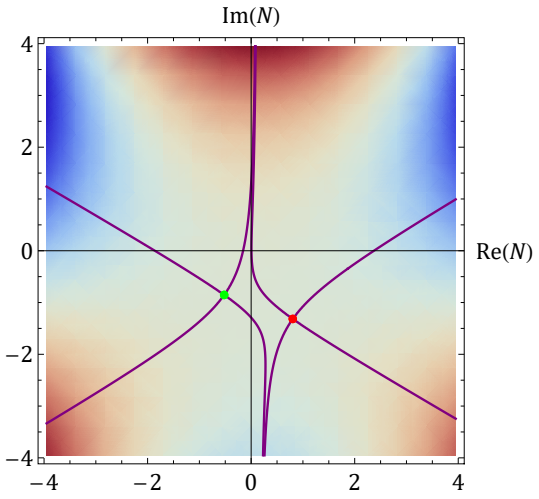

(b) $N_-[\gamma_+]$ (green dot) and $N_+[\gamma_+]$ (red dot).

Figure 4.4: $\alpha = 1$, $\beta = 0$ and $a_{\rm f} = 1$, $\phi_{\rm f} = 0.5$ (complex N). Density plot of the weighting $\text{Re}[iS^{\text{on-shell}}_{\text{saddle}}]$ and flow lines in the complex N plane. Steepest descent (resp. ascent) contours are those lines emanating from the saddle points and plunging into blue (resp. red) regions. The path integral is defined by integrating along the steepest descent contours.

descent and ascent contours associated with each saddle point geometry. We draw one

graph for each value of γ. Each graph contains one compact and one non-compact saddle point.

If we choose as original integration contour the Lorentzian metric line (i.e., the real N line), as was done for the no-boundary without scalar field 2.2, we can deform it into the steepest descent contours of the two saddle points for each graph. From the perspective that the standard big bang evolution and our late universe are both described by Lorentzian metrics, this integration contour sounds the most natural. This naturalness idea is nevertheless challenged by the complex metric criterion (see chapter 6), from which it appears that the integration contour would preferably follow the Euclidean axis instead.

Evaluation of the no-boundary wavefunction

Following our prescription for the no-boundary wavefunction (4.1.22), we must sum over the two relevant values of the initial conditions parameter γ. This yields, to leading order in $\hbar$,

$$\Psi[x_{\mathrm{f}}, y_{\mathrm{f}}] = e^{\frac{i}{\hbar}S(N_+[\gamma_-])} + e^{\frac{i}{\hbar}S(N_-[\gamma_+])} + e^{\frac{i}{\hbar}S(N_+[\gamma_+])} + e^{\frac{i}{\hbar}S(N_-[\gamma_-])}\,. \tag{4.2.8}$$

The saddle point geometries are pairwise complex conjugates of each other, so this wavefunction is real. The next step of our analysis consists in determining **which saddle point(s) actually dominate this wavefunction**, i.e., which have the highest weighting[3]. The saddle point lapse values (4.2.1) are in this case: $N_\pm = -\Pi_x^0 \pm \sqrt{x_{\mathrm{f}} + (\Pi_x^0)^2}$, so the on-shell action (4.1.19) evaluated on them gives:

$$S_{\text{on-shell}}[N_\pm] = \frac{N_\pm^3}{6} + \frac{N_\pm^2 \Pi_x^0}{2} - \frac{N_\pm x_{\mathrm{f}}}{2} + \frac{y_{\mathrm{f}}\Pi_y^0 - x_{\mathrm{f}}\Pi_x^0}{2} \tag{4.2.9}$$

$$= \mp \frac{\sqrt{x_{\mathrm{f}} + (\Pi_x^0)^2}^3}{3} + \frac{(\Pi_x^0)^3}{3} + \frac{y_{\mathrm{f}}\Pi_y^0}{2}\,. \tag{4.2.10}$$

What are the values of Π_x^0 and Π_y^0 for the different saddle points? The two possible solutions for γ are given from equation (4.2.5) by

$$\gamma_\mp = \frac{\phi_{\mathrm{f}}}{2} \mp \frac{i}{2}\,\mathrm{arcsin}\left(|\sinh(\phi_{\mathrm{f}})|\sqrt{a_{\mathrm{f}}^2\cosh^2(\phi_{\mathrm{f}}) - 1}\right). \tag{4.2.11}$$

Compact saddle point geometries correspond to the lapse values $N_+[\gamma_-]$ and $N_-[\gamma_+]$. The initial momenta evaluated in these γ values give:

$$\Pi_x^0(\gamma_\mp) \equiv i\cosh(2\gamma_\mp) = \pm\sinh^2(\phi_{\mathrm{f}})\sqrt{a_{\mathrm{f}}^2\cosh^2(\phi_{\mathrm{f}}) - 1} + i\cosh^2(\phi_{\mathrm{f}})\sqrt{1 - a_{\mathrm{f}}^2\sinh^2(\phi_{\mathrm{f}})}\,, \tag{4.2.12}$$

[3]On this point our prescription (4.1.22) is debatable, because it could be that other values of γ lead to higher weightings and dominate the wavefunction, even if they don't correspond to compact geometries. As mentioned before, it may in this case be necessary to consider the complex metric criterion for ruling out initial values of the scalar field that are "too complex" and recover the results presented here.

$$\Pi_y^0(\gamma_\mp) \equiv i\sinh(2\gamma_\mp) = \pm\frac{\sinh(2\phi_\mathrm{f})}{2}\sqrt{a_\mathrm{f}^2\cosh^2(\phi_\mathrm{f})-1} + \frac{i\sinh(2\phi_\mathrm{f})}{2}\sqrt{1-a_\mathrm{f}^2\sinh^2(\phi_\mathrm{f})}. \tag{4.2.13}$$

We have assumed $\phi_\mathrm{f} > 0$, and we restrict solutions to the region I of the phase space, where $a_\mathrm{f}^2\cosh^2(\phi_\mathrm{f}) > 1$ and $a_\mathrm{f}^2\sinh^2(\phi_\mathrm{f}) < 1$. In the expressions (4.2.12) and (4.2.13), the imaginary parts of the initial momenta do not depend on the choice of saddle point, while the real parts only differ by a sign. Therefore, since the weighting is determined by the imaginary part of the on-shell action, $e^{-\mathrm{Im}(S)}$, the comparison of the weighting for the different saddle points will only depend on the first term, $\mp\frac{1}{3}\sqrt{x_\mathrm{f}+(\Pi_x^0)^2}^3$, in the expression (4.2.10). We examine this term in more detail for the four saddle points:

$$\sqrt{x_\mathrm{f}+(\Pi_x^0(\gamma_\mp))^2}^3 = (A \pm iB)^{3/2} \equiv \rho^{3/2}e^{\pm 3i\theta/2}\,, \quad \text{where } A,\, B,\, \rho,\, \theta \in \mathbb{R}\,; \tag{4.2.14}$$

$$\text{and } \begin{cases} A = a_\mathrm{f}^2\cosh(2\phi_\mathrm{f}) + \sinh^4(\phi_\mathrm{f})\Big(a_\mathrm{f}^2\cosh^2(\phi_\mathrm{f})-1\Big) - \cosh^4(\phi_\mathrm{f})\Big(1-a_\mathrm{f}^2\sinh^2(\phi_\mathrm{f})\Big)\,; \\ B = 2\sinh^2(\phi_\mathrm{f})\cosh^2(\phi_\mathrm{f})\sqrt{a_\mathrm{f}^2\cosh^2(\phi_\mathrm{f})-1}\sqrt{1-a_\mathrm{f}^2\sinh^2(\phi_\mathrm{f})}\,. \end{cases} \tag{4.2.15}$$

From its expression, the quantity B is always positive (and real in the region I), therefore the angle θ, defined in (4.2.14), is comprised between 0 and π. On the other hand, A is real but its sign depends on the final set of conditions, $\{a_\mathrm{f}, \phi_\mathrm{f}\}$. With this rewriting, we can express the imaginary part of the on-shell action for each saddle point geometry:

$$\begin{cases} \mathrm{Im}(S^{\text{compact}}_{\text{on-shell}}[N_-[\gamma_+]]) = \mathrm{Im}\left(\frac{1}{3}\sqrt{x_\mathrm{f}+(\Pi_x^0(\gamma_+))^2}^3\right) = -\frac{1}{3}\rho^{3/2}\sin(3\theta/2)\,; \\ \mathrm{Im}(S^{\text{non-compact}}_{\text{on-shell}}[N_-[\gamma_-]]) = \mathrm{Im}\left(\frac{1}{3}\sqrt{x_\mathrm{f}+(\Pi_x^0(\gamma_-))^2}^3\right) = +\frac{1}{3}\rho^{3/2}\sin(3\theta/2)\,; \\ \mathrm{Im}(S^{\text{non-compact}}_{\text{on-shell}}[N_+[\gamma_+]]) = \mathrm{Im}\left(-\frac{1}{3}\sqrt{x_\mathrm{f}+(\Pi_x^0(\gamma_+))^2}^3\right) = +\frac{1}{3}\rho^{3/2}\sin(3\theta/2)\,; \\ \mathrm{Im}(S^{\text{compact}}_{\text{on-shell}}[N_+[\gamma_-]]) = \mathrm{Im}\left(-\frac{1}{3}\sqrt{x_\mathrm{f}+(\Pi_x^0(\gamma_-))^2}^3\right) = -\frac{1}{3}\rho^{3/2}\sin(3\theta/2)\,. \end{cases} \tag{4.2.16}$$

Therefore, the compact saddle point geometries will dominate over the non-compact ones if and only if

$$\sin\left(\frac{3\theta}{2}\right) > 0\,, \quad \Leftrightarrow \quad 0 < \theta < \frac{2\pi}{3}\,, \quad \Leftrightarrow \quad \frac{A}{B} = \cot(\theta) > -\frac{1}{\sqrt{3}}\,. \tag{4.2.17}$$

In figure 4.5, we plot the region of the phase space $\{a_\mathrm{f}, \phi_\mathrm{f}\}$ where the condition (4.2.17) is satisfied, and find it entirely covers the region I where complex saddle point geometries are defined. Therefore, the non-compact saddle point geometries are exponentially suppressed compared to compact geometries within region I. We conclude that, also in the presence of a complex scalar field, we recover the usual result that **the no-boundary wavefunction is dominated by initially compact and regular geometries**.

One subtelty remains in interpreting the wavefunction (4.2.8), because it is dominated

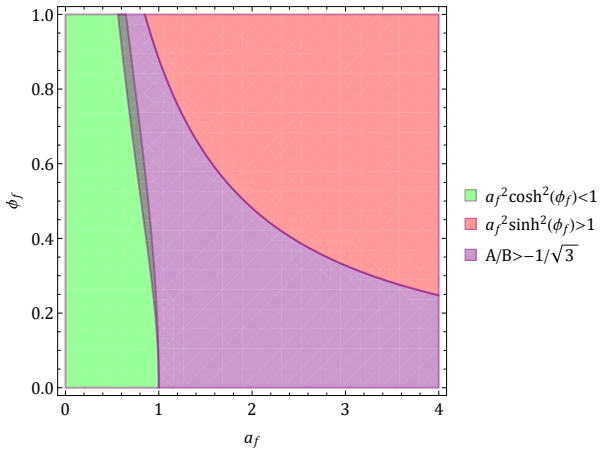

Figure 4.5: The region where the compact saddle points dominate over the non-compact ones is entirely covering the region I where complex saddle points are defined. Our analysis assumed that we were outside the green and red regions, so from this picture nothing can be inferred about these regions.

by two saddle point geometries of equal weight:

$$\Psi[a_{\rm f},\phi_{\rm f}] \approx \exp\left(\frac{i}{\hbar} S^{\rm compact}_{\text{on-shell}}(N_+[\gamma_-])\right) + \exp\left(\frac{i}{\hbar} S^{\rm compact}_{\text{on-shell}}(N_-[\gamma_+])\right). \tag{4.2.18}$$

This would predict a strong interference between two universes, but as shown in [6], the addition of perturbations leads to an efficient decoherence effect for growing scale factor. Therefore, for sufficiently large value $a_{\rm f} \gg 1$, the wavefunction is given by a single dominant saddle point geometry, for example $N_+[\gamma_-]$. Since $a_{\rm f}$ must be large and that the existence of complex saddle point is conditioned by $a_{\rm f}^2 \sinh(\phi_{\rm f})^2 < 1$, the final scalar field value $\phi_{\rm f}$ must be small. We can then Taylor-expand the on-shell action of the dominant saddle point around $\phi_{\rm f} = 0$ and find:

$$S^{\rm compact}_{\text{on-shell}}(N_+[\gamma_-]) = -\frac{1}{3}\left[\sqrt{a_{\rm f}^2-1}^{\,3} + i\right] - \frac{1}{2}\left[\sqrt{a_{\rm f}^2-1} - i\right] a_{\rm f}^2\phi_{\rm f}^2 + \mathcal{O}(\phi_{\rm f}^4)\,, \tag{4.2.19}$$

so to quadratic order in $\phi_{\rm f}$, the weighting of the dominant saddle point geometry is:

$$|\Psi[a_{\rm f},\phi_{\rm f}]| \approx \left|e^{\frac{i}{\hbar} S^{\rm compact}_{\text{on-shell}}(N_+[\gamma_-])}\right| = e^{-\operatorname{Im}(S^{\rm compact}_{\text{on-shell}}(N_+[\gamma_-]))/\hbar} = e^{\frac{1}{3\hbar}\left(1-\frac{3}{2}a_{\rm f}^2\phi_{\rm f}^2\right)} \quad \text{for } a_{\rm f}\,\phi_{\rm f} \ll 1\,. \tag{4.2.20}$$

This result (4.2.20) shows that the probability is higher when $\phi_{\rm f}$ is smaller. This is a generic result of the no-boundary wavefunction. Then the highest probability occurs for the limit where the scalar sits at the minimum of the $\cosh(2\phi)$ potential. In this limit, γ tends to zero and the non-compact saddles disappear. This limit corresponds to the pure gravity case with a cosmological constant, but also including fluctuations of the scalar field, that provide a sub-dominant contribution to the wavefunction.

The classicality of the final spacetime obtained can be proven by considering the

leading order changing rates of the imaginary and real parts of the on-shell action (4.2.19):

$$\left|\frac{\partial \operatorname{Im}(S)}{\partial a_{\mathrm{f}}} \Big/ \frac{\partial \operatorname{Re}(S)}{\partial a_{\mathrm{f}}}\right| \sim \frac{\phi_{\mathrm{f}}^2}{a_{\mathrm{f}}} \ll 1\,, \qquad \left|\frac{\partial \operatorname{Im}(S)}{\partial \phi_{\mathrm{f}}} \Big/ \frac{\partial \operatorname{Re}(S)}{\partial \phi_{\mathrm{f}}}\right| \sim \frac{1}{a_{\mathrm{f}}} \ll 1\,. \tag{4.2.21}$$

This means that at large scale factor, the wavefunction's amplitude varies slowly compared to its phase. This branch of the wavefunction is thus of WKB form and therefore, in the region I of phase space, we predict a classical spacetime with a classical background evolution.

4.2.3 Region II: imaginary saddle points.

Region II corresponds to a very small size of the universe: $a_{\mathrm{f}}^2 \cosh(2\phi_{\mathrm{f}}) < 1$. There, the solutions for γ (4.2.5) are purely real. Therefore the saddle point lapse values (4.2.1) are purely imaginary, as well as the initial momenta Π_x^0 (4.2.12) and Π_y^0 (4.2.13), and so the classical solutions $\bar{x}$ and $\bar{y}$ given in (4.1.15) are purely real. It follows that the on-shell action evaluated on the saddle points (4.1.19) is purely imaginary. Therefore the wave function of each saddle point geometry is a pure amplitude:

$$\psi \propto e^{\text{real number}}\,. \tag{4.2.22}$$

Such a wavefunction doesn't lead to a WKB evolution. We conclude that in the region II of phase space, the universe is still in its nucleation phase (analogous to the tunneling phase of a particle in a barrier potential, where time is purely Euclidean).

Analysis of the saddle point solutions

Similarly to the previous case, we illustrate this case by a numerical example with $a_{\mathrm{f}} = 0.2$, $\phi_{\mathrm{f}} = 1$. In figure 4.6 we present the time evolution of the imaginary and real parts of the scale factor and scalar field, for each saddle point geometry. Then in figure 4.7 we show, for each value of γ, the density plot of the no-boundary wavefunction weighting $(-\operatorname{Im}[S])$, the associated compact and non-compact saddle points and their steepest descent and ascent paths in the complexified lapse plane.

We can analyze the saddle point solutions generically. For the compact saddle point solutions, the classical solutions (4.1.15) $\bar{x}$ and $\bar{y}$ both start from 0 when $t = 0$. $\bar{x}$ describes a downward-facing parabola (since N^2 is negative), while $\bar{y}$ forms a straight line ($\beta = 0$). Also, the gradient of $\bar{x}$ in $t = 0$ is always bigger than that of $\bar{y}$, because in region II, γ is real so $|\tanh(2\gamma)| < 1$:

$$\left|\frac{\dot{\bar{y}}(t)}{\dot{\bar{x}}(t)}\right|_{t=0} = \frac{\Pi_x^0}{\Pi_y^0} = |\tanh(2\gamma_{II})| < 1\,. \tag{4.2.23}$$

Finally, at the end point of the trajectory $t = 1$, we find that $\bar{x}(1) > \bar{y}(1)$ because $\cosh(2\phi_{\mathrm{f}}) > \sinh(2\phi_{\mathrm{f}})$. Therefore, we can conclude that

$$\forall\, t \in (0,1):\ \bar{x}(t) > \bar{y}(t) \ \Rightarrow\ \bar{a}(t) = (\bar{x}(t)^2 - \bar{y}(t)^2)^{1/4} \in \mathbb{R}\,. \tag{4.2.24}$$

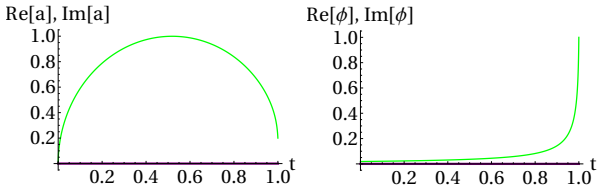

(a) Compact Euclidean geometry $N_-[\gamma_-]$.

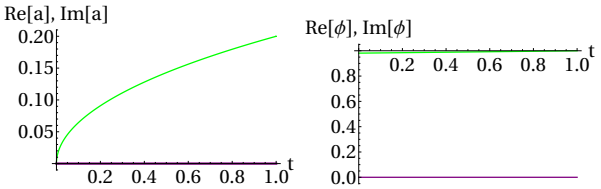

(b) Compact Euclidean geometry $N_+[\gamma_+]$.

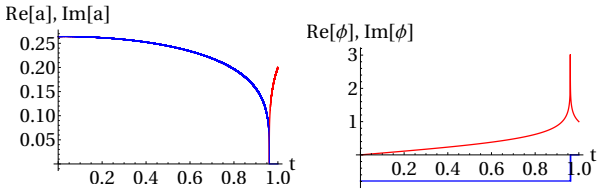

(c) Non-compact Euclidean geometry $N_+[\gamma_-]$.

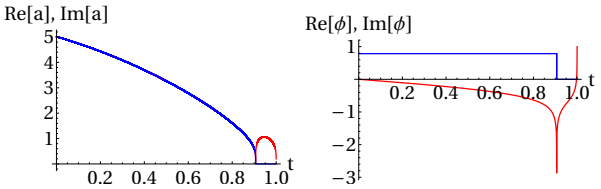

(d) Non-compact Euclidean geometry $N_-[\gamma_+]$.

Figure 4.6: Numerical evolution of fields in region II. The parameters are $\alpha = 1$, $\beta = 0$, $a_\mathrm{f} = 0.2$, $\phi_\mathrm{f} = 1$. The γ values are then: $\gamma_- = 0.0189$, $\gamma_+ = 0.981$, and the corresponding saddle point lapse values: $N_-[\gamma_-] = -1.92i$, $N_+[\gamma_-] = -0.0782i$, $N_+[\gamma_+] = -0.0208i$ and $N_-[\gamma_+] = -7.24i$. We find two compact saddle point geometries – $N_+[\gamma_+]$ and $N_-[\gamma_-]$ – and two non-compact ones – $N_+[\gamma_-]$ and $N_-[\gamma_+]$. Same color conventions as in figure 4.3. Note that the imaginary part of the scalar typically jumps when the scale factor passes through zero, as the imaginary part of the scalar itself changes there, given that it is obtained by taking a fourth root $a = (x^2 - y^2)^{1/4}$.

This proves that in region II, **compact saddle point geometries are purely Euclidean**.

Consider non-compact saddle points now. From the regularity condition, $\bar{x}(0) = 0$. But since the compactness condition is not satisfied, $\bar{y}(0) = y_\mathrm{f} - 2N\Pi_y^0$ takes an arbitrary non zero real value, so that the combination $\bar{x}(0)^2 - \bar{y}(0)^2$ is real and negative. At the end point of the trajectory, we still have that $\bar{x}(1) > \bar{y}(1)$, so that $\bar{x}(1)^2 - \bar{y}(1)^2$ is real and positive. We can then apply the *mean value principle* to the function $\bar{a}(t)^4 = \bar{x}(t)^2 - \bar{y}(t)^2$: there must exist a point in the trajectory $t_0 \in (0, 1)$ where $\bar{a}(t_0)^4 = 0$. This argument shows that in region II, **non-compact saddle point geometries always exhibit a singular bounce in the course of their evolution**. The solutions described by these geometries are then non-physical, since perturbations would blow up at the singularity and make the associated action infinite.

Evaluation of the wavefunction

We evaluate the wavefunction obtained in region II by using the Picard-Lefschetz theory for selecting the saddle points contributing to the path integral. Observing the example depicted in 4.7, where compact saddle point geometries are represented in green and non-compact ones in red, we find that if we take as contour of integration a parallel to the real lapse axis as we did for region I, we get a contribution from one compact ($N_+[\gamma_+]$) and one non-compact ($N_+[\gamma_-]$) saddle point. This is due to the fact, true for any point in region II, that the location of the compact and non-compact saddle points is reversed with respect to the real axis for the two values of γ. The no-boundary wavefunction found

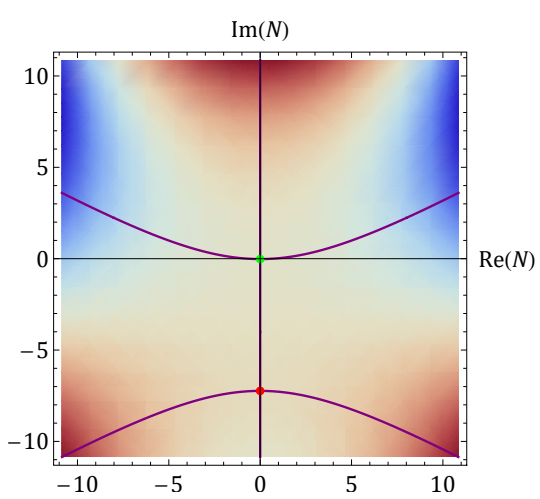

(a) $N_-[\gamma_-]$ (green dot) and $N_+[\gamma_-]$ (red dot).

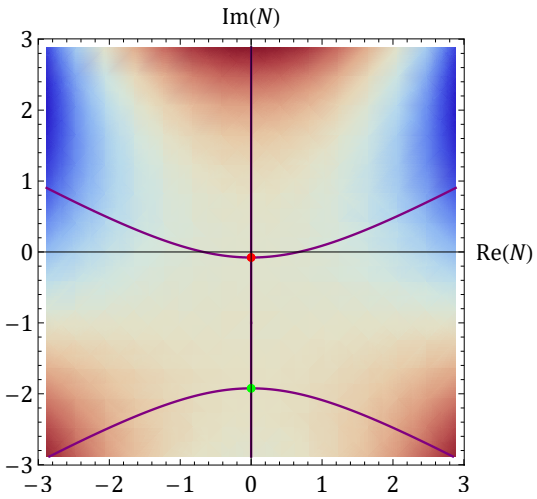

(b) $N_+[\gamma_+]$ (green dot) and $N_-[\gamma_+]$ (red dot).

Figure 4.7: Parameters: $\alpha = 1$, $\beta = 0$, $a_\mathrm{f} = 0.2$, $\phi_\mathrm{f} = 1$ (N is purely imaginary). Density plot of the weighting $\mathrm{Re}[iS^{\text{on-shell}}_{\text{saddle}}]$ and flow lines in the complex N plane.

from Picard-Leschetz theory is then at semi-classical level:

$$\Psi[x_\mathrm{f}, y_\mathrm{f}] \approx e^{\frac{i}{\hbar} S_{\text{on-shell}}(N_+[\gamma_-])} + e^{\frac{i}{\hbar} S_{\text{on-shell}}(N_+[\gamma_+])} . \tag{4.2.25}$$

In the previous paragraph, we found that non-compact saddle point geometries in region II always contain a singular bounce, which makes their action diverge in the presence of perturbations. These saddle points therefore do not contribute to the wavefunction.

In the original study of the no-boundary wavefunction including a scalar field [39], where the field space definition of the no-boundary proposal was used, it was advocated that saddle point geometries containing a singular bounce should be part of the path integral, because the singular bounce can always be avoided by deforming the time path in the complex plane. The fields evolution along such a time path would then be regular. By Cauchy's theorem, such deformation of the time path are allowed as long as no singularity is crossed. However here this is not the case: as can be seen from figure 4.6c, the scalar field becomes singular on the bounce in the original time path, so a singularity is necessarily crossed in the deformation.

We point out that such bouncing geometries, made regular by deforming the time path into the complex plane, have been studied as possible alternatives to the beginning of the universe [78, 79]. In the chapter 6 of this thesis, we will study a criterion on complex metrics coming from quantum field theory, which precisely rules out those bounces.

Let us make two more remarks on this question. First, we are evaluating the path integral in the constant lapse gauge [80], and therefore we consider the saddle point geometry with constant lapse as the fundamental one. This specific choice of gauge in defining the gravitational path integral is debatable and may be the subject of future studies. Second, in the non-compact saddle point geometries, the variables x and y possess a perfectly regular evolution in time. Singularities appear only when transforming back

to the original field variables a and ϕ, and the transformation itself is ill-defined at the singularity. Nevertheless, the variables a and ϕ are those with a physical meaning, so we view them as more fundamental. Non-compact saddle point solutions are thus discarded despite the regularity of the x and y field variables.

The wavefunction finally remains with one relevant saddle point:

$$\Psi[a_{\rm f}, \phi_{\rm f}] \approx e^{\frac{i}{\hbar} S^{\rm compact}_{\text{on-shell}}(N_+[\gamma_+])}, \tag{4.2.26}$$

with the on-shell action on the compact saddle point geometry given at quadratic order in $\phi_{\rm f}$ by:

$$S(N_+[\gamma_+]) = -\frac{i}{3}\left(1-\sqrt{1-a_{\rm f}^2}^{\,3}\right) + \frac{i}{2}\left(1-\sqrt{1-a_{\rm f}^2}\right) a_{\rm f}^2\phi_{\rm f}^2 + \mathcal{O}(\phi_{\rm f}^4)\,. \tag{4.2.27}$$

This purely imaginary action leads to a pure amplitude for the wavefunction: it grows from zero at $a_{\rm f} = 0$ until the boundary of the region II, $a_{\rm f}^2\cosh(2\phi_{\rm f}) < 1$, is reached. A phase develops only when the universe grows beyond this boundary into the region I.

As in the pure gravity case [76], the compact geometry selected by the Picard-Lefschetz theory, $N_+[\gamma_+]$, corresponds to less than a half-sphere. In contrast, the other compact geometry, $N_-[\gamma_-]$, corresponds to more than a half-sphere, as can be seen in figure 4.6. This ensures that in the limit where the final scale factor $a_{\rm f}$ goes to 0, the geometry dominating the wavefunction is the vanishing geometry, rather than the full-sphere. The opposite would have been the sign that a non-trivial topology dominates the path integral.

4.2.4 Region III: real saddle points.

This last region is defined by $a_{\rm f}^2\sinh^2(2\phi_{\rm f}) > 1$. The imaginary part of γ is there given by $\mathrm{Im}(\gamma) = \pi/4 + n\cdot\pi/2$ with $n \in \{-1, 0\}$. Therefore,

$$\cosh(2\gamma) = i(-1)^n \sinh(2\,\mathrm{Re}[\gamma])\,, \quad \text{and} \quad \sinh(2\gamma) = i(-1)^n\cosh(2\,\mathrm{Re}[\gamma])\,, \tag{4.2.28}$$

are purely imaginary, implying that the initial momenta Π_x^0, Π_y^0 and the classical solutions $\bar{x}(t), \bar{y}(t)$ are purely real (for all $t \in (0,1)$). This makes the saddle point lapse values (4.2.1) and the on-shell action evaluated on those geometries (4.1.7) also purely real. Whatever saddle points dominate the wavefunction, it will take the form:

$$\Psi[x_{\rm f}, y_{\rm f}] = \sum e^{i\cdot\text{real number}}, \tag{4.2.29}$$

meaning that all the relevant saddle points get the same amplitude. This wavefunction does not describe a true quantum state, and instead furnishes a collection of classical evolutions. Furthermore, we will now prove that **the classical solutions found in region III are non-physical**, as they always encounter a singular bounce.

The classical solution $\bar{x}(t)$ describes in this case an upward facing parabola, because

$N^2 > 0$. The classical solution $\bar{y}(t)$ still forms a straight line. Consider first the compact saddle points. There we start from $\bar{x}(0) = \bar{y}(0) = 0$, with the initial gradient of $\bar{y}$ larger than that of $\bar{x}$:

$$\left|\frac{\dot{\bar{y}}(t)}{\dot{\bar{x}}(t)}\right|_{t=0} = |\coth(\mathrm{Re}[\gamma])| > 1\,. \tag{4.2.30}$$

Since at the end point we get $\bar{x}(1) > \bar{y}(1)$, we conclude that there must exist a time point $t_\star \in (0,1)$ where the two curves $\bar{x}(t)$ and $\bar{y}(t)$ intersect, so that $\bar{a}(t_\star) = 0$. This shows that compact saddle point geometries contain a singular bounce where perturbations blow up. Following the line of arguments develop for the region II, these saddle points are then excluded from the path integral. Turning to non-compact saddle points, we initially find $\bar{x}(0)^2 - \bar{y}(0)^2 < 0$ and at the end point, $\bar{x}(1)^2 - \bar{y}(1)^2 > 0$. As for the non-compact saddle point of region II, by the mean value principle there must be a point $t_\star \in (0,1)$ where the geometry vanishes, $\bar{a}(t_\star) = 0$, giving us another singular bounce.

We conclude that in region III, there are no physically acceptable solutions. This is not a problem because this region is not continuously connected to the pure gravity case $\phi_\mathrm{f} \to 0$. This result simply means that there is a maximal bound on ϕ_f that lead to classical spacetime, and this bound is $a_\mathrm{f}^2 \sinh^2(\phi_\mathrm{f}) < 1$.

4.3 AdS potential

We now turn to the negative hyperbolic cosine potential ($\alpha = -1$, $\beta = 0$), represented in red in figure 4.1. This potential is prototypical of those appearing in string compactifications, at least for small values of the scalar field[4]. The interest of this potential is also that at its maximum in $\phi = 0$, we recover the pure Anti-de Sitter case, studied in [53, 76]. There it was found that the AdS path integral is formally completely analogous to a no-boundary path integral, including the requirement for a regularity condition in the interior of the geometry.

4.3.1 Compactness condition

The saddle point geometries for the AdS potential are given by:

$$N_\pm^\mathrm{saddle} = i\cosh(2\gamma) \pm \sqrt{-\cosh^2(2\gamma) - a_\mathrm{f}^2\cosh(2\phi_\mathrm{f})}\,. \tag{4.3.1}$$

As for the positive hyperbolic cosine potential 4.2, the constraint equation together with the regularity condition implies that $\bar{x}(t=0) = 0$ is always satisfied. Therefore, the compactness condition, $\bar{a}(t=0) = 0$, only requires that $\bar{y}(t=0) = 0$. This condition on the classical solution (4.1.15) is satisfied for the lapse value $N_\mathrm{compact} = a_\mathrm{f}^2\sinh(2\phi_\mathrm{f})/(2i\sinh(2\gamma))$. Equating this expression with the saddle point lapse expres-

[4]The typical string compactification potential would in addition be bounded by below and thus turn upward for large ϕ).

sions (4.3.1), we obtain an equation for γ:

$$a_{\rm f}^2 \sinh^2(2\phi_{\rm f}) - 4\sinh(2\gamma)\sinh(2\gamma - 2\phi_{\rm f}) = 0\,, \tag{4.3.2}$$

whose solution in the complex plane are given by:

$$\begin{cases} 2\gamma^{\rm I}_{\mp} = \mp\cosh^{-1}\left(\sqrt{1 + \dfrac{\sinh^2(2\phi_{\rm f})}{4}\left(2 + a_{\rm f}^2\cosh(2\phi_{\rm f}) - \sqrt{\left(2 + a_{\rm f}^2\cosh(2\phi_{\rm f})\right)^2 - a_{\rm f}^4}\right)}\right); \\ 2\gamma^{\rm II}_{\mp} = \mp\cosh^{-1}\left(\sqrt{1 + \dfrac{\sinh^2(2\phi_{\rm f})}{4}\left(2 + a_{\rm f}^2\cosh(2\phi_{\rm f}) + \sqrt{\left(2 + a_{\rm f}^2\cosh(2\phi_{\rm f})\right)^2 - a_{\rm f}^4}\right)}\right). \end{cases} \tag{4.3.3}$$

The solutions $\gamma^{\rm I}_-$ and $\gamma^{\rm II}_+$ are defined for $\phi_{\rm f} > 0$, while $\gamma^{\rm I}_+$ and $\gamma^{\rm II}_-$ are defined for $\phi_{\rm f} < 0$. For the explicit derivation of this result, see the appendix B.2.

For each choice of final boundary conditions $(a_{\rm f}, \phi_{\rm f})$, we find four saddle point solutions, two compact ($N_+[\gamma^{\rm I}]$ and $N_-[\gamma^{\rm II}]$), and two non-compact ($N_+[\gamma^{\rm II}]$ and $N_-[\gamma^{\rm I}]$). All those γ values are real, so the saddle point lapse values (4.3.1) are purely imaginary. This implies that the on-shell action evaluated on these saddle points (4.1.7) is also purely imaginary. Therefore, e^{iS} is a pure amplitude and the no-boundary wavefunction will not contain any phase, i.e., it doesn't lead to classical spacetime.

4.3.2 Saddle point geometries and lapse integration

We illustrate again the fields evolution for the four different saddle points (see figure 4.8), and the structure of flow lines (see figure 4.9) with the numerical example $a_{\rm f} = 2$, $\phi_{\rm f} = 0.1$.

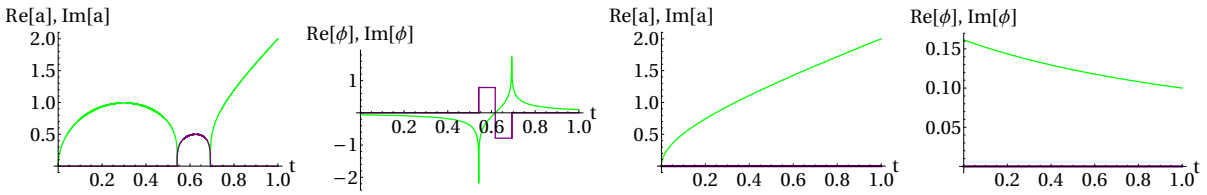

(a) Compact Euclidean geometry $N_+[\gamma^{\rm I}_-]$.

(b) Compact Euclidean geometry $N_-[\gamma^{\rm II}_+]$.

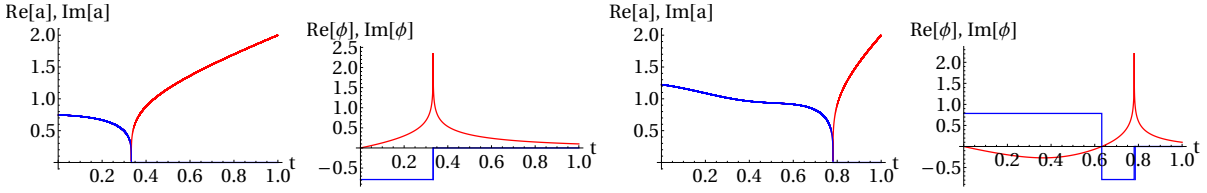

(c) Non-compact Euclidean geometry $N_-[\gamma^{\rm I}_-]$.

(d) Non-compact Euclidean geometry $N_+[\gamma^{\rm II}_+]$.

Figure 4.8: Fields evolution in time, for the four saddle point geometries. Parameters are: $\alpha = -1$, $\beta = 0$, $a_{\rm f} = 2$, $\phi_{\rm f} = 0.1$, (N is purely imaginary). The relevant numerical values are $\gamma^{\rm I}_- = -0.0615$, $N_+[\gamma^{\rm I}_-] = 3.26i$, $N_-[\gamma^{\rm I}_-] = -1.25i$; $\gamma^{\rm II}_+ = 0.162$, $N_-[\gamma^{\rm II}_+] = -1.23i$, $N_+[\gamma^{\rm II}_+] = 3.33i$. Same conventions as in Fig. 4.3.

.

For this example, we find a singular bounce within the evolution of the two non-compact saddle point geometries, $N_+[\gamma^{\rm II}]$, $N_-[\gamma^{\rm I}]$, as well as for the compact saddle point

geometry $N_+[\gamma^{\mathrm{I}}]$. Using the argument developed in 4.2.2, the contribution of these geometries to the wavefunction is suppressed by the blowing-up of fluctuations at the singularity. Moreover, as in section 4.2, one can show analytically that these singular bounces occur for any final boundary conditions $(a_{\mathrm{f}}, \phi_{\mathrm{f}})$.

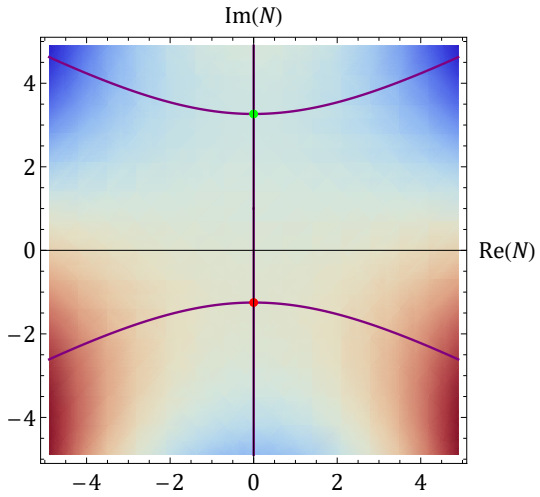

(a) $N_+[\gamma^{\mathrm{I}}_-]$ (green dot) and $N_-[\gamma^{\mathrm{I}}_-]$ (red dot).

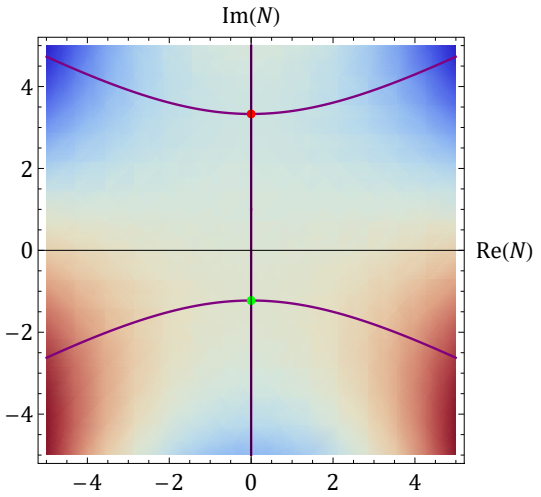

(b) $N_-[\gamma^{\mathrm{II}}_+]$ (green dot) and $N_+[\gamma^{\mathrm{II}}_+]$ (red dot).

Figure 4.9: Case $\alpha = -1$, $\beta = 0$, $a_{\mathrm{f}} = 2$, $\phi_{\mathrm{f}} = 1$. Density plot of the weighting $\mathrm{Re}[iS^{\text{on-shell}}_{\text{saddle}}]$ and flow lines in the complex N plane. Same conventions as in Fig. 4.4.

The only saddle point geometry left is $N_-[\gamma^{\mathrm{II}}]$. From the lapse integration given by Picard-Lefschetz theory, this saddle point (lower half plane in 4.9b) will be selected only if the integration contour runs along the lower imaginary axis in the lapse complexified plane (in order to obtain a real valued wavefunction, we can define the path integral as a sum of two contours, one running from $-i\infty$ up to the upper saddle point, and then along the steepest descent contour on the left, and the second mirroring the first with respect to the imaginary axis: this provides two complex conjugate contributions as in the pure gravity case [53, 76]).

The no-boundary wavefunction is then approximated by

$$\Psi[a_{\mathrm{f}}, \phi_{\mathrm{f}}] \approx e^{\frac{i}{\hbar} S^{\text{compact}}_{\text{on-shell}}(N_-[\gamma^{\mathrm{II}}_+])}, \text{ with} \tag{4.3.4}$$

$$S^{\text{compact}}_{\text{on-shell}}(N_-[\gamma^{\mathrm{II}}_+]) = -\frac{i}{3}\left((a_{\mathrm{f}}^2+1)^{3/2}-1\right) - \frac{i}{2}\left((a_{\mathrm{f}}^2+1)^{1/2}-1\right) a_{\mathrm{f}}^2\phi_{\mathrm{f}}^2 + \mathcal{O}(\phi_{\mathrm{f}}^4)\,. \tag{4.3.5}$$

To conclude, we have shown that in approximately AdS space, the prescription to define the path integral with a momentum condition instead of a Dirichlet condition on the interior also works once a scalar field is included.

4.4 Exponential potential

We now consider the simple exponential potential, $V(\phi) \propto e^{2\phi}$, described in our model by parameters $\alpha = \beta$, and drawn in green in figure 4.1. Classically, this potential possesses

inflationary scaling solutions with a constant equation of state, see [39]. Nevertheless, it is nowhere flat, and therefore it doesn't contain any de Sitter limit, in contrast with the hyperbolic cosine potential.

The scaling symmetry present in this model allows for some simplifications, in particular there is a unique expression for the saddle point lapse value (4.1.21),

$$N^0_{\text{saddle}} = -\frac{ia_{\text{f}}^2}{2}\exp(2\phi_{\text{f}} - 2\gamma)\,. \tag{4.4.1}$$

The regularity condition together with the constraint equation ensures in this case that $\bar{x}(0) = -\bar{y}(0)$. Therefore, the initial scale factor is always compact: $\bar{a}(0) = \sqrt[4]{\bar{x}(0)^2 - \bar{y}(0)^2}$. However, it turns out that if $\bar{x}(0)$ and $\bar{y}(0)$ do not also vanish independently, then the momentum of the scale factor, $\dfrac{a\dot{a}}{N}$, blows up as $t \to 0$. To avoid this divergence, we must impose that:

$$\bar{x}(t=0) = x_{\text{f}} - \alpha N^2 - 2Ni\cosh(2\gamma) = 0\,. \tag{4.4.2}$$

That condition (4.4.2) applied on the saddle point geometry, N^0_{saddle}, leads to the equation:

$$a_{\text{f}}^2\cosh(2\phi_{\text{f}}) + \frac{\alpha a_{\text{f}}^4}{4}e^{4\phi_{\text{f}}-4\gamma} - a_{\text{f}}^2\cosh(2\gamma)e^{2\phi_{\text{f}}-2\gamma} = 0\,, \tag{4.4.3}$$

which can be solved for $\gamma \in \mathbb{C}$ and yields the solutions:

$$\begin{cases} \gamma^{\text{I}}_{(n)} = \dfrac{1}{4}\ln\left(\dfrac{1 - a_{\text{f}}^2\frac{\alpha}{2}e^{2\phi_{\text{f}}}}{e^{-4\phi_{\text{f}}}}\right) + in\cdot\dfrac{\pi}{2} \quad \text{for } n \in \{0,1\}\,; \\ \gamma^{\text{II}}_{(n)} = \dfrac{1}{4}\ln\left(\dfrac{a_{\text{f}}^2\frac{\alpha}{2}e^{2\phi_{\text{f}}} - 1}{e^{-4\phi_{\text{f}}}}\right) + i\left(\dfrac{\pi}{4} + n\cdot\dfrac{\pi}{2}\right) \quad \text{for } n \in \{-1,0\}\,; \end{cases} \tag{4.4.4}$$

whose respective regions of validity, represented in figure 4.10 for $\alpha = 1/2$, are

$$\text{region I:} \quad a_{\text{f}}^2\frac{\alpha}{2}e^{2\phi_{\text{f}}} < 1\,; \qquad \text{region II:} \quad a_{\text{f}}^2\frac{\alpha}{2}e^{2\phi_{\text{f}}} > 1\,. \tag{4.4.5}$$

The stability condition $\text{Im}(\Pi^0_x) > 0$ will not be satisfied for $\gamma^{\text{I}}_{(1)}$, so this solution can be ruled out immediately.

For this case, we find one compact saddle point for each value of γ. We look closer to their geometry. In region I, the imaginary part of γ implies that the momenta Π^0_x, Π^0_y and the saddle point lapse values (4.4.1) are purely imaginary. Therefore, once again the wavefunction constructed from these geometries is a pure amplitude and we do not obtain a classical spacetime. In region II on the contrary, the imaginary part of γ leads to purely real momenta, real saddle point lapse values and real on-shell action evaluated on these saddle points. The wavefunction should then describe a collection of classical solutions that all have the same weighting. Nevertheless, all geometries of region II contain a

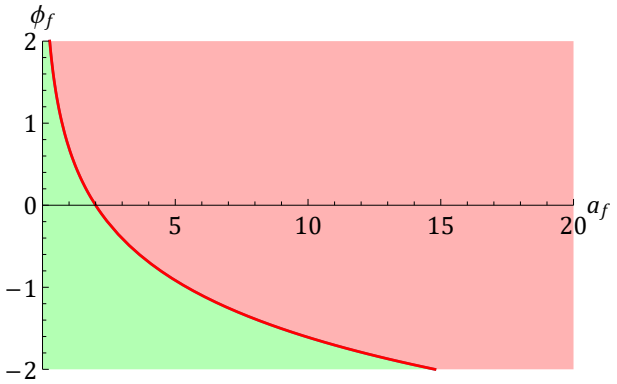

Figure 4.10: Phase space regions delimited by the condition $a_{\rm f}^2 \frac{\alpha}{2} e^{2\phi_{\rm f}} = 1$ (red curve), with $\alpha = 1/2$. In the red region, the saddle point value for the lapse is purely real. In the green region, the saddle point value for the lapse is purely imaginary.

singular bounce in their evolution[5]. The proof is straightforward and similar to that of subsection 4.2.3. As also discussed in there, singular geometries are excluded from the path integral, as they lead to the blowing-up of perturbations.

Therefore, for the pure exponential potential, we don't find any regular no-boundary solutions that could predict a classical evolution of the fields.

4.5 An unrealistic potential

The last model we consider is a hyperbolic sine potential ($\alpha = 0$, $\beta = 1$), represented in orange in figure 4.1. This is a special case, because this potential is not prototypical of any known physical situation. It is unbounded from below and steep for negative values, though not enough to possess ekpyrotic solutions [81], it doesn't possess a slow-roll region or a de Sitter like minimum, and it resembles the hyperbolic cosine potential only at large values of the scalar field $\phi_{\rm f} \ll 1$, where we haven't found any classical spacetime. Indeed our analysis will confirm that this potential does not allow for any no-boundary solutions.

4.5.1 Compactness condition

The saddle point lapse values are:

$$N^{\pm}_{\rm saddle} = i \sinh(2\gamma) \pm \sqrt{-\sinh^2(2\gamma) - a_{\rm f}^2 \sinh(2\phi_{\rm f})}\,. \tag{4.5.1}$$

In this case, the regularity condition and constraint equation imply that $\bar{y}(0) = 0$. The compactness condition reads $\bar{x}(0) = 0$, which translates into the requirement that $N_{\rm compact} = a_{\rm f}^2 \cosh(2\phi_{\rm f})/(2i\cosh(2\gamma))$. Equating this expression to the saddle point values

[5]This fact was already noted in [39].

(4.5.1), we find two equations for $\gamma \in \mathbb{C}$, which are solved by:

$$\begin{cases} \gamma^{\mathrm{I}}_{(n)} = -\frac{1}{2}\cosh^{-1}\left(\frac{\cosh(2\phi)}{2}\sqrt{2 - a_{\mathrm{f}}^2\sinh(2\phi_{\mathrm{f}}) + \sqrt{a_{\mathrm{f}}^4 + (2 - a_{\mathrm{f}}^2\sinh(2\phi_{\mathrm{f}}))^2}}\right) \\ \qquad + i\frac{n\cdot\pi}{2} \text{ with } n \in \{0,1\}\,; \\ \gamma^{\mathrm{II}}_{(n)} = \frac{1}{2}\cosh^{-1}\left(\sqrt{1 - \frac{\cosh^2(2\phi_{\mathrm{f}})}{4}\left(2 - a_{\mathrm{f}}^2\sinh(2\phi_{\mathrm{f}}) - \sqrt{a_{\mathrm{f}}^4 + (2 - a_{\mathrm{f}}^2\sinh(2\phi_{\mathrm{f}}))^2}\right)}\right) \\ \qquad + i\left(\frac{\pi}{4} + \frac{n\cdot\pi}{2}\right),\ n \in \{-1,0\}\,. \end{cases} \tag{4.5.2}$$

These expressions are both valid for any final boundary conditions $(a_{\mathrm{f}}, \phi_{\mathrm{f}})$. Again, the solution $\gamma^{\mathrm{I}}_{(1)}$ violates the stability condition $\mathrm{Im}(\Pi^0_x) > 0$ so it is immediately ruled out.

4.5.2 Analysis of the saddle point geometries

The geometries with γ^{II} have $\mathrm{Im}[2\gamma^{\mathrm{II}}] = \pi/2 + n\cdot\pi,\ n \in \{-1,0\}$, so that the initial momenta Π^0_x, Π^0_y and the saddle point lapse values are purely real. Analogously to similar cases in the previous sections, those saddle point geometries are found to contain a singular bounce and are therefore discarded from the path integral.

We can then focus on geometries with γ^{I}_0. The imaginary part is $\mathrm{Im}(2\gamma^{\mathrm{I}}_0) = 0$, so that the initial momenta Π^0_x, Π^0_y and the saddle point lapse values are purely imaginary. We get two saddle point geometries, one compact $(N_-[\gamma^{\mathrm{I}}_{(0)}])$ and one non-compact $(N_+[\gamma^{\mathrm{I}}_{(0)}])$. These two geometries are Euclidean, because they correspond to real field values a and ϕ throughout their time evolution, and their lapse value is purely imaginary. Their field evolution are represented in figure 4.11, and their steepest descent and ascent contours in the complexified lapse plane are depicted in figure 4.12, for the numerical values $a_{\mathrm{f}} = 2$ and $\phi_{\mathrm{f}} = 1$.

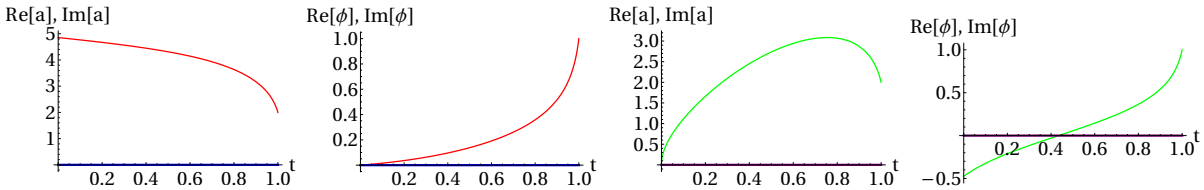

(a) Non-compact Euclidean geometry $N_+[\gamma^{\mathrm{I}}_{(0)}]$. (b) Compact Euclidean geometry $N_-[\gamma^{\mathrm{I}}_{(0)}]$.

Figure 4.11: Case $\alpha = 0$, $\beta = 1$, $a_{\mathrm{f}} = 2$, $\phi_{\mathrm{f}} = 1$, with N imaginary. The relevant numerical values are $\gamma^{\mathrm{I}}_{(0)} = -0.475$, $N_+[\gamma^{\mathrm{I}}_{(0)}] = 2.87i$, $N_-[\gamma^{\mathrm{I}}_{(0)}] = -5.06i$. Geometry associated to the different saddle points. Same conventions as in figure 4.3.

From this numerical example, we see that if we choose the Lorentzian axis as contour of integration, it can be deformed into the steepest descent contour of the compact saddle point (in green). The wavefunction defined by this path integral can be semi-classically approximated by:

$$\Psi[a_{\mathrm{f}}, \phi_{\mathrm{f}}] \approx e^{\frac{i}{\hbar}S^{\mathrm{compact}}_{\mathrm{saddle}}(N_-[\gamma^I_{(0)}])}\,, \text{ with at linear order in } \phi_{\mathrm{f}}: \tag{4.5.3}$$

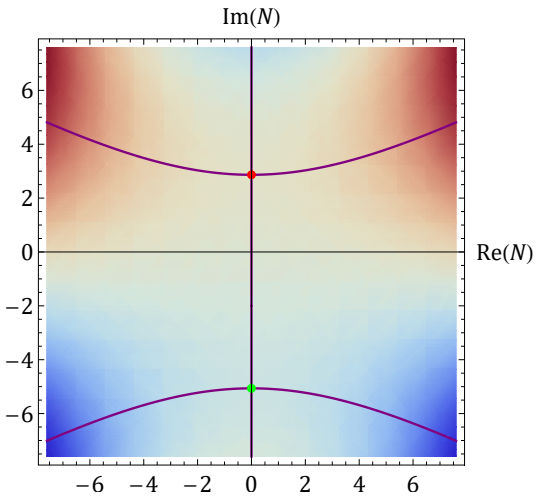

Figure 4.12: Case $\alpha = 0$, $\beta = 1$, $a_\mathrm{f} = 2$, $\phi_\mathrm{f} = 1$. Density plot of the weighting $\mathrm{Re}[iS^{\text{on-shell}}_{\text{saddle}}]$ and flow lines in the complex N plane. Same conventions as in figure 4.4. $N_-[\gamma^{\mathrm{I}}_{(0)}]$ (green dot) and $N_+[\gamma^{\mathrm{I}}_{(0)}]$ (red dot).

$$S^{\text{compact}}_{\text{saddle}}(N_-[\gamma^I_{(0)}]) = -\frac{i}{2}\left(3a_\mathrm{f}^2\sqrt{\sqrt{a_\mathrm{f}^4+4}+2} - \sqrt{\sqrt{a_\mathrm{f}^4+4}-2}^{\,3}\right) + \frac{i}{2}\sqrt{\sqrt{a_\mathrm{f}^4+4}-2}\; a_\mathrm{f}^2\phi_\mathrm{f} + \mathcal{O}(\phi_\mathrm{f}^2)\,.$$

This wavefunction is a pure amplitude. It could describe the nucleation of the universe at small scale factor, as in the region II of the hyperbolic cosine. The difference is that here, this solution is valid for any a_f value, so this nucleation is not followed by a classical evolution. Therefore, these saddle point geometries do not predict the emergence of classical spacetime. The wavefunction actually resembles the quasi-AdS case of section 4.3, except that we used a different contour of integration in the path integral's definition.

Overall, we find that **for the hyperbolic sine potential, the no-boundary wavefunction does not lead to the emergence of classical spacetime**. This illustrates the predictive power of the no-boundary wavefunction: within this proposal, only a few scalar potentials can actually lead to our classical early universe, such as flat-enough positive regions of the potential (inflationary regions [35, 37]), or steep-enough and negative regions of the potential (ekpyrotic no-boundary instantons [82, 36]).

4.6 Discussion

In this chapter, we have built an important step in the understanding of the no-boundary proposal, in particular its implementation in terms of a sum over regular metrics, i.e., the no-boundary proposal defined with a momentum condition. We have studied how this implementation can be generalized to include the description of a scalar field in the early universe, for various prototypes of the scalar potential. The consistent inclusion of a scalar field is a necessary step in the perspective of constructing a more realistic version of the no-boundary wavefunction, which encapsulates matter fields, and can lead to the

standard hot big bang evolution.

We have shown that, in the presence of a scalar field, classical spacetime can only emerge if the scalar potential is of slow-roll type, and in this case, we find that the scalar field goes to 0 at large values of the scale factor. If the final scalar field value is too large, no physical classical evolution can reach this configuration. For AdS-like potentials, we recover pure amplitude wavefunctions giving rise to Euclidean spacetime, similarly to the case without a scalar field. Those Euclidean pure amplitude wavefunctions are also found in the slow-roll type of potential, when considering very small scale factor values. For an exponential potential, we find either a Euclidean spacetime, or a region without any classical evolution, depending on the final configuration of scalar field and scale factor.

One peculiarity of the saddle point geometries in the presence of a scalar field, is that they always (except for the exponential potential) come in pairs, one being regular and compact initially at the no-boundary point, the other being only regular but non-compact. Nevertheless these non-compact geometries are always sub-dominant in the path integral.

Another key feature of our solutions is that the initial value of the scalar field at the no-boundary point always depends on the final boundary conditions. This actually poses a strong non-causality puzzle, which questions the validity of our prescription for the no-boundary wavefunction. This puzzle can be resolved either by assuming that quantum gravity is inherently non-causal, or by considering that the scalar field must take real (or not too complex) values and then construct a different prescription, e.g., summing on all γ values. Such a restriction could in particular follow from the application of the KS criterion for complex metrics (which will be the subject of chapter 6), because this criterion necessitates scalar fields to be real (generalization of the KS criterion, in particular considering effects of dimensional compactifications [77], still allow a certain range of complex values for the scalar field). Note that for Euclidean spacetimes, there is no notion of causality anyway. Restricting the scalar field to lie on the extrema of the potential can have interesting implications for the observations. Since the no-boundary wavefunction scales as $e^{1/(\hbar V(\phi))}$, low values of the potential are preferred. For a theory containing many scalar fields, as is expected for instance in string heterotic models, the most probable configuration consists of having all scalar fields lying on the lowest minimum of their potential. This feature would explain why all the coupling constants in our universe are observed to be time-independent. But this configuration would also leave an empty universe, so it is preferable that at least one of these scalar fields stands on a local maximum of the potential. This scalar field could then lead to an inflationary phase and generate density perturbations. Making such a scenario viable requires a better knowledge of the precise structure of the potential, which should possess a local maximum where large perturbations can be generated and next to a stable minimum where inflation can end. This is an open problem, but we have shown here that for a suitable dynamical theory, the no-boundary proposal still provides a consistent theory for the initial conditions of the universe.

Before moving on to the next part of this thesis, we make two last remarks. First, we have encountered many singular bouncing solutions in the geometries, both for compact and non-compact saddle points. On this point, we stress that our implementation of the no-boundary proposal relies on a minisuperspace ansatz. This ansatz is equivalent to making a strong symmetry reduction, and implies we are throwing away many degrees of freedom (by only considering homogeneous fields). Therefore, it is always necessary to verify a posteriori that the symmetry reduction was indeed consistent, i.e., that we didn't get rid of important contributions. In particular, the solutions containing a singular bouncing imply a blowing up of the perturbations at the singularity: these solutions are thus inconsistent with the minisuperspace ansatz. Finally, the prescription of the no-boundary proposal implies a choice of both boundary conditions and of the contours of integration. These choices are however connected, and in this chapter we have found that negative potentials require near-Euclidean geometries, while positive potentials require near-Lorentzian geometries. This question will also be reconsidered with the KS criterion for complex metrics in chapter 6.

Part II

Semi-classical constraints on the early universe

Chapter 5

Finite amplitude criterion

In this final part of the thesis, we depart from our previous focus on the no-boundary proposal and enlarge our perspective to other early universe models. The main ambition of this thesis is to study the gravitational path integral. In this third part, we investigate in particular the consequences of considering the path integral quantization at the semi-classical level, on a plethora of models for the early universe. First, in this chapter we construct a criterion based on the consistency of probability amplitudes defined through the path integral. Then in the next chapter, we apply a criterion for complex metrics, stemming from the consistency of matter fields path integrals in quantum field theory, to the case of early universe models.

In the context of the path integral quantization, cosmological amplitudes give the probability amplitudes for transitioning between two cosmological configurations, $\Phi_{\rm i}$ and $\Phi_{\rm f}$:

$$\mathcal{A}[\Phi_{\rm i} \to \Phi_{\rm f}] \equiv \int_{\Phi_{\rm i}}^{\Phi_{\rm f}} \mathcal{D}\Phi \, e^{iS[\Phi]/\hbar} \approx \sum_{\text{saddles}} \mathcal{N} \, e^{iS^{\text{classical}}_{\text{saddle}}[\Phi]/\hbar} \,. \tag{5.0.1}$$

The cosmological configurations typically consist of a spacetime hypersurface, on which all field values or their momenta are specified. Our definition of cosmological amplitudes (5.0.1) makes use of the Lorentzian path integral, which weights every path by a phase proportional to the Lorentzian action of all the fields (including the metric field), $S[\Phi]$. A minimal requirement for the path integral quantization to be consistent is then that the cosmological amplitude gives a finite contribution for any pair of field configurations "in the past", or up to current configurations. We call this *the finite amplitude criterion*. From the semi-classical approximation, which estimates the path integral by its leading (classical) order in the expansion in Planck's constant[1], as spelled out in (5.0.1), we find that a necessary requirement for obtaining a finite amplitude, is that the classical action evaluated on the saddle point configurations[2] is itself finite. We will show that this simple criterion already leads to stringent constraints on the cosmological models.

[1] The normalization factor $\mathcal{N}$, present in the semi-classical expression for the amplitude, will be unimportant for our considerations in this chapter.

[2] We recall that saddle points of an action are (generically complex) classical solutions to the equations of motion of this action.

We point out that the action is required to be finite only on-shell (e.g., evaluated on the saddle points). Off-shell actions are generically infinite, and this feature can be viewed as causing the uncertainty principle in quantum mechanics. Requiring a finite classical action is nevertheless not sufficient to ensure a finite amplitude, and in particular quantum interferences between several saddle point solutions can sometimes lead to instabilities. The stability of the configurations described by the cosmological amplitudes is therefore also a necessary requirement, which we will probe when possible. In this sense, the finite amplitude criterion goes beyond classical considerations and enables us to scrutinize some quantum aspects.

Figure 5.1: Theories studied in this chapter against the finite amplitude criterion. Dashed (respectively plain) nodes represent theories where the criterion is necessarily violated (respectively satisfied under certain conditions). These conditions, and more details on the characteristics of each model, are given in the table 5.1 and in the main text.

Scenario	Specifics	Sec.	Results and conclusions
Standard cosmological models	+ scalar field	5.1.1	Yes if $\forall\phi$, $\lvert V(\phi)\rvert < \infty$, four-volume $< \infty$. In FLRW/B9: Yes if $a^3 V \overset{t\to 0}{\sim} t^p$, $p > -1$.
	+ perfect fluid $p = w\rho$	5.1.2	In FLRW: Yes if $-1 < w < +1$.
	Black holes	5.1.3	Yes: singularity always in the future.
Inflation	First phase of evolution	5.2.1	No: $S^{(\text{classical})}_{\text{on-shell}} < \infty$ but interferences $\Rightarrow$ unstable semi-classical amplitudes.
	Eternal inflation	5.2.2	No: $S_{\text{on-shell}} \to \infty$.
	Transient & non-eternal	5.2	Yes.
Bounce	contracting phase with $p = w\rho$	5.3.1	Yes **if and only if** $w > 1 \Leftrightarrow$ pure ekpyrotic phase.
Cyclic universe (EH action in FLRW)	Exactly cyclic: $\exists P$ s.t. $\forall t : a(t) = a(t+P)$	5.3.2	No: $S_{\text{on-shell}} \to \infty$, and moreover, it violates the second law of thermodynamic.
	a larger at each cycle, but cyclic in local quantities, e.g., H	5.3.2	Yes: a reaches 0 in finite proper time, but universe becomes geodesically incomplete.
No-boundary proposal	Defined with initial momentum/regularity condition	5.4	Yes: $S_{\text{on-shell}} < \infty$ and stable semi-classical amplitudes.
$(\text{Riem})^n$ higher-curvature theories	Quadratic gravity ($n = 2$)	5.5.4	Yes: $S_{\text{on-shell}} < \infty$ only for accelerating (possibly anisotropic) backgrounds.
	$n \geq 3$ on Lorentzian FLRW bckg	5.5.3	$k = 0$: Yes if n is bounded and $\exists$ sufficiently accelerated expansion. $k \neq 0$: No, $S_{\text{on-shell}} \to \infty$.
	All n included	5.5.3	No for all FLRW solutions.
Emergent and loitering universes	k-essence theory (e.g. ghost condensate)	5.6.1	Yes, but other issues (e.g., unitarity violation of fluctuations).
	(beyond-)Horndeski	5.6.1	Yes for some models, at least at bckg level.
	Loitering phase in EH action	5.6	Yes, also with a scalar field and a perfect fluid action.
	Loitering phase in string cosmology	5.6.2	Dilaton gravity: No, $S_{\text{on-shell}} \to \infty$. Non-pert. curvature corr. in α' [83]: Yes.

Table 5.1: Summary of the results of this work. In the last column, "yes" and "no" refer to whether the finite amplitudes criterion is satisfied or not. The fact that these theories satisfy the finite amplitude criterion doesn't mean that they are exempt of any other inconsistencies.

Before we embark on the task of studying early universe models against this criterion, we must make several remarks. First, we insist on the fact that in the definition of the amplitudes (5.0.1), because we are performing the path integral also on the gravitational sector, the spacetime geometry is not fixed from the onset. Therefore, the total time elapsed between the initial and final configuration will not necessarily be specified. Since we will in particular focus on early universe models, we will sometimes consider a initial

configuration in the infinite past, and sometimes some finite time ago. Our second remark concerns the type of models that can be constrained by this criterion. Obviously, we can only restrict models possessing an action description. In particular, if the degrees of freedom drastically change in the early universe, e.g., by reaching a non-geometric phase such as in [84], then the amplitude definition we have given here will not apply anymore. Then, our third remark aims to underline the strong potential of our criterion, by illustrating it with the example of quadratic gravity studied in [85]. There it was found that demanding the finiteness of the classical action restricts possible backgrounds near the big-bang to accelerating scale factors (in this chapter we will see how this result can be improved). Therefore, quadratic gravity imposes strict initial conditions which are favorable to inflation. Independently of whether or not quadratic gravity turns out to be a viable theory for the early universe, this highlights how a semi-classical criterion can form a strong selection principle for the initial conditions of the early universe. Finally, we must note that already more than forty years ago, a finite action criterion was put forward by Barrow and Tipler (BT) [86], and was also recently updated in [87]. Although this criterion is very similar to the one we develop in this chapter, its motivation is deeply different and leads to remarkably contrasting consequences. BT's finite action principle requires the classical action, evaluated over the *entire history of the universe*[3] to be finite. This stems from the consideration that the action is a fundamental physical quantity, from which all the dynamic of the system is derived, and it should therefore be finite. This represents a (too) strong requirement, as it implies that the far future can affect the past history of the universe. This criterion is thus more constraining than ours at the classical level, but it nevertheless lacks the sensitivity to quantum aspects that we can achieve.

The results we will present in this chapter were published in [2]. In figure 5.1, we have represented schematically all the cosmological models that we will study against our finite amplitude criterion in this chapter. Then in table 5.1 we summarize the same results in more detail, and refer to specific sections of the chapter where those results are derived. These results will then be discussed in detail in the discussion section of this chapter 5.7. The next sections of this chapter rely and present the results of [2].

5.1 Standard cosmological models

We first confront the finite amplitude criterion with the standard cosmological model presented in the introductory chapter 1. This describes a universe obeying the basic action of general relativity. We will consider two simple types of matter fields, first a canonical scalar field 5.1.1, and then some perfect fluid matter fields 5.1.2, as appeared in the hot big bang model 1. We will also say a word about boundary terms and black hole solutions in the context of this criterion 5.1.3.

[3]By entire, we mean the whole four-manifold describing the universe's geometry.

5.1.1 Canonical scalar field

Scalar fields are the simplest matter fields we can add to general relativity, and we have seen (see chap. 3) that for a homogeneous and isotropic early universe, a scalar field is generically enough to describe the effects of matter close to the beginning of spacetime, and can generate an inflationary mechanism 1.2.

The action for general relativity minimally coupled to a canonical scalar field is:

$$S_{\text{scalar}} = \int \mathrm{d}^4x\,\sqrt{-g}\left(\frac{M_{\text{Pl}}^2}{2}R - \frac{1}{2}\partial_\mu\phi\partial^\mu\phi - V(\phi)\right). \tag{5.1.1}$$

The equations of motion for this action are the Einstein field's equations (1.1.9), $R_{\mu\nu} - \frac{1}{2}Rg_{\mu\nu} = \frac{1}{M_{\text{Pl}}^2}T_{\mu\nu}$, where $T_{\mu\nu}$ is the energy-momentum tensor of the scalar field,

$$T_{\mu\nu} = \partial_\mu\phi\partial_\nu\phi + g_{\mu\nu}\left(-\frac{1}{2}\partial_\alpha\phi\partial^\alpha\phi - V(\phi)\right). \tag{5.1.2}$$

The finite amplitude criterion can be satisfied only if the on-shell action, evaluated on classical solutions of the equations of motion, is finite. To probe this, we substitute the field equations into the action[4]. We take the trace of the equations of motion (1.1.9), $M_{\text{Pl}}^2R = -T = \partial_\mu\phi\partial^\mu\phi + 4V(\phi)$, and use it to replace the first term in the action (5.1.1), yielding the simple on-shell action,

$$S_{\text{scalar}}^{\text{on-shell}} = \int \mathrm{d}^4x\sqrt{-g}\,V(\phi). \tag{5.1.3}$$

The expression (5.1.3) leads to key consequences concerning the finite amplitude criterion. We consider a final configuration at time $t = t_0$: $\phi(t_0) = \phi_{\text{f}} \in \mathbb{R}$ and $g_{ij}(t_0) = h_{ij}$. Then the on-shell action (5.1.3) will be finite if:

1. the scalar **potential is bounded everywhere**: $\forall\phi$, $|V(\phi)| < \infty$, and the **four-volume** up to the final configuration in $t = t_0$ **is finite**: $\mathcal{V} = \left(\int \mathrm{d}^3x \int^{t_0} \mathrm{d}t\,\sqrt{-g}\right) < \infty$;

2. in the past, the scalar potential $V(\phi)$ decreases sufficiently fast as to render the on-shell action finite when integrating back to infinite past (genesis scenario, see section 5.6).

In this section we concentrate on the first possibility where **the four-volume $\mathcal{V}$ must be finite** to ensure the finiteness of the on-shell action. In this case, the actual behavior of the scalar field and the exact shape of the geometry are of no importance to the finite amplitude criterion. The finiteness of the four-volume has two immediate consequences:

[4]By doing so, we allow for cancellations between gravity and matter terms. This is justified by the fact that in quantum gravity, we do not expect a strong distinction between gravity and matter, and indeed in supersymmetry for example, all fields are described in the same multiplet, while in string theory, gravity as well as matter is described by strings.

1. the universe must have had a beginning in time, $t = 0$;

2. the spatial volume of the universe must be finite. This is automatic for a closed universe and can be achieved with adequate non-trivial topology for flat and open universes. From now on we thus set the spatial volume to unity for clarity.

We point out that the four-volume can stay perfectly finite although the curvature blows up in the approach of the beginning of time, as is the case in the presence of Bianchi IX anisotropies. We recall that in Euler's angles $\psi, \theta \in [0, \pi]$ and $\phi \in [0, 2\pi]$, the Bianchi IX metric reads (3.1.4):

$$\begin{aligned} \mathrm{d}s^2_{\mathrm{B_{IX}}} = -\mathrm{d}t^2 + a^2\Big[e^{-4\beta_+}(\mathrm{d}\psi + \cos\theta\,\mathrm{d}\phi)^2 + e^{2(\beta_+ + \sqrt{3}\beta_-)}(\sin\psi\,\mathrm{d}\theta - \cos\psi\sin\theta\,\mathrm{d}\phi)^2 \\ + \; e^{2(\beta_+ - \sqrt{3}\beta_-)}(\cos\psi\,\mathrm{d}\theta + \sin\psi\sin\theta\,\mathrm{d}\phi)^2\Big]\,, \end{aligned} \tag{5.1.4}$$

for the scale factor $a(t)$ and the anisotropies $\beta_\pm(t)$. Even though it is well-known that a generic approach to the initial singularity is governed by the mixmaster equations [88] where the anisotropies blow up, the overall volume is nevertheless given by $\sqrt{-g} = a^3 \sim t$, so that the four-volume stays finite.

This feature enables to soften the condition that the scalar potential must be bounded everywhere for certain homogeneous backgrounds such as FLRW or Bianchi IX, whose metric can be generically written as: $\mathrm{d}s^2 = -\mathrm{d}t^2 + a(t)^2\mathrm{d}\mathbf{x}^2$. Then their on-shell action (5.1.3) gives

$$S^{\text{on-shell}}_{\text{scalar}} \propto \int_0^{t_0} \mathrm{d}t\, a^3 V(\phi)\,, \tag{5.1.5}$$

which remains finite as long as the rate of divergence of $a^3V(\phi)$ is strictly slower than that of t^{-1} as $t \to 0$, and that this quantity is bounded everywhere else. For instance, for the following exact solution in FLRW[5]:

$$V(\phi) = V_0\,\exp\left(\sqrt{\frac{2}{s}}\,\phi\right),\ \text{with } s > 1/3 \ \Rightarrow\ \begin{cases} a(t) = t^s\,, \\ \phi(t) = -\sqrt{2s}\ln\left(t\sqrt{\dfrac{V_0}{s(3s-1)}}\right), \end{cases} \tag{5.1.6}$$

we find that $a^3V(\phi) \propto t^{3s-2}$ so that even though the scalar potential diverges as $V(\phi) \propto t^{-2}$, the on-shell action remains finite. However, the argument developed here requires us we trust the scalar potential over an infinite field range. This is a strong assumption which generically fails for example in string compactifications [9].

Finally, we point out that in the case of vacuum, or if the potential vanishes identically, $V(\phi) = 0$, e.g., in the case of a massless scalar field, then the on-shell action (5.1.3) also

[5] The requirement $s > 1/3$ constrains the pressure-to-energy density ratio, w, to lie in the range $(-1, 1)$. In this range, the anisotropies will typically dominate the approach to the big bang, so the exact FLRW solution presented here is not generic, but it serves an illustrative purpose. The argument presented here is also valid in the presence of anisotropies even though there are no simple exact solutions known in that case.

vanishes. This would imply that the finite amplitude criterion is satisfied regardless of the four-volume of the universe. However, if the only matter field is such a massless scalar (or in vacuum), no measurement of transition amplitudes can be made, since the propagation speed of matter equal that of light. Any physical apparatus would be massive and would alter the matter content, and render the on-shell action non zero.

5.1.2 Perfect fluid matter fields

As we have seen in chapter 1, many matter types of cosmological relevance are well approximated by perfect fluids of energy density ρ and pressure p. The equation of state relating pressure and energy density reads: $p = w\rho$. Then the trace of the energy-momentum tensor is $T = \rho(3w-1)$ in four-dimensions, and as in the previous subsection, the on-shell action of gravity with a perfect fluid [89, 90] can be simplified by replacing its first term using the trace of Einstein's equations: $M_{\rm Pl}^2 R = -T$, so that:

$$S_{\rm fluid}^{\text{on-shell}} = \int \mathrm{d}^4x\,\sqrt{-g}\,\frac{M_{\rm Pl}^2}{2}R + \int \mathrm{d}^4x\,\sqrt{-g}\,p = \frac{1}{2}\int \mathrm{d}^4x\,\sqrt{-g}\,(1-w)\rho\,. \tag{5.1.7}$$

This on-shell action vanishes when $\rho = 0$ (vacuum) and when $w = 1$ (stiff fluid). For the same reasons as established in the last paragraph of the previous subsection, these cases are not realistic.

We restrict to FLRW flat universes, $\mathrm{d}s^2 = -\mathrm{d}t^2 + a(t)^2(\mathrm{d}x^2 + \mathrm{d}y^2 + \mathrm{d}z^2)$. Assuming that the equation of state is $w > -1$, the equations of motions stemming from the gravity with perfect fluid action lead to the solution:

$$a \propto t^{\frac{2}{3(1+w)}}\,, \quad \rho \propto a^{-3(1+w)} \propto t^{-2}\,, \quad S_{\rm fluid}^{\text{on-shell}} \propto \int_0^{t_0} t^{-\frac{2w}{1+w}}\mathrm{d}t \propto t_0^{\frac{1-w}{1+w}} - \lim_{t\to 0} t^{\frac{1-w}{1+w}}\,. \tag{5.1.8}$$

The time integral giving the on-shell action in (5.1.8) is convergent only if $-1 < w \leq 1$. $w = 1$ gives the stiff fluid just discussed above, while $w = -1$ gives an effective cosmological constant. The background solution is then given by a flat de Sitter spacetime, which we analyze in detail in the section devoted to inflationary models 5.2.

For now, we conclude that the finite amplitude criterion is satisfied by any perfect fluid with equation of state $-1 < w < 1$ (if we assume a finite spatial volume of the universe), despite the generic presence of a curvature singularity and the blowing up of the energy density at the beginning of time.

5.1.3 Boundary terms and black holes

Before moving on to more speculative models for the early universe, we address here two questions related to the general relativity action.

The first concerns boundary terms that must be included in the gravity action in order

to make the variational principle well-posed,

$$\pm \int_{\partial M} \mathrm{d}^3x \, \sqrt{h} \, K \, . \tag{5.1.9}$$

This is the Gibbons-Hawking-York term, constructed from the determinant of the three-dimensional metric h on the boundary surface ∂M and from the trace of the extrinsic curvature on this same surface, K. The cosmological amplitudes we defined in (5.0.1) possess two boundaries (hypersurfaces corresponding to the initial and final configurations ϕ_i and ϕ_f). Let us assume for now that those hypersurfaces are spacelike and correspond to some initial and final time which bound the time integration of the action, t_i and t_f. Evaluated on the final boundary, the term (5.1.9) will always give a finite contribution to the on-shell action, because there all field values and their derivatives are finite. On the initial boundary, we first remark that a boundary term is only needed if we fix Dirichlet boundary conditions, e.g., if we fix the field space values. For cases where we fix the momentum values instead, such as in the no-boundary proposal defined with a regularity condition (see sections 2.2, 4 and 5.4), and for some emergent scenarios (see section 5.6), we do not require a GHY boundary term. When we have initial Dirichlet boundary conditions, we must study the finiteness of the boundary term (5.1.9). For example, on the perfect fluid solution with FLRW background we found in the previous subsection (5.1.8), the boundary term reads:

$$K \propto \frac{\dot{a}}{a} \, , \ \sqrt{h} \propto a^3 \ \Rightarrow \ \left(\pm \int_{\partial \mathcal{M}} \mathrm{d}^3x \, \sqrt{h} \, K \right) \propto \ a^2 \dot{a} \ \propto \ t^{\frac{1-w}{1+w}} \, . \tag{5.1.10}$$

In that case, the conditions for satisfying the finite amplitude criterion are unaltered by the boundary term. For the general relativity with a canonical scalar field case we studied in 5.1.1, we must also make sure that the variational principle with respect to the scalar field is well-posed. For the action (5.1.1), we find:

$$0 = \delta_\phi S = \int_{t_\mathrm{i}}^{t_\mathrm{f}} \mathrm{d}t \int_{\partial \mathcal{M}} \mathrm{d}^3x \, \sqrt{-g} \, (\Box \phi - V_{,\phi}) \cdot \delta\phi - \left[\int_{\partial \mathcal{M}} \mathrm{d}^3x \, \sqrt{h} \, n^\mu \nabla_\mu \phi \cdot \delta\phi \right]_{t_\mathrm{i}}^{t_\mathrm{f}} \, , \tag{5.1.11}$$

with $\nabla_\mu \nabla^\mu$ the d'Alembertian and n^μ the unit vector normal to the hypersurface ∂M. The variation principle is well-posed only if the term "$\sqrt{h} \, n^\mu \, \nabla_\mu \phi$" does not diverge on the boundary ∂M. In FLRW for instance, we typically have $a \propto t^{1/3}$ and $\phi \propto \ln(t)$ in the approach to the big bang, so that $\sqrt{h} \, n^\mu \, \nabla_\mu \phi \sim a^3 \dot{\phi} \propto t^0$ and the variational principle is well-posed. We emphasize with this example that even if the classical solution diverges on the initial boundary, it is perfectly fine to fix the functional variation $\delta\phi(t_\mathrm{i} = 0) = 0$.

The second point of concern within the general relativity action is whether the finite amplitude criterion is in adequation with the existence of black holes. Black holes are vacuum solutions to the Einstein's equations possessing enclosed spacetime singularity where the classical action blows up. However, these singularities always classically reside

in the future, because space and time are swapped at the event horizon[6]. Since we have defined cosmological amplitudes only up to current time configurations, black hole spacetimes satisfy the criterion. We mention that on this point, the finite action criterion of Barrow and Tippler gives different results, since there the action is evaluated on the entire spacetime, hence including the future singularity in the black hole interior. This is also the viewpoint adopted in the recent paper [92], where the authors suggest that since we expect quantum gravity theories to resolve singularities, the divergence of the black hole entire action could be used as a criterion for viable quantum gravity theories.

5.2 Inflationary phases

Here we start our study of models going beyond the standard hot big bang cosmological model, against the finite amplitude criterion. One of the most prominent and studied theory, proposed in order to explain some of the puzzling features arising in the standard cosmological model due to the initial conditions required, is the theory of inflation. In addition, inflation also provides a mechanism for explaining how quantum fluctuations amplify and turn into the density perturbations observed in the CMB. We have already reviewed the salient characteristics of this theory and explained how it resolves the aforementioned puzzles in section 5.2. Here we will confront several models of inflation against the finite amplitude criterion. In particular we will consider models where inflation describes the first phase of evolution of the universe 5.2.1, and then we will study a generic type of inflationary models possessing a so-called *eternal* phase 5.2.2.

5.2.1 Inflation as the first phase of evolution

In this subsection, we consider an inflationary phase preceding the radiation-dominated phase of evolution in the standard hot big-bang model, and reaching all the way back to an initial singularity. We neglect for now all effects related to eternal inflation, that will be treated in the next subsection.

As developed in the introductory chapter in section 1.2.3, inflation can be modeled by a simple scalar field evolving in a sufficiently flat potential, $V(\phi)$. In order for the inflationary phase to resolve the flatness and horizon problems, we have seen that it must have an equation of state $p = w_\phi \rho$, with $-1 < w_\phi < -1/3$. Using the equations developed in the previous section on perfect fluids, in a FLRW background the scale factor evolves close to the beginning of time as $a(t) \propto t^{\frac{2}{3(1+w_\phi)}}$. Moreover, the Friedmann equation implies that $V(\phi) \simeq 3M_{\rm Pl}^2 H^2 \propto t^{-2}$, and hence we can evaluate the on-shell action back to a vanishing scale factor $a(t=0) = 0$ as (5.1.3):

$$S_{\text{on-shell}} = \int \mathrm{d}^4x \sqrt{-g}\, V(\phi) = \int_0^{t_\mathrm{f}} \mathrm{d}t\, a^3 V(\phi) \propto \int_0^{t_\mathrm{f}} \mathrm{d}t\; t^{\frac{2}{1+w_\phi}-2}\,. \tag{5.2.1}$$

[6]When rotation and/or charge are included, the singularities reside near the Cauchy horizon, which represents future infinity inside the black hole [91].

Because of the inflationary range for w_ϕ recalled above, this on-shell action yields a finite result close to the initial singularity. This argument is valid for the FLRW background metric, which is a very symmetric ansatz. The past incompleteness of inflation [93] however ensures that the action for inflation will generically be finite when going back to the beginning of time.

As we emphasized at the beginning of this chapter, the finiteness of the classical action is a necessary but not sufficient condition, in order for the cosmological amplitude (5.0.1) to be finite. In [94], it was shown that the quantum amplitude of inflation contains two saddle point solutions, whose interference leads to instabilities. Explicitly, we consider the cosmological amplitude to grow from an initial scale factor a_i to a final, larger value of the scale factor a_f in an inflationary phase with a slow-roll potential. For simplicity we approximate the scalar field to a constant value. This approximation is legitimated by the slow-roll regime. There are two classical solutions respecting these boundary conditions. The first grows monotonically from a_i to a_f (expanding solution), and the second first contract from a_i to zero size and then bounces back to a_f (bouncing solution). They are represented in figure 5.2. These two saddle points contribute to the cosmological ampli-

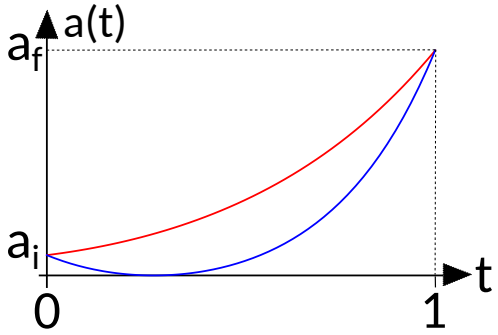

Figure 5.2: When specifying the boundary conditions that the universe evolves from an initial size a_i to a final size a_f, the semi-classical amplitude for inflation involves an interference between two background solutions. One solutions expands (red), while the other bounces before reaching the desired final size (blue). The interference between the two solutions causes an instability in the fluctuations. The time coordinate in the above plot has been rescaled to run over the fixed range $0 \leq t \leq 1$.

tude with an equal weight. In the limit when the initial scale factor goes to zero, those two classical solutions merge. Consider now perturbations around these background solutions. Using the standard Bunch-Davies vacuum, the perturbations around the expanding solution obey a Gaußian distribution, but around the bouncing solution, they obey an inverse Gaußian distribution (this is due to the fact that the bouncing solution is the time reverse of the expanding solution. Therefore, perturbations around the bouncing solution start in the unstable Bunch-Davies mode, which is the time reverse of the stable mode). Unfortunately, in the limit where the initial scale factor a goes to 0, it turns out that the unstable perturbations are dominant (see [94] for details). We conclude that the cosmological amplitude for inflation, when the phase of inflation reaches back to the initial singularity $a_\mathrm{i} \to 0$, is unstable and therefore this amplitude is not well defined.

To bypass this problem, we can either assume that:

- inflation did not occur. In that case, another mechanism is required to solve the flatness and horizons problems of the standard hot big-bang model, and also generate the primordial density fluctuations. Standard alternatives to inflation include bouncing and emergent cosmologies, both discussed later on in this chapter;

- inflation did occur, but was not the first phase of evolution. This leaves open the question of what happened before, and what are the initial conditions required for inflation to start. In this case, if the initial scale factor $a_{\rm i}$ is large enough, the bouncing solution get suppressed in the path integral [94]. The cosmological amplitude is therefore finite and stable at the beginning of inflation. Nevertheless, such a transient inflationary phase can still cause a blowing up amplitude if one reaches an eternal inflation regime. This will be discussed in the next subsection;

- inflation is the first phase of evolution, but the boundary conditions at the big bang exclude the unstable, bouncing solution which then doesn't contribute to the amplitude. This requires quantum boundary conditions and cannot be realized within classical gravity. The no-boundary wavefunction, which we have already studied at length in the previous chapters, is one example of such quantum initial conditions. We will confront it to the finite amplitude criterion in section 5.4.

5.2.2 Eternal inflation

Eternal inflation is a regime of evolution that is reached when the scalar potential is very flat, as is generically the case during a slow-roll inflationary phase. The inflaton (scalar field generating inflation) evolution can be decomposed into a classical evolution rolling down the potential, and stochastic jumps accounting for the quantum fluctuations of the field (see figure 5.4). The amplitude of the stochastic jumps depends on the height of the potential, while the classical slow-roll depends on the slope of the potential. If the potential is very flat, quantum jumps can become significant and prevent the universe from exiting the inflationary phase, by constantly creating new inflationary regions of spacetime. This is the regime of eternal inflation, schematically depicted in figure 5.3.

In this subsection, we show that the cosmological amplitude associated with an eternal inflation regime necessarily diverges. In cosmology, we cannot directly measure the scale factor a of our universe. Rather, we can measure the Hubble rate $H = \dot{a}/a$. Because of the Friedmann equation, the Hubble rate gives us the energy density of the universe. For inflation, the energy density is well approximated by the inflaton potential, $V(\phi) \simeq 3M_{\rm Pl}^2 H^2$. Therefore, the scalar field value ϕ is a useful substitute to the energy density (and the expansion rate), and we will thus calculate transition amplitudes from an initial field value $\phi_{\rm initial}$, lying in the inflationary region of the potential, up to a final field value $\phi_{\rm critical}$, which corresponds to the end of the inflation regime, where the reheating

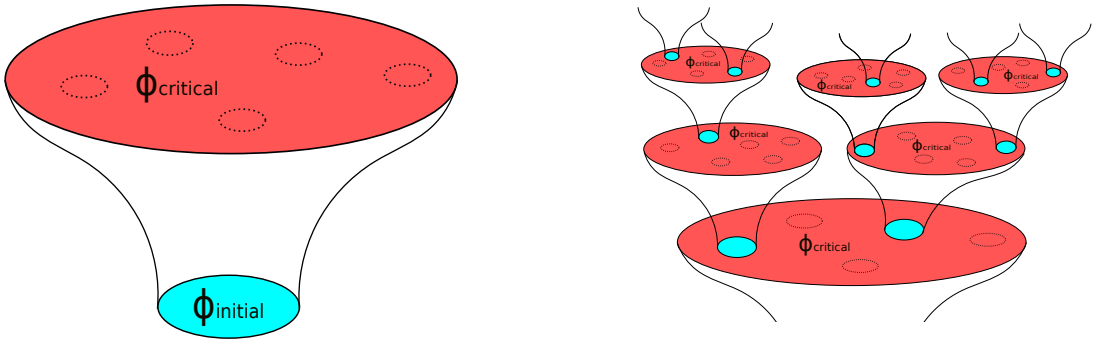

(a) No eternal inflation (b) Eternal inflation

Figure 5.3: The inflaton field evolves via a combination of classical rolling down the potential combined with random quantum jumps. When the classical rolling dominates, nearly the entire inflationary region ends inflation approximately simultaneously and then undergoes reheating followed by the ordinary hot big bang evolution. This is depicted in the left panel above, with orange denoting inflation and green the regions that have reheated. By contrast, if the quantum jumps are sufficiently important, then some regions will perpetuate inflation, as drawn in the right panel. The dashed ellipses indicate sample regions where inflation has just ended, and which (in our calculation) act as a proxy for our current state of the universe. We cannot possibly distinguish these sample regions at the end of inflation so we must include all of them.

mechanism occurs (we assume that whenever inflation ends, a radiation-dominated phase of the standard cosmological model starts).

We perform the explicit calculation by restricting to a linear potential,

$$V(\phi) = V_0 - \alpha(\phi - \phi_{\text{initial}})\,, \tag{5.2.2}$$

for some parameters $V_0 \in \mathbb{R}$ and $\alpha > 0$. The argument will hold for any positive potential such that $V(\phi_{\text{initial}}) > V(\phi_{\text{critical}})$ (see figure 5.4). A similar construction (also generalizing to other types of potential) can be found in [95]. The evolution of the inflaton field in this potential can be described by Starobinsky's stochastic formalism [61]: at the semi-classical level, the probability $P[\phi, t]$ that the inflaton takes the value ϕ at time t is given by the Fokker-Planck equation:

$$\partial_t P[\phi,t] = \frac{1}{2}\left(\frac{H^3}{4\pi^2}\right)\partial_\phi^2 P[\phi,t] + \frac{1}{3H}\partial_\phi\left[(\partial_\phi V)P[\phi,t]\right]\,. \tag{5.2.3}$$

For a very flat potential, we can approximate the expansion rate H by a constant and define a time coordinate everywhere and shift it such that $\phi(0) = \phi_{\text{initial}}$. The solution to the Fokker-Planck equation (5.2.3) is a Gaußian probability distribution:

$$P[\phi,t] = \frac{1}{\sqrt{2\pi}\,\sigma(t)}\exp\left[-\frac{(\phi-\mu(t))^2}{2\sigma(t)^2}\right]\,, \tag{5.2.4}$$

where the mean $\mu(t)$ describes the classical rolling evolution, while the standard deviation

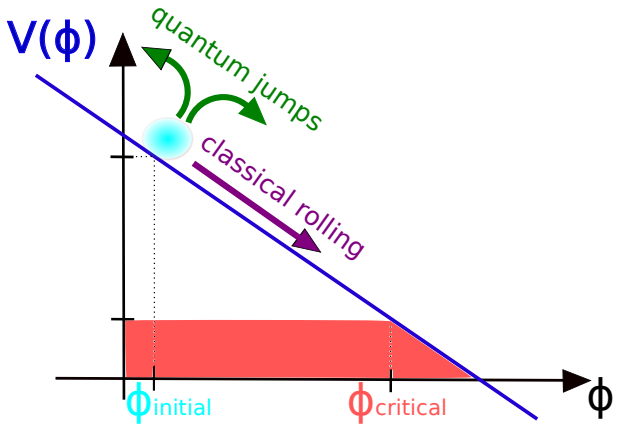

Figure 5.4: Representation of the stochastic formalism for inflation, for the potential (5.2.2). The inflaton field (in orange) rolls down the potential classically, but also undergoes quantum jumps up or down the potential. When the inflaton reaches the value ϕ_{critical}, it exits the inflationary regime. Depending on the slope α and on the expansion rate H (i.e., the potential value), either the classical evolution will dominate, and inflation will end (figure 5.3a), or the quantum jumps will prevail, and lead to an eternal inflation regime (figure 5.3b).

$\sigma(t)$ describes the Brownian motion due to the stochastic jumps of the inflaton:

$$\mu(t) = \phi_{\text{i}} + \frac{\alpha}{3H}t\,, \qquad \sigma^2(t) = \frac{H^3}{4\pi^2}t\,. \tag{5.2.5}$$

Our aim is to calculate the action associated with the regions of spacetime transitioning from ϕ_{initial} to ϕ_{critical}, i.e., the region of spacetime that stays inside the inflationary regime. By definition, ϕ_{critical} is the value for which the slow-roll parameter $\epsilon(\phi)$ reaches unity:

$$\epsilon(\phi_{\text{critical}}) \equiv \frac{M_{\text{Pl}}^2}{2V(\phi)^2}\left(\partial_\phi V(\phi)\right)^2\Big|_{\phi=\phi_{\text{critical}}} = 1 \;\Leftrightarrow\; \phi_{\text{critical}} \equiv \phi_{\text{initial}} + V_0/\alpha - M_{\text{Pl}}/\sqrt{2}\,. \tag{5.2.6}$$

Interpreting the probability $P[\phi, t]$ as the fraction of the universe where the scalar field value is ϕ at time t, the action over the region which is in the inflationary region of the potential $\phi < \phi_{\text{critical}}$ is thus:

$$S_{\text{inflation}} = \int_{t=0}^{t=t_{\text{f}}} \mathrm{d}t\, a^3\, P[\phi < \phi_{\text{critical}}, t] \cdot V(\phi)\,. \tag{5.2.7}$$

The lower and upper time limit of integration correspond to the beginning and end of inflation. The volume factor a^3 stems from the metric determinant, $\sqrt{-g}$, and has been normalized by the probability $P[\phi < \phi_{\text{critical}}, t] = \int_{-\infty}^{\phi_{\text{critical}}} P[\phi, t]\mathrm{d}\phi$, which gives the fraction of spacetime where the scalar field value is smaller than ϕ_{critical}. This way we restrict to regions of spacetime that are inside the inflationary phase. We insist on the fact that the volume factor results from the covariance of the action and does not represent a measure of some sort (in contrast to the argument used in [95]). Crucially, the upper limit of integration t_{f} must be extended to $+\infty$ in the case of eternal inflation, because all regions where inflation came to an end are indistinguishable (all dashed ellipses regions

in figure 5.3). This does not mean that we consider the infinite future evolution of the universe, since this only restricts to regions of spacetime that are inside the inflationary phase. We can calculate the probability of being inside the inflationary phase using the linear potential (5.2.2):

$$\begin{aligned} P[\phi < \phi_{\text{critical}}, t] = \int_{-\infty}^{\phi_{\text{critical}}} P[\phi, t]\, \mathrm{d}\phi &= \int_{-\infty}^{\phi_{\text{critical}}} \mathrm{d}\phi\, \frac{\sqrt{2\pi}}{H^{3/2}\sqrt{t}} e^{-\frac{2\pi^2}{H^3 t}\left(\phi - \phi_{\text{initial}} - \frac{\alpha}{3H}t\right)^2} \\ &= \frac{1}{2}\mathrm{erfc}\left[\frac{\phi_{\text{initial}} - \phi_{\text{critical}} + \frac{\alpha}{3H}t}{\frac{H}{2\pi}\sqrt{2Ht}}\right] \\ &\simeq \frac{3H^{5/2}}{2\pi^{3/2}\alpha\sqrt{2t}} \exp\left[-\frac{2\pi^2\alpha^2}{9H^5}t\right], \qquad (t \gg H^5/\alpha^2)\,. \end{aligned} \tag{5.2.8}$$

We then obtain a lower bound on the action (5.2.7) by using the relation valid during inflation: $3M_{\text{Pl}}^2 H^2 \approx V(\phi) \gtrsim V(\phi_{\text{critical}})$, as well as the scale factor evolution: $a(t) \simeq a_0 \exp(H\,t)$. Plugging these relations and the result (5.2.8) in the expression for the action (5.2.7), we get:

$$S_{\text{inflation}} \gtrsim \frac{a_0^3 V(\phi_{\text{critical}})^{9/4}}{3^{1/4}(2\pi)^{3/2}\alpha M_{\text{Pl}}^{5/2}} \int_{t=0}^{t=+\infty} \frac{\exp\left(3Ht - \frac{2\pi^2\alpha^2}{9H^5}t\right)}{\sqrt{t}} \mathrm{d}t\,. \tag{5.2.9}$$

In $t = 0$, this integral converges. The interesting limit is the late time limit when $t \to +\infty$. There the convergence of the integral depends on the sign of the exponential's argument:

$$\text{If } (3H^2)^3 > 2\pi^2\alpha^2\,, \text{ then the action diverges as } t \to \infty. \tag{5.2.10}$$

The condition $(3H^2)^3 > 2\pi^2\alpha^2$ is the exact condition that defines the regime of eternal inflation,

$$\frac{|V_{,\phi}|}{V^{3/2}} < \frac{1}{\sqrt{2}\,\pi M_{\text{Pl}}^3}\,. \tag{5.2.11}$$

This proof translates to other types of potential (see [95]): when the potential satisfies the eternal inflation criterion (5.2.11), then the action of the full inflationary spacetime region diverges. Therefore, the cosmological amplitude of eternal inflation is ill-defined. Conversely, potentials which violate the eternal inflation criterion, lead to a convergent action of the full inflationary region and to meaningful cosmological amplitudes (5.0.1).

We raise two remarks on the above calculation:

1. The same result can be obtained by considering a more local point of view, i.e., by following individual worldlines, and showing that the expectation value for the time spent in the inflationary phase diverges under the same conditions as the action (5.2.9). This expectation value can be calculated as:

$$\langle t_{\text{f}} \rangle = \int_0^{+\infty} \mathrm{d}t\; a(t)^3 P[\phi < \phi_{\text{critical}}, t] \cdot t\,, \tag{5.2.12}$$

where the probability $P[\phi < \phi_{\text{critical}}, t]$ accounts for the splitting of worldlines that happens each time a quantum jump occurs. When the potential does not lead to eternal inflation, the time (5.2.12) tends toward the classical rolling time, i.e., the classical time it takes for the scalar field to roll down from ϕ_{initial} to ϕ_{critical};

2. We stress that the stochastic approach we have developed in this subsection is an effective description, which is particularly efficient for flat potentials [96], such as those we are confronted to in the context of slow-roll inflation. Indeed, when calculating the probability (5.2.4), we have approximated the quantum fluctuations of the inflaton field by random jumps, effectively treating the fields classically. Using this effective description, the only relevant quantity to compute is the action of the expectation values of the scalar fields, $S(\langle\phi\rangle)$. If we want to go beyond this effective approach, we could calculate the amplitude of probability of reaching the scalar field value ϕ from a pure path integral approach. Here we present a short outline of such a calculation but do not make it precise: because inflation is very efficient in decohering the universe [97], it is reasonable to assume a classical evolution in between quantum jumps. Then the amplitude is given by a sum over all field configurations which have undergone a specific number n of jumps:

$$\mathcal{A} \approx \sum_n \int \mathcal{D}g_{\mu\nu}\mathcal{D}\phi\, e^{\frac{i}{\hbar}S} \approx \sum_n \mathcal{V}_{\text{infl}}^{(n)}\, e^{A(n)}\, e^{\frac{i}{\hbar}S_{\text{phase}}(n)}\,. \tag{5.2.13}$$

The amplitude $A(n)$ gives the likelihood of undergoing n jumps upward on the potential, and the volume factor $\mathcal{V}_{\text{infl}}^{(n)}$ accounts for the volume produced by the inflationary expansion for each up-jump. The total time of integration in the action $S_{\text{phase}}(n)$ depends on n, so that the factor $\mathcal{V}_{\text{infl}}^{(n)}\, e^{A(n)} \sim a^3 P[\phi < \phi_{\text{critical}}, t_{\text{f}}(n)]$ will diverge at large n similarly to what occurred in the stochastic framework.

Before concluding, we point out that in the paper [95], it was shown that the eternal inflation requirements on the potential (5.2.11) are exactly equivalent to the requirements coming from the de Sitter swampland conjectures [98, 99, 100]. The very same requirements imply a violation of the finite amplitude criterion, suggesting that Swampland conjectures could already be implied by semi-classical physics alone, and would not require input from quantum gravity. Said differently, this suggests that in order to find presumed de Sitter vacua in string theory, it is necessary to go beyond the semi-classical approximation.

Our general conclusion from this section on inflation, is that the semi-classical, cosmological amplitude (5.0.1) is ill-defined whenever the inflationary phase reaches back all the way to the initial singularity, or if the inflaton potential satisfies the eternal inflation criterion. Otherwise, a transient and non-eternal inflationary phase can satisfy the finite amplitude criterion, and play a key role in solving the puzzles of the early universe.

5.3 Bouncing and cyclic universes

In this section we explore one of the main alternative to inflation for describing the early universe and solving the paradoxes that arise in the standard hot big bang evolution: **bouncing models**. The flatness problem, which we used to advocate for inflation in 1.2, requires that the spatial curvature term in Friedmann equation, $k/(aH)^2$, shrinks sufficiently before the radiation-dominated epoch, in order to explain its extremely small value measured from the CMB. Inflation realizes this shrinking by assuming an accelerated expanding phase, but in fact other types of evolution can achieve the same aim, for instance if we are in a contracting instead of expanding universe. Sticking to a perfect fluid description with equation of state $p = w\rho$, this spatial curvature term gives:

$$\frac{k}{(aH)^2} \sim t^{\frac{2}{3}\frac{1+3w}{1+w}}. \tag{5.3.1}$$

In a contracting universe, this term will shrink for any ratio $w > -1/3$. The flatness problem can thus also be solved by a long contracting phase, followed by a bounce leading to the standard hot big bang evolution. Many such models have been proposed, see for instance [101] for a review.

In addition to solving the hot big bang puzzles, inflation also generates the nearly scale-invariant power spectrum observed for the scalar fluctuations in the CMB. This is also achievable through certain contracting phases, like matter dominated $w = 0$ phases, or phases driven by an ekpyrotic field $w > 1$ and such models represent testable alternatives to inflation. We point out however, that in matter-dominated contracting phases, anisotropies are typically unstable, while ekpyrotic contracting phase violate the null energy condition (NEC)[7], and hence require a new, beyond the standard model, type of matter.

That being said, we now study the finite amplitude criterion in the two main scenarios preceding a bounce: in the first, the universe is contracting forever in the past (**single bounce scenario**), and in the second, it undergoes a series of contracting and expanding phases in a cyclic manner (**cyclic universe**). In these two scenarios, the physical time runs all the way back to negative infinity.

5.3.1 Single bounce

Using the equations derived for perfect fluids, we can calculate the classical on-shell action for a contracting phase running from $t = -\infty$ to $t = -t_\mathrm{b}$ as:

$$S_{\text{bounce}}^{\text{on-shell}} = \frac{1}{2}\int_{-\infty}^{-t_\mathrm{b}} \mathrm{d}t\, a^3(1-w)\rho \propto \int_{-\infty}^{-t_\mathrm{b}} (1-w)t^{\frac{-2w}{1+w}}\mathrm{d}t$$

[7] The null energy condition states that for any future-pointing null vector k^μ, the stress-energy tensor must be such that the quantity $T_{\mu\nu}k^\mu k^\nu \geq 0$. For the case of a perfect fluid, it translates into the requirement that $\rho + p \geq 0$. The role of the NEC and of the other energy conditions is not totally understood, but for example all the known matter composing the standard model satisfies the NEC.

$$\propto \left[(1-w)(-t_{\rm b})^{\frac{1-w}{1+w}} - (1-w)\lim_{t\to-\infty} t^{\frac{1-w}{1+w}}\right], \qquad (5.3.2)$$

This on-shell action is finite if and only if $w > 1$, i.e., if the only matter field present in the asymptotic past is an ekpyrotic scalar. Matter and radiation would then only be produced later on, during the reheating phase [19]. Similarly to the case of a scalar field in 5.1.1, the well-definiteness of the amplitude in this case implies that we trust the effective description in terms of a perfect fluid over a infinite range of ϕ, in order to reach $t = -\infty$. This assumption is questionable, especially in view if the distance conjecture stemming from string compactification [100]. This is nevertheless allowed at the semi-classical level.

The additional contributions coming from the bouncing phase, and from the following standard hot big bang phase, are non-singular and hence, at least at the background level, yield a finite on-shell action. We insist on the fact that this holds at the background level, because the perturbed action could bring instabilities and divergences and thus violates the finite amplitude criterion. We study in more details the effect of perturbed actions in the section 5.5.

5.3.2 Cyclic universes

In this case we focus on the on-shell action deriving from the Einstein-Hilbert term in FLRW (so we leave aside possible cancellations between gravity and matter terms):

$$S_{\rm EH} \propto \int_{-\infty}^{t_0} a^3(\dot{H}+2H^2){\rm d}t = \sum_{n=0}^{\infty}\int_{t-n-1}^{t-n} a^3(\dot{H}+2H^2){\rm d}t\,, \qquad (5.3.3)$$

where we have subdivided the integration on each cycle $\{t_{-n-1}, t_{-n}\}$, for $n \in \mathbb{N}$, with $-\infty = t_{-\infty} < \cdots < t_{-2} < t_{-1} < t_0$, and each t_n correspond to a bouncing time (and t_0 is the present time).

We distinguish two different types of cyclic behavior for a universe experiencing such an infinite series of bounces in the limit $t \to -\infty$:

1. the universe is **exactly cyclic**: there exist a time period, P, such that the scale factor $a(t) = a(t+P)$ for any $t \in (-\infty, t_0)$. In this case, the integrand of (5.3.3) is non zero for each cycle, and therefore the infinite sum generically diverges. In any case, this type of cyclic behavior contradicts the second law of thermodynamics, according to which the maximal scale factor should grow from one cycle to the next, as time evolves. This brings us to a second type of cyclic behavior:

2. the maximal scale factor gets smaller at each cycle when evolving back in time, and is asymptotically zero. Nevertheless, some physical quantities such as the expansion rate H are periodic: $H(t) = H(t+P)$. In this case, the integrand in (5.3.3) is asymptotically zero when $n \to \infty$, and the sum may converge. Examples of this behavior are found in [102, 103, 104, 105, 106, 107, 108], where the average Hubble parameter H is approximately constant, so the average volume of each cycle grows

exponentially. The universe is then de Sitter-like when averaging over cycles, and we recover the result that, classically, the action is finite.[8]

Overall, bouncing and cyclic universes are highly constrained by the finite amplitude criterion. We will come back to non-singular universes, which represent another alternative to inflation, in the section concerning loitering and emergent cosmologies 5.6, and we will find that it is easier to construct a model compatible with the finite amplitude criterion in that case. But for now, we go back again to the no-boundary proposal, this time confronted against the finite amplitude criterion.

5.4 No-boundary proposal

The no-boundary proposal is evidently very well suited to the finite amplitude criterion, since it precisely gives a prescription for obtaining a well-defined transition amplitude given a dynamical model of the universe. We recalled in the introductory chapter 2.2 that the no-boundary wavefunction was originally defined as the path integral summing over initially compact and regular four-manifolds, having as only boundary a certain final hypersurface. This definition naturally leads to well-defined, finite cosmological amplitudes. It simultaneously avoids singularities in spacetime and in the on-shell, saddle point action. It thus represents the archetypal semi-classical solution for the early universe. Furthermore, we have shown in chapter 3 that no-boundary solutions would still exist when the dynamical models considered possess higher-order terms stemming from loop corrections to general relativity [1]. This is a first indication that no-boundary solutions might even persist in the full quantum gravity framework, and not only at the semi-classical level.

Therefore, the no-boundary solution by definition satisfies the finite amplitude criterion. The only difficulty lies in implementing practically this "pure" definition of the no-boundary proposal for specific dynamical models. We have elaborated on this issue in the introductory chapter 2.2, where we have seen that, previously to this thesis, the state-of-the-art understanding was that such a practical implementation of the no-boundary proposal was possible only when summing over initially regular metrics (i.e., the momentum condition). Indeed the adverse implementation of the no-boundary proposal, summing over initially compact geometries (i.e., field condition) leads to unstable perturbations when applying the Picard-Lefschetz theory for evaluating the Lorentzian path integral. In the next chapter 6, we will challenge this view, and show that in the context of the complex metric criterion we will develop there, the field definition of the no-boundary proposal may also lead to a well-defined and consistent definition of the path integral, and hence lead to finite cosmological amplitudes.

[8] Whether or not a quantum instability arises – as discussed in section 5.2.1 for inflation – is not obvious. Also, in the case where $\langle H \rangle_P > 0$ and $\langle a \rangle_P \to 0$ as $t \to -\infty$, where $\langle \rangle_P$ means the time average over the cycle period P, the spacetime is necessarily geodesically incomplete [93].

5.5 Higher-curvature term theories

All previous sections of this chapter have focused on dynamical models of the early universe based on general relativity, with an action given by the Einstein-Hilbert term:

$$S_{\rm EH} = \frac{M_{\rm Pl}^2}{2}\int \mathrm{d}^4x\,\sqrt{-g}\,R\,, \tag{5.5.1}$$

sometimes supplemented by a cosmological constant and/or boundary terms. General relativity is nevertheless known to be non-renormalizable [23, 24, 25], and hence loop corrections at order $\hbar^n$ induce terms involving the Riemann tensor to the power $n+1$. These terms may become relevant when approaching the initial spacetime singularity. As we did for the no-boundary solution in chapter 3, we are now going to consider higher curvature actions in the context of the cosmological amplitude. This analysis has been initiated in [85], where quadratic gravity in particular was found to restrict the early universe evolution to homogeneous, isotropic and accelerating backgrounds, thus setting the ideal conditions for an inflationary phase to begin. We will review and improve this analysis in the present chapter.

Generically, we here consider theories of the form:

$$S = \frac{1}{2}\int \mathrm{d}^4x\,\sqrt{-g}\,f(R_{\mu\nu\rho\sigma})\,, \tag{5.5.2}$$

where $f(R_{\mu\nu\rho\sigma})$ is an arbitrary scalar polynomial of the Riemann tensor. This action is the same that we studied in chapter 3 in the particular case of a closed FLRW background (3.2.2).

5.5.1 Specificities of quadratic gravity

Within higher curvature theories of the form (5.5.2), **quadratic gravity** occupies a special place, as it forms a renormalizable theory of gravity [109, 110], and is used in the favored inflationary mechanism [61] to explain the latest observations of the 2018 Planck survey [111]. We have already introduced quadratic gravity and some of its features in chapter 3. In particular, we recall that the action of quadratic gravity when coupled to general relativity reads:

$$S_{\rm quad} = \int \mathrm{d}^4x\,\sqrt{-g}\left(\frac{M_{\rm Pl}^2}{2}R + \frac{\omega}{3\sigma}R^2 - \frac{1}{2\sigma}C^2 + \theta\,\mathcal{G}\right), \tag{5.5.3}$$

$$\text{with}\quad \begin{cases} C^2 \equiv C_{\mu\nu\rho\sigma}C^{\mu\nu\rho\sigma} = R_{\mu\nu\rho\sigma}R^{\mu\nu\rho\sigma} - 2R_{\mu\nu}R^{\mu\nu} + \dfrac{1}{3}R^2 \quad \text{(Weyl tensor)}, \\ \mathcal{G} = R_{\mu\nu\rho\sigma}R^{\mu\nu\rho\sigma} - 4R_{\mu\nu}R^{\mu\nu} + R^2 \quad \text{(Gauß-Bonnet term)}\,. \end{cases}$$

The coefficient ω, σ and θ are coupling constants. The Gauß-Bonnet combination $\mathcal{G}$ yields a total derivative and doesn't participate in the dynamics. The relevance of quadratic

gravity stems from the fact that it can both be treated as a complete gravity theory as it stands, or as the easiest example of adding higher-curvature terms to general relativity in an effective field theory approach, and for that reason we use it as a leading example throughout this section. As we recalled in 3.3.1, the main blemish of quadratic gravity is the debated presence of ghosts violating unitarity. In that case, the finite amplitude criterion is necessarily violated as soon as we consider perturbations, at least when considering quadratic gravity as a complete theory. However in the effective field theory approach, the ghost issue can be resolved thanks to higher-order quantum corrections, or can simply be discarded as outside of the regime of validity of the EFT. In any case, here we again ignore the ghost problem and concentrate our analysis on background solutions.

Note that also in more general $f(R_{\mu\nu\rho\sigma})$ theories, a ghost appears if the theory stops at a given order in the curvature tensor. It can be re-summed and disappear only for an infinite series of higher-curvature terms. Low-energy expansions of string theory are of this type and additionally contain terms with derivatives acting on the Riemann tensor (see [62, 68] and the sections 3.3.4 and 3.4.3 where we have studied the no-boundary solutions for such actions).

5.5.2 Boundary term for higher curvature theories

When calculating cosmological amplitudes, as already emphasized in the case of general relativity in section 5.1.3, we must also study the impact of the surface term, especially when fixing the metric on the initial boundary in the path integral. For $f(R_{\mu\nu\rho\sigma})$ theories, the surface term has been studied in [112]. There, the authors found that using the ADM decomposition of the metric (2.1.1), $\mathrm{d}s^2 = -N^2\mathrm{d}t^2 + h_{ij}(\mathrm{d}x^i + N^i\mathrm{d}t)(\mathrm{d}x^j + N^j\mathrm{d}t)$, the generalization of the GHY boundary term is given by

$$S_{\text{boundary}}[f] = -\int_{\partial M} \mathrm{d}^3x\,\sqrt{h}\,\Psi^{ij}[f]K_{ij}\,, \qquad \text{with} \quad \delta\Psi^{ij}\big|_{\partial M} = 0\,, \tag{5.5.4}$$

where K_{ij} is the extrinsic curvature on the boundary hypersurface ∂M and

$$\Psi^{ij}[f] \equiv -\frac{1}{2}h^{ik}h^{jl}n^\mu n^\nu \frac{\partial f}{\partial R^{\mu k\nu l}}\,, \tag{5.5.5}$$

with $n^\mu = (1/N, -N^i/N)$ denoting the unit normal vector to ∂M. Adding the boundary term (5.5.4) to the bulk action (5.5.2) trades the boundary condition on the extrinsic curvature K_{ij} for a boundary condition on Ψ^{ij}. This generically involves new degrees of freedom: fixing Ψ^{ij} may not only fix the metric, but also restricts additional scalar or tensor degrees of freedom.

We consider a few $f(R_{\mu\nu\rho\sigma})$ theories as examples to illustrate the impact of such a boundary term:

1. First we check that the boundary term of the **Ricci scalar** recovers the expected GHY result of the Einstein-Hilbert action. In the ADM metric and using the sym-

metries of the Riemann tensor, we decompose:

$$R = g^{\mu\rho} g^{\nu\sigma} R_{\mu\nu\rho\sigma} = h^{ik} h^{jl} R_{ijkl} - 2 n^\mu n^\rho h^{ij} R_{\mu i \rho j} \,, \tag{5.5.6}$$

from which we calculate the expression $\Psi_{ij}[R]$ as:

$$\Psi^{ij}[R] \equiv -\frac{1}{2} h^{ik} h^{jl} n^\mu n^\nu \frac{\partial R}{\partial R_{\mu i \nu j}} = h^{ij} \,. \tag{5.5.7}$$

Therefore, the integrand of the boundary action (5.5.4) is $\Psi^{ij} K_{ij} = h^{ij} K_{ij} \equiv K$ and we indeed recover the GHY result (5.1.9). In this case, fixing the quantity $\Psi^{ij}[R]$ is strictly equivalent to fixing the three-metric h_{ij} on the boundary hypersurface.

2. From the above, we can directly treat the theories based solely on the Ricci scalar $f = f(R)$. By making use of the Taylor-expansion of the f function, it is sufficient to consider the functions $f_n(R) = R^n$. For these the quantity Ψ_{ij} is: $\Psi^{ij}[R^n] = n h^{ij} R^{n-1}$,[9] hence fixing Ψ_{ij} requires both to fix the three-metric h_{ij} and to set the Ricci scalar R on the boundary hypersurface. Therefore, in this case fixing the boundary condition additionally restricts a new scalar degree of freedom. This is consistent with the fact that $f(R)$ theories are known to be equivalent to GR plus a scalar field [114].

3. Finally we consider **terms of second order in curvature** appearing in quadratic gravity. First for the Ricci tensor squared $R^{\mu\nu} R_{\mu\nu}$, whose ADM decomposition reads:

$$\begin{aligned} R^{\mu\nu} R_{\mu\nu} &= R_{ij} R^{ij} - 2 n^\mu n^\nu h^{ij} R_{\mu i} R_{\nu j} + n^\mu n^\nu n^\alpha n^\beta R_{\mu\nu} R_{\alpha\beta} \\ &= (R^k{}_{ikj} - n^\mu n^\nu R_{\mu i \nu j}) R^{ij} - 2 n^\mu n^\nu h^{ij} (R^k{}_{\mu k i} - n^\alpha n^\beta R_{\alpha\mu\beta i}) R_{\nu j} \\ &\quad + n^\mu n^\nu n^\alpha n^\beta (R^k{}_{\mu k \nu} - n^\rho n^\sigma R_{\rho\mu\sigma\nu}) R_{\alpha\beta} \,, \end{aligned} \tag{5.5.8}$$

we calculate the Ψ_{ij} quantity as:

$$\Psi^{ij}[R_{\mu\nu} R^{\mu\nu}] = -n_\alpha n_\beta (g^{\alpha\beta} R^{ij} + h^{ij} R^{\alpha\beta}) \,. \tag{5.5.9}$$

Similarly, for the Riemann tensor:

$$\begin{aligned} R^{\mu\nu\rho\sigma} R_{\mu\nu\rho\sigma} &= R^{ijkl} R_{ijkl} + n^\mu n^\nu n^\alpha n^\beta \left(4 R_{\mu i \nu j} R_\alpha{}^i{}_\beta{}^j + 2 R_{ij\mu\nu} R^{ij}{}_{\alpha\beta} \right) \\ &\quad + 4 n^\mu n^\nu n^\rho n^\alpha n^\beta n^\gamma R_{\mu\nu\rho i} R_{\alpha\beta\gamma}{}^i + 4 n^\mu n^\alpha R_{\mu i j k} R_\alpha{}^{ijk} \,, \end{aligned} \tag{5.5.10}$$

we find:

$$\Psi^{ij}[R_{\mu\nu\rho\sigma} R^{\mu\nu\rho\sigma}] = -4 n_\alpha n_\beta R^{\alpha i \beta j} \,. \tag{5.5.11}$$

[9] More generally for $f = f(R)$, one recovers the known result (e.g., [113]): $\Psi^{ij}[f(R)] = h^{ij} f_{,R}$.

From these two results and the previous points implying $\Psi_{ij}[R^2] = 2h_{ij}R$, we calculate the boundary term of the Weyl tensor squared:

$$\Psi^{ij}[C^2] = -n_\alpha n_\beta\Big(4R^{\alpha i\beta j} - 2(g^{\alpha\beta}R^{ij} + h^{ij}R^{\alpha\beta}) - \frac{2}{3}Rh^{ij}g^{\alpha\beta}\Big) = -4n_\alpha n_\beta C^{\alpha i\beta j}\,. \tag{5.5.12}$$

This result indeed matches with the boundary term for C^2 found in [115]. In contrast, the boundary term for the Gauß-Bonnet combination $\mathcal{G}$ cannot be obtained through the method exposed in [112], as it is a degenerate topological term in four-dimensional spacetime. Instead, the correct surface term for $\mathcal{G}$ (i.e., enabling the imposition of Dirichlet boundary conditions $\delta g_{\mu\nu}|_{\partial M} = 0$) is given by the Myers action [116, 117]:

$$\Psi^{ij}[\mathcal{G}] = 2\left(JK^{ij} - 2G^{ij}_{\rm b}\right), \tag{5.5.13}$$

where $G^{\rm b}_{ij}$ is the Einstein tensor constructed from the boundary-induced metric h_{ij} and

$$J \equiv -h^{ij}\left(-\frac{2}{3}K_{il}K^{lp}K_{pj} + \frac{2}{3}KK_{il}K^{l}{}_{j} + \frac{1}{3}K_{ij}(K_{lp}K^{lp} - K^2)\right). \tag{5.5.14}$$

5.5.3 Higher-curvature terms on FLRW backgrounds

We can now investigate the finiteness of cosmological amplitudes of interest. We start with the simplest backgrounds, namely, FLRW metrics with spatial curvature $k = -1, 0, +1$ for open, flat, or closed spatial slices. On such backgrounds, we have seen in chapter 3 that the action of a $f(R_{\mu\nu\rho\sigma})$ theory is greatly simplified [1]:

$$S = \int \mathrm{d}t\, a^3 N \sum_{p_1,p_2\in\mathbb{N}} c_{p_1,p_2}\Big(A_1^{(k)}\Big)^{p_1} A_2^{p_2}\,, \tag{5.5.15}$$

for some real coefficients c_{p_1,p_2} and with

$$A_1^{(k)} = \frac{\dot{a}^2 + kN^2}{a^2N^2} \quad \text{and} \quad A_2 = \frac{\ddot{a}N - \dot{a}\dot{N}}{aN^3}\,. \tag{5.5.16}$$

The order in the Riemann tensor of the expression $f(R_{\mu\nu\rho\sigma})$ is $P = p_1 + p_2$. The Friedmann constraint equation for the action (5.5.15) is given by (3.2.14) (working again in the constant lapse gauge $\dot{N} = 0$):

$$\begin{aligned}\sum_{p_1,p_2} c_{p_1,p_2}\Bigg[&2p_1(p_2-1)\frac{a\dot{a}^2}{N^2}A_2^{p_2}\Big(A_1^{(k)}\Big)^{p_1-1} + (1-p_2)a^3A_2^{p_2}\Big(A_1^{(k)}\Big)^{p_1}\\ &+ p_2(p_2-1)\frac{a\dot{a}\,\dddot{a}}{N^4}A_2^{p_2-2}\Big(A_1^{(k)}\Big)^{p_1} - p_2(2p_1+p_2-3)\frac{a\dot{a}^2}{N^2}A_2^{p_2-1}\Big(A_1^{(k)}\Big)^{p_1}\Bigg] = 0\,.\end{aligned} \tag{5.5.17}$$

This constraint equation can be used to simplify the action (5.5.15) on-shell, as we did for general relativity in section 5.1.2. We illustrate this with quadratic gravity.

Finite amplitude criterion for quadratic gravity on FLRW

The Weyl tensor vanishes on FLRW backgrounds, so the action of quadratic gravity coupled to GR (5.5.3) simplifies to:

$$\begin{aligned} S_{\text{quad}} &= \int \mathrm{d}^4x\,\sqrt{-g}\left(\frac{M_{\text{Pl}}^2}{2}R+\frac{\omega}{3\sigma}R^2+\theta\,\mathcal{G}\right) \\ &= \int \mathrm{d}t\left[3M_{\text{Pl}}^2\left(\frac{a\dot{a}^2}{N}+aNk+\frac{a^2\ddot{a}}{N}\right)+\frac{12\omega}{\sigma}\left(\frac{\dot{a}^4}{aN^3}+\frac{2k\dot{a}^2}{aN}+\frac{Nk^2}{a}+\frac{2\dot{a}^2\ddot{a}}{N^3}+\frac{2k\ddot{a}}{N}+\frac{a\ddot{a}^2}{N^3}\right)\right. \\ &\qquad \left.+24\theta\left(\frac{\dot{a}^2\ddot{a}}{N^3}+\frac{k\ddot{a}}{N}\right)\right]. \end{aligned} \tag{5.5.18}$$

The Friedmann constraint (5.5.17) then reads

$$0=3M_{\text{Pl}}^2\left(\frac{a\dot{a}^2}{N^2}+ak\right)+\frac{12\omega}{\sigma}\left[-\frac{3\dot{a}^4}{aN^4}-\frac{2k\dot{a}^2}{aN^2}+\frac{k^2}{a}-\frac{a\ddot{a}^2}{N^4}+\frac{2\dot{a}^2\ddot{a}}{N^4}+\frac{2a\dot{a}a^{(3)}}{N^4}\right]. \tag{5.5.19}$$

We use this equation to replace the term proportional to k^2/a in the action, leading to:

$$\begin{aligned} S_{\text{quad}}^{\text{on-shell}} = \int \mathrm{d}t\left[3M_{\text{Pl}}^2\frac{a^2\ddot{a}}{N}+\frac{24\omega}{\sigma}\left(\frac{2\dot{a}^2}{aN}\left(\frac{\dot{a}^2}{N^2}+k\right)+\frac{a\ddot{a}^2}{N^3}-\frac{a\dot{a}a^{(3)}}{N^3}+\frac{k\ddot{a}}{N}\right)\right. \\ \left.+24\theta\frac{\ddot{a}}{N}\left(\frac{\dot{a}^2}{N^2}+k\right)\right]. \end{aligned} \tag{5.5.20}$$

Considering the ansatz[10] $a(t)\sim t^s$ for the approach to the initial singularity in $t\to 0$, we find that the terms making up this on-shell action (5.5.20) all scale as:

$$t^{3s-1},\quad t^{3s-3}\quad\text{or}\quad t^{s-1}. \tag{5.5.21}$$

Therefore, the on-shell action of quadratic gravity converges as long as $s>1$. This means that the background solution must expand in an accelerated manner close to the initial singularity.

We must also make sure that the boundary terms are well behaved. For the action (5.5.18), they read

$$S_{\text{boundary}}^{\text{quad}} = -\int \mathrm{d}^3x\sqrt{h}\left[M_{\text{Pl}}^2\,K+\frac{2\omega}{3\sigma}\,RK+4\theta\left(J-2G^{\text{b}}_{ij}K^{ij}\right)\right]. \tag{5.5.22}$$

[10]This ansatz is generic in the presence of standard matter, to the exception of a pure cosmological constant. In that case, the Riemann tensor is finite and constant everywhere and will not diverge in the approach to the big bang. However we then encounter the "incompleteness" problem described in section 5.2, namely that the two classical background solutions interfere and fail to reproduce a stable ground state for the perturbations when $t\to 0$ [94].

On a FLRW background, we have

$$K = K_{ij}h^{ij} = \frac{\dot{a}}{aN}h_{ij}h^{ij} = \frac{\dot{a}}{aN}\,, \quad J = \frac{2\dot{a}^3}{N^3a^3}\,, \quad G^{\rm b}_{ij}K^{ij} = -\frac{3k\dot{a}}{Na^3}\,, \tag{5.5.23}$$

so using again the ansatz $a(t) \sim t^s$, we find that the boundary terms also yield the exponents t^{3s-1} (GHY term), t^{3s-3}, and t^{s-1}. Thus we recover the result that in an inflationary background (which may arise directly as a solution of pure quadratic gravity or from a coupling to a scalar field with a sufficiently flat potential), quadratic gravity leads to a finite action in the approach to the big bang [85].

Finite amplitude criterion for generic higher-curvature action on FLRW

Now we can extend this method to the general action (5.5.15). Using the ansatz $a \sim t^s$, we find that in the approach to the big bang,

$$A_1^{(k)} \sim t^{-2} + k \cdot t^{-2s}\,, \qquad A_2 \sim t^{-2}\,, \tag{5.5.24}$$

so the behavior will be very different depending on the spatial curvature k.

- In the spatially flat case $\mathbf{k = 0}$, the lowest time dependence of the action (5.5.15) is $t^{1+3s-2P}$. Therefore this action is finite for $s > (2P_{\rm max} - 1)/3$, where $P_{\rm max}$ is the highest order of $P = p_1 + p_2$ that appears in the action ($P_{\rm max} \geq 3$ for a theory that is at least cubic in curvature). All the terms of the constraint equation go like t^{3s-2P}, so on the on-shell action, we can in general get rid of the highest order in t and keep as condition for finiteness, $s > (2P_{\rm max} - 3)/3 \geq 1$. This leads to a divergence in the action, unless the quantity $P_{\rm max}$ is bounded. Thus, on flat FLRW, generic $f(R_{\mu\nu\rho\sigma})$ theories have finite on-shell action only if they have a bounded order in the Riemann tensor, and if the scale factor undergoes sufficiently accelerated expansion[11].

- When the spatial sections are not flat, $\mathbf{k \neq 0}$, it becomes impossible to keep the action finite. The action (5.5.15) contains terms with $p_1 + 1$ different dependences in t:

$$t^{1+3s-2P+2(1-s)\cdot j} \quad \text{with} \quad j \in \{0, \ldots, p_1\}\,. \tag{5.5.25}$$

  The $j = 1$ and $j = 2$ terms yield the conditions

$$s > 2P - 3 \quad \text{and} \quad s < 5 - 2P\,, \tag{5.5.26}$$

  which are mutually exclusive since $P = p_1 + p_2 \geq 2$. If we try to ease this tension by using the constraint equation (5.5.17), we find that its time dependence when

[11] Note that here we haven't assumed any symmetry-induced cancellations between different on-shell terms in the action, as our emphasis was on generic theories. An outstanding exception are $f(R)$ theories, for which the higher-curvature terms are in fact spurious and can be replaced by a scalar field.

$a \sim t^s$ goes as

$$t^{3s-2P+2(1-s)\cdot j} \quad \text{with} \quad j \in \{0, \dots, p_1\}\,. \tag{5.5.27}$$

Therefore, the constraint equation enable us to replace the order $t^{3s-2P+2(1-s)p_1}$ by a combination of the p_1 other orders in t in the on-shell action, but for $p_1 > 2$ this does not suffice to resolve the contradiction (5.5.26). We conclude that generically (i.e., not in special cases as $f(R)$ theory as explained in the previous footnote), the on-shell action blows up whenever the Riemann tensor order is larger than 2 for non-spatially flat FLRW backgrounds.

Overall, these results teach us that the finite amplitude criterion is highly constraining for higher-curvature theories of gravity. If the highest power in the Riemann tensor, $P_{\max}$, is larger than 2, the criterion eliminates all Lorentzian FLRW backgrounds with non-zero spatial curvature. When the spatial curvature is zero instead, it retains only highly accelerating backgrounds with $s > (2P_{\max} - 3)/3$ for $a \sim t^s$. This implies that for the infinitely-many higher-curvature terms expected in string theory from loop corrections, all Lorentzian FLRW backgrounds with standard matter contributions are ruled out by the finite amplitude criterion. A Lorentzian big bang thus become impossible, and the only way out is to depart from Lorentzian metrics as in the no-boundary proposal (see 5.4). In this case we find a finite cosmological amplitude even for an action containing an infinite sum of higher-curvature terms.

Our results also underline once again the special role played by quadratic gravity: it allows for Lorentzian non-spatially flat FLRW backgrounds, but only if they are accelerating (i.e., inflation-like solutions). Next we carry further the study of quadratic gravity, by including anisotropies.

5.5.4 Quadratic gravity on anisotropic backgrounds

The generic Belinskii-Khalatnikov-Lifshitz (BKL) approach to spacetime singularities in ordinary general relativity was found in the 70's as the Kasner solution [88]. This solution is strongly anisotropic, and even though the mean scale factor scales as $a \sim t^{1/3}$ when $t \to 0$, the anisotropies themselves blow up. Such highly anisotropic backgrounds continue to form the generic solution for the approach of spacetime singularities when higher-order curvature terms are added to the gravity action.

Besides, we have shown in the previous subsection that the on-shell action of quadratic gravity remains finite when $t \to 0$ only if the background is accelerating, that is if $a \sim t^s$ with $s > 1$ when $t \to 0$. Therefore, the generic Kasner solutions are ruled out by the finite amplitude criterion for quadratic gravity. It implies that if accelerating background solutions to quadratic gravity do exist, they become the relevant saddle point solutions, even if they are non-generic. Our aim for this subsection is to study such accelerating, anisotropic solutions to quadratic gravity.

$R + R^2 +$ matter action

We consider the action: $R + R^2 +$ matter. It is equivalent to the action: R+inflationary scalar field+matter in the Einstein frame. We analyze anisotropies by considering a Bianchi-I type of metrics:

$$\mathrm{d}s^2_{\mathrm{BI}} = -\mathrm{d}t^2 + a^2 \left(e^{2(\beta_+ + \sqrt{3}\beta_-)} \mathrm{d}x^2 + e^{2(\beta_+ - \sqrt{3}\beta_-)} \mathrm{d}y^2 + e^{-4\beta_+} \mathrm{d}z^2 \right), \tag{5.5.28}$$

where the functions $\beta_\pm(t)$ characterize the time dependent anisotropies. The Friedmann constraint equation of this system reads:

$$3M^2_{\mathrm{Pl}} H^2 = 3(\dot{\beta}^2_+ + \dot{\beta}^2_-) + \rho_{\mathrm{infl}} + \rho_w, \tag{5.5.29}$$

where the matter is taken to be a perfect fluid $p = w\rho$ so that we find from the continuity equation $\rho_w \propto a^{-3(1+w)}$. We can also integrate the equation of motion for the anisotropies, $\ddot{\beta}_\pm + 3H\dot{\beta}_\pm = 0$, to obtain the scaling of their derivatives: $\dot{\beta}_\pm \propto a^{-3}$. The Friedmann equation (5.5.29) therefore becomes:

$$3M^2_{\mathrm{Pl}} H^2 = \frac{3\sigma_0^2}{a^6} + \rho_{\mathrm{infl}} + \frac{\rho_0}{a^{3(1+w)}}, \tag{5.5.30}$$

where we have defined the energy densities for anisotropies and matter at the reference scale $a = 1$ as respectively: $\sigma_0^2 \equiv (\dot{\beta}^2_+ + \dot{\beta}^2_-)|_{a=1}$ and $\rho_0 \equiv \rho_w(a = 1)$. Our solution must be accelerating, $a \propto t^s$ with $s > 1$, so that $H \propto t^{-2}$ and the inflationary scalar field has a constant energy density ρ_{infl}. Therefore, we find that in the approach to the spacetime singularity $t \to 0$, the anisotropic energy density, $3\sigma_0^2/a^6$, dominates the dynamic and leads to a Kasner solution. There exists no dynamical solution to the $R + R^2$ action which is accelerating all the way back to the big bang.

Full quadratic gravity action

We now add the Weyl squared term to the previous action, and recover the full quadratic gravity coupled to GR, (5.5.3)[12]. In this case, **exact anisotropic inflationary solutions** do exist [118], and for a Bianchi-I metric with $a(t) = e^{Ht}$, $\beta_\pm(t) = \sigma_\pm \cdot t$ and $\rho_{\mathrm{infl}} = \Lambda$, they are given by:

$$\begin{cases} H^2 = \dfrac{4}{27}\dfrac{\Lambda}{M^2_{\mathrm{Pl}}}(2 - \omega) - \dfrac{M^2_{\mathrm{Pl}}}{36}\sigma\,, \\ \Sigma^2 \equiv \dot{\beta}^2_+ + \dot{\beta}^2_- = \sigma^2_+ + \sigma^2_- = \dfrac{2}{27}\dfrac{\Lambda}{M^2_{\mathrm{Pl}}}(1 + 4\omega) + \dfrac{M^2_{\mathrm{Pl}}}{18}\sigma\,. \end{cases} \tag{5.5.31}$$

These solutions exist if the coupling constants ω and σ of quadratic gravity (5.5.3) are such that the constant quantities H^2 and Σ^2 defined above are positive. These solutions

[12]The Gauß-Bonnet term is irrelevant from the dynamical perspective, but will be considered again when we study the finiteness of the on-shell action

are non-generic, and are really intrinsic to quadratic gravity because they do not have a well-defined limit for $1/\sigma \to 0$ (where we recover GR). They are also non-singular (the four-curvature is bounded for $t \in [-\infty, t_0]$). Note that similar solutions also exist for other types of Bianchi metrics (II, IV, VIh and VIIh, see [119, 118, 120, 121]).

Now that we have some accelerating, anisotropic solutions for quadratic gravity, we verify that they indeed satisfy the finite amplitude criterion. Their on-shell bulk action (5.5.3) reads:

$$S_{\text{quad}} = S_{\text{E-H}} + S_{R^2} + S_{C^2} + S_{\mathcal{G}}\,, \tag{5.5.32}$$

with

$$\begin{aligned}
S_{\text{E-H}} &\equiv \frac{M_{\text{Pl}}^2}{2}\int \mathrm{d}^4x\,\sqrt{-g}\,R \\
&= 3M_{\text{Pl}}^2\int_{-\infty}^{t_0}\mathrm{d}t\,a^3\left[H^2+\frac{\ddot{a}}{a}+(\dot{\beta}_+^2+\dot{\beta}_-^2)\right] = \frac{M_{\text{Pl}}^2 e^{3Ht_0}}{H}\left(2H^2+\Sigma^2\right); \qquad (5.5.33)\\
S_{R^2} &\equiv \frac{\omega}{3\sigma}\int \mathrm{d}^4x\,\sqrt{-g}\,R^2 \\
&= \frac{12\omega}{\sigma}\int_{-\infty}^{t_0}\mathrm{d}t\,a^3\left[H^2+\frac{\ddot{a}}{a}+(\dot{\beta}_+^2+\dot{\beta}_-^2)\right]^2 = \frac{4\omega}{\sigma}\frac{e^{3Ht_0}}{H}\left(2H^2+\Sigma^2\right)^2; \qquad (5.5.34)\\
S_{C^2} &\equiv -\frac{1}{2\sigma}\int \mathrm{d}^4x\,\sqrt{-g}\,C^2 \\
&= -\frac{6}{\sigma}\int_{-\infty}^{t_0}\mathrm{d}t\,a^3\Big[(\ddot{\beta}_+^2+\ddot{\beta}_-^2)+2H(\dot{\beta}_-\ddot{\beta}_-+\dot{\beta}_+\ddot{\beta}_+-2\dot{\beta}_+^3+6\dot{\beta}_-^2\dot{\beta}_+) \\
&\qquad\qquad +H^2(\dot{\beta}_+^2+\dot{\beta}_-^2)+4(\dot{\beta}_+^2+\dot{\beta}_-^2)^2+4(\dot{\beta}_-^2\ddot{\beta}_+-\dot{\beta}_+^2\ddot{\beta}_++2\dot{\beta}_-\ddot{\beta}_-\dot{\beta}_+)\Big] \\
&= -\frac{2}{\sigma}\frac{e^{3Ht_0}}{H}\left(4H\sigma_+(3\sigma_-^2-\sigma_+^2)+H^2\Sigma^2+4\Sigma^4\right); \qquad (5.5.35)\\
S_{\mathcal{G}} &\equiv \theta\int \mathrm{d}^4x\,\sqrt{-g}\,\mathcal{G} \\
&= 24\,\theta\int_{-\infty}^{t_0}\mathrm{d}t\,a^3\left[H^2\left(\frac{\ddot{a}}{a}-2(\dot{\beta}_+^2+\dot{\beta}_-^2)\right)+2\left(\dot{\beta}_-^2\ddot{\beta}_++2\dot{\beta}_-\ddot{\beta}_-\dot{\beta}_+-\dot{\beta}_+^2\ddot{\beta}_+\right)\right. \\
&\qquad\qquad \left.-\frac{\ddot{a}}{a}\left(\dot{\beta}_-^2+\dot{\beta}_+^2\right)+H\left(6\dot{\beta}_-^2\dot{\beta}_+-2(\dot{\beta}_-\ddot{\beta}_-+\dot{\beta}_+\ddot{\beta}_++\dot{\beta}_+^3)\right)\right] \\
&= 8\,\theta\frac{e^{3Ht_0}}{H}\left(H^4-3H^2\Sigma^2+2H\sigma_+(3\sigma_-^2-\sigma_+^2)\right). \qquad (5.5.36)
\end{aligned}$$

The associated boundary terms are (the factor 2 in front comes from the 1/2 in the definition of (5.5.2)):

$$\begin{aligned}
S_{\text{E-H}}^{\text{boundary}} &= -2\cdot\frac{M_{\text{Pl}}^2}{3}\int \mathrm{d}^3x\sqrt{h}h^{ij}K_{ij} = -\frac{2M_{\text{Pl}}^2}{3}\left[a^3H\right]_{-\infty}^{t_0} = -\frac{2M_{\text{Pl}}^2}{3}e^{3Ht_0}H; \qquad (5.5.37)\\
S_{R^2}^{\text{boundary}} &= -2\cdot\frac{\omega}{3\sigma}\int \mathrm{d}^3x\,\sqrt{h}\,\Psi^{ij}[R^2]K_{ij} = -\frac{4\omega}{3\sigma}\left[a^3Rh^{ij}K_{ij}\right]_{-\infty}^{t_0} \\
&= -\frac{24\omega}{\sigma}\left[a^3H\left(\frac{\ddot{a}}{a}+H^2+(\dot{\beta}_+^2+\dot{\beta}_-^2)\right)\right]_{-\infty}^{t_0} = -\frac{24\omega}{\sigma}e^{3Ht_0}H\left(2H^2+\Sigma^2\right); \qquad (5.5.38)\\
S_{C^2}^{\text{boundary}} &= -2\cdot\left(-\frac{1}{2\sigma}\right)\int \mathrm{d}^3x\,\sqrt{h}\,\Psi^{ij}[C^2]K_{ij} = -\frac{4}{\sigma}\left[a^3n_0n_0C^{0i0j}K_{ij}\right]_{-\infty}^{t_0}
\end{aligned}$$

$$= \frac{12}{\sigma}\left[a^3 H\left(\dot\beta_-^2+\dot\beta_+^2\right)+a^3\left(6\dot\beta_-^2\dot\beta_+-2\dot\beta_+^3+\dot\beta_-\ddot\beta_-+\dot\beta_+\ddot\beta_+\right)\right]_{-\infty}^{t_0}$$

$$= \frac{12}{\sigma}e^{3Ht_0}\left(H\Sigma^2+2\sigma_+(3\sigma_-^2-\sigma_+^2)\right); \tag{5.5.39}$$

$$S_{\mathcal{G}}^{\text{boundary}} = -2\cdot\theta\int \mathrm{d}^3x\,\sqrt{h}\,\Psi^{ij}[\mathcal{G}]K_{ij} = -4\theta\left[J-2G^{\mathrm{b}}_{ij}K^{ij}\right]_{-\infty}^{t_0}$$

$$= -8\theta\left[a^3\left(H-2\dot\beta_+\right)\left(2H\dot\beta_++H^2+(\dot\beta_+^2-3\dot\beta_-^2)\right)\right]_{-\infty}^{t_0}$$

$$= -8\theta e^{3Ht_0}\left(H^3-3H\Sigma^2-2\sigma_+(\sigma_+^2-3\sigma_-^2)\right). \tag{5.5.40}$$

All these bulk and boundary contributions to the on-shell action are finite (and the Gauß-Bonnet contributions even sum to zero). This proves that **the solution** (5.5.31) **satisfies the finite amplitude criterion at least at the background level**. Nevertheless, we find that this solution is unstable under perturbations. We expect quantum fluctuations to naturally occur in the anisotropies, and therefore we must study the time evolution in the addition of small perturbations. The results of our numerical analysis are displayed in figure 5.5. We have initialized the exact anisotropic and inflating solution (constant Σ^2

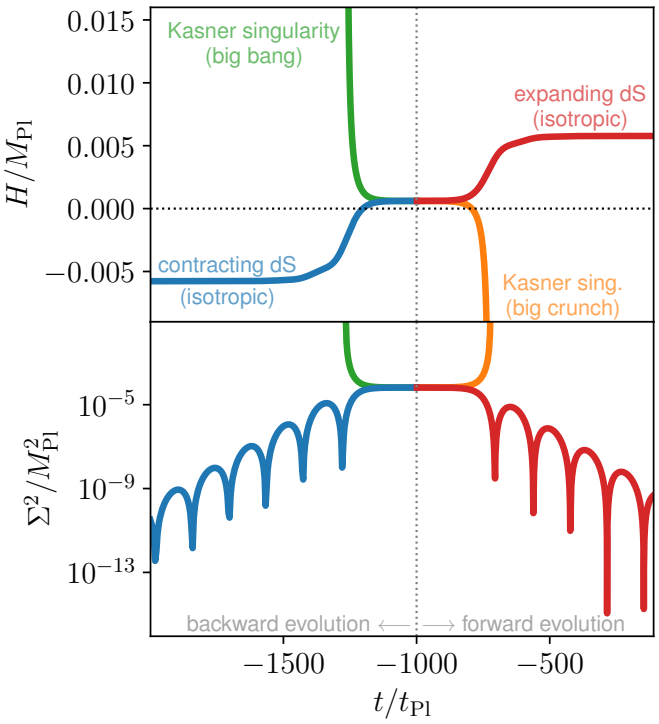

Figure 5.5: Time evolution of the anisotropies $\Sigma^2 \equiv \dot\beta_+^2+\dot\beta_-^2$ and of the Hubble expansion rate H in quadratic gravity with a cosmological constant Λ, starting from the exact anisotropically inflating solution (5.5.31) at $t_{\mathrm{ini}} = -1000\,t_{\mathrm{Pl}}$ and adding small perturbations about $\ddot\beta_\pm = 0$ and $\dot H = 0$. We have used the values $\Lambda = 10^{-4}M_{\mathrm{Pl}}^4$, $\sigma = 10^{-3}$ and $\omega = 1/10$. Without loss of generality, we set $\dot\beta_- \equiv 0$, so Σ^2 is fully determined by $\dot\beta_+^2$. Small perturbations in the initial conditions are implemented in this example with $\ddot\beta_+(t_{\mathrm{ini}}) = \pm 10^{-5}\sigma_+ M_{\mathrm{Pl}}$, and $\dot H(t_{\mathrm{ini}})$ is set such that the constraint equation is satisfied initially.

and H) at $t = -1000\,t_{\mathrm{Pl}}$. Toward the future, either the anisotropies grow and the universe re-collapses (orange curves), or the anisotropies shrink to zero and the universe reaches an isotropic de Sitter expansion phase (red curves). To the past, either the anisotropies blow

up and the universe collapses with a Kasner-type metric (green curves), or it bounces from a contracting de Sitter phase, while anisotropies are small (blue curves). Therefore, this solution is not a past-attractor,[13] but if it is the only one allowed by the finite amplitude criterion, and that this criterion acts as a selection rule for the initial conditions of the universe, then this solution can evolve into an isotropic inflationary phase.

We conclude that for quadratic gravity, the finite amplitude criterion is very restrictive and only allows accelerated expansion near the big bang singularity, though we have found that anisotropies are also allowed[14]. Nevertheless, such anisotropic beginnings are allowed only under the most favorable conditions, because accelerated expansion is efficient in suppressing anisotropies dynamically.

If the finite amplitude criterion indeed acts as a selection rule for actions of the early universe, then quadratic gravity naturally leads to initial conditions favorable for inflation. One last caveat to this scenario, which we leave for future work, concerns whether the incompleteness problem of inflation discussed in section 5.2 also applies to quadratic gravity.

5.6 Emergent and loitering universes

Loitering or *Quasi-static* universes are another class of non-singular cosmological models that differ from the bouncing and cyclic universes we studied previously in section 5.3, but also offer an alternative scenario to inflation in the very early universe.

In these models, the universe reaches an asymptotically Minkowski phase in the infinite past, meaning that $a \to$ constant and $H, \dot{H} \to 0$ when $t \to -\infty$. Such scenarios can naturally satisfy the finite amplitude criterion in ordinary general relativity, because the integrand of the Einstein-Hilbert action (5.3.3) vanishes in the limit $t \to -\infty$. The on-shell action also remains finite in the presence of a scalar field or perfect fluid matter field, because from the Einstein field's equations, the loitering limit is equivalent to $\rho \to 0$ or $V(\phi) \to 0$, while $a \to$ constant and $t \to -\infty$.

Loitering phase can however not be dynamically generated within the ordinary general relativity framework, or using usual matter fields. Instead, it requires to turn to **modified gravity theories** or to a full quantum theory such as **string theory**. In this section we explore these two possibilities and see how the loitering phase can emerge, and whether it can indeed lead to finite cosmological amplitudes in these contexts.

[13] The only known past attractors in quadratic gravity are in fact a Kasner-like anisotropic solution and a radiation-like isotropic solution [118, 122]. They are both non-accelerating and so are ruled out by the finite amplitude criterion.

[14] This refines the analysis of [85], where it was shown that the finite amplitude criterion only allows for isotropic and homogeneous beginnings in the context of quadratic gravity. However, the arguments were making use of the divergence of the off-shell action, which by itself does not imply an ill-defined amplitude. Here we have rectified this analysis by using the on-shell action. In any case the result we get is very similar to the one obtained previously, so the conclusions are overall preserved.

5.6.1 Emergent universe from the EFT approach and modified gravity

The first type of cosmological models enabling the emergence of a loitering phase is based on modified gravity theories, e.g., Horndeski and beyond-Horndeski. We adopt an effective field theory approach, without presuming any UV-complete theory. We will look for solutions within the modified gravity theories for which $a(t \to -\infty) \to$ constant. The universe must then exit the loitering phase in order to attain a subsequent hot big bang evolution, and this is only possible if $\dot{H} > 0$ during a certain period, i.e., the null energy condition must be violated[15]. This exiting step justifies the name of "emergent" or "genesis" scenario. This approach for constructing loitering phases has been applied to a plethora of modified gravity models [123, 124, 125, 126, 127, 128, 129, 130, 131, 132]. Here we will focus in particular on Horndeski, beyond-Horndeski and related theories.

Example in k-essence theory

The theory of k-essence [133, 134] is one of the simplest extension of general relativity, and simply introduces a scalar field, ϕ, that enters the action as a generic function of itself and of its kinetic term, $X \equiv -\partial_\mu\phi\,\partial^\mu\phi/2$:

$$S_{k\text{-essence}} = \int \mathrm{d}^4x\,\sqrt{-g}\left(\frac{M_{\rm Pl}^2}{2}R + P(X,\phi)\right). \tag{5.6.1}$$

The equations of motion are the Einstein field equations (1.1.9) with stress-energy tensor:

$$T_{\mu\nu}^{k\text{-essence}} = P g_{\mu\nu} + P_{,X}\partial_\mu\phi\partial_\nu\phi\,. \tag{5.6.2}$$

Taking the trace of the Einstein field equation (1.1.9) then gives the relation: $-M_{\rm Pl}^2 R = T^{k\text{-essence}} = 4P - 2XP_{,X}$, which can then be used to simplify the on-shell action (5.6.1) into:

$$S_{k\text{-essence}}^{\text{on-shell}} = \int \mathrm{d}^4x\,\sqrt{-g}\,(XP_{,X} - P)\,. \tag{5.6.3}$$

Exiting the loitering phase requires a period of the evolution where the NEC is violated. The interest of the k-essence theory is precisely that a cosmological background violating the NEC for a certain time period naturally emerges from the ghost condensation of the scalar field [135]. We display this mechanism here by following [136]. We assume the function P can be split into a kinetic and potential part: $P(X,\phi) = K(X) - V(\phi)$. For a ghost condensate, the kinetic function is given by $K(X) = (2X - M^4)^2/(8\Lambda)$, where we have introduced two new mass scales, $\Lambda^{1/4}$ and M. The ghost condensate forms at the kinetic energy $X = M^4/2$.

The trace of the stress-energy tensor is $T = 3p - \rho$, therefore on FLRW background,

[15] The violation of the null energy condition is a necessary requirement for obtaining a non-singular cosmology.

the energy density and its sum with the pressure are:

$$\rho = 3P - T^{k\text{-essence}} = 2XP_{,X} - P = \frac{X(2X - M^4)}{\Lambda} - \frac{(2X - M^4)^2}{8\Lambda} + V(\phi)\,, \tag{5.6.4}$$

$$\rho + p = 2XP_{,X} = \frac{X(2X - M^4)}{\Lambda}\,. \tag{5.6.5}$$

At the ghost condensate $X = M^4/2$, we find that $\rho = V(\phi)$ and $\rho + p = 0$. Therefore, a loitering phase will be reached if $V(\phi) \to 0$ when $t \to -\infty$.

The simplest form of the scalar field that satisfy the ghost condensation condition is: $\phi(t) = M^2 t$. By adding small fluctuations around it, $\phi(t) = M^2 t + \delta\phi(t)$, we find the Einstein field's equations at second order in the fluctuation's derivative as:

$$3M_{\rm Pl}^2 H^2 = \rho = \frac{M^6}{\Lambda}\delta\dot{\phi} + V(\phi) + \mathcal{O}(M^4\delta\dot{\phi}^2/\Lambda)\,, \tag{5.6.6}$$

$$-2M_{\rm Pl}^2 \dot{H} = \rho + p = \frac{M^6}{\Lambda}\delta\dot{\phi} + \mathcal{O}(M^4\delta\dot{\phi}^2/\Lambda)\,. \tag{5.6.7}$$

As for the equation of motion for the scalar field, $(P_{,X} + 2XP_{,XX})\ddot{\phi} + 3HP_{,X}\dot{\phi} + P_{,X\phi}\dot{\phi}^2 - P_{,\phi} = 0$, it becomes at second order in the fluctuation's derivative:

$$\frac{M^4}{\Lambda}(\delta\ddot{\phi} + 3H\delta\dot{\phi}) + \mathcal{O}(M^2\delta\dot{\phi}^2/\Lambda) = -V_{,\phi}\,. \tag{5.6.8}$$

Using the ansatz $V(\phi) \propto \phi^{-2\alpha}$ for $\alpha \in \mathbb{N}$, we get $V(\phi), V_{,\phi}(\phi) \to 0$ when $\phi \to -\infty$, so the equation of motion (5.6.8) implies that $\delta\dot{\phi} \to 0$ when $t \to -\infty$. Therefore from the Einstein field's equations (5.6.6) and (5.6.7), we find that $H, \dot{H} \to 0$ when $t \to -\infty$: we indeed reach a loitering phase asymptotically in the past.

Next we show that this loitering phase is followed by a NEC violating time period. Specifying for example to $V(\phi) = V_0\,\Lambda^{1/2}\phi^{-2}$, and considering the limit $t \to -\infty$ where $H \to 0$ and $|\delta\phi| \ll |M^2 t|$, the equation (5.6.8) can be integrated to yield

$$\delta\dot{\phi} \simeq -\frac{V_0\Lambda^{3/2}}{M^{10}t^2}\,, \tag{5.6.9}$$

with the initial condition $\delta\dot{\phi}(t \to -\infty) = 0$. This implies that $\delta\dot{\phi} < 0$ and from equation (5.6.7), $\dot{H} \propto -\delta\dot{\phi} < 0$: the NEC is violated. This NEC violating period will then come to an end when the universe reaches a certain energy level where a reheating mechanism occurs, and the newly produced particles would lead to the standard hot big bang evolution.

Now that we have explicitly demonstrated how a loitering phase can occur within the k-essence theory, we can confront it with the finite amplitude criterion. Considering the on-shell action (5.6.3), we find that for the FLRW background solution described above,

it yields to leading order when $t \to -\infty$:

$$S^{\text{on-shell}}_{k\text{-essence}} = \int \mathrm{d}^4x\,\sqrt{-g}\left[\frac{4X^2 - M^8}{8\Lambda} + V(\phi)\right] \simeq \int_{-\infty} \mathrm{d}t\, a_0^3 \left[\frac{M^6}{2\Lambda}\delta\dot{\phi} + V(\phi)\right], \qquad (5.6.10)$$

where a_0 is the constant scale factor reached during the loitering phase when $H \to 0$. From the construction of the ghost condensate, we have that $V(\phi)$, $\delta\dot{\phi} \to 0$ when $t \to -\infty$. The overall on-shell action thus vanishes in the limit $t \to -\infty$, and so the finite amplitude criterion is satisfied at background level.

However, such a simple ghost condensate as presented here usually suffers from issues as gradient instabilities, strong coupling or unitarity violation [137]. Moreover, once again this construction requires the effective scalar potential to be valid on an infinite range of the scalar field. More involved models such as Horndeski and beyond-Horndeski theories can be constructed, that behaves better under certain aspects, but so far it has been impossible to construct a NEC-violating model that avoids any inconsistency, especially when considering large perturbations around the background.

Horndeski theory and beyond

Many genesis scenarios studied within Horndeski theory and beyond have been claimed to be stable against linear perturbations. For each of them, we could study the finiteness of their on-shell action evaluated on the background solution when $t \to -\infty$, and then check that no instability (e.g., ghost, gradient instabilities) arises when considering linear perturbations. If it is the case, then a fixed-wavelength perturbation evolved back to $t \to -\infty$ must reached a Minkowski vacuum, so that the on-shell action of such a perturbation is finite. For example, for the beyond-Horndeski models presented in [129, 138], the background solution and on-shell action in the asymptotic past reduce to the early model of [123], which satisfies the finite amplitude criterion.

However, all those theories are only effective field theories that describe physics only up to a certain cutoff scale. They are assumed to arise from the integration out of heavy degrees of freedom in a more-complete UV theory. Therefore, these theories only make sense if the background energy remains below this cutoff, otherwise one enters a strongly coupled regime where the EFT breaks down. Even if this is satisfied, as in [139, 131, 140], the strong coupling scale shrinks as we look far back in time, making the regime over which the EFT is valid smaller and smaller.

We conclude that effective models of loitering cosmology in the very early universe using Horndeski theory and beyond do not indicate an immediate violation of the finite amplitudes criterion (it can certainly be satisfied at the background level), but those models have their limitations (by virtue of being EFTs), and more analysis is needed to demonstrate their proper robustness.

5.6.2 Loitering phase in string cosmology

Going beyond the EFT framework, loitering phases very naturally arise when string theory is applied to early universe cosmology. The theory of string gas cosmology [141] uses new degrees of freedom coming from strings to describe the very early universe. More precisely, it is based on the thermodynamics of a gas of closed strings in a $(d+1)-$dimensional compact space (such as a torus $\mathbb{T}^d$ of radius R, $d=9$ for the usual superstring model), with three different types of string modes obeying three different equations of states: momentum modes having $p=\rho/d$ (where p,ρ are as usual the fluid pressure and energy density), winding modes with $p=-\rho/d$, and oscillating pressureless modes $p=0$. There is a T-duality symmetry transforming winding modes into momentum ones and vice-versa, when the radius R transforms into its inverse $1/R$. In this model, the universe would start in a quasi-static phase where the winding modes dominate at the Hagedorn temperature (the maximal temperature for a gas of strings). This is the loitering phase where $H\to 0$. It would then transition into a radiation-dominated phase driven by momentum modes in three external dimensions, while the six remaining internal dimensions stay compact, with a radius R of about the string length ℓ_s, and do not evolve any more. This can be explained by the fact that one-dimensional strings tend to annihilate preferentially in three spatial directions [141]. In practice however, it is difficult to find an existing string cosmology background solution recovering such a loitering phase $a\to$ constant when $t\to-\infty$. In this subsection, we consider two attempts of implementation of this scenario into specific string theories. The first considers only the low-energy, tree-level interactions, while the second also encapsulates non-perturbative curvature corrections.

Example in dilaton gravity

As a first example, we consider the low-energy, tree-level effective theory of string theory known as dilaton gravity in $d+1$ spacetime dimensions,

$$S_\mathrm{dilaton}=\frac{1}{2\ell_\mathrm{s}^{d-1}}\int \mathrm{d}^{d+1}x\,\sqrt{-g}\,e^{-2\phi}\left(R+4\partial_\mu\phi\partial^\mu\phi\right)+S_\mathrm{m}\,, \tag{5.6.11}$$

where ℓ_s is the string length, ϕ is the dilaton field, and S_m represents the action of additional matter content. This action ignores any possible potential for the dilaton field and sets the string theory Neveu-Schwarz–Neveu-Schwarz (NS-NS) two-form to zero. We restrict our analysis to an FLRW background for simplicity. Introducing the shifted dilaton $\Phi=2\phi-d\cdot\ln a$ and writing the scale factor as $a=e^\lambda$, we can integrate by part and find:

$$S_\mathrm{dilaton}=\frac{1}{2\ell_\mathrm{s}^{d-1}}\int \mathrm{d}t\,e^{-\Phi}\left(d\cdot\dot\lambda^2-\dot\Phi^2\right)+S_\mathrm{m}. \tag{5.6.12}$$

For the matter action, we assume a gas of strings with momentum and winding modes contributing equally, with respective equation of state $p=\rho/d$ and $p=-\rho/d$, so that the total pressure vanishes. With this matter content, the equations of motion stemming

from the action (5.6.12) admit a loitering solution of the form:

$$\dot{\lambda} \sim \frac{1}{t^2}\,, \quad \Phi \sim -2\ln(-t)\,, \quad (t \to -\infty). \tag{5.6.13}$$

For this solution, the kinetic energy of the shifted dilaton, $\dot{\Phi}^2 \sim 4/t^2$, and the Hubble parameter $H \propto \dot{\lambda}$, both tend to zero in the asymptotic past, so that we reach a loitering phase with $a \to$ constant. Moreover, the energy density also tends to a constant, since $\rho \propto a^{-d}$. By substituting this solution into the action (5.6.12), we find the on-shell action to leading order in $t \to -\infty$ to be:

$$S_{\text{on-shell}} \sim \int_{-\infty} \mathrm{d}t\ (-4+\rho)\ . \tag{5.6.14}$$

Despite the vanishing of the Hubble parameter and the kinetic term, this on-shell action diverges when $t \to -\infty$. This divergence is due to the non-minimal coupling to the dilaton, $e^{-\Phi} \sim t^2$, which blows up when we integrate back to the infinite past. We conclude that the dilaton gravity model of string cosmology does not satisfy the finite amplitude criterion.

Example with non-perturbative curvature corrections

With dilaton gravity, we have restricted ourselves to tree-level interaction and the first order in curvature corrections. Going beyond that gets very complicated, especially in string theory. Nevertheless, recent developments indicate that curvature corrections to all orders in $\alpha' \sim \ell_{\rm s}^2$ can be expressed in a simple form when restricted to homogeneous backgrounds [142], thanks to $\mathrm{O}(d,d)$ symmetry [143, 144]. The FLRW action with no NS-NS two-form field would then read:

$$S = \frac{1}{2\ell_{\rm s}^{d-1}} \int \mathrm{d}t\, a^d e^{-2\phi} \left[-4\dot{\phi}^2 + 4d\dot{\phi}H - d^2H^2 - F(H)\right] + S_{\rm m}\,, \tag{5.6.15}$$

where the function $F(H)$ contains the α' corrections,

$$F(H) = 2d\sum_{k=1}^{\infty}(-\alpha')^{k-1}c_k 2^{2k} H^{2k}\,. \tag{5.6.16}$$

The coefficients c_k must be determined from full string theory calculations, order by order. To zeroth order, it is known that $c_1 = -1/8$, but determining c_2 to first order in α' is already a very difficult task. So instead we keep the c_k coefficients arbitrary and only assume that the infinite sum in $F(H)$ is convergent. In this case, it has been shown that in the string frame, de Sitter-like solutions with $H =$ constant can exist in vacuum [142, 145] and in the presence of matter [146, 147].

Recently, this theory was applied to a very early universe loitering phase in string gas cosmology [83]. In the regime where the string gas is dominated by the winding modes

$p = -\rho/d$, one finds a non-perturbative solution in α':

$$\phi(t) = \frac{d-1}{2} Ht\,, \qquad H = \text{const.}\,, \qquad a(t) \propto e^{Ht}\,. \tag{5.6.17}$$

The on-shell action (5.6.15) (neglecting the matter action) evaluated on this solution then yields:

$$S_{\rm SF}^{\text{on-shell}} \propto \int_{-\infty} a^d e^{-2\phi} \mathrm{d}t = \int_{-\infty} e^{Ht} \mathrm{d}t < +\infty\,. \tag{5.6.18}$$

This integral converges in the string frame (SF) and therefore, the on-shell action is finite when $t \to -\infty$.

However, the loitering phase only appears when making the conformal transformation to the Einstein frame (EF):

$$a_{\rm E} = e^{-2\phi/(d-1)} a\,, \qquad \mathrm{d}t_{\rm E} = e^{-2\phi/(d-1)} \mathrm{d}t\,, \qquad \phi_{\rm E} = \frac{2}{\kappa} \frac{1}{\sqrt{d-1}} \phi\,, \tag{5.6.19}$$

for $\kappa^2 \equiv M_{\rm Pl}^{1-d}$. The Einstein frame is the physical frame, in the sense that all additional matter must be coupled in this frame. Therefore the tools we can use to measure the amplitudes are made of this matter, so the finiteness of the on-shell action must be satisfied in this frame. We can translate the SF solution (5.6.17) into the EF as:

$$a_{\rm E} = a_0\,, \quad t_{\rm E} = -\frac{e^{-Ht}}{H}\,, \quad \phi_{\rm E}(t_{\rm E}) = -\frac{\sqrt{d-1}}{\kappa} \ln(H(-t_{\rm E}))\,, \tag{5.6.20}$$

where we used $a(t) \equiv a_0 e^{Ht}$. This confirms that the theory admits a loitering phase in the EF where $H_{\rm E} \equiv \mathrm{d}a_{\rm E}/\mathrm{d}t_{\rm E} = 0$. The dilaton evolution (5.6.20) implies that

$$\frac{\mathrm{d}\phi_{\rm E}}{\mathrm{d}t_{\rm E}} = \frac{\sqrt{d-1}}{\kappa(-t_{\rm E})} \to 0 \quad \text{when} \quad t_{\rm E} \to -\infty\,. \tag{5.6.21}$$

Therefore, the on-shell action in the Einstein frame, neglecting the matter contributions, reads:

$$S^{(\rm EF)} = \int_{-\infty} \mathrm{d}t_{\rm E}\, a_{\rm E}^d \left[\frac{3}{\kappa^2} \left(2H_{\rm E}^2 + \frac{\mathrm{d}H_{\rm E}}{\mathrm{d}t_{\rm E}} \right) + \frac{1}{2} \left(\frac{\mathrm{d}\phi_{\rm E}}{\mathrm{d}t_{\rm E}} \right)^2 + \mathcal{O}(\alpha') \right] \propto \int_{-\infty} \mathrm{d}t_{\rm E}\, a_{\rm E}^d\, \mathcal{O}(\alpha')\,. \tag{5.6.22}$$

Let us now prove that the α' correction terms also vanish on-shell in the limit $t \to -\infty$. In the string frame, these terms enter the action (5.6.15) as:

$$S(\alpha') \propto \int \mathrm{d}t\, a^d e^{-2\phi} A(H)\,, \quad \text{with} \quad A(H) = 2d \sum_{k=2}^{\infty} (-\alpha')^{k-1} c_k (2H)^{2k}\,, \tag{5.6.23}$$

which transforms in the Einstein frame into:

$$\int \mathrm{d}t\, a^d e^{-2\phi} A(H) = \int \mathrm{d}t_{\rm E}\, a_{\rm E}^d e^{2\kappa\phi_{\rm E}/\sqrt{d-1}} A(H)\,. \tag{5.6.24}$$

The SF Hubble rate H can be expressed in terms of EF quantities as:

$$H = \frac{1}{a}\frac{\mathrm{d}a}{\mathrm{d}t} = \frac{e^{-\kappa\phi_{\mathrm{E}}/\sqrt{d-1}}}{a_{\mathrm{E}}} \cdot \frac{\mathrm{d}\left(a_{\mathrm{E}} e^{\kappa\phi_{\mathrm{E}}/\sqrt{d-1}}\right)}{\mathrm{d}t} = \frac{\kappa}{\sqrt{d-1}}\frac{\mathrm{d}\phi_{\mathrm{E}}}{\mathrm{d}t} = \frac{\kappa}{\sqrt{d-1}}\frac{\mathrm{d}\phi_{\mathrm{E}}}{\mathrm{d}t_{\mathrm{E}}} e^{-\kappa\phi_{\mathrm{E}}/\sqrt{d-1}} . \tag{5.6.25}$$

In the asymptotic past, H is still a constant and $\phi_{\mathrm{E}} \to -\infty$ in the Einstein frame, and therefore the α' correction terms in the action (5.6.24) vanish on-shell.

This model thus provides an example of loitering phase in the Einstein frame within string cosmology, which satisfies the finite amplitude criterion.

5.7 Discussion

In this chapter, we have confronted a new criterion, based on the consistency of the path integral amplitudes for gravitational theories, with a large panel of early universe cosmological models. This criterion bares resemblance to the finite action criterion studied by Barrow and Tipler earlier on [86, 87], in particular both criteria require a finite spatial volume for the universe, and they eliminate histories for which the action diverges when approaching a cosmological singularity. They also differ on important points, for instance our criterion has the advantage of not constraining past configurations of the universe based on its future evolution, and in addition, it is sensitive to some quantum mechanical aspects beyond the semi-classical level, thanks to its path integral formulation.

In the context of this thesis, where our aim is to improve the understanding of the gravitational path integral, this criterion is a helpful resource for categorizing the various early universe models, and we have shown here that it can act as a powerful sieve. We review here the main conclusions of our work, which are also summarized in the table 5.1.

In ordinary general relativity, the finite amplitude criterion is not very constraining and overall, it maintains the BKL mixmaster solutions as the typical approach to cosmological singularities. Specifically, it demands finite four-volume and matter fields behaving in a usual way (i.e., bounded potential for a scalar field or equation of state $w \in (-1, +1)$ for a perfect fluid). Black holes are also consequent with our criterion.

Besides, the non-renormalizability of GR and the various puzzles arising in the early phases of the standard hot big-bang evolution compel us to consider alternative theories of the very early universe. While remaining within the framework of general relativity, the most popular modification to the standard hot big-bang evolution, which solves its horizon and flatness puzzles, is the addition of an inflationary phase before the radiation-dominated epoch. We have found that if inflation is thought of as the very first phase of evolution, going all the way back to the big bang, then it violates the finite amplitude criterion because of quantum interference instabilities. Even if it is not the first phase of evolution, satisfying the criterion also requires to avoid the eternal inflation regime. Intriguingly, the eternal inflation regime is also conjectured to be part of the Swampland [95]. This hints toward a link between the Swampland constraints and our criterion,

suggesting that the Swampland may be a feature already of the semi-classical theory and not only of the full quantum gravity theory[16]. Therefore, an inflationary phase is consequent with the finite amplitude criterion only if it is transient and non-eternal. This means that either we must consider other explanations to the horizon and flatness problems, or we must find an alternative early phase which naturally leads to the initial conditions required for inflation to start. The latter is typically difficult to achieve, but is the approach of the no-boundary proposal, whose formulation in terms of a gravitational path integral makes it particularly well suited to the finite amplitude criterion. In fact, this whole chapter could be summarized by the question: is it possible to find another early universe model that enables to define semi-classical cosmological amplitudes as well as the no-boundary proposal? The main difficulty of the no-boundary proposal is to practically implement the formal definition in a consistent manner, as we reviewed in the introductory chapter 2.2 and in the first part of this thesis. We also come back to this point in the last chapter of this thesis (chapter 6).

Alternative explanations of the horizon and flatness puzzles are for example provided by bouncing and cyclic models. Bounces are allowed by the criterion only if they admit an ekpyrotic scalar field as their unique matter content, while cyclic models are allowed only if they are not exactly cyclic, but instead reach a null scale factor in the asymptotic past while conserving cyclicity in certain local quantities such as the Hubble rate. These bouncing models always imply a violation of the null energy condition, and hence require the appearance of new physics.

By further considering theories beyond general relativity, we have found that the finite amplitude criterion becomes very constraining. Quadratic gravity only allows accelerating solutions, though they can also be anisotropic. This means that quadratic gravity leads to the right initial conditions for inflation to start. Whether a quantum interference instability also arises when a quadratic gravity inflation phase goes all the way back to the big bang remains an open problem. In this case, the finite amplitude criterion changes what is typical and special: the generic mixmaster behavior is ruled out by the criterion, and thus accelerating, inflating backgrounds become the rule and not the exception anymore. For actions containing cubic or higher-order terms in the Riemann tensor, the implications of the criterion get even stricter. Lorentzian FLRW backgrounds are all excluded, except for sufficiently accelerated solutions on a spatially flat background and with a finite number of higher-order terms. This stands in contrast with the results of chapter 3, where all higher order actions we examined admitted a no-boundary solution on closed FLRW background.

Finally, we investigated a last alternative to inflation, that can only be realized within beyond-GR theories: loitering or emerging universes. We found that loitering phases based on EFT kind of theories generically satisfy the finite amplitude criterion, but until

[16]In a parallel manner, the Trans-Planckian censorship conjecture [22] is another semi-classical consistency requirement which is equivalent to certain swampland conditions [148].

now no such model is entirely free of other inconsistencies such as unitarity violations, strong coupling problems, etc. Loitering phase also naturally arise within string cosmology. There we found that the simplest model based on the tree-level, low energy dilaton gravity action cannot satisfy the finite amplitude criterion, while the more complete action containing non-perturbative curvature corrections does satisfy the criterion.

We conclude this chapter by noting that the finite amplitude criterion also connects to Penrose's Weyl curvature hypothesis [149]. By noting that the Weyl curvature is very small for cosmological singularities, while being very large at black hole singularities, Penrose conjectured that it was related to the gravitational entropy, and thus the increase of Weyl curvature would be linked to the second law of thermodynamics. Our results could explain the smallness of the Weyl curvature in initial configurations such as a cosmological singularity: for the no-boundary solution, the most probable spacetimes are those which are highly symmetric and isotropic; for quadratic gravity, the criterion restrict to very symmetric backgrounds; loitering phases for their parts, only satisfy the criterion if anisotropies are kept small. Overall, we see that the finite amplitude criterion selects early universe scenarios which have a small Weyl curvature at early times.

In the next chapter, we pursue our study of the semi-classical consistency of early cosmological models, by looking at another criterion, stemming this time from the consistency of matter fields path integrals, and which restricts how complex the metric components can get.

Chapter 6

Complex metrics criterion

6.1 Necessity for a complex metric criterion

In physics, complex numbers play a crucial yet intriguing role. What seemed to be merely a mathematical artifact necessary for solving third order polynomial equations, turned out to stand at the core of quantum mechanics, describing the very dynamic of quantum objects through Schrödinger's equation. In gravitation as well, several cases of complex metrics appear naturally, for example when considering the thermodynamic of Kerr black holes [55]. Indeed, Gibbons and Hawking found that, similarly to the case of Schwarschild black holes, Kerr black holes' thermodynamic can be recovered by analytically continuing the Kerr metric to complex time, using a Wick-rotation. Because of the crossed angular-time term present in the Kerr metric, the Wick-rotation leads in this case to a fully complex spacetime, and not a mere Euclidean one. Another example where complex metrics play an essential role is in the no-boundary proposal (2.2). There the path integral sums over complex metrics, hence replacing the cosmological singularity of Lorentzian spacetime by a regular geometry.

Nevertheless, as various examples demonstrate, we cannot simply complexify any real metric, and expect to obtain physical results. For instance, Witten showed that analytically continued flat four-dimensional spacetime gives rise to zero action wormhole solutions [150]. If physical, those solutions should be included in a gravitational path integral with the same weighting than classical solutions. This would clearly contradicts our (lack of) observations, and we therefore expect such wormhole solutions to be non physical, and excluded from the path integral in some way. Witten also discusses another type of pathological complex solutions, that we will here call the *n four-sphere no boundary solutions*[1]. These solutions are constructed starting from the simplest instanton geometry for the no-boundary proposal, described explicitly in section 2.2 and depicted in figure 2.1. By gluing below the lower-half four-sphere of the original no-boundary instanton a new full four-sphere, we obtain a different instanton solution. This procedure can be

[1]These many-sphere configurations were first described in [151], where it was found that by considering the Vilenkin saddle points ($n < 0$), the integral could be made convergent. However here we discard those saddle points, as we have seen in section 2.2 that they are associated with blowing-up fluctuations.

repeated as many time as desired, hence creating n different instanton solutions. The *2 four-sphere no-boundary solution* is depicted in figure 6.1, along a graphical representation of a possible time path it corresponds to. Assuming these newly constructed instantons

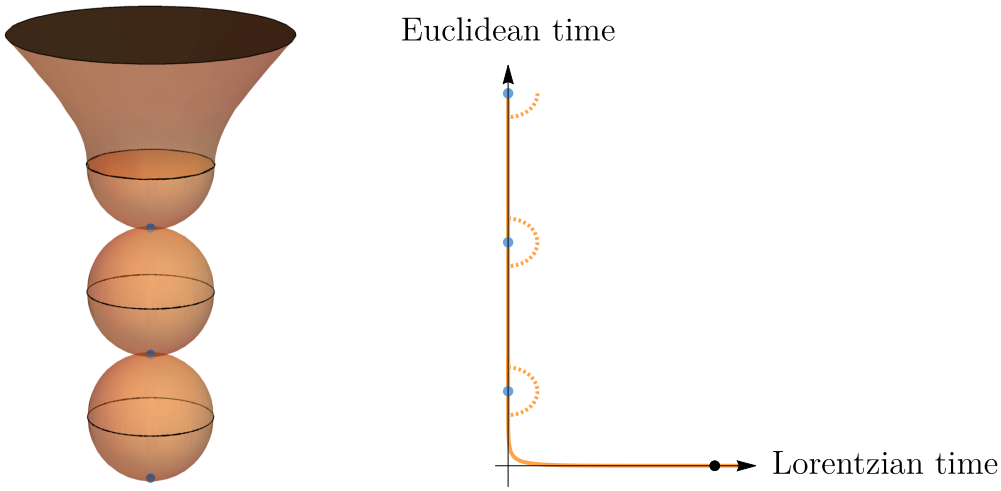

Figure 6.1: *Left:* Spacetime depiction of the no-boundary solution with two additional spheres glued onto the original South Pole. 'Time' evolves forwards from bottom to top: it is Euclidean when the geometries are spheres and Lorentzian when it becomes the hyperboloid. *Right:* Graphical representation of the time path (orange curve) in the complex time plane. The horizontal axis represents Lorentzian time (real t, imaginary τ) and the vertical axis Euclidean time (imaginary t, real τ). The curve changes direction at the moment of the Wick rotation (of 90° in the complex plane). The blue dots indicate the south poles of the Euclidean spheres, and the black dot indicates the late-time Lorentzian de Sitter geometry. The dotted orange curves show possible deformations of the time path such that the zeroes of the scale factor are avoided by going into the Lorentzian direction.

are physical, we can calculate their contribution to the wavefunction of the universe at the semi-classical level (i.e., by performing a saddle-point approximation), and we find:

$$\Psi \sim \exp\left[-\left(\mathbf{n}+\frac{1}{2}\right)\frac{\mathcal{I}(S^4)}{\hbar}+i\varphi\right] = \exp\left[\frac{4\pi^2}{\hbar H^2}\left(2\mathbf{n}+1+i\sqrt{q_1 H^2-1}^{\,3}\right)\right], \tag{6.1.1}$$

where $\mathcal{I}(S^4) = 16\pi^2/H^2$ is the on-shell Euclidean Einstein-Hilbert action of the four-sphere, φ is the phase given by the de Sitter hyperboloid in spatially flat space, and q_1 is the value of the scale factor squared evaluated on the final hypersurface. The amplitude of the wavefunction is found by this calculation to grow exponentially with the number n of four-sphere we glued below the original no-boundary instanton. Therefore, the total wavefunction summing over all these contributions would blow up as $n \to \infty$. This blowing up is non-sensical and therefore, as for the vanishing action wormholes, these geometries must be excluded of the gravitational path integral if we want it to be defined consistently.

We point out that the time path followed in figure 6.1 is not rigid, as a change in the complex time path does not modify the on-shell action used in the semi-classical calculation (at least as long as the boundary conditions are unchanged). This follows from the fundamental theorem of calculus for analytic complex functions: if the complex time

path reside in a simply connected open domain $\subset \mathbb{C}$ where the Lagrangian is holomorphic, then Cauchy's theorem holds. This result is notably not valid in the presence of large anisotropies, because in this case singularities appear in the complex domain, and prevent the time path to be deformed at will [152]. In this chapter we restrict to isotropic backgrounds, so we can deform time path contours without concern.

From the few examples described here, it is clear that certain complex metrics are needed for a successful description of quantum gravity, while others must be discarded. This argument calls for some sort of criterion that could distinguish physical from nonsensical complex metrics for quantum gravity. This chapter aims to develop such a criterion in the specific context of quantum cosmology.

The criterion we will study was devised by Kontsevich and Segal [153] in the prospect of constructing a new axiomatic description of quantum field theories on fixed curved backgrounds. In this context, they considered complex metrics to form an allowable background, if any free matter field theory could be consistently coupled to this background.

In section 6.2 of this chapter, we rederive this allowability criterion, and we also show how it in fact extends an earlier result by Louko and Sorkin [154] for two-dimensional complex scalar fields. We also motivate the application of this criterion to quantum gravity, that was initiated by Witten [150], by showing that it efficiently separates the examples described above, allowing physical geometries and discarding nonsensical ones. The rest of the chapter is then dedicated to the application of the allowability criterion to several models of the early universe cosmology, significantly extending the results of [150, 155]. First, we explain in section 6.3 the techniques used to assess the (non-)allowability of off-shell complex metrics. Then we apply the criterion to Lorentzian metrics (section 6.4), to classical transition solutions between two de Sitter geometries (section 6.5), to quantum bouncing cosmologies that avoid the initial spacetime singularity (section 6.6), and finally, to off-shell configurations in the no-boundary proposal, defined either by the sum over compact geometries or by the sum over regular geometries (section 6.7). The results we obtain are discussed in section 6.8 and are schematically summarized in figure 6.2.

The rest of this chapter follows and presents the results of [4].

6.2 Allowability criterion for complex metrics

In this section we will motivate and rederive the allowability criterion for complex metrics studied in this chapter. It is based on the work of Louko and Sorkin [154], Kontsevich and Segal [153] and Witten [150]. We will hence designate this criterion as the LSKSW criterion, or simply the allowability criterion.

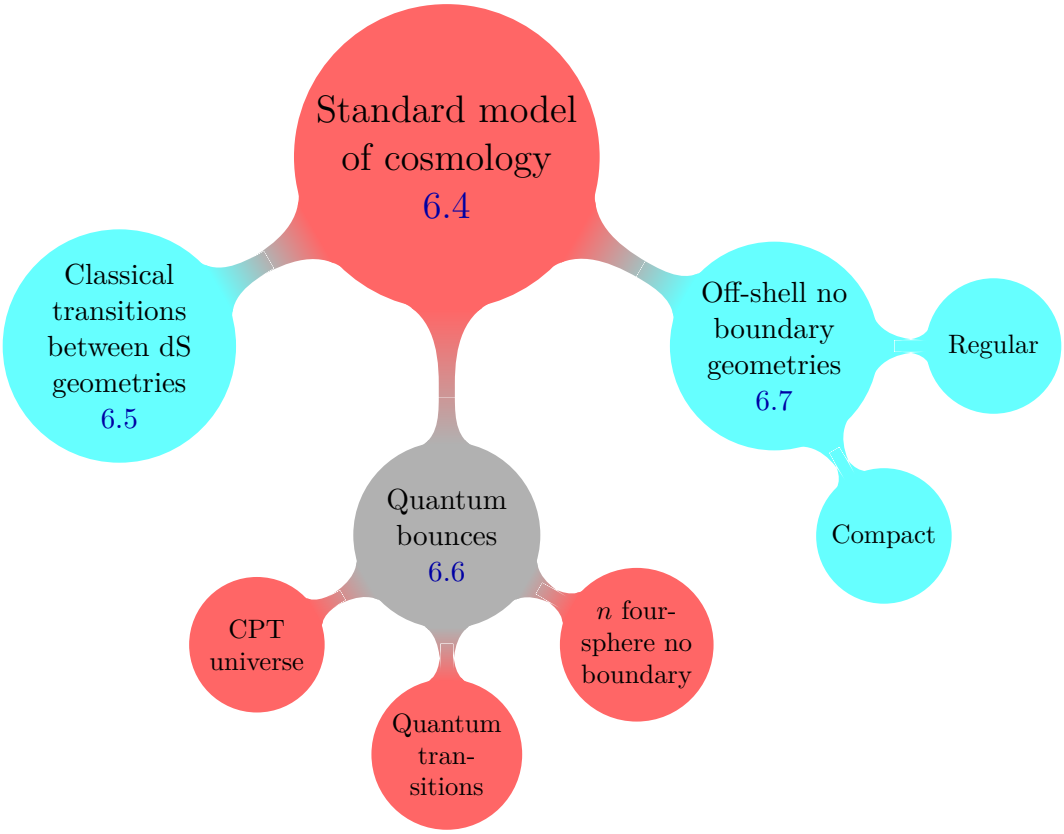

Figure 6.2: (Non-)Allowability of the different early universe cosmology model studied in this chapter. Red means that the metric is discarded, gray means that no conclusion can be reached, and cyan means that an allowed complex metric can be defined. This simplistic representation does not account for the specificities and subtleties described in the core of the text and in the discussion (section 6.8).

6.2.1 A first allowability criterion for scalar fields in two dimensions

In 1995, Louko & Sorkin [154] formulated a first allowability criterion for scalar fields in the context of topology change in $1+1$ dimensions. The variational principle for deriving equations of motions from the Einstein-Hilbert action of general relativity requires the use of smooth and invertible metrics. But sometimes, non-invertible metrics arise in physically interesting cases, for example in topology changes in two spacetime dimensions. There, non-invertible metrics are needed to compute the fundamental vertex of string theory (see figure 6.3). The study of these string theory vertices hence inclined Louko and Sorkin to

Figure 6.3: Trousers (left) and yarmulke (right) geometries: examples of non-invertible 2D metrics possessing a crotch singularity (in red). The trousers geometry is used to compute the fundamental vertex of string theory.

extend the class of metrics entering the definition of the EH action by relaxing the non-

invertibility assumption, to make topology changes kinematically possible. In this aim, they studied two-dimensional Lorentzian analytic metrics vanishing at one single point, and regularised these spacetimes using a simple $+i\epsilon$ prescription. They fixed the sign of the regulator by requiring that the massless scalar field's action has a positive imaginary part (assuming that the scalar field ϕ is real valued on the regularized spacetime):

$$\text{For } S[\phi] = -\frac{1}{2}\int \mathrm{d}^2x\,\sqrt{-g}\,g^{\mu\nu}\partial_\mu\phi\partial_\nu\phi\,,\ \text{where } g \equiv \det(g_{\mu\nu}):\quad \mathrm{Im}(S[\phi]) > 0\,. \tag{6.2.1}$$

This condition implies that the path integral of this scalar field is convergent on the regularized spacetime:

$$\int \mathcal{D}_\phi\,\exp\left(\frac{i}{\hbar}S[\phi]\right) < \infty\,. \tag{6.2.2}$$

Louko and Sorkin also noted that, after diagonalization of the metric, $g_{\mu\nu} = \mathrm{diag}(\lambda_{(0)}, \lambda_{(1)})$, the convergence condition (6.2.1) was equivalent to:

$$\mathrm{Im}[\sqrt{-g}] = \mathrm{Im}[\sqrt{-\lambda_{(0)}\lambda_{(1)}}] < 0\,. \tag{6.2.3}$$

They further speculated on the possibility of defining a similar criterion for other types of matter fields such as an electromagnetic field strength.

6.2.2 Complex metrics in QFT on fixed curved backgrounds

Aiming to replace the axiom sets of quantum field theory, Kontsevich and Segal [153] recently characterised complex background geometries as allowable if any free p-form field theory could be coupled to these backgrounds in a consistent manner. The precise definition (Definition 2.1 of [153]) states that, on a spacetime manifold $\mathcal{M}$ of dimension $D \geq 2$, the complex invertible metric $\boldsymbol{g}$ is **allowable** if the kinetic part of the Euclidean action for any real non-zero p-form gauge field $\boldsymbol{A}$ with associated q-form field strength $\boldsymbol{F} = \mathbf{d}\boldsymbol{A}$ ($q = p+1$) has a positive real part:

$$\begin{aligned}&\mathcal{I}_q[\boldsymbol{A}] = \frac{1}{2q!}\int_{\mathcal{M}} \mathrm{d}^Dx\,\sqrt{\det(\boldsymbol{g})}\,g^{\mu_1\nu_1}\cdots g^{\mu_q\nu_q}F_{\mu_1\cdots\mu_q}F_{\nu_1\cdots\nu_q}\,;\\ &\boldsymbol{g}\text{ is allowable if }\forall\, q \leq D\,,\ \mathrm{Re}\,(\mathcal{I}_q[\boldsymbol{A}]) > 0\,.\end{aligned} \tag{6.2.4}$$

In that case, the Euclidean path integral constructed from this action is convergent:

$$\int \mathcal{D}\boldsymbol{A}\,\exp\left(-\mathcal{I}_q[\boldsymbol{A}]/\hbar\right) < \infty\,. \tag{6.2.5}$$

Note that for $q = 0$, we don't have an interpretation in terms of the field strength of a gauge field. This case corresponds to a scalar field mass term, already discussed by Louko and Sorkin [154] in two dimensions. Let us demonstrate that the Louko and Sorkin criterion (6.2.1) matches this general criterion (6.2.4) in that case. We consider the action

of a real massive scalar field on a Lorentzian background:

$$\begin{aligned} S[\phi] &= -\frac{1}{2}\int \mathrm{d}t\, \mathrm{d}^{D-1}x\, \sqrt{-g_{\mathrm{L}}}\left(g_{\mathrm{L}}^{\mu\nu}\partial_\mu\phi\partial_\nu\phi + m^2\phi^2\right) \\ &= +\frac{i}{2}\int \mathrm{d}\tau\, \mathrm{d}^{D-1}x\, \sqrt{g_{\mathrm{E}}}\left(g_{\mathrm{E}}^{\mu\nu}\partial_\mu\phi\partial_\nu\phi + m^2\phi^2\right) = i\mathcal{I}[\phi]\,, \end{aligned} \tag{6.2.6}$$

where we used the Wick rotation $t = -i\tau$ for the second equality to transform the Lorentzian background metric into the Euclidean one, as this leads to the correct relation between the Lorentzian and Euclidean actions, $iS[\phi] = -\mathcal{I}[\phi]$. The convergence of the Lorentzian path integral requires:

$$\mathrm{Im}\left(S[\phi]\right) > 0 \;\Leftrightarrow\; \mathrm{Im}\left[\sqrt{-g_{\mathrm{L}}}\right] < 0\,, \tag{6.2.7}$$

while the convergence of the Euclidean path integral requires:

$$\mathrm{Im}\left(i\mathcal{I}[\phi]\right) = \mathrm{Re}\left(\mathcal{I}[\phi]\right) > 0 \;\Leftrightarrow\; \mathrm{Re}\left[\sqrt{g_{\mathrm{E}}}\right] > 0\,. \tag{6.2.8}$$

Equations (6.2.7) and (6.2.8) are completely equivalent if the requirements $\mathrm{Re}[\sqrt{g}] > 0$ and $\mathrm{Im}[\sqrt{-g}] < 0$ are. This happens only if the following sign choice: $\sqrt{-g_{\mathrm{L}}} = -i\sqrt{g_{\mathrm{E}}}$, is taken when calculating the square root of the Lorentzian determinant. This choice is consistent with the + sign usually taken when evaluating the square root of the determinant of a Lorentzian metric. This shows that the allowability criterion really applies to any complex metric, be it Euclidean, Lorentzian, or any linear combination of the two. For convenience and to avoid ambiguity, we will focus on the Euclidean version of the criterion (6.2.4) for the rest of this chapter.

Kontsevich and Segal proved that their definition of allowable metrics possesses a simple **pointwise formulation** (see Theorem 2.2 of [153] and its proof). This formulation will be very handy to apply directly the criterion to many early universe metrics.

Consider a specific spacetime point of the manifold, $x \in \mathcal{M}$. The allowability definition is exactly equivalent to the pointwise condition:

$$\mathrm{Re}\left[\sqrt{\det(\boldsymbol{g}(x))}\, g^{\mu_1\nu_1}(x)\cdots g^{\mu_q\nu_q}(x) F_{\mu_1\cdots\mu_q}(x) F_{\nu_1\cdots\nu_q}(x)\right] > 0\,, \tag{6.2.9}$$

for any real and non-zero q-form $\boldsymbol{F}$, $q \in \{0, \cdots, D\}$. We analyze this condition for successive values of q.

1. First, for $q = 0$, we recover the Louko-Sorkin condition (6.2.1), which implies, as we explained in the paragraph above, that $\mathrm{Re}\left[\sqrt{\det(\boldsymbol{g})}\right] > 0$.

2. From $q = 1$, we obtain that the real part of the matrix $G \equiv \sqrt{\det(\boldsymbol{g}(x))}\,\boldsymbol{g}(x)$ is positive-definite. This means that the real and imaginary parts of this matrix can be simultaneously diagonalized using a real basis. Then, the inverse matrix $G^{-1} = \frac{\boldsymbol{g}(x)}{\sqrt{\det(\boldsymbol{g}(x))}}$ is also diagonal in this basis. Because $\sqrt{\det(\boldsymbol{g}(x))}$ is a scalar value,

$\boldsymbol{g}(x)$ itself is then diagonal, and we can write:

$$g_{\mu\nu}(x) = \lambda_{(\mu)}(x)\delta_{\mu\nu}\,, \tag{6.2.10}$$

where no summation on the μ index is implied. We therefore obtain that:

$$\sqrt{\det(\boldsymbol{g}(x))} = \prod_{\mu=1}^{D} \sqrt{\lambda_{(\mu)}(x)}\,, \tag{6.2.11}$$

and the condition found from $q = 0$ (1) translates into

$$\mathrm{Re}\left(\prod_{\mu=0}^{D} \sqrt{\lambda_{(\mu)}(x)}\right) > 0 \;\Leftrightarrow\; \sum_{\mu=1}^{D} \frac{\mathrm{Arg}[\lambda_{(\mu)}(x)]}{2} < \frac{\pi}{2}\,. \tag{6.2.12}$$

3. Considering now all subsequent $q > 1$, the condition (6.2.9) implies that for any subset $\mathcal{S} \subset \{1, 2, \cdots, D\}$,

$$\mathrm{Re}\left(\sqrt{\det(\boldsymbol{g}(x))} \prod_{\mu\in S} (\lambda_{(\mu)}(x))^{-1}\right) > 0\,, \tag{6.2.13}$$

$$\Leftrightarrow \sum_{\mu\in\bar{\mathcal{S}}} \frac{\mathrm{Arg}[\lambda_{(\mu)}(x)]}{2} - \sum_{\mu\in\mathcal{S}} \frac{\mathrm{Arg}[\lambda_{(\mu)}(x)]}{2} < \frac{\pi}{2}\,, \tag{6.2.14}$$

where $\bar{\mathcal{S}} = \{1, 2, \cdot, D\} \setminus \mathcal{S}$. Since this must be true for any subset $\mathcal{S}$, it implies that the metric $\boldsymbol{g}$ is allowable if and only if, for all $x \in \mathcal{M}$,

$$\Sigma(x) \equiv \sum_{\mu=0}^{D-1} \left|\mathrm{Arg}\left[\lambda_{(\mu)}(x)\right]\right| < \pi. \tag{6.2.15}$$

This is the pointwise formulation of the allowability criterion, which we will use in the rest of this chapter. We call $\Sigma(x)$ the *LSKSW or allowability function*, and the inequality, $\Sigma(x) < \pi$, the *LSKSW or allowability bound*.

Before applying the allowability bound to early universe cosmologies, let us comment on the different working assumptions used in [153] to formulate this criterion.

1. **Why is it sufficient to consider p-form gauge fields?**
   The restriction of the condition (6.2.4) to the case of p-form gauge fields is due to the fact that these are the only bosonic fields which possess a gauge-invariant stress energy tensor ($\boldsymbol{F}$), that is necessary for coupling the theory to gravity in a curved spacetime. Additionally, we only consider *non-interacting* field theories, because even in flat spacetime, we do not know any interacting UV complete theories of massless fields except for p-forms.

2. **Why do we restrict to *real* gauge fields?**
   In [153], the goal is ultimately to give an Hilbert space interpretation of the path

integral, in order to obtain unitary quantum field theories. A Euclidean transition amplitude can be written in the Schrödinger picture as a bra and a ket sandwiching an evolution operator, $\Psi[1 \to 2] = \langle 2| e^{-\tau \hat{H}/\hbar} |1\rangle$ (with $\hat{H}$ the Hamiltonian operator). This transition amplitude also corresponds to a path integral fixed at its two ends. Therefore, a quantum state composed of an evolved ket, $|\psi_1\rangle = e^{-\tau \hat{H}/\hbar} |1\rangle$, can be viewed as a path integral fixed at only one of its ends. When the path integral sums over *real* matter fields, it can be carried out along the real line, and the integration contour is defined locally in field space. But if the matter fields are allowed to take complex values, then the path integral is defined via analytic continuation, and the thimbles in the complexified field space define the contour of integration, but depend on the two ends of integration. With only one end given, the thimbles cannot be specified, so the definition of quantum states using the path integral is not possible.

There is yet another argument for why real matter fields are sufficient, when $p \geq 1$ (i.e., not for scalar fields). In these cases, the field configurations contains certain integer variables (e.g., the monopole numbers, the instanton numbers, or the fluxes), and integers cannot be analytically continued. This would, however, only lead to a weaker global, and not a local, restriction [150]. See [156] for a study of no-boundary proposal with internal fluxes.

Given the results found in the chapter 4 of this thesis, it may be desirable that scalar fields, in particular, remain real-valued (or have a small complex component) and at an extremum of their potential. This would avoid the strong non-localities stemming from the dependence of the South-Pole values of the scalar field on the final size of the universe 4.6. This was recently studied in [77] by applying the LSKSW criterion to higher-dimensional spacetimes, and inspecting its consequences on e.g., the volume moduli scalar field coming from the compactification to lower dimensions.

6.2.3 Allowability criterion for quantum gravity

In [150], Witten speculated on the validity of the allowability criterion, not only for QFTs on fixed curved backgrounds, but also in the context of quantum gravity. Of course, due to our present lack of knowledge about quantum gravity, no formal proof can be given. But as argued in the introduction of this chapter 6.1, we expect some criterion for complex metrics to exist, and Witten showed that, at the semi-classical level, the present allowability criterion is very well suited to quantum gravity. In particular, he demonstrated that the Hartle-Hawking saddle points used in the no-boundary proposal and the Kerr metric describing rotating black holes are both allowed. Conversely, he proved that the analytically continued flat 4D spacetime leading to zero-action wormholes is not allowed by the criterion. The simple Lorentzian metric $\mathrm{d}s^2 = -\mathrm{d}t^2 + \sum_{i=1}^{D-1} \mathrm{d}x_i^2$ is also not allowed, but lies on the boundary of the allowable metrics' space. We will develop

this example further, in particular by studying deformation of time path contours, in section 6.4. The pathological *n four sphere no boundary solution* described in the previous subsection is also found not to be allowed, and we will come back to this in more details in 6.6.

In the rest of this chapter, we apply the allowability criterion to quantum cosmology, including off-shell configurations, extending what was initiated in [150, 155]. The reason why we also consider off-shell geometries is because the overall aim of this criterion is to define quantum gravity using the path integral approach consistently. However, as is evident from the no-boundary proposal case detailed in 2.2, the full gravitational path integral also sums over off-shell geometries. In the next section 6.3, we will explain why this fact, together with the deformation of time path contours allowed by Cauchy's integral theorem, renders the determination of allowability more subtle. We will then present three analytical techniques, that will be used afterward to assess the allowability of on- and off-shell metrics.

6.3 Methodology

The condition (6.2.15) characterizes allowable complex metrics in a simple and straightforward manner. But in practice, determining whether a given metric satisfies this condition or not can turn into an involved task, because of the possibility to deform time contours continuously without altering observable variables. So it is sometimes possible to find a specific time contour for which the metric becomes allowable, even if it was not initially. In the first subsection we will describe how to optimize this time contour. We will then present two analytical methods that allow to determine the allowability of a specific metric. All the methods described in this section are particularly appropriate to study minisuperspace models, with a metric parameterized by several functions of time only. For the rest of this chapter, we actually only consider homogeneous metrics, so that the allowability function, $\Sigma(x)$, only depends on time and not on space. The first two methods we describe are conceptually simple, but not always conclusive, while the last one, presented in section 6.3.3, is more intricate, but always conclusive.

6.3.1 Optimizing deformations of the time contour

References [150, 155] found that the on-shell metric of the no-boundary solution is allowed by deforming the time contour in the complex plane, in order to find a time path where the allowability bound is satisfied everywhere. Similarly, we consider a metric to be allowable if there exists a continuous and differentiable deformation of the time contour that keeps the boundary points fixed, and such that the allowability bound is satisfied at all time. This is justified by the fact that, as long as there is no hole in the domain, such a change does not alter the value of the action nor of any observable quantities such as

the transition amplitude calculated from the path integral.

Allowability of a complex metric can therefore be proven by finding one time path that satisfies the allowability bound. This can be done in a time-consuming and not very efficient manner, by running an optimization algorithm on the value of the LSKSW function. The optimization parameters characterize the time path in a judicious way, and the algorithm runs until it finds a set of parameters for which $\Sigma(t) < \pi\,,\ \forall\, t$.

We work with a normalized time variable such that the boundary conditions of a particular solution are set at an initial time $t = 0$ and a final time $t = 1$. We then promote the real, straight path from $t = 0$ to $t = 1$ to a complex path $t(u) : [0, 1] \mapsto \mathbb{C}$ such that $t(0) = 0$ and $t(1) = 1$. The time path function further depends on n real parameters, $\vec{c} = (c_1, c_2, \cdots, c_n) \in \mathbb{R}^n$, so we write it as $t(u, \vec{c})$. The optimization procedure finds the parameters (restricted to some compact domain $\mathcal{A} \subset \mathbb{R}^n$) minimizing the maximal value in time of the $\Sigma(t)$ function, and assesses whether this minimum satisfies the allowability bound:

$$\min_{\vec{c}\in\mathcal{A}} \max_{u\in[0,1]} \Sigma(t(u;\vec{c})) < \pi\,.^{2} \tag{6.3.1}$$

This method is not very efficient because it requires two nested optimizations which are quite time-consuming, and in the case of a negative result, it is not conclusive: the parametrization might not be appropriate, or the domain $\mathcal{A}$ not extended enough. We present more conclusive techniques in the next subsections, but this numerical optimization is useful to **develop intuition about allowable metrics**.

For this purpose, we have used the following parametrization (with a 5-dimensional parameter space). It consists of a linear combination of the straight path, with the addition of the first three terms of a Fourier series in the complex time direction, and a power-law function (inspired by the path that worked in [155]) that starts by following the Euclidean-time direction and then smoothly interpolates to the Lorentzian-time direction:

$$\begin{aligned} t(u; c_1, \ldots, c_5) = c_5\Big[u + ic_1\sin(\pi u) + ic_2\sin(2\pi u) + ic_3\sin(3\pi u)\Big] \\ + (1 - c_5)e^{i(\vartheta-\pi/2)}\Big[\,(1 - (1 - u)^{c_4})\sin(\vartheta) + iu^{c_4}\cos(\vartheta)\Big]\,. \end{aligned} \tag{6.3.2}$$

The angle $\vartheta \equiv \mathrm{Arg}(-N)$ is used to rotate the power-law part of the path as a function of the fixed lapse N, for a given (on- or off-shell) solution. We explored several numerical ranges for the parameters $c_1, \cdots, c_5$. We found many successful paths with the Fourier coefficients $c_1, c_2, c_3 \in [-1/2, 1/2]$, the power-law coefficient $c_4 \in [1, 10]$, and the linear weighting coefficient $c_5 \in [0, 1]$. In the figures 6.11, 6.17 and 6.18, this numerical opti-

[2] The numerical implementation of this optimization problem was carried out using the basin-hopping algorithm [157] of the `SciPy Python` package [158]. We performed two nested basin-hopping optimizations: at every point $\vec{c}$ in the parameter space $\mathcal{A}$ explored by the outer minimization, an inner maximization is called over $u \in [0, 1]$ to find the global maximum of Σ. If this maximum is below π, the algorithm is stopped; otherwise, the optimization over $\mathcal{A}$ is continued until a certain number of iterations has been reached. This cannot guarantee that the value on the left-hand side of (6.3.1) is truly a global minimum, but it is often sufficient to find local minima. When performing an optimization for many different metrics, we took advantage of parallelization using the `multiprocessing` package.

mization (when successful) was used in conjunction with the more analytic techniques described below.

6.3.2 Checking for uncrossable ridges

Sometimes, it is possible to immediately check whether a certain solution violates the allowability bound for any time paths. Let us split the diagonalized homogeneous metric into its temporal and spatial parts:

$$\mathrm{d}s^2 = -f(t)\mathrm{d}t^2 + \sum_{j=1}^{D-1} q_{(j)}(t)(\sigma^j)^2 = -f(t(u))t'(u)^2\mathrm{d}u^2 + \sum_{j=1}^{D-1} q_{(j)}(t(u))(\sigma^j)^2\,, \tag{6.3.3}$$

where the σ^js are differential 1-forms on the spatial hypersurface. The allowability function then reads

$$\Sigma(t(u)) \equiv \Sigma_{\text{temporal}}(t(u)) + \Sigma_{\text{spatial}}(t(u)) = \left|\mathrm{Arg}\left[-f(t(u))t'(u)^2\right]\right| + \sum_{j=1}^{D-1}\left|\mathrm{Arg}\left[q_{(j)}(t(u))\right]\right|\,. \tag{6.3.4}$$

Because of the absolute values, both the temporal and the spatial parts of the allowability function are always positive: $\Sigma_{\text{temporal}}(t(u)) \geq 0$ and $\Sigma_{\text{spatial}}(t(u)) \geq 0$, and therefore

$$\Sigma(t(u)) \geq \max\left\{\Sigma_{\text{temporal}}(t(u)), \Sigma_{\text{spatial}}(t(u))\right\}. \tag{6.3.5}$$

Therefore, it is **sufficient to prove that the spatial allowability bound:**

$$\Sigma_{\text{spatial}}(t(u)) < \pi\,,\ \forall\, u \in [0,1]\,, \tag{6.3.6}$$

is always violated for any connected path between $t(0) = 0$ and $t(1) = 1$, in order for the full allowability bound to be violated (or at best saturated if $\Sigma = \pi$) for this metric.

This condition is very useful because it only depends on the position $t(u)$ of the time paths in the complex plane and not on the tangent $t'(u)$ of the paths, which makes its verification easier.

Checking if the spatial allowability bound (6.3.6) is always violated: In practice, we restrict ourselves to a bounded, closed domain of the complex plane, $\mathcal{B} \subset \mathbb{C}$. If the real part of the time path grows monotonically (so that Lorentzian time never stops or turns around), then this sets the restriction $\mathrm{Re}(t) \in [0,1]$. Similarly, we can set some bound on how far in the imaginary direction a time path can go, e.g., $\mathrm{Im}(t) \in [-1,1]$ (in this case, $\mathcal{B}$ is rectangular). We need to check whether there exists a simply connected subset, $\mathcal{S} \subseteq \mathcal{B}$, containing the points $t = 0$ and $t = 1$, and such that $\Sigma_{\text{spatial}}(t) < \pi\ \forall\, t \in \mathcal{S}$. If there is no such region $\mathcal{S}$, then the time paths within $\mathcal{B}$ inevitably have to cross a region where $\Sigma_{\text{spatial}}(t) \geq \pi$ in order to connect the starting and ending points, hence violating the full allowability bound. In many cases, even if $\mathcal{B}$ is compact, it can be enough to

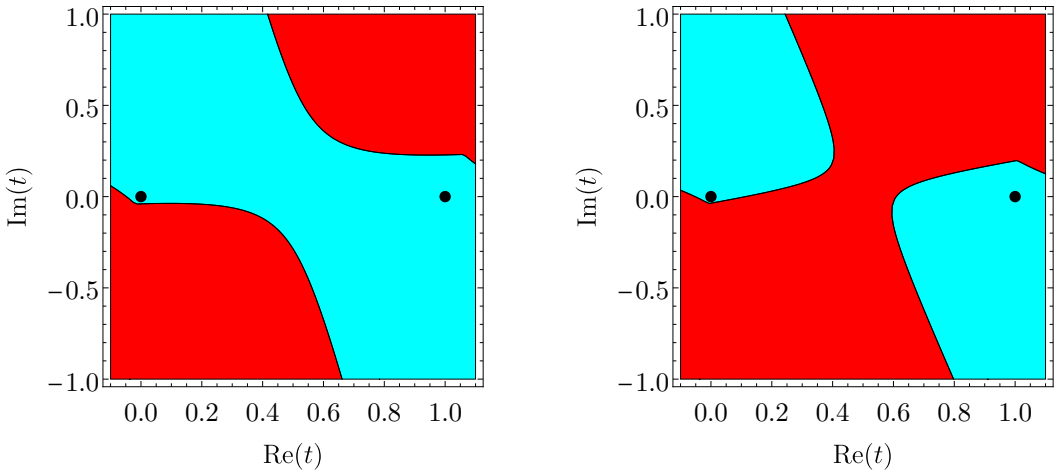

Figure 6.4: An example of the ridge obstruction picture in the complexified t plane. The *seas* (cyan regions) are where $\Sigma_{\text{spatial}}(t) < \pi$, and the *ridges* (red regions) are where $\Sigma_{\text{spatial}}(t) \geq \pi$. On the left, one has an example where the ridges do not present an obstruction and where we can find a simply connected smooth path between $t = 0$ and $t = 1$ (represented in both pictures by the black dots) along which $\Sigma_{\text{spatial}}(t) < \pi$. Whether the LSKSW bound can actually be satisfied along such a path is however not guaranteed and must be decided based on other methods. On the right, one has an example where there is a ridge obstructing the way between $t = 0$ and $t = 1$. This implies that the LSKSW bound is necessarily violated.

convince oneself that the result in fact holds true for $\mathcal{B}$ extending to positive and negative imaginary infinity.

Pictorially, the obstruction resembles a *ridge* exceeding the *sea* of $\Sigma_{\text{spatial}} < \pi$ points and blocking the way between $t = 0$ and $t = 1$; as an example see figure 6.4. This **no-ridge condition** is very useful when studying specific early universe cosmological models. There, we will focus on homogeneous and isotropic metrics, which are solutions to general relativity with a cosmological constant for various boundary conditions. In particular, we will study classical transitions (see 6.5), as well as the no-boundary proposal with Neumann-Dirichlet and Dirichlet-Dirichlet boundary conditions. The path integral for all those scale factor solutions will involve summing over geometries in the complex plane for the lapse N. Thus, for any fixed value of N, we have a metric for which we can write down the allowability function $\Sigma(t)$ and apply the no-ridge condition[3]. We display the results obtained by assessing the no-ridge criterion in figure 6.5. These results are already very informative: the no-ridge criterion renders non-allowable large portions of the geometries, especially at large $|N|$. This is a new indication of the potential power of the allowability criterion to constrain complex metrics that should be non-allowable in path integrals.

[3]In practice, we assess this criterion by using a 'walking algorithm': upon discretizing the region $\mathcal{B}$, one starts from $t = 0$ and explores the complex time plane by trying to go forwards in $\text{Re}(t)$ in small increments and reach $t = 1$, while always staying 'in the water', i.e., keeping $\Sigma_{\text{spatial}}(t) < \pi$. If it is impossible, we declare the metric non-allowable. While this is approximate in the sense that the numerical procedure has limited precision (given by the inverse lattice spacing) and in the sense that it is restricted to a bounded region of the complex plane, we have found the method to be perfectly robust.

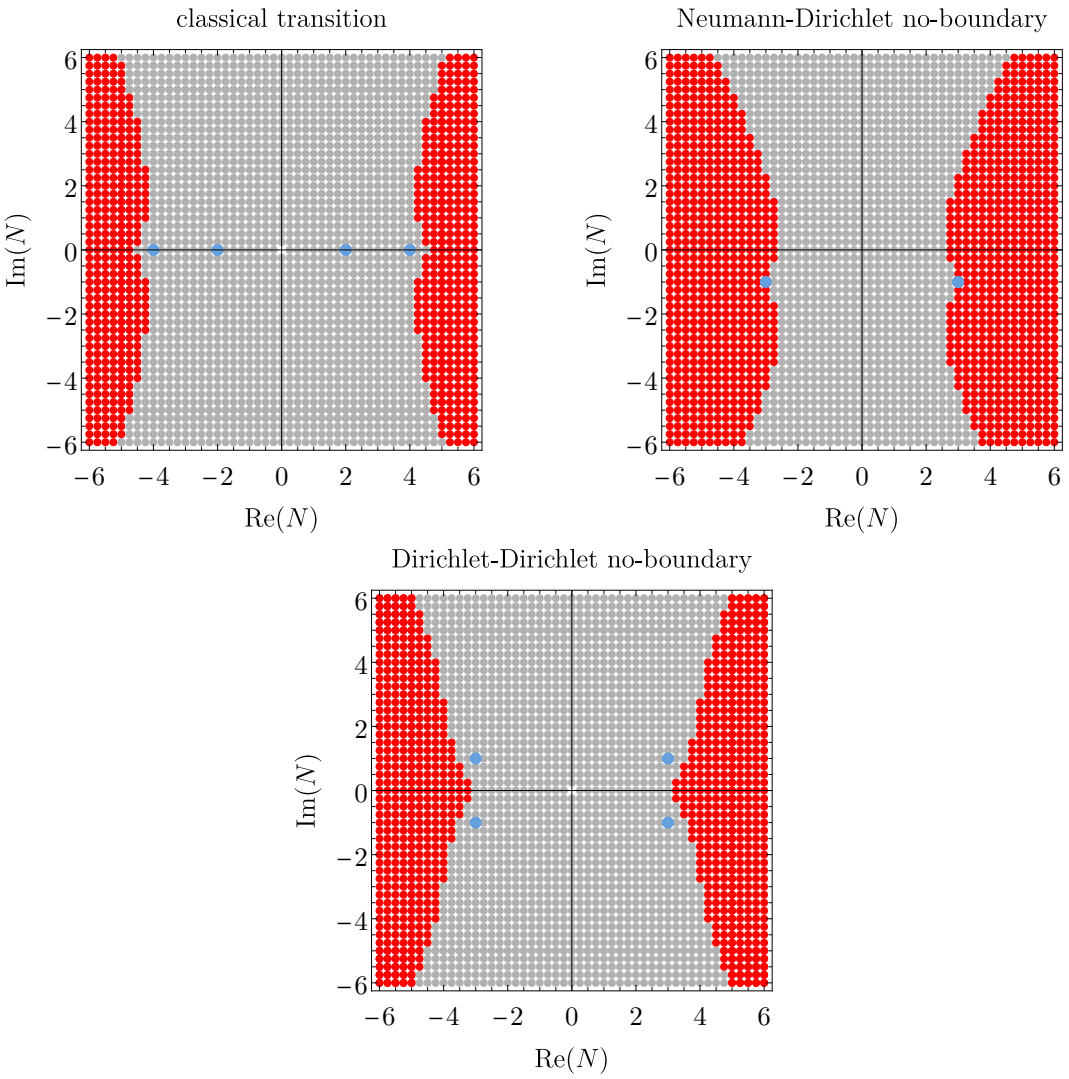

Figure 6.5: Results of the walking algorithm for different models studied later in this chapter. Red dots correspond to geometries for which a ridge was found (the allowability bound is violated). Grey dots represent geometries for which no obstruction is found and further investigation is needed. Saddle point geometries (i.e., classical solutions) are represented by blue dots.

6.3.3 Allowable time domains

In this subsection, we describe our best analytic method for assessing the allowability of a minisuperspace metric. We focus on a particular homogeneous and isotropic metric of the form of equation (6.3.3), which is very often used in minisuperspace quantum cosmology [159] and especially for the no-boundary proposal:

$$\mathrm{d}s^2 = -\frac{N^2}{q(t)}\mathrm{d}t^2 + q(t)\mathrm{d}\Omega^2_{(D-1)} = -\frac{N^2}{q(t(u))}t'(u)^2\mathrm{d}u^2 + q(t(u))\mathrm{d}\Omega^2_{(D-1)}\,. \tag{6.3.7}$$

This metric is a D-dimensional extension of the no-boundary metric we used in the introductory part on the no-boundary proposal 2.2 and in the chapter 4 on the inclusion of scalar fields in the no boundary picture. For this metric (6.3.7), the allowability criterion

reads:

$$\Sigma(t(u)) = \left|\mathrm{Arg}\left[-\frac{N^2}{q(t(u))}t'(u)^2\right]\right| + (D-1)\left|\mathrm{Arg}\Big[q(t(u))\Big]\right| < \pi\,, \quad \forall\, u \in [0,1]\,. \tag{6.3.8}$$

For a geometry that passed the **no-ridge condition**, i.e., for which there exist time paths $t(u)$ that satisfy the spatial allowability condition on all time, we find that

$$\pi - \Sigma_{\mathrm{spatial}}(t(u)) = \pi - (D-1)|\mathrm{Arg}[q(t(u))]| > 0\,, \ \forall\, u \in [0,1], \tag{6.3.9}$$

and therefore we can rewrite the allowability criterion (6.3.8) as:

$$-\pi+(D-1)\left|\mathrm{Arg}\Big[q(t(u))\Big]\right| < \mathrm{Arg}\left[-\frac{N^2}{q(t(u))}t'(u)^2\right] < \pi-(D-1)\left|\mathrm{Arg}\Big[q(t(u))\Big]\right|. \tag{6.3.10}$$

We want to isolate $t'(u)$ from the temporal part of the allowability function, $\Sigma_{\mathrm{temporal}}(t(u)) = \mathrm{Arg}\left[-\frac{N^2}{q(t(u))}t'(u)^2\right]$. This gives us an ordinary differential inequality. At each point in the complexified time plane, we thus obtain a range of directions $t'(u)$ for which the full allowability bound remains satisfied. Using properties of the complex argument, the inequalities (6.3.10) can be rewritten as

$$F_{\mathrm{min}}(t(u)) < \mathrm{Arg}\,[t'(u)] < F_{\mathrm{max}}(t(u)), \tag{6.3.11}$$

with

$$\begin{aligned} F_{\mathrm{min}}(t(u)) &\equiv -(n+1)\pi + \frac{D-1}{2}\left|\mathrm{Arg}\Big[q(t(u))\Big]\right| - \frac{1}{2}\mathrm{Arg}\left[\frac{N^2}{q(t(u))}\right], \\ F_{\mathrm{max}}(t(u)) &\equiv -n\pi - \frac{D-1}{2}\left|\mathrm{Arg}\Big[q(t(u))\Big]\right| - \frac{1}{2}\mathrm{Arg}\left[\frac{N^2}{q(t(u))}\right], \end{aligned} \tag{6.3.12}$$

and where $n \in \{-2,-1,0,1\}$ appears due to the fact that the principal value of the argument of a complex number has to remain within the range $(-\pi,\pi]$.

The inequalities (6.3.11) imply that, at any point $t(u) \in \mathbb{C}$, the slope of a time path $t'(u)$ passing through that point, has to lie within some interval delimited by $F_{\mathrm{min}}(t(u))$ and $F_{\mathrm{max}}(t(u))$, in order to respect the full allowability bound at that point. This provides lower and upper bounds on the allowable time paths: since the paths all start at $t(0) = 0$, one can solve the corresponding initial value problems (IVPs) for the ordinary differential equations[4]:

$$\mathrm{Arg}[t'_{\mathrm{min}}(u)] = F_{\mathrm{min}}(t_{\mathrm{min}}(u))\,, \tag{6.3.13a}$$

$$\mathrm{Arg}[t'_{\mathrm{max}}(u)] = F_{\mathrm{max}}(t_{\mathrm{max}}(u))\,. \tag{6.3.13b}$$

[4]Since F_{min} and F_{max} can take four different values each in order to have the correct principal value for the complex argument, one actually has to solve four IVPs for $t_{\mathrm{min}}(u)$ and four for $t_{\mathrm{max}}(u)$. It is nevertheless straightforward to then verify which solutions correspond to the correct lower and upper bounds.

From Petrovitch's inequality [160], the time paths $t(u)$ respecting the inequalities (6.3.11) have to lie within the curves $t_{\min}(u)$ and $t_{\max}(u)$ for all values of $u > 0$. The full allowability bound is satisfied if and only if the region within the curves $t_{\min}(u)$ and $t_{\max}(u)$ contains the required end point, $t = 1$.

Using this method, we can conclusively determine whether or not for a given metric, there exist time paths respecting the allowability bound, without having to find an actual allowable path[5]. This method is described pictorially in figures 6.9 and 6.10, and it was used in conjunction with the two previous ones described in this section, to obtain the figures 6.11, 6.17 and 6.18.

6.4 Lorentzian metrics

We start our investigation of the allowability of complex metrics in early universe cosmology by the simplest example, which is extensively used in standard cosmology: the Lorentzian metric. It was already proven in [150] that Lorentzian metrics are non-allowable, and always reside on the edge of the allowability domain. In this section, we further show that no smooth complex deformation of the time path can ever render any homogeneous Lorentzian metric allowable. In fact, we show that these metrics at best saturate the allowability bound.

We consider a homogeneous metric ansatz of the form (in particular, it could be a Bianchi spacetime of any type):

$$\mathrm{d}s^2 = -N^2\mathrm{d}t^2 + \sum_{j=1}^{D-1} a_{(j)}^2(t)(\sigma^j)^2\,, \tag{6.4.1}$$

whose allowability function reads

$$\Sigma(t) = \left|\mathrm{Arg}\left[-N^2\right]\right| + \sum_{j=1}^{D-1}\left|\mathrm{Arg}\left[a_{(j)}^2(t)\right]\right|\,. \tag{6.4.2}$$

If the metric (6.4.1) is real and Lorentzian for some solutions $a_{(j)}(t) \in [a_0, a_1]\ \forall\, t \in [t_0, t_1]$, then the lapse N and the scale factors squared $a_{(j)}^2(t)$ are real valued everywhere. Therefore, the allowability bound is saturated with $\Sigma(t) = \pi\,,\ \forall\, t \in [t_0, t_1]$.

Consider now some smooth complex time path $t(u)$ with the same starting and ending points: $t(0) = t_0 \in \mathbb{R}$ and $t(1) = t_1 \in \mathbb{R}$. Then the metric (6.4.1) and its allowability function (6.4.2) respectively become:

$$\mathrm{d}s^2 = -N^2t'(u)^2\mathrm{d}u^2 + \sum_{j=1}^{D-1} a_{(j)}^2(t(u))(\sigma^j)^2\,, \tag{6.4.3a}$$

[5]In practice, the method of the maximal and minimal curves involves solving a few initial value problems using numerical algorithms. This implies a certain level of numerical imprecision, but it has proven to be robust.

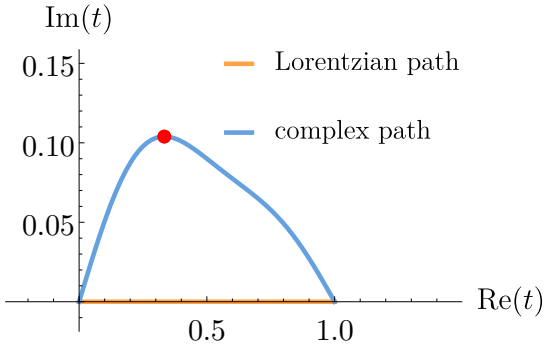

Figure 6.6: Example of a smooth deformation of the time path between $t_0 = 0$ and $t_1 = 1$ in the complex plane. The point $t(u_\star)$ is plotted in red, where the tangent of the complex path is parallel to the real axis, and thus where $\mathrm{Arg}[t'(u_\star)] = 0$.

$$\Sigma(t(u)) = \left|\mathrm{Arg}\left[-N^2 t'(u)^2\right]\right| + \sum_{j=1}^{D-1} \left|\mathrm{Arg}\left[a^2_{(j)}(t(u))\right]\right| . \tag{6.4.3b}$$

Then for $t(u) \in \mathbb{C}\,,\ \forall\, u \in (0,1)$, the scale factor becomes complex, and the spatial part of the allowability function may become non-zero. To reduce $\Sigma(t(u))$ below π, we need a time path such that $\Sigma_{\text{temporal}} < \pi - \Sigma_{\text{spatial}}$. But since the time path must start and end on the real-t axis, at t_0 and t_1 respectively, the time trajectory must 'turn around' in the imaginary direction. Then there is at least one point $u_\star \in (0,1)$ along the trajectory, for which $\mathrm{Im}[t'(u_\star)] = 0$ and where $t'(u_\star)$ is purely real and positive (assuming again the real part of time always grows monotonically). At that point, we then have $\mathrm{Arg}[t'(u_\star)] = 0$ (see figure 6.6 for a graphical representation) and

$$\Sigma_{\text{temporal}}(t(u_\star)) = \pi\,,\ \text{so that}\ \Sigma(t(u_\star)) \geq \pi\,. \tag{6.4.4}$$

Therefore, the allowability bound is violated (or again, at best saturated[6]) at that point.

The way to regularize all these metrics, described in [150] (see also [161]), is to add a factor $(1 \mp i\epsilon)$, $0 < \epsilon \ll 1$, to the time-time component of the metric. This is not a smooth deformation, because the two choices of sign $(\mp)$ are not smoothly related. The regularization implies a change in the value of the action, so it is a true deformation of the metric and not just a rewriting.

Before ending this section, we comment on the meaning of metrics that saturate the allowability bound (i.e., such that $\Sigma = \pi$ everywhere, as in the case of real Lorentzian metrics described in this section). Saturation is synonym of **conditionally convergent path integrals**, which may or may not be problematic. Reasonable quantum field theories cannot be properly defined on backgrounds violating the allowability bound ($\Sigma > \pi$), since they lead to divergent path integrals, but this is not necessarily true for metrics

[6]Saturation is generally not even realized with a complex time path here since it could only occur if $a^2_{(j)}(t(u_\star))$ had a phase of $2n\pi$, $n \in \{1, 2, \cdots\}$, in every spatial direction j (a phase of 0 is excluded since $t(u_\star)$ itself would have a non-zero phase). However, since the phases of the $a^2_{(j)}$s vary continuously from 0 at the start of the path, one would necessarily cross another location where at least one of the phases is π, and hence where the allowability bound is violated.

saturating the bound. Conditionally convergent integrals are more subtle to treat than traditional Gaußian-like integrals, and as path integrals they dependent on the order of integration. Therefore, absolute convergence is favorable, and that is why the allowability bound ($\mathrm{Re}(\mathcal{I}) > 0$ or $\Sigma < \pi$) does not allow for equality. But let us note that Picard-Lefschetz theory, described in detail in section 2.2, is exactly the right tool to define conditionally convergent integrals, re-writing them as sums of absolutely convergent integrals. In this sense, Picard-Lefschetz theory enables to define conditionally convergent integral without ambiguities. Applying this procedure to gravity hence seems the obvious thing to do [51]. However, as we will observe in all the specific examples we study next [150, 155], it turns out that the integration contours selected by the Picard-Lefschetz method, run into regions that do not satisfy the allowability bound: in all cases we have studied, **the steepest descent integration contours provided by Picard-Lefschetz theory are cut off by the allowability regions**. This is one of the most important results of this chapter [4], and we will elaborate on it in more details in the discussion section 6.8.

6.5 Classical transitions

In this section, we study transition amplitudes between two classical solutions of general relativity in a closed ($k = 1$) four-dimensional spacetime, in the presence of a positive cosmological constant Λ and without matter fields. The classical solution in this case is given by the de Sitter cosmology, and is a good approximation of the inflationary period of the standard model of cosmology we described in 1.2 (assuming the inflaton is constant).

More generically, we can use the ADM decomposition of the metric [27]:

$$\mathrm{d}s^2 = -N^2\mathrm{d}t^2 + \beta_i \mathrm{d}t\mathrm{d}x_i + h_{ij}\mathrm{d}x^i\mathrm{d}x^j \,, \tag{6.5.1}$$

where N is the lapse, $\boldsymbol{\beta}$ is the shift, and $\boldsymbol{h}$ is the metric on the spatial hypersurfaces. Then the transition amplitude between two three-dimensional hypersurfaces $\Sigma_0, \Sigma_1 \subset \mathcal{M}$ is defined as the gravitational path integral:

$$\Psi[\Sigma_0 \to \Sigma_1] = \int_{\Sigma_0}^{\Sigma_1} \mathcal{D}N\, \mathcal{D}\boldsymbol{\beta}\, \mathcal{D}\boldsymbol{h}\, \exp\left(\frac{i}{\hbar} \int_{\mathcal{M}} \mathrm{d}^4x \sqrt{-g} \left(\frac{R}{2} - \Lambda \right) + \sum_{n=0,1} b_n \int_{\Sigma_n} \mathrm{d}^3x \sqrt{\det(\boldsymbol{h})}\, K \right), \tag{6.5.2}$$

where R is the four-dimensional Ricci scalar and K is the trace of the three-dimensional extrinsic curvature tensor on the hypersurfaces $\Sigma_{0,1}$ bounding the four-manifold $\mathcal{M}$. The coefficients $b_n \in \{-1, 0, 1\}$ in front of the GHY surface terms determine the type of boundary conditions we impose. For example, when considering the transition amplitude between two large, classical values of the scale factor, we have $b_0 = -1$ and $b_1 = 1$.

In this section we study transition amplitudes between two large, classical de Sitter geometries. We study the allowability bound on the saddle points corresponding to these

transitions (already considered in [77]), but also on the off-shell geometries that we sum over in the gravitational path integral (6.5.2).

Because we are considering the early universe cosmology, as we have established in the introductory chapter 1, we can use a FLRW type of metric to good approximation, and hence restrict to minisuperspace. We thus use the same simplified ansatz as for the no-boundary metric (see 2.2):

$$\mathrm{d}s^2 = -\frac{N^2}{q(t)}\mathrm{d}t^2 + q(t)\mathrm{d}\Omega^2_{(3)}\,, \tag{6.5.3}$$

where $q(t)$ is the squared-scale factor and N is the lapse function. This enables us to perform calculations analytically. We recall that for Dirichlet-Dirichlet boundary conditions $q(0) = q_0$ and $q(1) = q_1$ ($q_0 \leq q_1$), the classical solutions to the Einstein-Hilbert action read (see equation (2.2.13)):

$$\bar{q}(t) = \frac{\Lambda}{3}N^2 t(t-1) + (q_1 - q_0)\,t + q_0\,. \tag{6.5.4}$$

The on-shell (in the scale factor, but not in the lapse) action is then given by

$$S_{\text{on-shell}}(N) = 2\pi^2\left[\frac{\Lambda^2}{36}N^3 + \left(3 - \frac{\Lambda(q_0+q_1)}{2}\right)N - \frac{3(q_1-q_0)^2}{4N}\right]. \tag{6.5.5}$$

The gravitational path integral then reduces to a simple integral over the lapse:

$$\Psi \sim \int_{\mathcal{C}} \mathrm{d}N\, e^{\frac{i}{\hbar}S_{\text{on-shell}}(N)}\,, \tag{6.5.6}$$

along some contour $\mathcal{C}$ in the complex plane. This integral can be performed in the saddle point approximation. Saddle point geometries correspond to the values of the lapse N that minimize the on-shell action (6.5.5):

$$N_{\text{SP}} = \frac{3}{\Lambda}\left(\pm\sqrt{\frac{\Lambda q_1}{3} - 1} \pm \sqrt{\frac{\Lambda q_0}{3} - 1}\right). \tag{6.5.7}$$

These four saddle point lapse values are real valued as long as the scale factor is never smaller than the waist of the de Sitter hyperboloid (i.e., $3/\Lambda \leq q_0 \leq q_1$). The geometries they described are Lorentzian homogeneous metrics, as those discussed in section 6.4. They hence reside on the boundary of the domain of allowable complex metrics. The two inner saddle point geometries (which are time reversals of one another) describe expanding de Sitter solutions, where the scale factor monotonically increases from q_0 to q_1. The outer saddle point geometries (again, time reversals of one another) describe classical de Sitter bouncing solutions, where the scale factor first decreases from q_0 to the waist of the de Sitter hyperboloid ($q = 3/\Lambda$) and from there increases again up to q_1 (see figure 6.7). In the rest of this section, we study the structure of the lapse integral (6.5.6). We analyze the

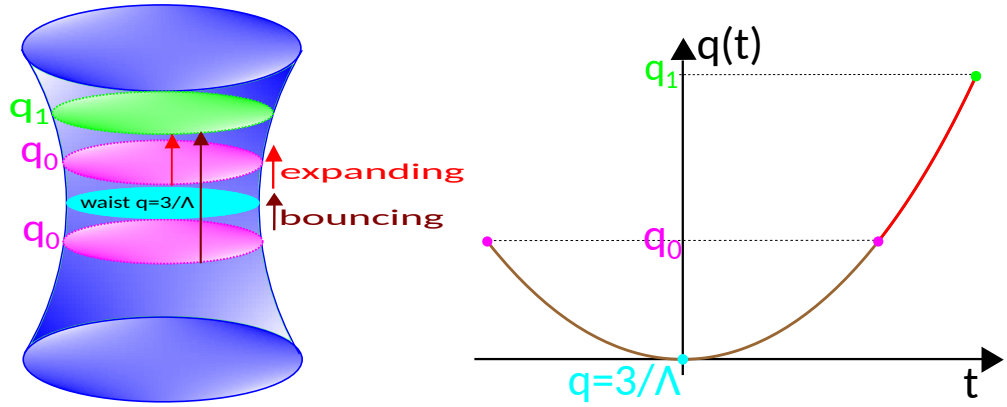

Figure 6.7: Classical de Sitter solutions between q_0 and q_1. Expanding solution in red, and bouncing solution in brown.

(non-)allowability of all the metrics entering this integral. These metrics all satisfy the scale-factor equation of motion, but they can be off-shell regarding the lapse constraint.

6.5.1 Analytical arguments for the (non-)allowability of off-shell metrics entering the gravitational path integral

First, we consider large absolute values of the lapse, $|N| \gg 1$. Writing $N = |N|e^{i\mathrm{Arg}(N)}$, the classical solution is in that case well approximated by

$$\bar{q}(t) \overset{|N|\to\infty}{\simeq} \frac{\Lambda}{3}|N|^2 e^{2i\mathrm{Arg}(N)} t(t-1)\,, \text{ for } t \neq 0, 1\,. \tag{6.5.8}$$

Any simply connected complex time path $t(u)$ must necessarily cross the line $\mathrm{Re}[t(u^*)] = 1/2$ if it evolves continuously from $t = 0$ to $t = 1$. On this location we write $t(u^*) = 1/2 + i\rho$ for some $\rho \in \mathbb{R}$. Then $t(u^*)(t(u^*)-1) = -1/4 - \rho^2$ is a negative real number. The spatial part of the allowability function then reads at $t(u^*) = 1/2 + i\rho$:

$$\begin{aligned}\Sigma_{\text{spatial}}\left[t(u^*) = 1/2 + i\rho\right] &= 3|\mathrm{Arg}\left[\bar{q}(1/2 + i\rho)\right]| \\ &\overset{|N|\to\infty}{\simeq} 3\left|\mathrm{Arg}\left[\left(-\frac{1}{4} - \rho^2\right)\frac{\Lambda}{3}|N|^2 e^{2i\mathrm{Arg}(N)}\right]\right|, \\ &= 3|\pm\pi + 2\mathrm{Arg}(N)|\,.\end{aligned} \tag{6.5.9}$$

The spatial allowability bound therefore implies that when $|N| \to \infty$, if

$$|\pm\pi + 2\mathrm{Arg}(N)| \geq \frac{\pi}{3}\,, \tag{6.5.10}$$

then the full allowability bound is violated and the metric is not allowable. We conclude that, asymptotically, off-shell metrics in the lapse integral (6.5.6) are not allowable when:

$$\mathrm{Arg}(N) \in \,]-\pi, -2\pi/3] \cup [-\pi/3, \pi/3] \cup [2\pi/3, \pi]\,, \tag{6.5.11}$$

leaving only two wedges centered on the Euclidean axis. This regions of non-allowability are depicted in figure 6.8. This implies that metrics with a large real part of the lapse are not allowable.

This is an important result of our work [4]. It can be understood from the fact that when the real part of the lapse gets very large, the squared-scale factor starts diving into negative values for some interval of time (because the first, negative term in (6.5.4) will dominate for values of t not near $0, 1$), so that the signature of the metric changes.

How large must $|N|$ be for the approximation (6.5.8) to hold? To estimate this, we use (6.5.4) to compute:

$$\begin{aligned}\bar{q}(t(u^*)) = \bar{q}(1/2 + i\rho) &= \frac{\Lambda|N|^2 e^{2i\mathrm{Arg}(N)}}{3}\left(-\frac{1}{4} - \rho^2\right) + \frac{q_1+q_0}{2} + i\rho(q_1 - q_0)\,, \\ &= -\frac{\Lambda|N|^2\,(1/4+\rho^2)}{3}e^{2i\mathrm{Arg}(N)} + \frac{(q_1+q_0)}{2}\sqrt{1+4\rho^2\left(\frac{q_1-q_0}{q_1+q_0}\right)^2}\,e^{i\varphi}\,, \end{aligned} \tag{6.5.12}$$

where $\varphi \equiv \mathrm{Arg}[(q_1+q_0)/2 + i\rho(q_1-q_0)]$. The large $|N|$ approximation is valid when the norm of the first complex number in (6.5.12) is much larger than the norm of the second one, i.e., when

$$|N|^2 \gg \frac{6(q_1+q_0)}{\Lambda\,(1+4\rho^2)}\sqrt{1+4\rho^2\left(\frac{q_1-q_0}{q_1+q_0}\right)^2}\,. \tag{6.5.13}$$

The combination of factors, $\sqrt{1+4\rho^2(q_1-q_0)^2/(q_1+q_0)^2}/(1+4\rho^2)$, is always contained between 0 and 1. The strongest constraint on $|N|$ then arises when it is equal to 1. Therefore, the approximation is always valid when

$$|N|^2 \gg \frac{6}{\Lambda}(q_1+q_0)\,. \tag{6.5.14}$$

For the numerical example presented in figure 6.11, we took $\Lambda = 3$, $q_0 = 2$ and $q_1 = 10$. Then the approximation is valid when $|N|^2 \gg 24$ (so if, e.g., $|N| \gtrsim 15.5$, then (6.5.14) is respected by at least one order of magnitude).

Second, we study the metrics lying on the Euclidean axis: $N = iN_{\mathrm{E}}$, $N_{\mathrm{E}} \in \mathbb{R}$. In this case, the classical solution for the scale factor squared is:

$$\bar{q}(t) = -\frac{\Lambda}{3}N_{\mathrm{E}}^2 t(t-1) + (q_1 - q_0)\,t + q_0\,. \tag{6.5.15}$$

This solution is real (and positive) when time is real, i.e., when the time path goes straight from 0 to 1 on the real-time axis: $\mathrm{Arg}[\bar{q}(t)] = 0$. Moreover, the time-time component of the metric for this solution is positive definite: $\mathrm{Arg}[-N^2/\bar{q}(t)] = \mathrm{Arg}[+N_{\mathrm{E}}^2/\bar{q}(t)] = 0$. This implies that the allowability function, $\Sigma(t)$, is constantly null on the real-time axis when the lapse is purely imaginary. The allowability bound is therefore trivially satisfied on the whole Euclidean axis. This result is also depicted on figure 6.8.

Note that for large values of the Euclidean lapse N_{E}, the classical solution behaves

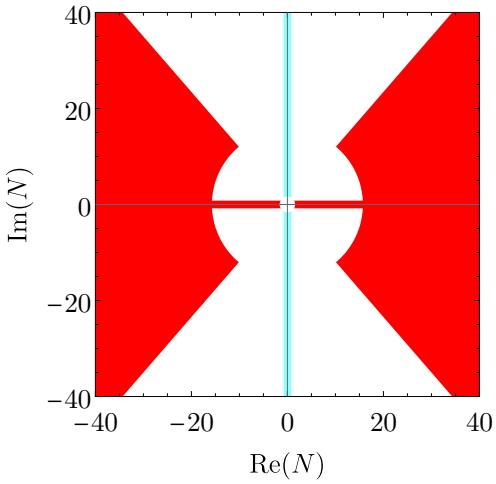

Figure 6.8: Analytical results for the classical transition from $q_0 = 2$ to $q_1 = 10$. The red regions represent the asymptotic region of non-allowability (6.5.11) (starting at $|N| = 15.5$) and the Lorentzian axis (shown to saturate the allowability bound in section 6.4). The Euclidean axis, highlighted in cyan, is allowable. The saddle point lapse values (6.5.7) are not shown, but they are located at $N_{\rm SP} = \pm 2, \pm 4$, so the region of particular interest for the path integral ($N \lesssim 6$) remains unconstrained at this point.

like $\bar{q}(t) \approx -\frac{\Lambda}{3} N_{\rm E}^2 t(t-1)$, so that the metric becomes

$$\begin{aligned} \mathrm{d}s^2 = \frac{N_{\rm E}^2}{\bar{q}(t)}\mathrm{d}t^2 + \bar{q}(t)\mathrm{d}\Omega_{(3)}^2 &\approx \frac{3}{\Lambda t(1-t)}\mathrm{d}t^2 + \frac{\Lambda}{3}N_{\rm E}^2 t(1-t)\mathrm{d}\Omega_{(3)}^2\,, \\ &= \frac{3}{\Lambda}\mathrm{d}T^2 + \frac{\Lambda}{12}N_{\rm E}^2\cos^2(T)\mathrm{d}\Omega_{(3)}^2\,. \end{aligned} \tag{6.5.16}$$

We defined here a new time coordinate T according to $2t - 1 \equiv \sin T$, with $-\pi/2 \leq T \leq \pi/2$. At very large lapse value $N_{\rm E}$, the metric approximately corresponds to a full (huge) four-sphere. It describes a Euclidean geometry starting out near zero (at q_0), expanding to a huge size and then shrinking again to almost zero (in fact to q_1).

6.5.2 Numerical assessment of the (non-)allowability of off-shell metrics

To assess the allowability of (off-shell) metrics everywhere else in the complex lapse plane, in particular around the saddle points and along the steepest descent contours, we need to apply the numerical methods described in section 6.3.

We allow deformations of the time path from $t = 0$ to $t = 1$ into any simply connected smooth path in the complexified time plane that leaves the end points fixed. We assess whether at least one path exists, such that the resulting metric is allowable. In particular, we here describe in details, and with a specific example, how the *minimum and maximum curves* method introduced in section 6.3.3 functions. This method relies on the fact that, at each point in the complex t plane, there is a range of directions for which the allowability bound is satisfied. We start from $t = 0$ and we follow both the path defined by choosing at each point the maximal angle allowed (the *maximal curve*), and the path

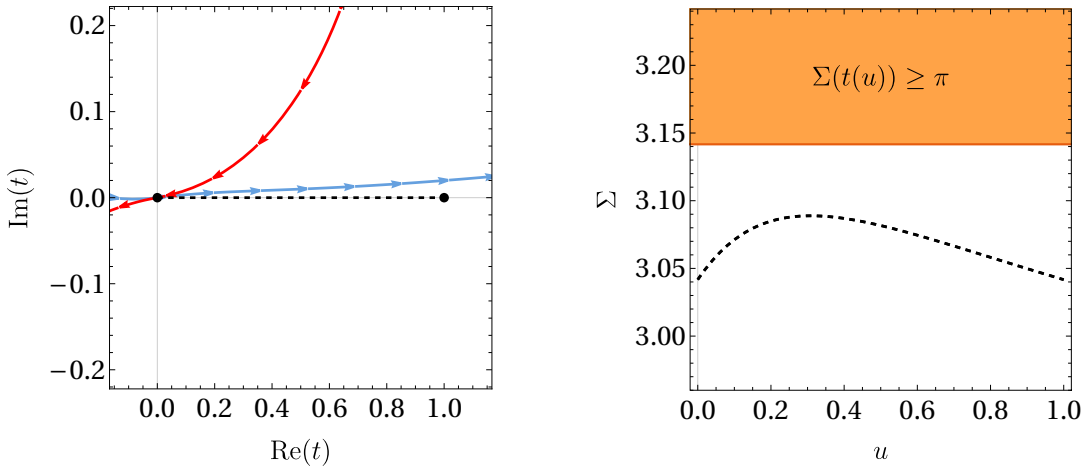

Figure 6.9: *Left*: Complexified time plane for a solution with classical boundary conditions slightly off-shell of the expanding saddle point: $N = 2 - i/10$. The numerical values are: $q_0 = 2$, $q_1 = 10$, and $\Lambda = 3$. Black dots in $t = 0$ and $t = 1$ indicate the end points of the time path specifying the metric. The blue directed line is the *maximal curve*, and the red directed line is the *minimal curve*. An allowable path, e.g., the dashed black line, must reside in between these two lines under forward time evolution ($\mathrm{Re}(t)$ must grow monotonically from 0 to 1). *Right*: Plot of the full $\Sigma(t(u))$ along the dashed line, and of the violated region where $\Sigma > \pi$ (in orange). This verifies that the dashed path $t(u)$ is allowable.

defined by choosing at each point the minimal angle allowed (the *minimal curve*). Any allowable paths must reside between these two lines. In figure 6.9, the minimal curve is represented in red, and the maximal curve in blue. So the allowed region contains the point $t = 1$, which means it can be reached via an allowable path, such as the dashed line drawn on this figure. This example corresponds to a **lapse value slightly off-shell of the expanding saddle point**. In the right panel we plot $\Sigma(t(u))$ and explicitly verify that the geometry defined by the dashed time path is indeed allowable.

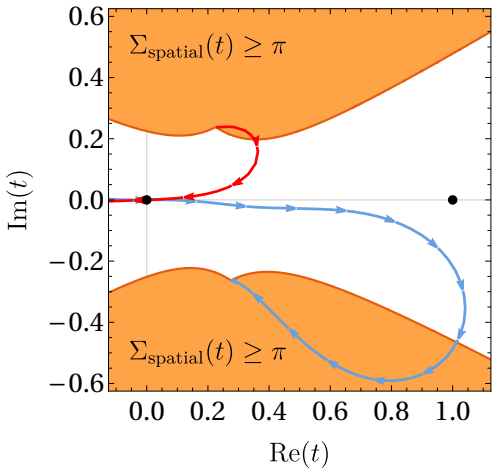

Figure 6.10: Complexified time plane of a solution with classical boundary condition, this time slightly off-shell of the bouncing saddle point: $N = 4 - i/10$. We have again $q_0 = 2$, $q_1 = 10$ and $\Lambda = 3$. The orange shaded regions represent regions where the spatial allowability bound (6.3.6) is violated. An allowable time path should link the $t = 0$ and $t = 1$ dots while remaining below the blue curve and avoiding the orange regions. This is not possible in this example, hence the metric is not allowable.

Now turning to a **lapse value slightly off-shell of the bouncing saddle point**, we find a different result, as illustrated in figure 6.10. There, it is impossible to draw a simply connected time path from $t = 0$ to $t = 1$ that remains below the blue curve and above the red one, and that also avoids the regions where the no-ridge condition is violated (see subsection 6.3.2). This is a first hint that bouncing saddle points will not always be approachable along minisuperspace allowable metrics.

6.5.3 Summary of results

Using all the tools explained in section 6.3, we determine the allowability of every point in the complexified lapse plane and display our results in figure 6.11. Our findings are summarized as follow [4]:

1. inner (expanding) saddle points are always reachable by allowable complex metrics, i.e., they are surrounded by the domain of allowability;

2. outer (bouncing) saddle points are not reachable through the minisuperspace metrics considered in our ansatz, for large enough final scale factor ($q_1 \gtrsim 2$). They are however reachable through a continuous integration contour in the space of allowable off-shell metrics but that do not follow the steepest-descent contour, i.e., departing from the minisuperspace ansatz 6.5.3.

3. small bouncing classical transition solution (with $q_1 \leq 2$) are reachable via allowable complex metrics in minisuperspace.

The result 2 points out the over-restrictive power of the minisuperspace setting. Outer bouncing saddle point geometries can in fact be reached through allowable metrics, but only when departing from the minisuperspace steepest descent contours. The following family of metrics:

$$\mathrm{d}s^2 = -(1 - i\varepsilon)^2 \frac{N^2}{\bar{q}(t)} \mathrm{d}t^2 + \bar{q}(t) \mathrm{d}\Omega^2_{(3)} \,, \tag{6.5.17}$$

defined for $\varepsilon \in]0, 1[$ and evaluated on the outer saddle point solution $(N_{\mathrm{SP}}, \bar{q}(t))$, forms a continuous path in the space of allowable[7] off-shell metrics, whose limit when $\varepsilon \to 0^+$ is the bouncing saddle point metric. The weighting of those metrics depends on ε, and they can be linked to an integration contour that asymptotically (i.e., at large lapse values) reaches the Euclidean axis.

The result 3 leads to an apparent paradox with respect to the previous result 2. Imagine a classical transition solution with only two saddle points, time reversals of each other. The initial and final scale factor values are chosen as: $q_0 = 1$ and $q_1 \gg 1$. By

[7] We quickly show that this family of solution is always allowable: the lapse $N = N_{\mathrm{SP}}$ is real, so along the real time path, the classical solution for $\bar{q}(t)$ (6.5.4) is also real, and we find:

$$\Sigma(t) = \left|\mathrm{Arg}[-(1 - i\varepsilon)^2]\right| = \left|\pi - \arctan\left(\frac{2\varepsilon}{1 - \varepsilon^2}\right)\right| < \pi \,, \ \forall\, \varepsilon \in]0, 1[\,. \tag{6.5.18}$$

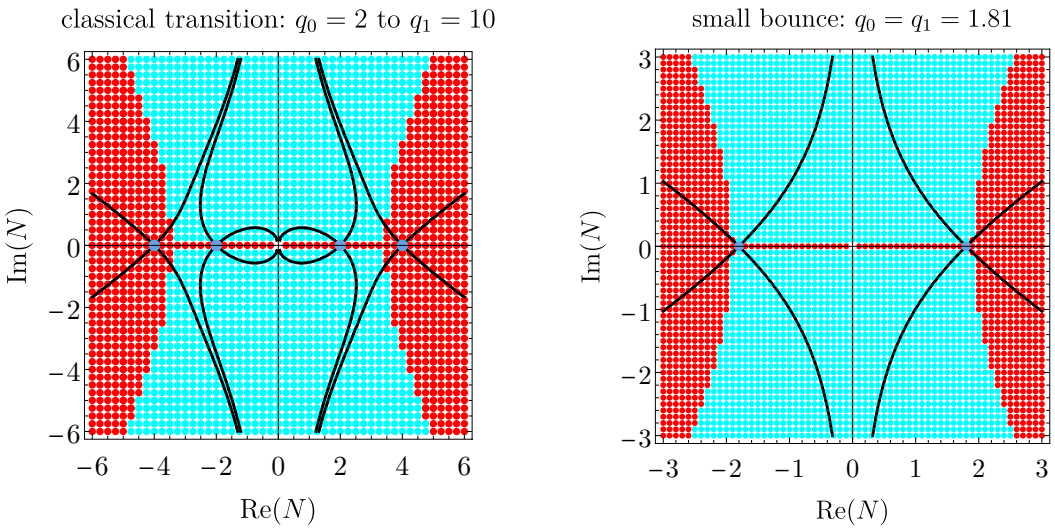

Figure 6.11: Complex lapse plane for two different classical transition solutions which both have $\Lambda = 3$. Blue dots indicate the lapse value at the saddle point geometries and black lines show the steepest descent and ascent contours found using Picard-Lefschetz theory. (Red) Cyan dots denote lapse values corresponding to a (non-)allowable metric. *Left:* Classical transition from a small scale factor, $q_0 = 2$, to a larger scale factor, $q_1 = 10$. The inner saddle point geometries $N_{\rm SP} = \pm 2$ (expanding solutions) are reachable via allowable complex metrics (see 1). The outer saddle point geometries $N_{\rm SP} = \pm 4$ (classical bouncing solutions) are not reachable via allowable metrics within this restricted minisuperspace (see 2). *Right:* Classical transition with $q_0 = q_1 = 1.81$. The saddle point geometries (classical bouncing solutions) are reachable by allowable metrics along the steepest descent contours (see 3).

gluing the contracting saddle with the expanding one (both reachable within the space of allowable metrics in minisuperspace), we would obtain exactly the same classical solution as a large bouncing saddle with $q_0 = q_1 \gg 1$ (which is apparently not reachable via the same space of allowable metrics in minisuperspace). This apparent paradox is resolved by realizing that:

1. the transitions amplitude of the two scenarios differ: in the first case, a measurement is made when the universe is small (at $q_0 = 1$), providing a prior knowledge that conditions the amplitude. This prior knowledge does not exist in the second case of a large bounce.

2. assuming we approach the two saddle points through off-shell metrics with a non-zero imaginary part of the lapse, then the two classical solutions are not equal anymore ($q(t)$ possesses an imaginary part and the two allowability functions $\Sigma(t)$ differ).

Our results on the allowability criterion for de Sitter classical transitions clearly highlight the difficulty in properly defining contours of integration for the gravitational path integral. Convergence of the pure gravitational part of the path integral designates the steepest-descent paths as the right contours of integration. Those paths are however sometimes conflicting with the convergence of the matter fields path integral, given by

the allowability criterion. When this happens, it is necessary to elucidate whether some other integration contours, departing from the minisuperspace steepest-descent path (such as (6.5.17)), exist and can render the saddle point geometries reachable. We come back to this crucial point later on in section 6.7, when analyzing the allowability criterion for no-boundary solutions.

6.6 Quantum bouncing cosmologies

So far we have applied the allowability criterion to classical solutions of the Einstein equations, namely to Lorentzian geometries and to classical de Sitter geometries. The main interest of the path integral approach to cosmology, is that it enables us to also study quantum solutions to the Einstein equations, such as the no-boundary solution which will be the focus of next section. Here we concentrate on another type of quantum solutions: quantum bounces.

The dynamical evolution of particles given by quantum mechanic is richer than that of classical mechanic. Classically forbidden transitions, such as the tunneling across a potential barrier, are possible in quantum mechanics (though unlikely). They can also be suitably described by an evolution in complex time [162, 163, 164]. In the case of a barrier of potential $V(\phi)$, the particle wave $e^{-it\,\phi}$ is partly reflected at the barrier as in the classical case, but also acquires an exponentially decreasing part transmitted through the barrier in complex time: $\tau = it \;\rightarrow e^{-it\,\phi} = e^{-\tau\,\phi}$ (see figure 6.12). In the gravitational context,

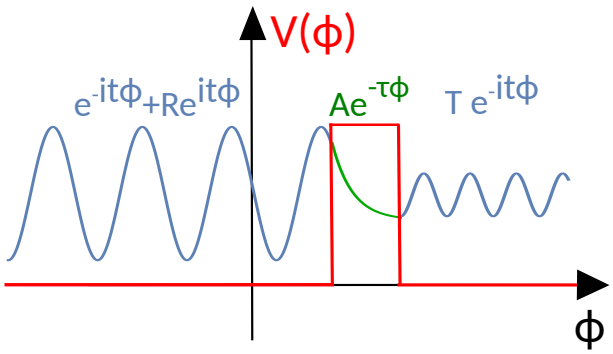

Figure 6.12: Quantum tunneling of a particle through a potential barrier $V(\phi)$, drawn in red. The particle is described by an incoming wave in blue, partially reflected at the left wall of the barrier potential, and partially tunneling through the barrier (green decreasing exponential). It is then transmitted with a damped amplitude on the right of the potential barrier.

one can similarly describe certain classically-forbidden, quantum solutions using complex metrics. This is the case e.g., for Coleman-de Luccia instantons. These are solutions to the Einstein-Hilbert equations, which describe the nucleation of a bubble of true vacuum, inside a region of false vacuum in the universe [165]. The complex metrics corresponding to Coleman-de Luccia instantons are purely Euclidean, and therefore they are allowed by the criterion. Yet another kind of quantum solution is the tunneling of (a part of) the universe from a contracting to an expanding phase. This tunneling bypasses the big bang

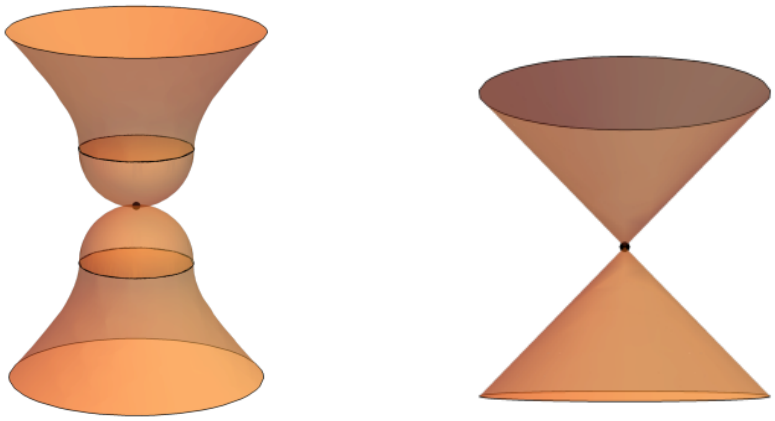

Figure 6.13: Quantum bouncing solutions studied in this section. *Left:* Back-to-back gluing of two no-boundary solutions, prototypical of the quantum bounces described in [166]. *Right:* Mirrored conical four-geometries representing the solution studied in [79, 167].

singularity by getting around it in the complexified metric space (see [166, 79, 167] for specific examples that use genuine complex metrics). Do such quantum solutions satisfy the allowability criterion?

Setting aside the complex nature of the scalar field (generalization of the allowability criterion to include complex scalar fields, notably from adopting a higher-dimensional point of view, are developed in [77]), the quantum bounces described in [166] can be modeled by a back-to-back gluing of no-boundary geometries, pictured on the left of figure 6.13. On the other hand, the quantum bouncing models presented in [79, 167], named two-sheeted or CPT symmetric universes, can be schematically represented by two conical four-universes mirrored at their tip, as illustrated on the right of figure 6.13. Here we study these two models against the allowability criterion.

Assuming a fixed cosmological constant Λ, which is equivalent to a real constant scalar field sitting at the extremum of its potential, the no-boundary solution in D dimensions is given by (2.2.5b):

$$a(t) = \frac{1}{H}\cosh(Ht)\,, \quad \text{with } H = \sqrt{\frac{2\Lambda}{(D-1)(D-2)}} \tag{6.6.1}$$

For real time $t \in (-\infty, +\infty)$, this hyperboloid describes a classical bounce from a contracting to an expanding universe, evading the big bang singularity without requiring a quantum transition. However, such a bounce requires extremely fine-tuned initial conditions and the presence of the smallest anisotropies would make this classical solution deviates in the contracting phase ($t < 0$). The anisotropies grow faster than the homogeneous curvature term and hence lead to a big crunch instead of the bounce (see [166]). This crunch can be circumvented by linking the contracting to the expanding hyperboloid via a path in the complexified time plane. The prototype shown in figure 6.13 correspond to two simple Wick rotations $\tau = it - \dfrac{\pi}{2H}$ from the contracting phase $t < 0$, and then

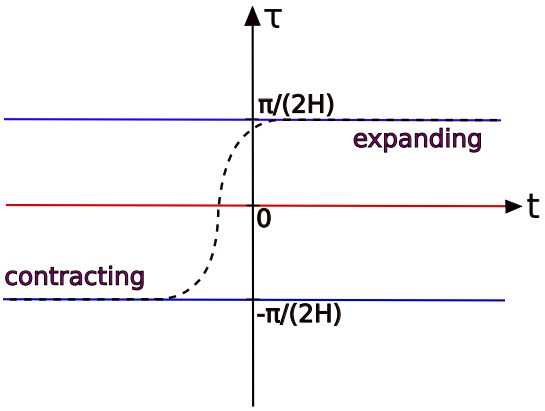

Figure 6.14: Lines of real (in blue) and pure imaginary (in orange) scale factor values in the complexified time plane, for $a(t) = \cosh(t)$. In this figure, real Lorentzian time is horizontal and Euclidean time vertical. One can model a quantum bounce (dashed black line) by linking a contracting universe to an expanding one at a different, parallel line of real field values, but such a path necessarily passes through a line on which the scale factor is imaginary (orange line).

$t = -i\left(\tau - \frac{\pi}{2H}\right)$ into the expanding phase $t > 0$. This prototype is not realistic because it crosses the no-boundary point $(0, 0)$ where the manifold degenerates to a point. This can be easily regularized by deforming it slightly away from $\mathrm{Re}(t) = 0$. A generic path in the complexified plane will be any continuous path linking the contracting universe (negative part of a horizontal line where $a(t)$ takes real values, e.g. $\tau = -\frac{\pi}{2H}$) to the expanding universe (positive part of another horizontal line where $a(t)$ takes real values, e.g. $\tau = \frac{\pi}{2H}$). This continuous path therefore necessarily crosses the horizontal line $\tau = 0$ in some point $\tilde{\tau} = ix$ with $x \in \mathbb{R}_0$. There the scale factor is $a(\tilde{\tau}) = -\frac{1}{H}\sin(H\tilde{\tau}) = \frac{i}{H}\sinh(Hx)$ so that $a^2(\tilde{\tau}) < 0$, and hence the allowability function gives:

$$\Sigma(\tilde{\tau}) > \Sigma_{\text{partial}}(\tilde{\tau}) \geq (D-1)\pi\,, \tag{6.6.2}$$

for a D–dimensional FLRW spacetime. Therefore, any quantum bounce defined in this way violates the allowability criterion.

From this argument, we can also prove that the many-sphere no-boundary solution, described in the introduction of this chapter 6.1 as a motivation for a complex metric criterion, violates the allowability criterion. At the anchor point of each additional sphere, the regularized time path that passes around the zeroes of the scale factor (i.e., following the dotted lines in figure 6.1) crosses a line where the scale factor is purely imaginary and where equation (6.6.2) is valid and thus the allowability bound is violated.

With hindsight, it is reassuring that those quantum bounces built out of approximate de Sitter solutions are excluded from the path integral, as they are always unstable, either at the perturbative, or at the background level. Indeed, no-boundary geometries, that forms the two halves of the prototype quantum bouncing solution depicted in figure 6.13, are known (see e.g., [168]) to come in pairs related by complex conjugation (i.e., corresponding to whether the contracting solution is linked to an expanding solution at

either positive or negative imaginary time values). One of these solutions exhibits a negative weighting, and thus occurs with exponentially suppressed probability (of order $e^{-|\mathcal{I}(S^4)|/\hbar}$, where $\mathcal{I}(S^4)$ is the action of the four-sphere with radius $1/H$). But in that case, fluctuations around the solution get a positive weighting proportional to the size of the fluctuations squared: fluctuations thus follow an inverse Gaußian probability distribution, so this solution is perturbatively unstable. The complex conjugate solution has stable perturbations, that obeys a Gaußian probability distribution, but it possesses a positive weighting (of order $e^{+|\mathcal{I}(S^4)|/\hbar}$). This means that such a solution should occur with higher probability than classical evolution, contradicting our actual experience: this solution is thus unstable at the background level. The exclusion of these unstable quantum bounces brings support to the validity of the allowability criterion.

We turn to the CPT symmetric universe described in [79, 167]. In this model, the universe doesn't undergo any inflationary phase, and instead it stays dominated by radiation all the way to the big bang. For a flat spatial section and in conformal time η, close to the big bang the metric approaches the form:

$$\mathrm{d}s^2 = \eta^2(-\mathrm{d}\eta^2 + \mathrm{d}x^2 + \mathrm{d}y^2 + \mathrm{d}z^2). \tag{6.6.3}$$

For $\eta \in \mathbb{R}$, this geometry describes two cones, one for $\eta > 0$ and one for $\eta < 0$, joined at their tips where η vanishes (see figure 6.13). The idea of [79] is to pass around the big bang at $\eta = 0$ by taking a continuous path in the complexified time plane.

If we take this path to be a simple semi-circle at a small radius, i.e., $\eta = re^{i\theta}$ with θ spanning $[0, \pi]$ and $r > 0$ kept constant, then at $\theta = \pi/2$ we have $\eta = ir$, so that $\eta^2 = -r$. From the spatial part of (6.6.3), we thus find that $\Sigma(\eta) \geq (D-1)\pi$, so this specific path violates the allowability bound $\forall D > 2$.

More generally, the locus of negative values of η^2 emanates radially from $\eta = 0$, so it is necessarily crossed by any continuous path passing from $\eta > 0$ to $\eta < 0$ while avoiding the singularity at $\eta = 0$. From this simple argument, it seems that the allowability criterion excludes the CPT symmetric universe altogether. One important caveat to this result is that in this model, the conformal symmetry might become manifest in the approach to the big bang [169, 170]. This would modify some of the assumptions that go into the derivation of the allowability bound, as the matter contributions would also have to obey the symmetry in question (i.e., we would deal only with CFT and not QFT). The possible matter types that must have convergent actions are then restricted, enlarging the space of allowed complex metrics. In particular, for exact conformal symmetry, the scale factor of the universe is not restricted at all. The precise implications of different types of symmetries and matter fields on the allowability criterion is an interesting open avenue to be explored in the future.

In this section we found that two specific, homogeneous quantum bouncing models relying on complex metrics, are ruled out by the allowability criterion. This does not

imply that no quantum bouncing model can satisfies the allowability criterion, but it suggests that generically, the criterion strongly constrains these models. In the future it would be interesting to study other quantum bounce models, to see whether we can find one which satisfies the allowability criterion, or whether we can find an argument to rule them all out.

6.7 No boundary solutions

The overarching aim of this thesis is to deepen our understanding of the gravitational path integral. In this perspective, we have already seen that the no-boundary proposal plays a key role as one of the only models where an analytical treatment of the four-dimensional gravitational path integral is feasible and has been carried out (though the end result is still subject to interpretation, in particular it is not clear what is and if there is a meaning to probabilities for a whole universe). So far, we have reviewed the state-of-the art concerning this proposal 2.2, exposing the two contrasted constructions of the no-boundary solution, based respectively on the sum over compact metrics and on the sum over regular metrics. We have then explored several features of the no-boundary solution in chapters 3 and 4. Finally, we have studied its relation to the finite amplitude criterion in chapter 5, where we found it was one of the few models of the early universe compatible with this criterion.

The no-boundary solution fully relies on complex metrics, so it is a natural playground to test the complex metric criterion. Additionally, we will see that the integration contours defining the path integral get modified when restricting to allowable complex metrics. We will review the two constructions of the no-boundary solution from the point of view of the allowability of metrics. For the momentum space, or sum over regular metrics definition, we prove that on-shell no-boundary geometries are allowable in any spacetime dimension D. Specifically, the on-shell solutions always reside on the boundary of the allowability domain and we can find fully allowable and appropriate integration contours for the path integral. In contrast, for the field space, or sum over compact metrics definition, we find that the on-shell no boundary solutions in four dimension are allowable, but in this case they reside in the middle of the allowability domain. Furthermore, the restrictions imposed by the allowability criterion could enable the definition of the path integral in this case as well, while avoiding the problems related to perturbative instabilities developed earlier 2.2.

6.7.1 Sum over regular metrics

We consider the minisuperspace ansatz in arbitrary D spacetime dimensions:

$$\mathrm{d}s^2 = -N^2\mathrm{d}t^2 + a(t)^2\mathrm{d}\Omega^2_{(D-1)}\,. \tag{6.7.1}$$

The spatial sections of this metric are $(D-1)$-spheres. The time coordinate t runs from $t=0$ to $t=1$. The Einstein-Hilbert action with a cosmological constant $\Lambda > 0$ reads:

$$S = \frac{1}{2}\int \mathrm{d}^D x\, \sqrt{-g}\,(R - 2\Lambda)\ . \tag{6.7.2}$$

Condition for regular metrics

We determine the condition for having regular metrics from the regularity of the Friedmann equation (obtained by varying the action (6.7.2) with respect to the lapse N):

$$\frac{\dot{q}^2}{4N^2} + 1 = \frac{2\Lambda}{(D-1)(D-2)} q\,. \tag{6.7.3}$$

This equation is regular at $q=0$ if $\dot{q} = \pm 2Ni$. This means that the expansion rate must be imaginary: the metric must start out Euclidean near $q=0$. The choice of sign for $\dot{q}$ corresponds to the effective choice of Wick rotation. Stability of perturbations demands to choose the positive sign [44]:

$$\dot{q}\big|_{\text{origin}} = 2Ni \qquad \text{(regularity condition)}\,. \tag{6.7.4}$$

This regularity condition is imposed on the initial hypersurface $t=0$. It corresponds to a Neumann boundary condition. On the final hypersurface $t=1$, we can simply impose a Dirichlet boundary condition $q(t=1) = q_1$. The wavefunction given by the no-boundary proposal is then given by the following path integral:

$$\Psi(q_1) = \int \mathcal{D}N \int_{\dot{q}=2Ni}^{q=q_1} \mathcal{D}q\ \exp\!\left(\frac{i}{\hbar} S\right). \tag{6.7.5}$$

This has been studied in great details in four dimensions [52, 53, 76] (see section 2.2 for details). In particular, the integral over q can be performed by writing $q(t) = \bar{q}(t) + \mathcal{Q}(t)$, where $\bar{q}$ denotes a solution to the equation of motion that follows from the variation with respect to q,

$$\ddot{q} = \frac{4\Lambda N^2}{(D-1)(D-2)}\,, \tag{6.7.6}$$

while $\mathcal{Q}(t)$ is an arbitrary fluctuation satisfying the boundary conditions $\dot{\mathcal{Q}}(t=0) = \mathcal{Q}(t=1) = 0$. In four dimensions, the integral over $\mathcal{Q}$ is a Gaußian and simply yields a numerical factor. In general dimensions, this integral cannot be performed so easily, and we leave a full analysis for future work. We can nevertheless make progress by looking at solutions to the equation of motion, which for mixed Neumann-Dirichlet (ND) boundary conditions are given by (in four dimensions see equation (2.2.16)):

$$\bar{q}_{\text{ND}}(t) = \frac{2\Lambda N^2}{(D-1)(D-2)}(t^2-1) + 2Ni(t-1) + q_1\,. \tag{6.7.7}$$

The path integral then sums over a subset of these backgrounds, depending on the integration contour for N. Here we will study the structure of the complexified lapse plane in terms of allowability of metrics.

The location of the no-boundary saddle points $N_\pm$ is determined by:

$$\bar{q}_{\rm ND}(t=0)|_{N_\pm} = 0 \;\Rightarrow\; N_\pm = \frac{(D-1)(D-2)}{2\Lambda}\left(-i \pm \sqrt{\frac{2\Lambda}{(D-1)(D-2)}q_1 - 1}\right). \quad (6.7.8)$$

Allowability of the saddle point geometries

The first step is to verify the allowability of the saddle points (on-shell no-boundary solutions), using the methods described in section 6.3.

We consider deformations of the time path between $t = 0$ and $t = 1$. Similarly to what we did in section 6.5 for classical transitions, we start from $t = 0$ and we calculate the maximal and minimal curves, which correspond to the path defined by choosing at each point the maximal (respectively minimal) angle allowed. Any allowable path must lie in between these two curves. Therefore, the geometry is allowed if the point $t = 1$ lies between the minimal and the maximal curve. It is the case here for the saddle point geometries, as depicted in figure 6.15. The dashed line plotted in this figure is one allowable path, and it can be parameterized as:

$$t(u) = e^{i(\alpha-\pi/2)}\left[u(2-u)\sin(\alpha) + iu^2\cos(\alpha)\right], \quad \alpha \equiv -\mathrm{Arg}(N_+), \quad 0 \le u \le 1. \quad (6.7.9)$$

This calculation is valid in any dimensions if we choose the length unit such that $\Lambda = (D-1)(D-2)/2$. The on-shell no-boundary geometries for the sum over regular metrics satisfies the allowability criterion in any dimensions D.

Saddle points lie on the boundary of the allowability region

Our second step is to prove that saddle points always lie on the boundary of the allowability domain. This was shown in four dimensions in [155], here we generalize the proof to arbitrary spacetime dimensions. We consider the spatial allowability function defined earlier in (6.3.4)

$$\Sigma_{\rm spatial}(t) = (D-1)|\mathrm{Arg}(q(t))|, \quad (6.7.10)$$

and recall that the violation of the spatial allowability bound, $\Sigma_{\rm spatial} < \pi$, is sufficient to prove the violation of the full allowability bound. The strongest constraint occurs at $t = 0$. We study values of the lapse close to the saddle points:

$$N = N_\pm + \zeta, \quad \text{for some } \zeta \in \mathbb{C} \;\text{ with }\; |\zeta| \ll 1. \quad (6.7.11)$$

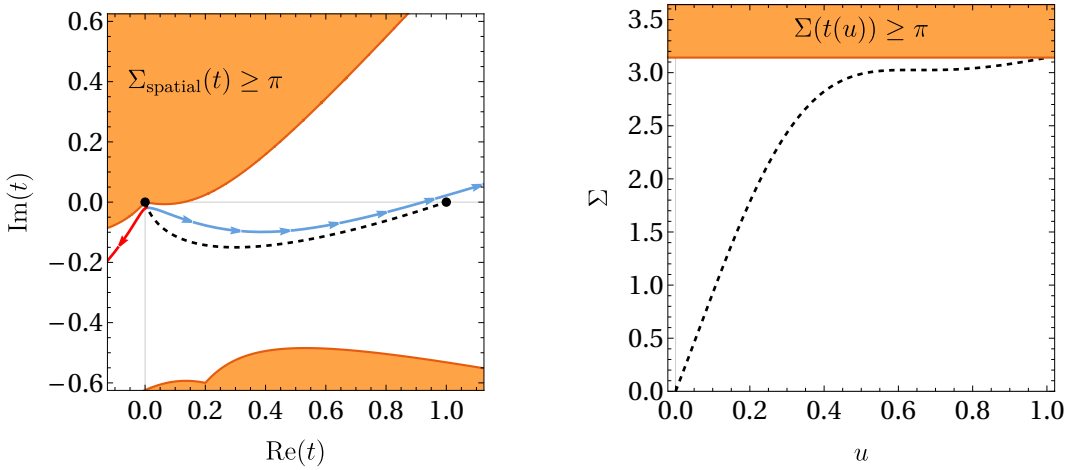

Figure 6.15: *Left*: Complexified t plane for the saddle point solutions with Neumann-Dirichlet boundary conditions. Here $q_1 = 10$ and $\Lambda = (D-1)(D-2)/2$. The shaded orange regions correspond to non-allowed metrics according to the spatial allowability criterion alone, i.e., in these regions $(D-1)|\text{Arg}(q)| \geq \pi$. Black dots reside at $t = 0$ and $t = 1$, indicating the end points of the time path specifying the metric. The maximal curve is plotted in blue, while the minimal curve is plotted in red – an allowable path must reside in between. See 6.3.3 for the derivation of these curves. The point $t = 1$ is reachable by an allowable path, such as the black dashed path. *Right*: Plot of the full allowability bound Σ along the black dashed path. This explicitly proves that this path is allowable, since the value of Σ is always below the limiting value π indicated by the orange regions.

At that lapse value, the no-boundary solution is given at first order in ζ by:

$$\bar{q}_{\text{ND}}(0) = \mp 2\zeta \sqrt{\frac{2\Lambda}{(D-1)(D-2)} q_1 - 1} + O(\zeta^2)\,. \tag{6.7.12}$$

We consider values $q_1 > (D-1)(D-2)/(2\Lambda)$, for which the final size of the universe is larger than the Hubble radius. Then the spatial allowability bound is satisfied only if:

$$(D-1)|\text{Arg}(q)| < \pi \;\Leftrightarrow\; \begin{cases} \dfrac{(D-2)\pi}{D-1} < \text{Arg}(\zeta) < \dfrac{D\pi}{D-1} \text{ around } N_+\,, \\ -\dfrac{\pi}{D-1} < \text{Arg}(\zeta) < \dfrac{\pi}{D-1} \text{ around } N_-\,. \end{cases} \tag{6.7.13}$$

This means that the allowability bound is violated in the surroundings of the saddle points, except within a narrow wedge pointing toward the other saddle point. This is illustrated in figure 6.16 for the cases $D = 7$ and $D = 100$, where the region of spatial non-allowability in $t = 0$ is plotted numerically for the entire complexified lapse plane, i.e. the region where

$$(D-1)|\text{Arg}(q(0))| \geq 0\,. \tag{6.7.14}$$

Therefore, the saddle points reside on the boundary of the allowability region for any spacetime dimensions.

In very large spacetime dimensions, the only region where the spatial allowability bound is not violated consists of a narrow cross-shaped domain that includes the Euclidean

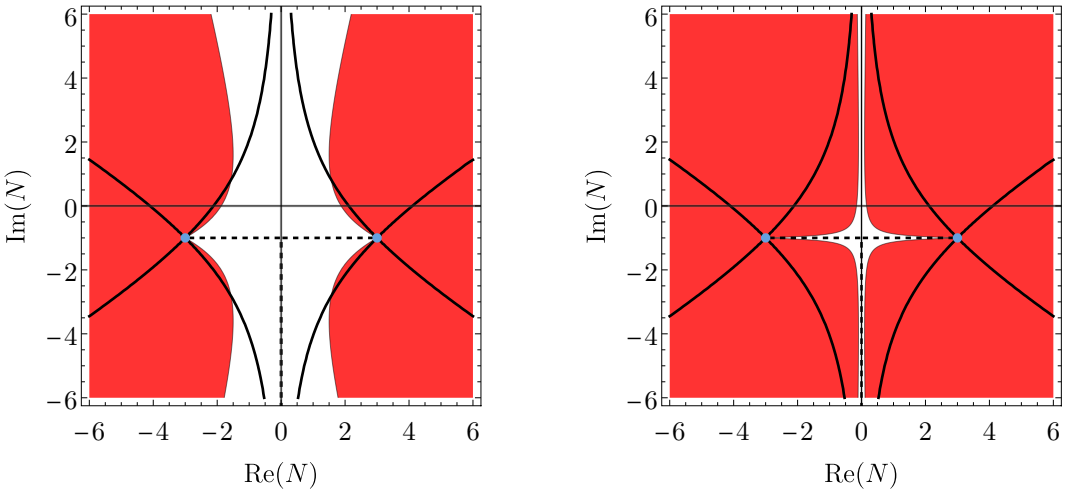

Figure 6.16: Red regions show the domain in the complexified lapse plane where the spatial allowability bound is violated, in 7 dimensions (left panel) and in 100 dimensions (right panel). We have used $\Lambda = (D-1)(D-2)/2$ and $q_1 = 10$. In any dimensions, the saddles (blue dots) remain on the boundary of the allowability domain. The full black curves depict the thimbles, and the dashed ones represent an example of T-shaped allowable integration contour.

axis and the segment joining the two saddle points. Therefore, the steepest descent contours lie completely inside the non-allowability region, so they cannot be used as integration contours for the path integral. However, we will prove that other allowable integration contours can be constructed (dashed lines in figure 6.16) and enable a proper definition of the path integral.

Numerical analysis of the full allowability regions in 4D

The above analysis only considered the spatial allowability bound. We need to resort to numerical techniques if we want to study the full allowability bound. For this we restrict to four dimensions again. Using the optimization techniques and the method of minimal and maximal curves described in section 6.3, we obtain the figure 6.17, where the red (respectively cyan) dots correspond to geometries where the full allowability is violated (respectively satisfied). We observe that the domain of non-allowability is larger than that obtained with the spatial allowability bound only (shaded orange region in this plot). However, the segment joining the two saddle points, as well as the lower Euclidean axis, lie inside the full allowability region. Next we show analytically that this property is true for arbitrary spacetime dimensions.

Full allowability on the T-shaped contour in arbitrary dimensions

We consider the T-shaped contour running horizontally from the saddle point toward the Euclidean axis and then from that point down the Euclidean axis. We prove here that this contour is always allowable and can thus be used as an integration contour for the path integral. Again we set the length unit such that $\Lambda = (D-1)(D-2)/2$.

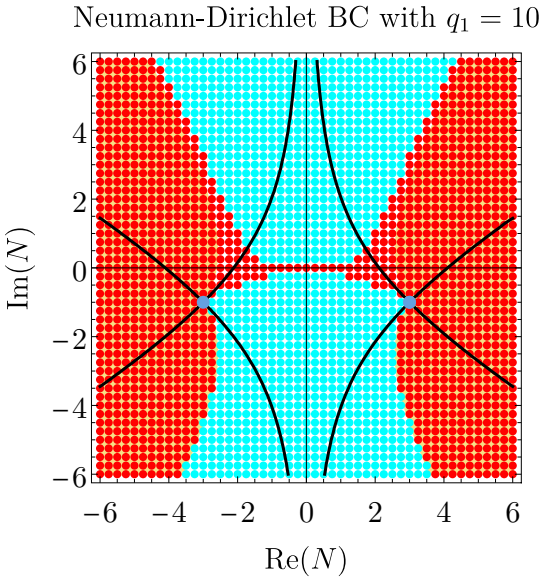

Figure 6.17: Numerical plot of the allowed (cyan) and disallowed (red) metrics in the complexified lapse plane satisfying initial Neumann and final Dirichlet conditions, as appropriate for a momentum space definition of the no-boundary wave function. Here $D = 4$, $\Lambda = 3$, $\dot{q}(t = 0) = +2Ni$, and $q(t = 1) = 10$. The shaded orange regions are the disallowed regions discussed and plotted in figure 6.16, in four dimensions here. The saddle points (in blue) reside at the boundary of the allowable domain. The steepest ascent/descent lines (in black) emanating from the saddle points largely intrude the non-allowable region. Nevertheless, integration contours residing entirely in the lower half plane remain allowed.

First we study metrics on the Euclidean axis: $N = iN_{\rm E}$. The no-boundary geometry reads:

$$\mathrm{d}s^2 = N_{\rm E}^2\,\mathrm{d}t^2 + \bar{q}_{\rm E}(t)\mathrm{d}\Omega^2_{(D-1)}\,, \quad \text{with } \bar{q}_{\rm E}(t) = q_1 + N_{\rm E}^2(1-t^2) + 2N_{\rm E}(1-t)\,. \tag{6.7.15}$$

For the real time path $t \in [0, 1]$, the temporal part of the allowability function is zero, because $N_{\rm E} \in \mathbb{R}$. Then $\bar{q}_{\rm E}(t)$ is also real so the spatial allowability function will be non-zero only if $\bar{q}_{\rm E}(t)$ becomes negative. For $N_{\rm E} < 0$, the lowest value of $\bar{q}_{\rm E}(t)$ is reached when $t = 0$:

$$\bar{q}_{\rm E}(0) = q_1 + |N_{\rm E}|^2 - 2|N_{\rm E}|\,, \tag{6.7.16}$$

which reaches its minimum when $|N_{\rm E}| = 1$: $q_{\rm min} = q_1 - 1 > 0$ and this value is positive if the universe size is larger than the Hubble radius, which is required in order to reach a classical universe. Therefore, the scale factor is always positive and the full allowability bound is satisfied on the whole Euclidean axis.

Next we consider the metrics on the segment joining the two saddle points, for which the lapse values are:

$$N = \mathcal{N} - i\,, \quad \text{with } \mathcal{N} \in \mathbb{R} \text{ and } |\mathcal{N}| < \sqrt{q_1 - 1}\,. \tag{6.7.17}$$

The no-boundary geometry is then:

$$\bar{q}(t) = (\mathcal{N}^2 - 1 - 2\mathcal{N}i)(t^2 - 1) + (2\mathcal{N}i + 2)(t - 1) + q_1 \,. \tag{6.7.18}$$

Here the scale factor becomes complex along the real time path, but because both $q(0)$ and $q(1)$ are real, there must exist a path $t(u) = v(u) + iw(u)$ along which $\bar{q}(t(u))$ stays real (and positive). On such a path, the spatial allowability function is zero. The full allowability function is then at most saturated, because the contribution from the temporal function is at most π. We determine the real path $t(u)$ by requiring the imaginary part of the scale factor to vanish:

$$\mathrm{Im}\Big(\bar{q}(t(u))\Big) = 2\Big(\mathcal{N}v(u) + w(u)\Big)\Big(\mathcal{N}w(u) - v(u) + 1\Big) = 0 \,, \tag{6.7.19}$$

$$\Leftrightarrow \quad w(u) = -\mathcal{N}v(u) \,, \text{ or } v(u) = \mathcal{N}w(u) + 1 \,. \tag{6.7.20}$$

Equation (6.7.20) defines two line segments that cross at the point $\left(\frac{1}{\mathcal{N}^2+1}, \frac{-\mathcal{N}}{\mathcal{N}^2+1}\right)$ in the complex time plane. Our real q time path is thus defined by following the first line where $t(u) = u - i\mathcal{N}u$ from $u = 0$ to the crossing point $u = 1/(\mathcal{N}^2 + 1)$, and then along the second line where $t(u) = u + i(u-1)/\mathcal{N}$ from the crossing point until $u = 1$. By plugging the expressions of the lines (6.7.20) into the real part of the scale factor,

$$\mathrm{Re}\Big(\bar{q}(t(u))\Big) = q_1 - (v(u) - 1)^2 + \mathcal{N}^2\Big(v(u)^2 - w(u)^2 - 1\Big) + w(u)\Big(2\mathcal{N}(2v - 1) + w(u)\Big) \,, \tag{6.7.21}$$

we find it is always positive on the range of parameters we consider. Finally, we can calculate the value of the allowability function along this path by considering the temporal part,

$$\Sigma(t) = \Sigma_{\text{temporal}}(t(u)) = \mathrm{Arg}\left(\frac{-N^2 t'(u)^2}{\bar{q}(t(u))}\right) = \mathrm{Arg}(-N^2 t'(u)^2) \tag{6.7.22}$$

$$= \begin{cases} \mathrm{Arg}((\mathcal{N}^2+1)^2) = 0 \quad \text{for} \quad 0 < u < 1/(\mathcal{N}^2+1) \,, \\ \mathrm{Arg}(-(\mathcal{N}^2+1)^2/\mathcal{N}^2) = \pi \quad \text{for} \quad 1/(\mathcal{N}^2+1) < u < 1 \,. \end{cases} \tag{6.7.23}$$

On the second line segment, the allowability bound is saturated. Slightly smoothing out the path can render it strictly satisfied. The higher the dimension, the closer this smoothed path must stay to the real q segment. We have therefore derived that the T-shaped region described in figure 6.16 is allowable up to arbitrarily high dimensions. The path integral can therefore be defined along the T-shaped contours, ending on the saddle points. How the wavefunction is altered by this change of contour is a question to be pursued in the future, but we expect the semi-classical approximation to remain substantively unchanged.

6.7.2 Sum over compact metrics

The previous subsection showed that the no-boundary proposal defined in momentum space (i.e., as a sum over regular metrics) can be restricted to sum over allowable metrics only, in any spacetime dimensions. Here we turn to the field space definition of the no-boundary proposal (i.e., as a sum over compact metrics) and repeat the analysis. We restrict to the four dimensional case only.

The compactness condition for metrics implies we impose an initial Dirichlet condition $q(t=0)=0$, in addition to the final Dirichlet condition $q(t=1)=q_1$. Apart from this, the construction of the no-boundary solution follows the same steps as in the previous subsection. The path integral over the scale factor is carried out by expanding around a classical background solution: $q(t)=\bar{q}_{\rm DD}(t)+\mathcal{Q}(t)$, with $\mathcal{Q}(t)$ an arbitrary fluctuation satisfying $\mathcal{Q}(0)=\mathcal{Q}(1)=0$. The background solution to the equations of motions (6.7.6) and satisfying the Dirichlet boundary condition is (see equation (2.2.13) with $q_0=0$):

$$\bar{q}_{\rm DD}(t)=\frac{\Lambda}{3}N^2t(t-1)+q_1t\,. \tag{6.7.24}$$

Again, the integral over $\mathcal{Q}$ is a Gaußian and only changes the measure by a factor $1/\sqrt{N}$, which we ignore at the semi-classical level. We are left with an ordinary integral over the lapse:

$$\Psi_{\rm DD}(q_1)=\int {\rm d}N\,\exp\left[\frac{2\pi^2 i}{\hbar}\left(\frac{\Lambda^2}{36}N^3+\left(3-\frac{\Lambda q_1}{2}\right)N-\frac{3q_1^2}{4N}\right)\right]. \tag{6.7.25}$$

The four saddle points of the integrand read:

$$N_{\rm SP}=\frac{3}{\Lambda}\left(\pm\sqrt{\frac{\Lambda q_1}{3}-1}\pm i\right)\,. \tag{6.7.26}$$

As recalled in detail in 2.2, the physical properties of the upper complex half plane and lower complex half plane saddle points strongly differ. The two saddle points in the lower half plane have an enhanced weighting $\exp\left(+\frac{1}{2\hbar}|\mathcal{I}(S^4)|\right)$ (where again $\mathcal{I}(S^4)$ is the action on a four-sphere of radius $H^{-1}=\sqrt{3/\Lambda}$), and perturbations around these geometries are stable. On the other hand, the two saddle points in the upper half plane have a suppressed weighting $\exp\left(-\frac{1}{2\hbar}|\mathcal{I}(S^4)|\right)$ and unstable perturbations. We have depicted again these saddle points and their associated steepest ascent/descent contours in the left panel of figure 6.18. We recall that in [44], this definition was discarded for being inconsistent, because lower half plane and upper half plane saddle points are linked by steepest descent contours, hence any integration contour including the stable (lower) saddle points, also necessarily includes the unstable (upper) ones. Here we focus on the structure of the metrics space in the light of the allowability bound, and study its impact on the definition of the no-boundary wavefunction.

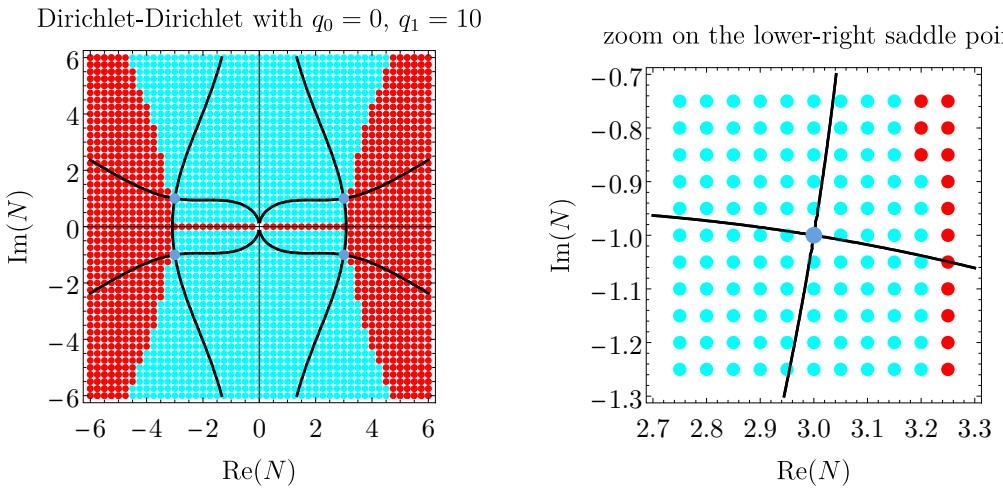

Figure 6.18: In the left panel, a numerical plot in the complexified lapse plane of the allowed (cyan) and disallowed (red) metrics satisfying initial and final Dirichlet conditions, as appropriate for a field space definition of the no-boundary wave function. Here $D = 4$, $\Lambda = 3$, $q(t = 0) = 0$, and $q(t = 1) = 10$. This time the saddle points (in blue) do not reside at the boundary of the allowable domain, but are surrounded by allowable metrics, as can be seen more clearly in the zoomed in version in the right panel.

We apply the numerical methods described in section 6.3, and display our results in figure 6.18. These are grids of geometries in the complexified lapse plane. Saddle points are represented by blue dots and their steepest descent and ascent contour by solid black lines. Cyan dots correspond to geometries for which the allowability bound is satisfied, and red dots to geometries for which it is violated. We raise two interesting features in these results:

1. the saddle points do no lie on the boundary of the allowability domain, in contrast with the result obtained for the momentum space definition. Instead, as evident from the magnified plot on the right of figure 6.18, saddle point geometries are surrounded by allowable metrics. This could mean that the momentum space and field space definitions are not Fourier transforms of each other, at least beyond the semi-classical limit;

2. all geometries on the Lorentzian (real lapse) axis saturate the allowability criterion. In the minisuperspace ansatz, this line divides the space of metrics into two separate halves, and cuts any integration contour crossing it. This therefore cuts the steepest descent contours linking stable and unstable saddle points, and removes this obstruction to a consistent definition of the no-boundary wavefunction. Within the assumptions presented in this section, we can define a no-boundary wavefunction in the field space definition, by restricting the contour of integration to the steepest descent contours in the lower complex half plane (coming from $-i\infty$ and passing through one of the saddle points). A real wave function (as advocated by Hartle and Hawking [38]) is obtained by summing the left and right contours with an equal weight.

Before ending this section, we emphasize that this analysis is restricted to the minisuperspace space of metrics. We cannot conclude from the above result whether the field space no-boundary wavefunction can be defined in full generality, i.e., whether or not there exist allowable metrics with zero weighting, satisfying the Dirichlet boundary conditions $q(0) = 0$, $q(1) = q_1$, for arbitrary $q_1 > 3/\Lambda$, and which can continuously link an integration contour stemming from a saddle in the lower-half plane to an integration contour stemming from a saddle in the upper-half plane. We can only conjecture that the full space of metrics will still be separated into two disconnected regions by the domain of non-allowability, keeping away stable from unstable saddle points. Proving such a conjecture would confirm that the original field space definition of the no-boundary proposal can indeed be made consistent.

6.8 Discussion

In this last chapter, we have investigated a second possible selection criterion for early universe models, also in the perspective of improving our understanding of the gravitational path integral. Before turning to the general conclusions of this thesis, let us review and discuss the main results obtained here. We have motivated why a criterion for complex metrics must exist in quantum gravity, and showed that the criterion developed by Kontsevich and Segal for quantum field theory on curved backgrounds seems a sensible sieve when applied to known quantum gravity models that make use of complex metrics. Taking this criterion seriously, we then applied it to several early universe models. To this aim, we developed an unambiguous methodology for studying the allowability function of on- and off-shell metrics. Lorentzian metrics always saturate the allowability bound. Classical transitions between two de Sitter geometries satisfy the bound, but highlight the limits of the minisuperspace ansatz. All the quantum bounce models we reviewed here violate the allowability bound. This raises the question of whether all quantum bounces are ruled out by this criterion. Finally, the no-boundary proposal, defined both in the momentum and in the field space, is compatible with the allowability criterion, not only on-shell but also along the off-shell metrics necessary to define the integration contour for the path integral. This allowability of off-shell metrics is key to a proper definition of the gravitational path integral beyond the semi-classical approximation. This last point is an important result, because until then the common understanding was that the field space definition of the no-boundary proposal could not lead to a consistent definition of the wavefunction of the universe. Restricting the path integral to the domain of allowable metrics not only enables a proper definition of the wavefunction in this case, but also reconcile the field space no-boundary definition with the momentum space one, as the integration contours in both cases now run along the negative Euclidean axis before reaching the lower half plane, stable Hartle-Hawking saddle points. In the conclusion we will elaborate on the many new avenues this work opens, and its significance in the construction of a meaningful path integral for quantum gravity.

Conclusion

Throughout this thesis, our aim was to advance the knowledge on the very early quantum stage of our universe, in particular through a better understanding of the gravitational path integral in cosmology. In this conclusion, we reflect on the different lessons we learned from the results we have obtained, and sketch the new avenues and next possible steps they opened.

First concerning the no-boundary proposal, we have learned in chapter 3 that despite being a semi-classical result, the no-boundary solution still exists when the theory of gravity is supplemented by higher-order corrections. These corrections are typically the perturbative quantum corrections we expect from known theories aiming to describe the UV-complete theory of quantum gravity, such as quadratic gravity, effective field theories of gravity, heterotic and type II string theories. This result is powerful, because it shows that all the covariant terms consisting of Riemann tensors, of covariant derivatives of the Riemann tensor, and of the metric (at least those we have analyzed) possess a no-boundary solution. It is made even stronger by the fact that Lorentzian backgrounds for their part, have been found in the chapter 5 to be inconsistent at the semi-classical level for theories including terms that are cubic or of higher-order in the Riemann tensor. This both indicates that results found at the semi-classical level may very well still hold at the perturbative level of the full quantum gravity, and that the no-boundary solution seems a particularly adequate description of the early universe, both semi-classically and beyond. An open question that remains is whether it is possible to **prove a general result on the existence of no-boundary solutions for any type of higher-order corrections.** This would formalize the statement that no-boundary solutions stay valid in perturbative quantum gravity.

Still regarding the no-boundary proposal, we have confirmed in chapter 4 the viability of the no-boundary proposal defined as a sum over regular metrics, by including a scalar field in its description. In addition to the compact and regular saddle point geometries, this definition also contains non-compact and regular saddle point geometries which come in pairs with the compact ones. Fortunately, we have found that these non-compact saddles are always subdominant in the wavefunction with respect to their compact counterpart. Besides, we have also highlighted a puzzle that was already present in earlier implementations of the no-boundary with a scalar field [39, 40]: the no-boundary wavefunction selects an initial scalar field value at the South Pole of the instanton (i.e., at the

big bang) which depends on the values of the scale factor and scalar field evaluated at the final hypersurface. This is a strong non-causal consequence which must be resolved before we obtain a completely well-defined implementation of the no-boundary proposal. One possible solution which can be investigated in the future, is to **generalize our prescription for the wavefunction definition** by summing over all possible initial values of the scalar field, and not only on those corresponding to at least one compact saddle point as we did in this work. This would automatically eliminate the non-causality problem, but would also require to prove that the compact saddle points are still the dominant contribution to the no-boundary wavefunction if we want to conserve the presumed Hartle-Hawking result for the no-boundary wavefunction. This does not seem to be the case from a first naive examination, because the potential of non-compact saddle points is generically null, so its weighting $\propto e^{1/(\hbar V(\phi))}$ would blow up and dominate the path integral. Nevertheless, we might be saved there by a first principle, which could for instance imply the complex metric criterion developed in chapter 6: indeed, at least in the few examples we studied in this thesis, the scalar potential $V(\phi)$ is null only if the scalar field ϕ has a large complex value. But the complex metric criterion requires matter fields to take real values, while a recent extension of this criterion considering it must apply to the 10 dimensional action of string theory allows for only small imaginary components of the scalar field [77].

Moving on to the semi-classical constraints on early universe models, we have studied two criteria following from semi-classical consistency requirements. The motivation behind this study is akin to the swampland program [8]: instead of searching for an ever increasing number of new solutions (vacua) of string theory, one looks for conditions ruling out certain candidates for the low-energy effective theory of quantum gravity. In most interesting and directly applicable cases, the swampland program only formulates conjectures whose formal proofs still lay far out of reach, for instance the de Sitter conjecture [98, 99] expects that (meta-)stable de Sitter vacua are excluded from string theory. In this thesis, instead of studying the full quantum gravity consistency, we analyzed the implications of requiring semi-classical consistency for cosmological models. Semi-classical considerations are obviously more easily tractable than full quantum gravity ones, especially thanks to the path integral. The other way around, semi-classical limits of cosmological models represent a good playground for testing the gravitational path integral and question its meaning. The main lesson that we have learned is that semi-classical physics is already very restricting and in some cases is already equivalent to some swampland conditions: coming back to the de Sitter conjecture example, this would mean that stable de Sitter vacua, if they exist, must necessarily be found beyond the semi-classical approximation. More particularly, we have found that according to the finite amplitude criterion in chapter 5, quadratic gravity occupies a peculiar situation, naturally leading to initial conditions favoring inflation, while being the only higher-order theory of gravity admitting Lorentzian background solutions. Eternal inflation and infla-

tion as a first phase of evolution are also ruled out, and **one open question concerns whether the latter is still ruled out in the case of quadratic inflation**. This overall suggests that efforts done in order to make sense of the ghost of quadratic gravity [60, 59] are worth pursuing. The no-boundary proposal is naturally semi-classically consistent, and emergent (or genesis) scenarios, which arise in particular in string cosmology where they are presently studied in the context of Matrix Models [171, 172, 173], can also be made semi-classically consistent in accordance with the finite amplitude criterion. Turning finally to the complex metric criterion studied in chapter 6, the principal lesson it taught us is that such a criterion can effectively modify the interpretation and even definition of the gravitational path integral. This last chapter opens many new avenues and research questions. First, all the quantum bouncing models we analyzed were ruled out by this criterion. **Is this a general feature of all quantum bounces**, and can we prove this? Further, our results on classical transitions in de Sitter spacetime have underlined the limitations of the minisuperspace ansatz. In the prospect of relaxing this ansatz, it would be interesting to **consider more general cosmological backgrounds such as the Bianchi IX model**, for which a no-boundary solution has also been found [174]. The scrutiny of the no-boundary proposal in the light of the complex metric criterion changed our view on the gravitational path integral. In this perspective, it would be interesting to **study also the AdS gravitational path integral** as initiated in [53], and to consider the existence of **Euclidean wormhole solutions** (see [175] for a first study of Euclidean wormholes in the context of the LSKSW criterion). Finally, a long-run goal would be to **relate the complex metric criterion to an underlying physical principle in quantum gravity**. Since the complex metric criterion is formally valid only for quantum field theories on fixed curved background, the ultimate criterion stemming from quantum gravity may well turn out to be less or more restrictive than the present LSKSW criterion. Nevertheless, our study confirms the previous expectation that the LSKSW criterion is adequate to the study of quantum gravity.

While waiting for observational probes in the next decades, the development of theoretical tests such as these two criteria seems crucial to assert the many early universe models and enable to focus the research effort on the models that pass these tests, such as the no-boundary proposal. Additionally, the study of these criteria can help improving our understanding of key physical principles and better deciphering the nature of quantum gravity.

Acknowledgements

First and foremost, I wish to deeply thank my supervisor Jean-Luc Lehners for having taught me so much and shared with me his ideas on cosmology, quantum gravity and our universe. Our discussions and shared research helped me develop my own thinking and research abilities. His encouragements and enthusiasm have been a constant boost throughout my time here.

It has been a real pleasure to also collaborate with Jérôme Quintin and Vincent Meyer. I have learned a lot about physics in our many (virtual) meetings, and our discussions have often challenged my perspectives.

I am very grateful to Robert Brandenberger and Lavinia Heisenberg for having hosted me during a two-months research trip in ETH Zürich in Autumn 2022, and having discussed with me their ideas of the early universe, offering me a fresh view on it.

My work has also benefited from lively physics discussions with Alice Di Tucci, Sebastian Bramberger, Jan Gerken, Ana Alonso-Serrano, Serena Giardino, George Lavrelashvili and Cédric Schoonen.

I acknowledge the support of the Max Planck Institute for Gravitational Physics (Albert Einstein Institute), particularly of my official supervisor and former institute's director Hermann Nicolai, and of Axel Kleinschmidt and Hadi Godazgar for organizing the IMPRS program. I thank all the administrative and IT staff of the AEI, in particular Darya Niakhaichyk for her continued administrative but also personal support, from my very first day in Germany. Thank you for making everyone at the AEI feel welcomed and at home, and for your commitment toward equal opportunities in the institute.

Finally, I am grateful to my friends and family in Belgium, Germany and Switzerland, which have supported me faithfully and steadily through my ups and downs. I am especially grateful to Cédric Schoonen for having encouraged and motivated me to do my best daily. The hard times we have been through these last years have reminded me how much you are all essential to my fulfillment.

Je souhaite dédier cette thèse à mon grand-père Lucien Carouy, décédé en 2022. L'avoir rendu fier est une grande source de joie, et même si je n'ai pas vraiment été dans l'espace, j'y vais régulièrement dans mes pensées.

Appendix A

Appendices to the chapter 3

A.1 Constraint equation of Riemann terms in the no-boundary ansatz

We plug the no-boundary ansatz (3.2.16) into the Friedmann constraint equation (3.2.14), and expand it at lowest orders in t. From (3.2.17) we know that at lowest order $A_1 = A_2 = \frac{a_3}{a_1 N^2}$. Therefore we get

$$0 = 2\pi^2 \sum_{p_1,p_2} c_{p_1,p_2} \Big[2p_1(p_2-1)\frac{a_1 t \cdot a_1^2}{N^2}\Big(\frac{a_3}{a_1 N^2}\Big)^{P-1} + p_2(p_2-1)\frac{a_1 t \cdot a_1 \cdot a_3}{N^4}\Big(\frac{a_3}{a_1 N^2}\Big)^{P-2} - p_2(2p_1+p_2-3)\frac{a_1 t \cdot a_1^2}{N^2}\Big(\frac{a_3}{a_1 N^2}\Big)^{P-1}\Big] + O(t^3)\,; \tag{A.1.1}$$

where we defined $P = p_1 + p_2$ for simplicity.
This leading order equation can be further simplified to

$$2\pi^2 \sum_{p_1,p_2} \frac{c_{p_1,p_2}}{N^{2P}} a_1^{4-P} a_3^{P-1} \left[2p_2 - 2p_1\right] t + O(t^3) = 0\,. \tag{A.1.2}$$

Let us now look at the next order. Because a is an odd function of t, and hence A_1 and A_2 are even functions of t (see (3.2.17)), the t^2 order of the Friedmann constraint will vanish. We directly consider the t^3 order of the Friedmann constraint:

$$\begin{aligned} 2\pi^2 \sum_{p_1,p_2} c_{p_1,p_2} \Big[& 2p_1(p_2-1)\frac{\big(a_1 t + \frac{a_3 t^3}{6}\big)\big(a_1 + \frac{a_3 t^2}{2}\big)^2}{N^2}\Big(\frac{a_3}{a_1 N^2} + \frac{a_3^2 - a_1 a_5}{12 N^4} t^2\Big)^{p_1-1}\Big(\frac{a_3}{a_1 N^2} + \frac{a_3^2 - a_1 a_5}{6 N^4} t^2\Big)^{p_2} \\ & + p_2(p_2-1)\frac{\big(a_1 t + \frac{a_3 t^3}{6}\big)\big(a_1 + \frac{a_3 t^2}{2}\big)\big(a_3 + \frac{a_5 t^2}{2}\big)}{N^4}\Big(\frac{a_3}{a_1 N^2} + \frac{a_3^2 - a_1 a_5}{12 N^4} t^2\Big)^{p_1}\Big(\frac{a_3}{a_1 N^2} + \frac{a_3^2 - a_1 a_5}{6 N^4} t^2\Big)^{p_2-2} \\ & - p_2(2p_1+p_2-3)\frac{\big(a_1 t + \frac{a_3 t^3}{6}\big)\cdot\big(a_1 + \frac{a_3 t^2}{2}\big)^2}{N^2}\Big(\frac{a_3}{a_1 N^2} + \frac{a_3^2 - a_1 a_5}{12 N^4} t^2\Big)^{p_1}\Big(\frac{a_3}{a_1 N^2} + \frac{a_3^2 - a_1 a_5}{6 N^4} t^2\Big)^{p_2-1} \\ & + (1-p_2)\big(a_1 t\big)^3\Big(\frac{a_3}{a_1 N^2}\Big)^P\Big] + \mathcal{O}(t^5) = 0\,. \end{aligned} \tag{A.1.3}$$

This can then be simplified to

$$2\pi^2 \sum_{p_1,p_2} \frac{c_{p_1,p_2}}{N^{2P}} a_1^{3-P} a_3^{P-2}\Big(a_3^2 \cdot G_3[p_1,p_2] + a_1 a_5 \cdot G_5[p_1,p_2]\Big) t^3 + \mathcal{O}(t^5) = 0\,, \tag{A.1.4}$$

with

$$G_3[p_1,p_2]=\frac{1}{6}\left(p_1^2-15p_1+6-4p_2^2+12p_2\right)\text{ and }G_5[p_1,p_2]=\frac{p_1(1-p_1)}{6}-\frac{2p_2(1-p_2)}{3}\,. \tag{A.1.5}$$

A.2 Constraint equations for $\mathcal{B}$ and $\mathcal{C}$ terms

Here we display the constraint equations of $\mathcal{B}$ terms where the no-boundary ansatz has been plugged in. Writing $\delta\mathcal{B}\equiv\frac{\delta}{\delta N}(a^3N\mathcal{B})$, we find

$$\begin{aligned}
\delta\mathcal{B}_1=&-12\left[\frac{4}{15a_1^6}\left(25a_3^3-29a_1a_3a_5+4a_1^2a_7\right)t^3\right]+\mathcal{O}(t^5)\,;\\
\delta\mathcal{B}_2=&-12\left[\frac{1}{15a_1^6}\left(85a_3^3-101a_1a_3a_5+16a_1^2a_7\right)t^3\right]+\mathcal{O}(t^5)\,;\\
\delta\mathcal{B}_3=&-36\left[\frac{2}{15a_1^6}\left(35a_3^3-43a_1a_3a_5+8a_1^2a_7\right)t^3\right]+\mathcal{O}(t^5)\,;\\
\delta\mathcal{B}_4=&-\frac{4}{5a_1^6}\left(35a_3^3-43a_1a_3a_5+8a_1^2a_7\right)t^3+\mathcal{O}(t^5)\,.
\end{aligned}$$

All those ∇^2R^2 terms possess a no-boundary solution which specifies a_7 in terms of a_1, a_3, and a_5, but where the latter are not specified by the ∇^2R^2 terms alone.

We now look at the constraint equations for $\mathcal{C}$ terms. Their expressions in terms of A_1, A_2, A_3 and A_4 are

$$\begin{aligned}
\mathcal{C}_1=&\,12\left[4\left[A_2(A_2-A_1)+\frac{2\dot{a}^2}{a^2N^2}(A_2-A_1)+\frac{\dot{a}}{aN}A_3\right]^2+\left[A_4-\frac{4\dot{a}^2}{a^2N^2}(A_2-A_1)+\frac{\dot{a}}{aN}A_3\right]^2\right];\\
\mathcal{C}_2=&\,12\left[A_4^2+\frac{4\dot{a}}{aN}A_3A_4+\frac{7\dot{a}^2}{a^2N^2}A_3^2+2A_4A_2(A_2-A_1)+4A_2^2(A_2-A_1)^2-\frac{4\dot{a}^2}{a^2N^2}A_4(A_2-A_1)\right.\\
&\left.+\frac{16\dot{a}^4}{a^4N^4}(A_2-A_1)^2+\frac{8\dot{a}^2}{a^2N^2}A_2(A_2-A_1)^2+\frac{10\dot{a}}{aN}A_3A_2(A_2-A_1)+\frac{4\dot{a}^3}{a^3N^3}A_3(A_2-A_1)\right];\\
\mathcal{C}_3=&\,36\left[\frac{3\dot{a}}{aN}A_3+2A_2(A_2-A_1)+A_4\right]^2;\\
\mathcal{C}_4=&\,12\left[A_4^2-\frac{4\dot{a}}{aN}A_3A_4+\frac{19\dot{a}^2}{a^2N^2}A_3^2+\frac{16\dot{a}}{aN}A_3A_2(A_2-A_1)-\frac{80\dot{a}^3}{a^3N^3}A_3(A_2-A_1)\right.\\
&\left.+\frac{160\dot{a}^4}{a^4N^4}(A_2-A_1)^2-\frac{48\dot{a}^2}{a^2N^2}A_2(A_2-A_1)^2+8A_2^2(A_2-A_1)^2\right];\\
\mathcal{C}_5=&\,12\left[A_4^2-\frac{2\dot{a}}{aN}A_3A_4+\frac{11\dot{a}^2}{a^2N^2}A_3^2-\frac{34\dot{a}^3}{a^3N^3}A_3(A_2-A_1)+\frac{8\dot{a}}{aN}A_3A_2(A_2-A_1)\right.\\
&+2A_4A_2(A_2-A_1)-\frac{6\dot{a}^2}{a^2N^2}A_4(A_2-A_1)+\frac{104\dot{a}^4}{a^4N^4}(A_2-A_1)^2-\frac{36\dot{a}^2}{a^2N^2}A_2(A_2-A_1)^2\\
&\left.+6A_2^2(A_2-A_1)^2\right];\\
\mathcal{C}_6=&\,36\left[\left[A_4+2A_2(A_2-A_1)\right]^2-\frac{12\dot{a}^2}{a^2N^2}(A_2-A_1)A_4-\frac{24\dot{a}^2}{a^2N^2}A_2(A_2-A_1)^2+\frac{3\dot{a}^2}{a^2N^2}A_3^2\right.\\
&\left.+\frac{12\dot{a}^3}{a^3N^3}(A_2-A_1)A_3+\frac{48\dot{a}^4}{a^4N^4}(A_2-A_1)^2\right].
\end{aligned}$$

Writing $\delta\mathcal{C} \equiv \frac{\delta}{\delta N}(a^3 N\mathcal{C})$, we find

$$\delta\mathcal{C}_1 = \frac{8t^3\left(3262a_1a_3^2a_5 + 60a_1^3a_9 - 2135a_3^4 - a_1^2\left(592a_3a_7 + 595a_5^2\right)\right)}{35a_1^9} + \mathcal{O}\left(t^5\right);$$
$$\delta\mathcal{C}_2 = \frac{4t^3\left(3528a_1a_3^2a_5 - 5a_1^2\left(161a_5^2 - 24a_1a_9\right) - 1995a_3^4 - 848a_1^2a_3a_7\right)}{35a_1^9} + \mathcal{O}\left(t^5\right);$$
$$\delta\mathcal{C}_3 = \frac{48t^3\left(133a_1a_3^2a_5 - 15a_1^2\left(7a_5^2 - 2a_1a_9\right) + 70a_3^4 + 128a_3a_7N^2\right)}{35a_1^9} + \mathcal{O}\left(t^5\right);$$
$$\delta\mathcal{C}_4 = \frac{8t^3\left(1008a_1a_3^2a_5 + 12a_1^3a_9 - 735a_3^4 - 19a_1^2\left(8a_3a_7 + 7a_5^2\right)\right)}{7a_1N^8} + \mathcal{O}\left(t^5\right);$$
$$\delta\mathcal{C}_5 = \frac{2t^3\left(13048a_1a_3^2a_5 - 5a_1^2\left(413a_5^2 - 48a_1a_9\right) - 8855a_3^4 - 2368a_1^2a_3a_7\right)}{35a_1^9} + \mathcal{O}\left(t^5\right);$$
$$\delta\mathcal{C}_6 = \frac{12t^3\left(2968a_1a_3^2a_5 - 15a_1^2\left(49a_5^2 - 8a_1a_9\right) - 1505a_3^4 - 848a_1^2a_3a_7\right)}{35a_1^9} + \mathcal{O}\left(t^5\right).$$

These six ∇^4R^2 terms all admit a regular no-boundary solution, for which the coefficient a_9 is fixed in terms of a_1, a_3, a_5 and a_7 at order t^3 of the constraint. This ensures the existence of a solution if these ∇^4R^2 terms are combined with Riemann terms and ∇^2R^2 terms, since a_9 is a new degree of freedom at order t^3.

A.3 Constraint equations from $\mathcal{D}$, $\mathcal{E}$ and $\mathcal{F}$ terms

Expressions of $\mathcal{D}$ terms as functions of A_1, A_2 and A_3:

$$\mathcal{D}_1 = 144\left[A_3^4 + \frac{16\dot{a}^2}{a^2N^2}A_3^2(A_2 - A_1)^2 + \frac{64\dot{a}^4}{a^4N^4}(A_2 - A_1)^4\right];$$
$$\mathcal{D}_2 = 48\left[3A_3^4 + \frac{24\dot{a}^2}{a^2N^2}A_3^2(A_2 - A_1)^2 + \frac{64\dot{a}^4}{a^4N^4}(A_2 - A_1)^4\right];$$
$$\mathcal{D}_3 = 48\left[A_3^4 + \frac{4\dot{a}^2}{a^2N^2}A_3^2(A_2 - A_1)^2 + \frac{40\dot{a}^4}{a^4N^4}(A_2 - A_1)^4\right];$$
$$\mathcal{D}_4 = 48\left[A_3^4 + \frac{16\dot{a}^3}{a^3N^3}A_3(A_2 - A_1)^3 + \frac{20\dot{a}^4}{a^4N^4}(A_2 - A_1)^4\right].$$

Expressions of $\mathcal{E}$ terms as functions of A_1, A_2, A_3 and A_4:

$$\begin{aligned}\mathcal{E}_1 =& 144(A_1^2 + A_2^2)\left[4\Big(\frac{\dot{a}}{aN}A_3 + \frac{2\dot{a}^2}{a^2N^2}(A_2 - A_1) + A_2(A_2 - A_1)\Big)^2\right.\\ &\left. + \Big(A_4 + \frac{4\dot{a}^2}{a^2N^2}(A_1 - A_2) + \frac{\dot{a}}{aN}A_3\Big)^2\right];\\ \mathcal{E}_2 =& 144(A_1^2 + A_2^2)\left[A_4^2 - \frac{4\dot{a}}{aN}A_4A_3 + \frac{19\dot{a}^2}{a^2N^2}A_3^2 + \frac{16\dot{a}}{aN}A_3A_2(A_2 - A_1) + \frac{80\dot{a}^3}{a^3N^3}A_3(A_1 - A_2)\right.\\ &\left. + 8A_2^2(A_2 - A_1)^2 + \frac{160\dot{a}^4}{a^4N^4}(A_2 - A_1)^2 - \frac{48\dot{a}^2}{a^2N^2}A_2(A_2 - A_1)^2\right];\\ \mathcal{E}_3 =& 144\left[A_2A_4 + \frac{\dot{a}}{aN}A_3(A_2 + 2A_1) - 2A_1A_2(A_1 - A_2) - \frac{4\dot{a}^2}{a^2N^2}(A_1 - A_2)^2\right]^2;\\ \mathcal{E}_4 =& 48\left[12A_1^2A_2^2(A_2 - A_1)^2 + 3A_2^2A_4^2 + 12A_1A_2^2(A_2 - A_1)A_4\right.\end{aligned}$$

$$+\frac{16\dot{a}^4}{a^4N^4}(A_2-A_1)^2(A_2^2-5A_1A_2+13A_1^2)-\frac{12\dot{a}}{aN}A_3A_2(A_2-A_1)\Big(A_4+2A_1(A_2-A_1)\Big)$$
$$-\frac{12\dot{a}^3}{a^3N^3}A_3(A_2-A_1)\Big(2(A_2-A_1)^2-4A_1(A_2-A_1)-3A_1A_2\Big)$$
$$-\frac{12\dot{a}^2}{a^2N^2}(A_2-A_1)\Big(3A_1A_2A_4-A_3^2(A_2-A_1)+6A_1^2A_2(A_2-A_1)\Big)+\frac{9\dot{a}^2}{a^2N^2}A_3^2A_2^2\Bigg];$$

$$\mathcal{E}_5=48\Bigg[4A_1^2\Big[\frac{\dot{a}}{aN}A_3+\frac{2\dot{a}^2}{a^2N^2}(A_2-A_1)+A_2(A_2-A_1)\Big]^2$$
$$+A_2^2\Big[A_4+\frac{\dot{a}}{aN}A_3+\frac{4\dot{a}^2}{a^2N^2}(A_1-A_2)\Big]^2\Bigg];$$

$$\mathcal{E}_6=48\Bigg[16\frac{\dot{a}^4}{a^4N^4}(A_2-A_1)^2(7A_1^2+3A_2^2)-12\frac{\dot{a}^2}{a^2N^2}A_2(A_2-A_1)^2(A_2^2+3A_1^2)$$
$$+2A_2^2(A_2-A_1)^2(A_2^2+3A_1^2)+\frac{\dot{a}^2}{a^2N^2}A_3^2(8A_1^2+11A_2^2)-4\frac{\dot{a}}{aN}A_3A_2^2A_4$$
$$+4\frac{\dot{a}}{aN}A_3A_2(A_2-A_1)(A_2^2+3A_1^2)+A_2^2A_4^2+16A_3\frac{\dot{a}^3}{a^3N^3}(A_1-A_2)(2A_2^2+3A_1^2)\Bigg];$$

$$\mathcal{E}_7=48\Bigg[\frac{16\dot{a}^4}{a^4N^4}(A_2-A_1)^2(A_1^2+A_2^2)+4A_1^2A_2^2(A_2-A_1)^2-\frac{8\dot{a}^3}{a^3N^3}A_3(A_2-A_1)(A_2^2-2A_1^2)$$
$$+\frac{\dot{a}^2}{a^2N^2}(4A_1^2+A_2^2)A_3^2+\frac{8\dot{a}^2}{a^2N^2}A_2^2A_4(A_1-A_2)+\frac{16\dot{a}^2}{a^2N^2}A_1^2A_2(A_2-A_1)^2$$
$$+\frac{2\dot{a}}{aN}A_2^2A_3A_4+\frac{8\dot{a}}{aN}A_1^2A_2A_3(A_2-A_1)+A_2^2A_4^2\Bigg]=\mathcal{E}_5\ ;$$

$$\mathcal{E}_8=48\Bigg[\frac{4\dot{a}^4}{a^4N^4}(A_2-A_1)^2(3A_2^2+18A_2A_1+19A_1^2)-\frac{8\dot{a}^3}{a^3N^3}A_3(A_2-A_1)(A_2^2+6A_2A_1+3A_1^2)$$
$$+\frac{\dot{a}^2}{a^2N^2}A_3^2(8A_2A_1+7A_2^2+4A_1^2)-\frac{24\dot{a}^2}{a^2N^2}A_1A_2(A_2-A_1)^2(A_2+A_1)$$
$$+\frac{8\dot{a}}{aN}A_2A_1A_3(A_2^2-A_1^2)-\frac{4\dot{a}}{aN}A_2^2A_3A_4+4A_2^2A_1(A_2-A_1)^2(A_2+A_1)+A_2^2A_4^2\Bigg].$$

Expressions of $\mathcal{F}$ terms through A_1, A_2, A_3 and A_4 quantities:

$$\mathcal{F}_1=144\Big[\frac{8\dot{a}^2}{a^2N^2}(A_2-A_1)^2+A_3^2\Big]\Big[2A_2A_1(A_2-A_1)-\frac{4\dot{a}^2}{a^2N^2}(A_2-A_1)^2$$
$$+\frac{\dot{a}}{aN}A_3(A_2+2A_1)+A_2A_4\Big];$$

$$\mathcal{F}_2=48\Big[-\frac{16\dot{a}^4}{a^4N^4}(A_2-A_1)^3(A_2+2A_1)-\frac{12\dot{a}^3}{a^3N^3}A_3(A_2-A_1)^2(A_2-2A_1)$$
$$+\frac{24\dot{a}^2}{a^2N^2}A_1A_2(A_2-A_1)^3+\frac{18\dot{a}^2}{a^2N^2}A_3^2A_1(A_1-A_2)+\frac{12\dot{a}^2}{a^2N^2}A_2A_4(A_2-A_1)^2$$
$$+\frac{6\dot{a}}{aN}A_3^3(A_1-A_2)+6A_3^2A_1A_2(A_2-A_1)+3A_2A_3^2A_4\Big];$$

$$\mathcal{F}_3=144\Big[\frac{2\dot{a}}{aN}A_1(A_2-A_1)+A_2A_3\Big]\Big[\frac{\dot{a}}{aN}A_3^2+\frac{4\dot{a}}{aN}A_2(A_2-A_1)^2+\frac{8\dot{a}^3}{a^3N^3}(A_2-A_1)^2+A_3A_4\Big];$$

$$\mathcal{F}_4=144\Big[\frac{2\dot{a}}{aN}A_1(A_2-A_1)+A_2A_3\Big]\Big[\frac{4\dot{a}}{aN}(A_2-A_1)^2(A_2-\frac{6\dot{a}^2}{a^2N^2})-\frac{2\dot{a}}{aN}A_3^2$$
$$+\frac{8\dot{a}^2}{a^2N^2}A_3(A_2-A_1)+A_3A_4\Big];$$

$$\mathcal{F}_5 = 48\Big[-\frac{8\dot{a}^4}{a^4N^4}(A_2-A_1)^3(A_2-3A_1) + \frac{2\dot{a}^3}{a^3N^3}A_3(A_2-A_1)^2(A_2+6A_1)$$
$$-\frac{4\dot{a}^2}{a^2N^2}A_2A_3^2(A_2-A_1) + \frac{2\dot{a}^2}{a^2N^2}A_2A_4(A_2-A_1)^2 + \frac{12\dot{a}^2}{a^2N^2}A_1A_2(A_2-A_1)^3$$
$$+\frac{\dot{a}}{aN}A_2A_3^3 + A_2A_3^2A_4\Big];$$
$$\mathcal{F}_6 = 48\Big[-\frac{2\dot{a}^4}{a^4N^4}(A_2-A_1)^3(9A_2+13A_1) + \frac{6\dot{a}^3}{a^3N^3}A_1A_3(A_2-A_1)^2 + \frac{2\dot{a}^2}{a^2N^2}A_3^2(A_2^2-A_1^2)$$
$$+\frac{12\dot{a}^2}{a^2N^2}A_1A_2(A_2-A_1)^3 + \frac{2\dot{a}}{aN}A_2^2A_3(A_2-A_1)^2 - \frac{2\dot{a}}{aN}A_2A_3^3 + A_2A_3^2A_4\Big];$$
$$\mathcal{F}_7 = 48\Big[\frac{8\dot{a}^4}{a^4N^4}(A_2-A_1)^3(A_2+A_1) + \frac{2\dot{a}^3}{a^3N^3}A_3(A_2-A_1)^2(2A_2+5A_1)$$
$$+\frac{2\dot{a}^2}{a^2N^2}A_1A_4(A_2-A_1)^2 - \frac{4\dot{a}^2}{a^2N^2}A_2A_3^2(A_2-A_1) + \frac{4\dot{a}^2}{a^2N^2}A_2(A_2-A_1)^3(A_2+2A_1)$$
$$+\frac{\dot{a}}{aN}A_2A_3^3 + A_2A_3^2A_4\Big];$$
$$\mathcal{F}_8 = 48\Big[\frac{2\dot{a}^4}{a^4N^4}(A_2-A_1)^3(5A_2-27A_1) - \frac{6\dot{a}^3}{a^3N^3}A_3(A_2-A_1)^2(2A_2-3A_1)$$
$$+\frac{12\dot{a}^2}{a^2N^2}A_1A_2(A_2-A_1)^3 + \frac{4\dot{a}^2}{a^2N^2}A_2A_3^2(A_2-A_1) + \frac{2\dot{a}}{aN}A_2^2A_3(A_2-A_1)^2$$
$$-\frac{2\dot{a}}{aN}A_2A_3^3 + A_2A_3^2A_4\Big].$$

We display here the constraint equations obtained for all $\mathcal{D}$, $\mathcal{E}$ and $\mathcal{F}$ terms (using again the notation $\delta\mathcal{D} \equiv \frac{\delta}{\delta N}(a^3N\mathcal{D})$ and similarly for $\mathcal{E}$ and $\mathcal{F}$):

$$\delta\mathcal{D}_1 = 144\Big[\Delta_1 + 16\Delta_3 + 64\Delta_2\Big] = \frac{384(a_3^2-a_1a_5)^3}{a_1^{15}}\,t^3 + \mathcal{O}\left(t^5\right);$$
$$\delta\mathcal{D}_2 = 12\Big[64\Delta_2 + 12\big[\Delta_1 + 8\Delta_3 + 16\Delta_2\big]\Big] = \frac{1408(a_3^2-a_1a_5)^3}{3a_1^{15}}\,t^3 + O\left(t^5\right);$$
$$\delta\mathcal{D}_3 = 2\Big[864\Delta_2 + 24\big[\Delta_1 + 4\Delta_3 + 4\Delta_2\big]\Big] = \frac{144(a_3^2-a_1a_5)^3}{a_1^{15}}\,t^3 + O\left(t^5\right);$$
$$\delta\mathcal{D}_4 = 4\Big[240\Delta_2 + 192\Delta_4 + 12\Delta_1\Big] = \frac{136(a_3^2-a_1a_5)^3}{a_1^{15}}\,t^3 + \mathcal{O}\left(t^5\right);$$
$$\delta\mathcal{E}_1 = 144\cdot\frac{4t^3}{105a_1^{15}}\Big[60a_1^2a_3^2(a_1a_9-a_3a_7) + 532a_1^2a_3a_5(a_3a_5-a_1a_7) - 3675(a_3^2-a_1a_5)^3$$
$$-3535a_1a_5(a_3^2-a_1a_5)^2 - a_1a_3(616a_5a_3+924a_1a_7)(a_3^2-a_1a_5)\Big] + \mathcal{O}\left(t^5\right);$$
$$\delta\mathcal{E}_2 = 144\cdot\frac{4t^3}{63a_1^{15}}\Big[36a_1^2a_3^2(a_1a_9-a_3a_7) + 420a_1^2a_3a_5(a_3a_5-a_1a_7) - 2793(a_3^2-a_1a_5)^3$$
$$-2765a_1a_5(a_3^2-a_1a_5)^2 - a_1a_3(1246a_5a_3+560a_1a_7)(a_3^2-a_1a_5)\Big] + \mathcal{O}\left(t^5\right);$$
$$\delta\mathcal{E}_3 = 144\cdot\frac{2t^3}{315a_1^{15}}\Big[180a_1^2a_3^2(a_1a_9-a_3a_7) + 588a_1^2a_3a_5(a_3a_5-a_1a_7) - 6860(a_3^2-a_1a_5)^3$$
$$-5915a_1a_5(a_3^2-a_1a_5)^2 - a_1a_3(-4046a_5a_3+2996a_1a_7)(a_3^2-a_1a_5)\Big] + \mathcal{O}\left(t^5\right);$$
$$\delta\mathcal{E}_4 = 48\cdot\frac{2t^3}{315a_1^{15}}\Big[540a_1^2a_3^2(a_1a_9-a_3a_7) + 3276a_1^2a_3a_5(a_3a_5-a_1a_7) - 23450(a_3^2-a_1a_5)^3$$
$$-22575a_1a_5(a_3^2-a_1a_5)^2 - a_1a_3(-4179a_5a_3+7644a_1a_7)(a_3^2-a_1a_5)\Big] + \mathcal{O}\left(t^5\right);$$

$$\delta\mathcal{E}_5 = \delta E_7 = 48\cdot\frac{t^3}{315a_1^{15}}\Big[360a_1^2a_3^2(a_1a_9-a_3a_7)+3192a_1^2a_3a_5(a_3a_5-a_1a_7)$$
$$-29470(a_3^2-a_1a_5)^3-28000a_1a_5(a_3^2-a_1a_5)^2$$
$$-a_1a_3(2240a_5a_3+7000a_1a_7)(a_3^2-a_1a_5)\Big]+\mathcal{O}\left(t^5\right);$$
$$\delta\mathcal{E}_6 = 48\cdot\frac{t^3}{315a_1^{15}}\Big[360a_1^2a_3^2(a_1a_9-a_3a_7)+4200a_1^2a_3a_5(a_3a_5-a_1a_7)-32795(a_3^2-a_1a_5)^3$$
$$-32305a_1a_5(a_3^2-a_1a_5)^2-a_1a_3(11396a_5a_3+6664a_1a_7)(a_3^2-a_1a_5)\Big]$$
$$+\mathcal{O}\left(t^5\right);$$
$$\delta\mathcal{E}_8 = 48\cdot\frac{t^3}{630a_1^{15}}\Big[720a_1^2a_3^2(a_1a_9-a_3a_7)+8400a_1^2a_3a_5(a_3a_5-a_1a_7)-65695(a_3^2-a_1a_5)^3$$
$$-64610a_1a_5(a_3^2-a_1a_5)^2-a_1a_3(22792a_5a_3+13328a_1a_7)(a_3^2-a_1a_5)\Big]$$
$$+\mathcal{O}\left(t^5\right);$$
$$\delta\mathcal{F}_1 = 144\cdot\frac{2(a_3^2-a_1a_5)t^3}{45a_1^{15}}\Big[235a_3^2(a_3^2-a_1a_5)-64a_1a_3(a_3a_5-a_1a_7)\Big]+\mathcal{O}\left(t^5\right);$$
$$\delta\mathcal{F}_2 = 48\cdot\frac{2(a_3^2-a_1a_5)t^3}{45a_1^{15}}\Big[105a_1a_5(a_3^2-a_1a_5)+12a_1a_3(a_3a_5-a_1a_7)-160(a_3^2-a_1a_5)^2\Big]$$
$$+\mathcal{O}\left(t^5\right);$$
$$\delta\mathcal{F}_3 = 144\cdot\frac{4(a_3^2-a_1a_5)t^3}{45a_1^{15}}\Big[60a_1a_5(a_3^2-a_1a_5)-18a_1a_3(a_3a_5-a_1a_7)+5(a_3^2-a_1a_5)^2\Big]$$
$$+\mathcal{O}\left(t^5\right);$$
$$\delta\mathcal{F}_4 = 144\cdot\frac{2(a_3^2-a_1a_5)t^3}{45a_1^{15}}\Big[-155a_1a_5(a_3^2-a_1a_5)+32a_1a_3(a_3a_5-a_1a_7)-30(a_3^2-a_1a_5)^2\Big]$$
$$+\mathcal{O}\left(t^5\right);$$
$$\delta\mathcal{F}_5 = 48\cdot\frac{(a_3^2-a_1a_5)t^3}{90a_1^{15}}\Big[725a_3^2(a_3^2-a_1a_5)-128a_1a_3(a_3a_5-a_1a_7)\Big]$$
$$+\mathcal{O}\left(t^5\right);$$
$$\delta\mathcal{F}_6 = 48\cdot\frac{(a_3^2-a_1a_5)t^3}{180a_1^{15}}\Big[-725a_1a_5(a_3^2-a_1a_5)+128a_1a_3(a_3a_5-a_1a_7)-265(a_3^2-a_1a_5)^2\Big]$$
$$+\mathcal{O}\left(t^5\right);$$
$$\delta\mathcal{F}_7 = 48\cdot\frac{(a_3^2-a_1a_5)t^3}{90a_1^{15}}\Big[725a_1a_5(a_3^2-a_1a_5)-128a_1a_3(a_3a_5-a_1a_7)+10(a_3^2-a_1a_5)^2\Big]$$
$$+\mathcal{O}\left(t^5\right);$$
$$\delta\mathcal{F}_8 = 48\cdot\frac{(a_3^2-a_1a_5)t^3}{180a_1^{15}}\Big[-725a_1a_5(a_3^2-a_1a_5)+128a_1a_3(a_3a_5-a_1a_7)-275(a_3^2-a_1a_5)^2\Big]$$
$$+\mathcal{O}\left(t^5\right).$$

Appendix B

Appendices to the chapter 4

B.1 Fluctuation integrals

The Wheeler-de Witt equation in field position space is obtained from the constraint (4.1.8)

$$\left[\hbar^2\left(\partial_x^2-\partial_y^2\right)-\frac{1}{4}\left(1-\alpha x-\beta y\right)\right]\Psi=0\,. \tag{B.1.1}$$

Assuming that the integrations of x and y have already been performed implies that the wave function can be written as an ordinary integral over the lapse, but with a currently unknown measure factor $m(N)$,

$$\Psi[x_{\rm f},y_{\rm f}]=\int {\rm d}N\, m(N)\, e^{iS_0^{\text{on-shell}}[x_{\rm f},y_{\rm f},N]/\hbar}\,. \tag{B.1.2}$$

We abbreviate the on-shell (in x and y) action (4.1.19) simply by S, and $x_{\rm f}$, $y_{\rm f}$ by x, y. Then

$$\hbar^2(\partial_x^2-\partial_y^2)\Psi=\int {\rm d}N\, m(N)\hbar^2\left(\frac{iS_{,xx}}{\hbar}-\frac{(S_{,x})^2}{\hbar^2}-\frac{iS_{,yy}}{\hbar}+\frac{(S_{,y})^2}{\hbar^2}\right)e^{iS/\hbar}\,. \tag{B.1.3}$$

Starting from (4.1.19), the explicit expressions are given by

$$S_{,x}=-\frac{\alpha N}{2}-\frac{\Pi_x}{2}\,;\quad S_{,xx}=0\,;\quad S_{,y}=-\frac{\beta N}{2}-\frac{\Pi_y}{2}\,;\quad S_{,yy}=0\,; \tag{B.1.4}$$

$$\Rightarrow (S_{,y})^2-(S_{,x})^2=\frac{1}{4}\left(N^2(\alpha^2-\beta^2)-2N(\alpha\Pi_x+\beta\Pi_y)+\Pi_y^2-\Pi_x^2\right)\,; \tag{B.1.5}$$

$$S_{,N}=\frac{N^2(\alpha^2-\beta^2)}{2}+N(\alpha\Pi_x+\beta\Pi_y)-\frac{(\alpha x+\beta y)}{2}\,; \tag{B.1.6}$$

$$\Rightarrow\ \text{if } \Pi_y^2-\Pi_x^2=1,\quad (S_{,y})^2-(S_{,x})^2=-\frac{S_{,N}}{2}+\frac{(1-\alpha x-\beta y)}{4}\,. \tag{B.1.7}$$

Inserting into the WdW equation we obtain

$$0=\int {\rm d}N m(N)\cdot\left[-\frac{S_{,N}}{2}\right]e^{iS/\hbar}\ \Leftrightarrow\ 0=\int {\rm d}N\left(-\frac{i\hbar}{2}\right)m_{,N}e^{iS/\hbar}\ \Leftrightarrow\ m=\text{const.} \tag{B.1.8}$$

which verifies that, with mixed Neumann-Dirichlet boundary conditions, the fluctuation integrals lead to no additional N dependence in the integrand of the lapse integral.

B.2 Solving for γ

In this appendix, we will present the details on how to solve for the initial conditions parameter γ, in order for a compact saddle point geometry to exist. We restrict our analysis to hyperbolic cosine potentials ($\alpha = \pm 1, \beta = 0$). For other potentials, the analysis is analogous.

B.2.1 $\alpha = 1$ and $\beta = 0$

We need to solve the following equation for $\gamma \in \mathbb{C}$:

$$a_{\mathrm{f}}^2 \sinh^2(2\phi_{\mathrm{f}}) + 4\sinh(2\gamma)\sinh(2\gamma - 2\phi_{\mathrm{f}}) = 0\,. \tag{B.2.1}$$

The real and imaginary parts of this equation must both hold separately. The imaginary part yields:

$$\sin(4\,\mathrm{Im}[\gamma])\sinh(4\,\mathrm{Re}[\gamma] - 2\phi_{\mathrm{f}}) = 0\,; \tag{B.2.2}$$

so we need either $\mathrm{Im}[\gamma] = k \cdot \pi/4$ for $k \in \mathbb{Z}$, or $\mathrm{Re}[\gamma] = \phi_{\mathrm{f}}/2$. We now analyze the real part of equation (B.2.1), $N_{\mathrm{compact}} = a_{\mathrm{f}}^2 \sinh(2\phi_{\mathrm{f}})/(2i\sinh(2\gamma))$, for these different cases.

1. $\mathrm{Re}[\gamma] = \phi_{\mathrm{f}}/2$: then the real part of (B.2.1) becomes

$$\sin^2(2\,\mathrm{Im}[\gamma]) = (a_{\mathrm{f}}^2\cosh^2(\phi_{\mathrm{f}}) - 1)\sinh^2(\phi_{\mathrm{f}})\,. \tag{B.2.3}$$

Solutions to this equation only exist if the right hand side is between 0 and 1, which translates into

$$a_{\mathrm{f}}^2\cosh^2(\phi_{\mathrm{f}}) > 1 \quad \text{and} \quad a_{\mathrm{f}}^2\sinh^2(\phi_{\mathrm{f}}) < 1\,. \tag{B.2.4}$$

When these conditions are satisfied, equation (B.2.3) possesses four families of solutions

$$\begin{cases} \gamma^{1,2(k)} = \dfrac{\phi_{\mathrm{f}}}{2} \mp \dfrac{i}{2}\left(\arcsin\left(|\sinh(\phi_{\mathrm{f}})|\sqrt{a_{\mathrm{f}}^2\cosh^2(\phi_{\mathrm{f}}) - 1}\right) + 2\pi\cdot k\right); \\ \gamma^{3,4(k)} = \dfrac{\phi_{\mathrm{f}}}{2} \mp \dfrac{i}{2}\left(\pi - \arcsin\left(|\sinh(\phi_{\mathrm{f}})|\sqrt{a_{\mathrm{f}}^2\cosh^2(\phi_{\mathrm{f}}) - 1}\right) + 2\pi\cdot k\right); \end{cases} \quad \forall k \in \mathbb{Z}\,. \tag{B.2.5}$$

We still need to make sure that we obtain only saddle points that admit stable fluctuations, i.e., which imply the correct orientation for the Wick rotation. This means that we must get rid of spurious solutions for which $a\dot{a}|_0 \to -iN$ (rather than $a\dot{a}|_0 \to +iN$) when $\phi \to 0$, i.e. we only keep solutions where

$$\Pi_x = \left.\frac{\dot{x}}{2N}\right|_0 = \left.\frac{a\dot{a}\cosh(2\phi) + a^2\dot{\phi}\sinh(2\phi)}{N}\right|_0 \xrightarrow{\phi\to 0} \left.\frac{a\dot{a}}{N}\right|_0 = +i\,. \tag{B.2.6}$$

Writing Π_x in terms of γ, we obtain

$$\Pi_x = i\cosh(2\gamma) = i\Big(\cosh(\phi_{\mathrm{f}})\cos(2\,\mathrm{Im}[\gamma]) + i\sinh(\phi_{\mathrm{f}})\sin(2\,\mathrm{Im}[\gamma])\Big)\,. \tag{B.2.7}$$

Expanding this expression at zeroth order in ϕ_{f}, the second term vanishes and we find, by

plugging in the solutions (B.2.5) for γ:

$$\begin{cases} \Pi_x^{1,2(k)} = i\cos\left(\mp\arcsin\left(|\sinh(\phi_\mathrm{f})|\sqrt{a_\mathrm{f}^2\cosh^2(\phi_\mathrm{f})-1}\right)+2\pi\cdot k\right) \xrightarrow{\phi_\mathrm{f}\to 0} +i\,; \\ \Pi_x^{3,4(k)} = i\cos\left(\mp\pi\pm\arcsin\left(|\sinh(\phi_\mathrm{f})|\sqrt{a_\mathrm{f}^2\cosh^2(\phi_\mathrm{f})-1}\right)+2\pi\cdot k\right) \xrightarrow{\phi_\mathrm{f}\to 0} -i\,. \end{cases} \tag{B.2.8}$$

We therefore exclude the last two families of solutions, $\gamma^{3,4(k)}$, and keep only the first two, $\gamma^{1,2(k)}$. Since γ only enters expressions through its hyperbolic sine or cosine, the value of k is unimportant and we can simply set it to 0. In the end we only have two values for γ:

$$2\gamma_\mp = \phi_\mathrm{f} \mp i\arcsin\left(|\sinh\phi_\mathrm{f}|\sqrt{a_\mathrm{f}^2\cosh^2(\phi_\mathrm{f})-1}\right). \tag{B.2.9}$$

The saddle point for the lapse computed from these γ values will be complex. These values of γ automatically satisfy the condition $\mathrm{Im}(\Pi_0^x) > 0$.

2. $\mathrm{Im}[\gamma] = k\cdot\pi/2$, $k\in\mathbb{Z}$: $\sin(2\,\mathrm{Im}[\gamma]) = 0$ and $\cos(2\,\mathrm{Im}[\gamma]) = (-1)^k$. All expressions then only depend on whether k is odd or even, so we can restrict to $k = 0, 1$. The real part of the equation (B.2.1) yields:

$$a_\mathrm{f}^2\sinh^2(2\phi_\mathrm{f}) = 4\sinh(2\,\mathrm{Re}[\gamma])\sinh(2\phi_\mathrm{f}-2\,\mathrm{Re}[\gamma])\,. \tag{B.2.10}$$

This admits a solution only if

$$\begin{aligned} & a_\mathrm{f}^2\sinh^2(2\phi_\mathrm{f}) < 4\left|\max_{\mathrm{Re}[\gamma]}\Big(\sinh(2\,\mathrm{Re}[\gamma])\sinh(2\phi_\mathrm{f}-2\,\mathrm{Re}[\gamma])\Big)\right| = 4\sinh^2(\phi_\mathrm{f})\,; \\ \Leftrightarrow\ & a_\mathrm{f}^2\cosh^2(\phi_\mathrm{f}) < 1\,. \end{aligned} \tag{B.2.11}$$

When this condition is satisfied, we find two solutions for each k value:

$$\begin{aligned} \gamma_\mp^{(k)} = \frac{1}{2}\cosh^{-1}\Bigg(\frac{1}{2}\Big[4+\sinh^2(2\phi_\mathrm{f})(2-a_\mathrm{f}^2\cosh(2\phi_\mathrm{f})) \\ \mp\sinh^2(2\phi_\mathrm{f})\sqrt{(2-a_\mathrm{f}^2\cosh(2\phi_\mathrm{f}))^2-a_\mathrm{f}^4}\Big]^{1/2}\Bigg) + ik\cdot\frac{\pi}{2}\,; \end{aligned} \tag{B.2.12}$$

which implies that

$$\begin{aligned} \Pi_{x\mp} = i\cosh(2\gamma_\mp) =& \frac{i(-1)^k}{2}\Big[4+\sinh^2(2\phi_\mathrm{f})(2-a_\mathrm{f}^2\cosh(2\phi_\mathrm{f})) \\ & \mp\sinh^2(2\phi_\mathrm{f})\sqrt{(2-a_\mathrm{f}^2\cosh(2\phi_\mathrm{f}))^2-a_\mathrm{f}^4}\Big]^{1/2} \in i\mathbb{R}\,, \end{aligned} \tag{B.2.13}$$

$$\begin{aligned} \Pi_{y\mp} = i\sinh(2\gamma_\mp) =& \frac{i(-1)^k}{2}|\sinh(2\phi_\mathrm{f})|\sqrt{(2-a_\mathrm{f}^2\cosh(2\phi_\mathrm{f}))\mp\sqrt{(2-a_\mathrm{f}^2\cosh(2\phi_\mathrm{f}))^2-a_\mathrm{f}^4}} \\ & \in i\mathbb{R}\,. \end{aligned} \tag{B.2.14}$$

We look at the limit of Π_x when $\phi_\mathrm{f}\to 0$ to exclude spurious solutions, and we find

$$\Pi_{x\mp}\to i(-1)^k\,; \tag{B.2.15}$$

thus we only keep $k = 0$ and we reject $k = 1$. Finally the γ values are

$$\gamma_{\mp} = \frac{1}{2}\cosh^{-1}\left(\sqrt{1+\frac{\sinh^2(2\phi_{\rm f})}{4}\Big((2-a_{\rm f}^2\cosh(2\phi_{\rm f}))\mp\sqrt{(2-a_{\rm f}^2\cosh(2\phi_{\rm f}))^2-a_{\rm f}^4}\Big)}\right).$$

Because these γ values are real, the saddle points for the lapse will be purely imaginary. These values of γ automatically satisfy the condition $\mathrm{Im}(\Pi_0^x) > 0$.

3. $\mathrm{Im}[\gamma] = \pi/4 + k\cdot\pi/2$: $\sin(2\,\mathrm{Im}[\gamma]) = (-1)^k$ and $\cos(2\,\mathrm{Im}[\gamma]) = 0$. All expressions will only depend on whether k is odd or even, so we can restrict to $k = 0, 1$. The real part of equation (B.2.1) becomes

$$a_{\rm f}^2\sinh^2(2\phi_{\rm f}) - 4\cosh(2\,\mathrm{Re}[\gamma])\cosh(2\,\mathrm{Re}[\gamma]-2\phi_{\rm f}) = 0\,, \tag{B.2.16}$$

which admits a solution only if

$$\begin{aligned} &a_{\rm f}^2\sinh^2(2\phi_{\rm f}) > 4\min_{\mathrm{Re}[\gamma]}(\cosh(2\,\mathrm{Re}[\gamma])\cosh(2\,\mathrm{Re}[\gamma]-2\phi_{\rm f})) = 4\cosh^2(\phi_{\rm f})\,,\\ &\Leftrightarrow\ a_{\rm f}^2\sinh^2(\phi_{\rm f}) > 1\,. \end{aligned} \tag{B.2.17}$$

This condition being fulfilled, we find the four following solutions:

$$\begin{aligned} \gamma_{\mp}^{(k)} = \mp\frac{1}{2}\cosh^{-1}&\left(\frac{1}{2}\sinh(2\phi_{\rm f})\sqrt{a_{\rm f}^2\cosh(2\phi_{\rm f})-2\mp\sqrt{\Big(a_{\rm f}^2\cosh^2(2\phi_{\rm f})-2\Big)^2-a_{\rm f}^4}}\right)\\ &+i\left(\frac{\pi}{4}+\frac{k\cdot\pi}{2}\right),\quad k\in\{-1,0\}\,. \end{aligned} \tag{B.2.18}$$

For these values of γ, we have a particular case where $\mathrm{Im}(\Pi_x^0) = 0$.

In this case it is not possible to take the limit $\phi_{\rm f}\to 0$, as this would contradict the condition (B.2.17). The saddle points for the lapse will be purely real.

B.2.2 $\alpha = -1$ and $\beta = 0$

In this case, the equation we must solve for $\gamma\in\mathbb{C}$ reads:

$$a_{\rm f}^2\sinh^2(2\phi_{\rm f}) - 4\sinh(2\gamma)\sinh(2\gamma-2\phi_{\rm f}) = 0\,. \tag{B.2.19}$$

Taking the imaginary part of this expression, we find

$$2a_{\rm f}^2\sin(4\,\mathrm{Im}[\gamma])\sinh(4\,\mathrm{Re}[\gamma]-2\phi_{\rm f}) = 0\,. \tag{B.2.20}$$

This is solved by $\mathrm{Im}[\gamma] = k\cdot\pi/4$ for $k\in\mathbb{Z}$, or $\mathrm{Re}[\gamma] = \phi_{\rm f}/2$. For each of these cases we examine the real part of equation (B.2.19):

1. $\mathrm{Re}[\gamma] = \phi_{\rm f}/2$: then we find

$$4\sin^2(2\,\mathrm{Im}[\gamma]) = -a_{\rm f}^2\sinh^2(2\phi_{\rm f}) - 4\sinh^2(\phi_{\rm f})\,. \tag{B.2.21}$$

This equation does not admit any solution for $a_\mathrm{f} > 0$ and $\phi_\mathrm{f} \in \mathbb{R}$.

2. $\mathrm{Im}[\gamma] = k \cdot \pi/2$, $k \in \mathbb{Z}$: then $\cos(2\,\mathrm{Im}[\gamma]) = (-1)^k$ and $\sin(2\,\mathrm{Im}[\gamma]) = 0$. Again we only keep $k = \{0, 1\}$. The real part of the equation for γ is

$$a_\mathrm{f}^2 \sinh^2(2\phi_\mathrm{f}) = 4 \sinh(2\,\mathrm{Re}[\gamma]) \sinh(2\,\mathrm{Re}[\gamma] - 2\phi_\mathrm{f})\,; \tag{B.2.22}$$

which yields the following constraint:

$$a_\mathrm{f}^2 \sinh^2(2\phi_\mathrm{f}) > 4 \min_{\mathrm{Re}[\gamma]} (\sinh(2\,\mathrm{Re}[\gamma]) \sinh(2\,\mathrm{Re}[\gamma] - 2\phi_\mathrm{f}))\,. \tag{B.2.23}$$

This minimum lies at $\mathrm{Re}[\gamma] = \phi_\mathrm{f}/2$ and hence implies $a_\mathrm{f}^2 \sinh^2(2\phi_\mathrm{f}) > -4\sinh^2(\phi_\mathrm{f})$. This condition is always satisfied, thus the equation (B.2.22) admits solutions for all values $a_\mathrm{f} > 0$ and $\phi_\mathrm{f} \in \mathbb{R}$, which are:

$$\begin{cases} \mathrm{Re}[\gamma_\mp^\mathrm{I}] = \mp \cosh^{-1}\left(\sqrt{1 + \dfrac{\sinh^2(2\phi_\mathrm{f})}{4}\left(2 + a_\mathrm{f}^2\cosh(2\phi_\mathrm{f}) - \sqrt{(2 + a_\mathrm{f}^2\cosh(2\phi_\mathrm{f}))^2 - a_\mathrm{f}^4}\right)}\right); \\ \mathrm{Re}[\gamma_\mp^\mathrm{II}] = \mp \cosh^{-1}\left(\sqrt{1 + \dfrac{\sinh^2(2\phi_\mathrm{f})}{4}\left(2 + a_\mathrm{f}^2\cosh(2\phi_\mathrm{f}) + \sqrt{(2 + a_\mathrm{f}^2\cosh(2\phi_\mathrm{f}))^2 - a_\mathrm{f}^4}\right)}\right). \end{cases} \tag{B.2.24}$$

We can further constrain the value of k by looking at the limit of Π_x when $\phi_\mathrm{f} \to 0$. In that case, (B.2.22) directly implies $\sinh^2(2\,\mathrm{Re}[\gamma]) \to 0$, so $\gamma \to 0$. Then

$$\Pi_x = i\cosh(2\gamma) = i(-1)^k \cosh(2\,\mathrm{Re}[\gamma]) \xrightarrow[\gamma\to 0]{} i(-1)^k\,; \tag{B.2.25}$$

so we recover the right limit $\Pi_x \to +i$ only for $k = 0$, so $\mathrm{Im}[\gamma] = 0$.

3. $\mathrm{Im}[\gamma] = \pi/4 + k \cdot \pi/2$, $k \in \mathbb{Z}$: here we have $\cos(2\,\mathrm{Im}[\gamma]) = 0$ and $\sin(2\,\mathrm{Im}[\gamma]) = (-1)^k$:

$$\begin{aligned} & a_\mathrm{f}^4 \sinh^2(2\phi_\mathrm{f}) = -4a_\mathrm{f}^2 \cosh(2\,\mathrm{Re}[\gamma]) \cosh(2\,\mathrm{Re}[\gamma] - 2\phi_\mathrm{f})\,; \\ \Rightarrow\ & a_\mathrm{f}^2 \sinh^2(2\phi_\mathrm{f}) < 4 \max_{\mathrm{Re}[\gamma]} (-\cosh(2\,\mathrm{Re}[\gamma]) \cosh(2\,\mathrm{Re}[\gamma] - 2\phi_\mathrm{f}))\,. \end{aligned} \tag{B.2.26}$$

This maximum lies at $\mathrm{Re}[\gamma] = \phi_\mathrm{f}/2$ and thus $a_\mathrm{f}^2 \sinh^2(2\phi_\mathrm{f}) < -4\cosh^2(\phi_\mathrm{f})$. This can never be satisfied for real values of a_f and ϕ_f.

B.3 Picard's little theorem

Picard's little theorem was formulated and proved in 1879 by Picard and states that [176]: *"Consider an entire [and non-constant] function $G(z)$ which never equals a certain finite value a. Then there cannot exist another finite value b, different from a, that $G(z)$ cannot equal."* An entire function is a holomorphic function defined on the whole complex plane. An holomorphic function $G : \mathbb{C} \to \mathbb{C}$ is a $\mathbb{C}$-differentiable function (the corresponding function $F : \mathbb{R}^2 \to \mathbb{R}^2 : (\mathrm{Re}[z], \mathrm{Im}[z]) \to (\mathrm{Re}[G(z)], \mathrm{Im}[G(z)])$ is differentiable at all points $(\mathrm{Re}[z], \mathrm{Im}[z]) = (x, y)$) such that the application $\mathbb{C} \to \mathbb{C} : z \to G'(z)$ is continuous on $\mathbb{C}$, and which moreover satisfies the

Cauchy-Riemann relations: for $G(x+iy) \equiv u(x,y) + iv(x,y)$,

$$\begin{cases} \dfrac{\partial u}{\partial x}(x,y) = \dfrac{\partial v}{\partial y}(x,y)\,, \\ \dfrac{\partial u}{\partial y}(x,y) = -\dfrac{\partial v}{\partial x}(x,y)\,. \end{cases} \tag{B.3.1}$$

Based on this definition, one can show that the function

$$V : \mathbb{C} \to \mathbb{C} : z \to \alpha \cosh(z) + \beta \sinh(z)\,, \tag{B.3.2}$$

(i.e., our potential) is holomorphic. Generically, for a potential that is an entire function, this theorem means that the constraint equation at $\tau = 0$, $a|_0^2\, V(\phi|_0) = 0$, is not only satisfied for closed geometries where $a|_0 = 0$, but also for situations where $V(\phi|_0) = 0$, which generically exist. There is one well-known exception given by the exponential potential, $V(\phi) = e^{\phi}$, which only vanishes at infinity when $\mathrm{Re}[\phi] < 0$. This is precisely the case we study when $\alpha = \beta$. That case put aside, this explains why for every γ, we find two regular saddle points; one compact and for which $\phi|_0 = \gamma$; and one non-compact for which $\phi|_0 \neq \gamma$, but where $V(\phi|_0) = 0$.

Moreover this is not specific to this potential, but is a generic feature of all entire functions. The only assumption we are making is that this potential of the scalar field can be extended to the complex plane. This is however a strong assumption, that can be questioned, in particular in view of the complex metric criterion (chapter 6).

Bibliography

[1] C. Jonas and J.L. Lehners, *No-boundary solutions are robust to quantum gravity corrections*, *Phys. Rev. D* **102** (2020) 123539.

[2] C. Jonas, J.L. Lehners and J. Quintin, *Cosmological consequences of a principle of finite amplitudes*, *Phys. Rev. D* **103** (2021) 103525.

[3] C. Jonas, J.L. Lehners and V. Meyer, *Revisiting the no-boundary proposal with a scalar field*, *Phys. Rev. D* **105** (2022) 043529.

[4] C. Jonas, J.L. Lehners and J. Quintin, *Uses of complex metrics in cosmology*, *JHEP* **08** (2022) 284.

[5] C. Kiefer, *Decoherence in quantum electrodynamics and quantum gravity*, *Phys. Rev. D* **46** (1992) 1658.

[6] J.J. Halliwell, *Decoherence in Quantum Cosmology*, *Phys. Rev. D* **39** (1989) 2912.

[7] Planck collaboration, N. Aghanim et al., *Planck 2018 results. I. Overview and the cosmological legacy of Planck*, *Astron. Astrophys.* **641** (2020) A1.

[8] C. Vafa, *The String landscape and the swampland*, `hep-th/0509212`.

[9] H. Ooguri and C. Vafa, *On the Geometry of the String Landscape and the Swampland*, *Nucl. Phys. B* **766** (2007) 21.

[10] J.M. Weisberg, J.H. Taylor and L.A. Fowler, *Gravitational waves from an orbiting pulsar*, *Scientific American* **245** (Oct., 1981) 74.

[11] LIGO Scientific, Virgo collaboration, B.P. Abbott et al., *Observing gravitational-wave transient GW150914 with minimal assumptions*, *Phys. Rev. D* **93** (2016) 122004.

[12] B.L. Webster and P. Murdin, *Cygnus x-1—a spectroscopic binary with a heavy companion ?*, *Nature* **235** (Jan, 1972) 37.

[13] A.G. Riess et al., *A 2.4% Determination of the Local Value of the Hubble Constant*, *Astrophys. J.* **826** (2016) 56.

[14] P.D. Group, P.A. Zyla, R.M. Barnett, J. Beringer, O. Dahl, D.A. Dwyer et al., *Review of Particle Physics*, *Progress of Theoretical and Experimental Physics* **2020** (08, 2020).

[15] R.A. Alpher, H. Bethe and G. Gamow, *The origin of chemical elements*, *Phys. Rev.* **73** (Apr, 1948) 803.

[16] A.H. Guth, *The Inflationary Universe: A Possible Solution to the Horizon and Flatness Problems*, *Phys. Rev. D* **23** (1981) 347.

[17] A.D. Linde, *A New Inflationary Universe Scenario: A Possible Solution of the Horizon, Flatness, Homogeneity, Isotropy and Primordial Monopole Problems*, *Adv. Ser. Astrophys. Cosmol.* **3** (1987) 149.

[18] V. Mukhanov, *Physical Foundations of Cosmology*, Cambridge University Press (2005), 10.1017/CBO9780511790553.

[19] L. Abbott, E. Farhi and M.B. Wise, *Particle production in the new inflationary cosmology*, *Physics Letters B* **117** (1982) 29.

[20] F.L. Bezrukov and M. Shaposhnikov, *The Standard Model Higgs boson as the inflaton*, *Phys. Lett. B* **659** (2008) 703.

[21] A.A. Starobinsky, *A New Type of Isotropic Cosmological Models Without Singularity*, *Phys. Lett. B* **91** (1980) 99.

[22] J. Martin and R.H. Brandenberger, *The TransPlanckian problem of inflationary cosmology*, *Phys. Rev. D* **63** (2001) 123501.

[23] G. 't Hooft and M. Veltman, *One-loop divergencies in the theory of gravitation*, *Annales de L'Institut Henri Poincare Section (A) Physique Theorique* **20** (Jan., 1974) 69.

[24] S. Deser and P. van Nieuwenhuizen, *One Loop Divergences of Quantized Einstein-Maxwell Fields*, *Phys. Rev. D* **10** (1974) 401.

[25] M.H. Goroff and A. Sagnotti, *The Ultraviolet Behavior of Einstein Gravity*, *Nucl. Phys. B* **266** (1986) 709.

[26] B.S. DeWitt, *Quantum Theory of Gravity. 1. The Canonical Theory*, *Phys. Rev.* **160** (1967) 1113.

[27] R. Arnowitt, S. Deser and C.W. Misner, *Dynamical structure and definition of energy in general relativity*, *Phys. Rev.* **116** (Dec, 1959) 1322.

[28] C. Kiefer, *Quantum gravity*, vol. 124, Clarendon, Oxford (2004).

[29] D. Brizuela, C. Kiefer and M. Krämer, *Quantum-gravitational effects on gauge-invariant scalar and tensor perturbations during inflation: The de Sitter case*, *Phys. Rev. D* **93** (2016) 104035.

[30] L. Chataignier, *Beyond semiclassical time*, arXiv:2205.09147.

[31] R.P. Feynman, *Space-time approach to non-relativistic quantum mechanics*, *Rev. Mod. Phys.* **20** (Apr, 1948) 367.

[32] S.W. Hawking, *Quantum gravity and path integrals*, *Phys. Rev. D* **18** (Sep, 1978) 1747.

[33] S. Hawking, *The Boundary Conditions of the Universe*, *Pontif. Acad. Sci. Scr. Varia* **48** (1982) 563.

[34] A. Vilenkin, *Classical and Quantum Cosmology of the Starobinsky Inflationary Model*, *Phys. Rev. D* **32** (1985) 2511.

[35] J.B. Hartle, S.W. Hawking and T. Hertog, *The Classical Universes of the No-Boundary Quantum State*, *Phys. Rev. D* **77** (2008) 123537.

[36] L. Battarra and J.L. Lehners, *On the No-Boundary Proposal for Ekpyrotic and Cyclic Cosmologies*, *JCAP* **12** (2014) 023.

[37] J.L. Lehners, *Classical Inflationary and Ekpyrotic Universes in the No-Boundary Wavefunction*, *Phys. Rev. D* **91** (2015) 083525.

[38] J.B. Hartle and S.W. Hawking, *Wave Function of the Universe*, *Phys. Rev. D* **28** (1983) 2960.

[39] L.J. Garay, J.J. Halliwell and G.A.M. Marugán, *Path-integral quantum cosmology: A class of exactly soluble scalar-field minisuperspace models with exponential potentials*, *Phys. Rev. D* **43** (Apr, 1991) 2572.

[40] G.W. Lyons, *Complex solutions for the scalar field model of the universe*, *Phys. Rev. D* **46** (Aug, 1992) 1546.

[41] R. Penrose, *Gravitational collapse and space-time singularities*, *Phys. Rev. Lett.* **14** (1965) 57.

[42] G.W. Gibbons, S.W. Hawking and M.J. Perry, *Path Integrals and the Indefiniteness of the Gravitational Action*, *Nucl. Phys. B* **138** (1978) 141.

[43] A. Di Tucci and J.L. Lehners, *No-Boundary Proposal as a Path Integral with Robin Boundary Conditions*, *Phys. Rev. Lett.* **122** (2019) 201302.

[44] J. Feldbrugge, J.L. Lehners and N. Turok, *No smooth beginning for spacetime*, *Phys. Rev. Lett.* **119** (2017) 171301.

[45] A. Di Tucci and J.L. Lehners, *Unstable no-boundary fluctuations from sums over regular metrics*, *Phys. Rev. D* **98** (2018) 103506.

[46] T.S. Bunch and P.C.W. Davies, *Quantum field theory in de Sitter space - Renormalization by point-splitting*, *Proceedings of the Royal Society of London Series A* **360** (Mar., 1978) 117.

[47] A. Vilenkin, *Creation of Universes from Nothing*, *Phys. Lett.* **117B** (1982) 25.

[48] T. Hertog and J. Hartle, *Holographic No-Boundary Measure*, *JHEP* **05** (2012) 095.

[49] J.M. Maldacena, *The Large N limit of superconformal field theories and supergravity*, *Adv. Theor. Math. Phys.* **2** (1998) 231.

[50] E. Witten, *Anti-de Sitter space and holography*, *Adv. Theor. Math. Phys.* **2** (1998) 253.

[51] J. Feldbrugge, J.L. Lehners and N. Turok, *Lorentzian Quantum Cosmology*, *Phys. Rev. D* **95** (2017) 103508.

[52] A. Di Tucci, J.L. Lehners and L. Sberna, *No-boundary prescriptions in Lorentzian quantum cosmology*, *Phys. Rev. D* **100** (2019) 123543.

[53] A. Di Tucci, M.P. Heller and J.L. Lehners, *Lessons for quantum cosmology from anti–de Sitter black holes*, *Phys. Rev. D* **102** (2020) 086011.

[54] J.W. York, *Role of conformal three-geometry in the dynamics of gravitation*, *Phys. Rev. Lett.* **28** (Apr, 1972) 1082.

[55] G.W. Gibbons and S.W. Hawking, *Action integrals and partition functions in quantum gravity*, *Phys. Rev. D* **15** (May, 1977) 2752.

[56] S. Hawking and J. Luttrell, *Higher derivatives in quantum cosmology: (i). the isotropic case*, *Nuclear Physics B* **247** (1984) 250 .

[57] H. van Elst, J.E. Lidsey and R.K. Tavakol, *Quantum cosmology and higher order Lagrangian theories*, *Class. Quant. Grav.* **11** (1994) 2483.

[58] K.S. Stelle, *Classical gravity with higher derivatives*, *General Relativity and Gravitation* **9** (Apr, 1978) 353.

[59] J.F. Donoghue and G. Menezes, *Unitarity, stability and loops of unstable ghosts*, *Phys. Rev. D* **100** (2019) 105006.

[60] A. Salvio, *Metastability in Quadratic Gravity*, *Phys. Rev. D* **99** (2019) 103507.

[61] A.A. Starobinsky, *Stochastic de Sitter (inflationary) stage in the early Universe*, *Lect. Notes Phys.* **246** (1986) 107.

[62] R. Metsaev and A. Tseytlin, *Order α' (two-loop) equivalence of the string equations of motion and the σ-model weyl invariance conditions: Dependence on the dilaton and the antisymmetric tensor*, *Nuclear Physics B* **293** (1987) 385 .

[63] N. Ohta and T. Torii, *Charged Black Holes in String Theory with Gauss-Bonnet Correction in Various Dimensions*, *Phys. Rev. D* **86** (2012) 104016 [arXiv:1208.6367].

[64] J.F. Donoghue, *General relativity as an effective field theory: The leading quantum corrections*, *Phys. Rev. D* **50** (1994) 3874.

[65] E. Calzetta, I. Jack and L. Parker, *Quantum gauge fields at high curvature*, *Phys. Rev. D* **33** (1986) 953.

[66] J.F. Donoghue and B.K. El-Menoufi, *Nonlocal quantum effects in cosmology: Quantum memory, nonlocal FLRW equations, and singularity avoidance*, *Phys. Rev. D* **89** (2014) 104062.

[67] E. Belgacem, Y. Dirian, S. Foffa and M. Maggiore, *Nonlocal gravity. Conceptual aspects and cosmological predictions*, *JCAP* **03** (2018) 002.

[68] M.B. Green, J.G. Russo and P. Vanhove, *Automorphic properties of low energy string amplitudes in various dimensions*, *Phys. Rev. D* **81** (2010) 086008.

[69] P. Fleig, H.P.A. Gustafsson, A. Kleinschmidt and D. Persson, *Eisenstein series and automorphic representations*, Cambridge University Press (2018).

[70] M.B. Green, J.H. Schwarz and E. Witten, *Superstring Theory Vol. 2*, Cambridge Monographs on Mathematical Physics, Cambridge University Press (2012), 10.1017/CBO9781139248570.

[71] J. M. Martín-García, *xact: Efficient tensor computer algebra for the wolfram language*, http://www.xact.es/.

[72] M.B. Green, M. Gutperle and P. Vanhove, *One loop in eleven-dimensions*, *Phys. Lett. B* **409** (1997) 177.

[73] M.B. Green, S.D. Miller, J.G. Russo and P. Vanhove, *Eisenstein series for higher-rank groups and string theory amplitudes*, *Commun. Num. Theor. Phys.* **4** (2010) 551.

[74] G. Bossard and V. Verschinin, $\mathcal{E}\nabla^4 R^4$ *type invariants and their gradient expansion*, *JHEP* **03** (2015) 089.

[75] P. Caputa and S. Hirano, *Airy Function and 4d Quantum Gravity*, *JHEP* **06** (2018) 106.

[76] J.L. Lehners, *Wave function of simple universes analytically continued from negative to positive potentials*, *Phys. Rev. D* **104** (2021) 063527.

[77] J.L. Lehners, *Allowable Complex Scalars from Kaluza-Klein Compactifications and Metric Rescalings*, arXiv:2209.14669.

[78] S.F. Bramberger, A. Di Tucci and J.L. Lehners, *Homogeneous Transitions during Inflation: a Description in Quantum Cosmology*, *Phys. Rev. D* **101** (2020) 063501.

[79] L. Boyle, K. Finn and N. Turok, *CPT-Symmetric Universe*, *Phys. Rev. Lett.* **121** (2018) 251301.

[80] C. Teitelboim, *Quantum Mechanics of the Gravitational Field*, *Phys. Rev. D* **25** (1982) 3159.

[81] J. Khoury, B.A. Ovrut, P.J. Steinhardt and N. Turok, *The Ekpyrotic universe: Colliding branes and the origin of the hot big bang*, *Phys. Rev. D* **64** (2001) 123522.

[82] L. Battarra and J.L. Lehners, *On the Creation of the Universe via Ekpyrotic Instantons*, *Phys. Lett. B* **742** (2015) 167.

[83] H. Bernardo, R. Brandenberger and G. Franzmann, *String cosmology backgrounds from classical string geometry*, *Phys. Rev. D* **103** (2021) 043540.

[84] P. Agrawal, S. Gukov, G. Obied and C. Vafa, *Topological Gravity as the Early Phase of Our Universe*, arXiv:2009.10077.

[85] J.L. Lehners and K.S. Stelle, *A Safe Beginning for the Universe?*, *Phys. Rev.* **D100** (2019) 083540.

[86] J.D. Barrow and F.J. Tipler, *Action principles in nature*, *Nature* **331** (Jan, 1988) 31.

[87] J.D. Barrow, *Finite Action Principle Revisited*, *Phys. Rev.* **D101** (2020) 023527.

[88] V. Belinskii, I. Khalatnikov and E. Lifshitz, *Oscillatory approach to a singular point in the relativistic cosmology*, *Advances in Physics* **19** (1970) 525.

[89] B.F. Schutz, *Perfect Fluids in General Relativity: Velocity Potentials and a Variational Principle*, *Phys. Rev. D* **2** (1970) 2762.

[90] J. Brown, *Action functionals for relativistic perfect fluids*, *Class. Quant. Grav.* **10** (1993) 1579.

[91] M. Dafermos, *Black holes without spacelike singularities*, *Commun. Math. Phys.* **332** (2014) 729.

[92] J.N. Borissova and A. Eichhorn, *Towards black-hole singularity-resolution in the Lorentzian gravitational path integral*, *Universe* **7** (2021) 48.

[93] A. Borde, A.H. Guth and A. Vilenkin, *Inflationary space-times are incompletein past directions*, *Phys. Rev. Lett.* **90** (2003) 151301.

[94] A. Di Tucci, J. Feldbrugge, J.L. Lehners and N. Turok, *Quantum Incompleteness of Inflation*, *Phys. Rev. D* **100** (2019) 063517.

[95] T. Rudelius, *Conditions for (No) Eternal Inflation*, *JCAP* **08** (2019) 009.

[96] P. Creminelli, S. Dubovsky, A. Nicolis, L. Senatore and M. Zaldarriaga, *The Phase Transition to Slow-roll Eternal Inflation*, *JHEP* **09** (2008) 036.

[97] C. Kiefer, D. Polarski and A.A. Starobinsky, *Quantum to classical transition for fluctuations in the early universe*, *Int. J. Mod. Phys. D* **7** (1998) 455.

[98] P. Agrawal, G. Obied, P.J. Steinhardt and C. Vafa, *On the Cosmological Implications of the String Swampland*, *Phys. Lett. B* **784** (2018) 271.

[99] G. Obied, H. Ooguri, L. Spodyneiko and C. Vafa, *De Sitter Space and the Swampland*, arXiv:1806.08362.

[100] H. Ooguri, E. Palti, G. Shiu and C. Vafa, *Distance and de Sitter Conjectures on the Swampland*, *Phys. Lett. B* **788** (2019) 180.

[101] R. Brandenberger and P. Peter, *Bouncing Cosmologies: Progress and Problems*, *Found. Phys.* **47** (2017) 797.

[102] J.D. Barrow and M.P. Dabrowski, *Oscillating Universes*, *Mon. Not. Roy. Astron. Soc.* **275** (1995) 850.

[103] P.J. Steinhardt and N. Turok, *Cosmic evolution in a cyclic universe*, *Phys. Rev. D* **65** (2002) 126003.

[104] P.J. Steinhardt and N. Turok, *The Cyclic model simplified*, *New Astron. Rev.* **49** (2005) 43.

[105] J.L. Lehners and P.J. Steinhardt, *Dark Energy and the Return of the Phoenix Universe*, *Phys. Rev. D* **79** (2009) 063503.

[106] J.D. Barrow and C. Ganguly, *Cyclic Mixmaster Universes*, *Phys. Rev. D* **95** (2017) 083515.

[107] J.D. Barrow and C. Ganguly, *The Shape of Bouncing Universes*, *Int. J. Mod. Phys. D* **26** (2017) 1743016.

[108] A. Ijjas and P.J. Steinhardt, *A new kind of cyclic universe*, *Phys. Lett. B* **795** (2019) 666.

[109] K.S. Stelle, *Renormalization of Higher Derivative Quantum Gravity*, *Phys. Rev. D* **16** (1977) 953.

[110] K.S. Stelle, *Classical Gravity with Higher Derivatives*, *Gen. Rel. Grav.* **9** (1978) 353.

[111] Planck collaboration, Y. Akrami et al., *Planck 2018 results. X. Constraints on inflation*, *Astron. Astrophys.* **641** (2020) A10.

[112] N. Deruelle, M. Sasaki, Y. Sendouda and D. Yamauchi, *Hamiltonian formulation of f(Riemann) theories of gravity*, *Prog. Theor. Phys.* **123** (2010) 169.

[113] E. Dyer and K. Hinterbichler, *Boundary Terms, Variational Principles and Higher Derivative Modified Gravity*, *Phys. Rev. D* **79** (2009) 024028.

[114] J.D. Barrow and S. Cotsakis, *Inflation and the Conformal Structure of Higher Order Gravity Theories*, *Phys. Lett. B* **214** (1988) 515.

[115] O. Hohm and E. Tonni, *A boundary stress tensor for higher-derivative gravity in AdS and Lifshitz backgrounds*, *JHEP* **04** (2010) 093.

[116] R.C. Myers, *Higher Derivative Gravity, Surface Terms and String Theory*, *Phys. Rev. D* **36** (1987) 392.

[117] N. Deruelle, N. Merino and R. Olea, *Einstein-Gauss-Bonnet theory of gravity: The Gauss-Bonnet-Katz boundary term*, *Phys. Rev. D* **97** (2018) 104009.

[118] J.D. Barrow and S. Hervik, *On the evolution of universes in quadratic theories of gravity*, *Phys. Rev. D* **74** (2006) 124017.

[119] J.D. Barrow and S. Hervik, *Anisotropically inflating universes*, *Phys. Rev. D* **73** (2006) 023007.

[120] J.D. Barrow and S. Hervik, *Simple Types of Anisotropic Inflation*, *Phys. Rev. D* **81** (2010) 023513.

[121] J. Middleton, *On The Existence Of Anisotropic Cosmological Models In Higher-Order Theories Of Gravity*, *Class. Quant. Grav.* **27** (2010) 225013.

[122] D. Müller, A. Ricciardone, A.A. Starobinsky and A. Toporensky, *Anisotropic cosmological solutions in $R + R^2$ gravity*, *Eur. Phys. J. C* **78** (2018) 311.

[123] P. Creminelli, A. Nicolis and E. Trincherini, *Galilean Genesis: An Alternative to inflation*, *JCAP* **11** (2010) 021.

[124] P. Creminelli, K. Hinterbichler, J. Khoury, A. Nicolis and E. Trincherini, *Subluminal Galilean Genesis*, *JHEP* **02** (2013) 006.

[125] S. Nishi and T. Kobayashi, *Generalized Galilean Genesis*, *JCAP* **03** (2015) 057.

[126] T. Kobayashi, M. Yamaguchi and J. Yokoyama, *Galilean Creation of the Inflationary Universe*, *JCAP* **07** (2015) 017.

[127] S. Nishi and T. Kobayashi, *Scale-invariant perturbations from null-energy-condition violation: A new variant of Galilean genesis*, *Phys. Rev. D* **95** (2017) 064001.

[128] D. Yoshida, J. Quintin, M. Yamaguchi and R.H. Brandenberger, *Cosmological perturbations and stability of nonsingular cosmologies with limiting curvature*, *Phys. Rev. D* **96** (2017) 043502.

[129] S. Mironov, V. Rubakov and V. Volkova, *Genesis with general relativity asymptotics in beyond Horndeski theory*, *Phys. Rev. D* **100** (2019) 083521.

[130] V. Volkova, S. Mironov and V. Rubakov, *Cosmological Scenarios with Bounce and Genesis in Horndeski Theory and Beyond*, *J. Exp. Theor. Phys.* **129** (2019) 553.

[131] Y. Ageeva, O. Evseev, O. Melichev and V. Rubakov, *Towards evading the strong coupling problem in Horndeski Genesis*, *Phys. Rev. D* **102** (2020) 023519.

[132] A. Ilyas, M. Zhu, Y. Zheng and Y.F. Cai, *Emergent Universe and Genesis from the DHOST Cosmology*, *JHEP* **01** (2021) 141.

[133] C. Armendariz-Picon, V.F. Mukhanov and P.J. Steinhardt, *A Dynamical solution to the problem of a small cosmological constant and late time cosmic acceleration*, *Phys. Rev. Lett.* **85** (2000) 4438.

[134] C. Armendariz-Picon, V.F. Mukhanov and P.J. Steinhardt, *Essentials of k essence*, *Phys. Rev. D* **63** (2001) 103510.

[135] N. Arkani-Hamed, H.C. Cheng, M.A. Luty and S. Mukohyama, *Ghost condensation and a consistent infrared modification of gravity*, *JHEP* **05** (2004) 074.

[136] C. Lin, R.H. Brandenberger and L. Perreault Levasseur, *A Matter Bounce By Means of Ghost Condensation*, *JCAP* **04** (2011) 019.

[137] C. de Rham and S. Melville, *Unitary null energy condition violation in P(X) cosmologies*, *Phys. Rev. D* **95** (2017) 123523.

[138] S. Mironov, V. Rubakov and V. Volkova, *Cosmological scenarios with bounce and Genesis in Horndeski theory and beyond*, arXiv:1906.12139.

[139] Y.A. Ageeva, O.A. Evseev, O.I. Melichev and V.A. Rubakov, *Horndeski Genesis: strong coupling and absence thereof*, *EPJ Web Conf.* **191** (2018) 07010.

[140] Y. Ageeva, P. Petrov and V. Rubakov, *Horndeski genesis: consistency of classical theory*, *JHEP* **12** (2020) 107.

[141] R.H. Brandenberger and C. Vafa, *Superstrings in the Early Universe*, *Nucl. Phys. B* **316** (1989) 391.

[142] O. Hohm and B. Zwiebach, *Duality invariant cosmology to all orders in α'*, *Phys. Rev. D* **100** (2019) 126011.

[143] K.A. Meissner and G. Veneziano, *Manifestly O(d,d) invariant approach to space-time dependent string vacua*, *Mod. Phys. Lett. A* **6** (1991) 3397.

[144] K.A. Meissner, *Symmetries of higher order string gravity actions*, *Phys. Lett. B* **392** (1997) 298.

[145] O. Hohm and B. Zwiebach, *Non-perturbative de Sitter vacua via α' corrections*, *Int. J. Mod. Phys. D* **28** (2019) 1943002.

[146] H. Bernardo, R. Brandenberger and G. Franzmann, *$O(d,d)$ covariant string cosmology to all orders in α'*, *JHEP* **02** (2020) 178.

[147] H. Bernardo and G. Franzmann, *α'-Cosmology: solutions and stability analysis*, *JHEP* **05** (2020) 073.

[148] A. Bedroya, *de Sitter Complementarity, TCC, and the Swampland*, arXiv:2010.09760.

[149] R. Penrose, *Singularities and time-asymmetry.*, in *General Relativity: An Einstein centenary survey* (S.W. Hawking and W. Israel, eds.), p. 581, Jan., 1979.

[150] E. Witten, *A Note On Complex Spacetime Metrics*, arXiv:2111.06514.

[151] J.J. Halliwell and R.C. Myers, *Multiple Sphere Configurations in the Path Integral Representation of the Wave Function of the Universe*, *Phys. Rev. D* **40** (1989) 4011.

[152] S.F. Bramberger, S. Farnsworth and J.L. Lehners, *Wavefunction of anisotropic inflationary universes with no-boundary conditions*, *Phys. Rev. D* **95** (2017) 083513.

[153] M. Kontsevich and G. Segal, *Wick Rotation and the Positivity of Energy in Quantum Field Theory*, *Quart. J. Math. Oxford Ser.* **72** (2021) 673.

[154] J. Louko and R.D. Sorkin, *Complex actions in two-dimensional topology change*, *Class. Quant. Grav.* **14** (1997) 179.

[155] J.L. Lehners, *Allowable complex metrics in minisuperspace quantum cosmology*, *Phys. Rev. D* **105** (2022) 026022.

[156] J.L. Lehners, R. Leung and K.S. Stelle, *How to create universes with internal flux*, *Phys. Rev. D* **107** (2023) 046006.

[157] D.J. Wales and J.P.K. Doye, *Global optimization by basin-hopping and the lowest energy structures of lennard-jones clusters containing up to 110 atoms*, *The Journal of Physical Chemistry A* **101** (Jul, 1997) 5111.

[158] P. Virtanen et al., *SciPy 1.0–Fundamental Algorithms for Scientific Computing in Python*, *Nature Meth.* **17** (2020) 261.

[159] J.J. Halliwell and J. Louko, *Steepest Descent Contours in the Path Integral Approach to Quantum Cosmology. 1. The De Sitter Minisuperspace Model*, *Phys. Rev. D* **39** (1989) 2206.

[160] M. Michel Petrovitch, *Sur une manière d'étendre le théorème de la moyenne aux équations différentielles du premier ordre*, *Mathematische Annalen* **54** (Sep, 1901) 417.

[161] M. Visser, *Feynman's $i\epsilon$ prescription, almost real spacetimes, and acceptable complex spacetimes*, *JHEP* **08** (2022) 129.

[162] C.M. Bender, D.C. Brody and D.W. Hook, *Quantum effects in classical systems having complex energy*, *J. Phys. A* **41** (2008) 352003.

[163] N. Turok, *On Quantum Tunneling in Real Time*, *New J. Phys.* **16** (2014) 063006.

[164] S.F. Bramberger, G. Lavrelashvili and J.L. Lehners, *Quantum tunneling from paths in complex time*, *Phys. Rev. D* **94** (2016) 064032.

[165] S.R. Coleman and F. De Luccia, *Gravitational Effects on and of Vacuum Decay*, *Phys. Rev. D* **21** (1980) 3305.

[166] S.F. Bramberger, T. Hertog, J.L. Lehners and Y. Vreys, *Quantum Transitions Through Cosmological Singularities*, *JCAP* **07** (2017) 007.

[167] L. Boyle and N. Turok, *Two-Sheeted Universe, Analyticity and the Arrow of Time*, arXiv:2109.06204.

[168] J. Feldbrugge, J.L. Lehners and N. Turok, *No rescue for the no boundary proposal: Pointers to the future of quantum cosmology*, *Phys. Rev. D* **97** (2018) 023509.

[169] S. Gielen and N. Turok, *Perfect Quantum Cosmological Bounce*, *Phys. Rev. Lett.* **117** (2016) 021301.

[170] S. Gielen and N. Turok, *Quantum propagation across cosmological singularities*, *Phys. Rev. D* **95** (2017) 103510.

[171] T. Banks, W. Fischler, S.H. Shenker and L. Susskind, *m theory as a matrix model: A conjecture*, *Phys. Rev. D* **55** (Apr, 1997) 5112.

[172] S. Brahma, R. Brandenberger and S. Laliberte, *Emergent cosmology from matrix theory*, *JHEP* **03** (2022) 067.

[173] S. Brahma, R. Brandenberger and S. Laliberte, *BFSS Matrix Model Cosmology: Progress and Challenges*, arXiv:2210.07288.

[174] O. Janssen, J.J. Halliwell and T. Hertog, *No-boundary proposal in biaxial Bianchi IX minisuperspace*, *Phys. Rev. D* **99** (2019) 123531.

[175] G.J. Loges, G. Shiu and N. Sudhir, *Complex saddles and Euclidean wormholes in the Lorentzian path integral*, *JHEP* **08** (2022) 064.

[176] E. Picard, *Sur une propriété des fonctions entières*, *Comptes rendus hebdomadaires des séances de l'Académie des Sciences* **88** (1879) 1024.